Clinical Physiology

PG-01

馬偕紀念醫院
MacKay Memorial Hospital

Establishment of the LC-MS/MS quantification method for serum free arachidonic and eicosapentaenoic acid

-Developmental and clinical practice of the tandem mass analytical method for free fatty acid

Tuen Jen Wang [a*], Chih Kuang Chuang [b], Chi Kuan Chen [a,c]
[a]Dept. of Laboratory Medicine, [b]Division of Genetics and Metabolism, Dept of Medical Research, and
[c]Dept of Pathology, Mackay Memorial Hospital, Taipei, Taiwan.

Background: Cerebrovascular and cardiovascular disease are the second and the forth most common causes of death in Taiwan, and both result in serious health injure and high mortality. The principle etiology of above diseases is arteriosclerosis which is caused by prolonged and slowly progressive inflammation on the vascular epithelium cells. Arachidonic acid (AA), Eicosapentaenoic acid (EPA) and their ratio in plasma are thought to be an accurate indication of the level of inflammation occurring within the body. In this study, a unique tandem mass spectrometry method that measures the ratio of Arachidonic acid (AA) to Eicosapentaenoic acid (EPA) in serum is proposed.

Method: An AB 4000 Q TRAP LC-MS/MS system with multiple reaction monitoring (MRM) mode was applied. Blood samples were collected from 50 normal adults after 12-hour fasting, and from 40 patients with increased C-Reactive Protein (CRP; normal reference range: <0.8mg/dl) of suffering atherosclerotic event. Serum samples were pretreated by organic solvent and hexane extraction, and the extract was ready for LC/MS/MS analysis.

Result: The within-run and between-run precisions (CV %) and the linearity of AA and EPA based on the IS were good (both less than 13.6%). The recovery of AA and EPA by using LC-MS/MS method (n=6) was 78.9% and 66.8% in average, respectively. The mean AA and EPA was 6.19 (±2.31) and 2.77 (±1.25) μg/mL in normal control (n=50) and 4.31 (±2.80), and 0.25 (±0.22) μg/mL in CRP increased patients (n=40), respectively. The average AA/EPA ratio was 2.21 in normal control and 16.6 in patients with increased CRP.

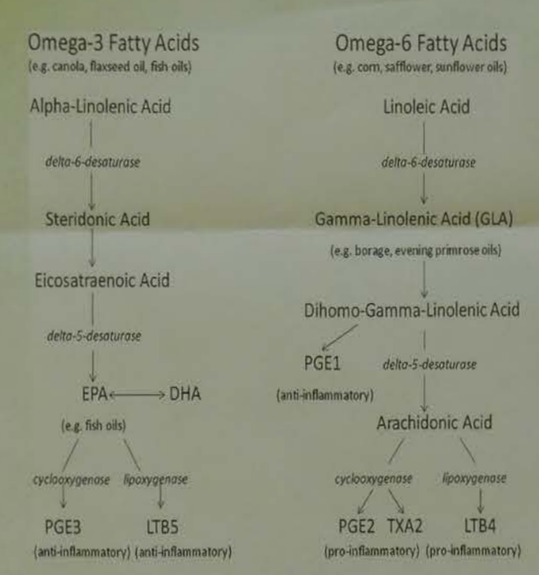

Figure1. Omega-3 and omega-6 fatty acids pathways in humans. (Martin & Stapleton, 2010)

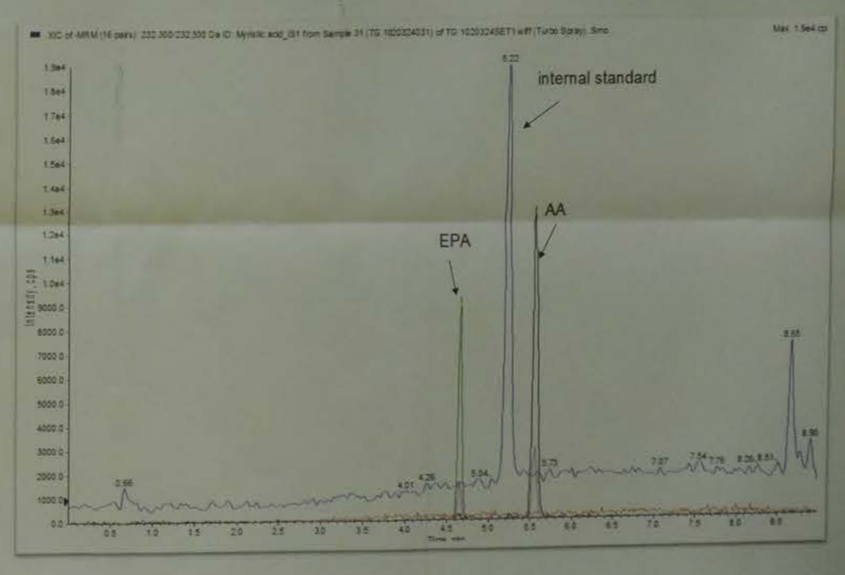

Figure2. MRM chromatography of Arachidonic acid(AA) and Eicosatrenoic acid (EPA) and its inetrnal standard (Myristic acid –D5) in blood sample.

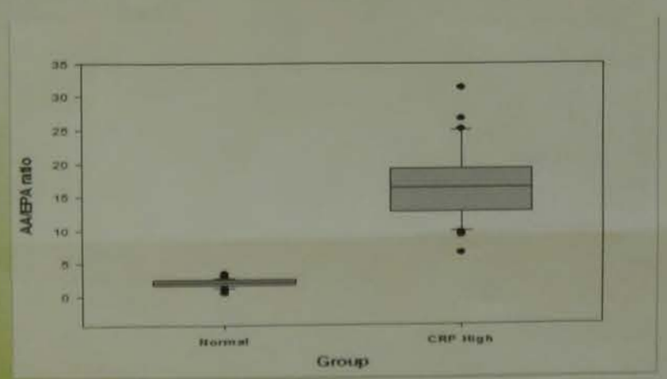

Figure3. Level of AA/EPA ratio are elevated in CRP high samples

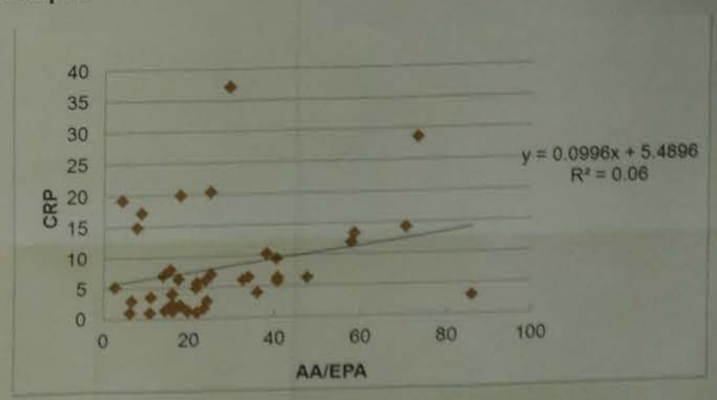

Figure4. Between CRP and AA/EPA ratio value is no correlation in CRP high samples.

Conclusion : The AA/EPA ratio is significantly elevated 7.5-fold in patients with high CRP value than that in normal control (p value < 0.001). Our results show that the AA and EPA quantitative analyses may provide valuable information for the monitoring chronic inflammation, such as arteriosclerosis. The LC-MS/MS is a specific, sensitive, validated, high throughput method and applicable for simultaneous quantification of AA and EPA in blood.

Clinical Physiology

PG-02

Preoperative language mapping with MEG in patients with temporal lobe epilepsy

Makoto Ishida[1,2], Masaki Iwasaki[3], Akitake Kanno[4], Kazutaka Jin[2], Suguru Asagi[1], Takashi Miki[1], Ryuta Kawashima[4], and Nobukazu Nakasato[1,2]

[1]Clinical Physiology Center, Tohoku University Hospital
[2]Department of Epileptology, Tohoku University Graduate School of Medicine
[3]Department of Neurosurgery, Tohoku University Graduate School of Medicine
[4]Institute of Development, Aging and Cancer, Tohoku University

TOHOKU UNIVERSITY

Purpose:
To investigate clinical utility of non-invasive language mapping with magnetoencephalography (MEG).

Methods:
This study included 28 right-handed patients with drug-resistant temporal lobe epilepsy (TLE) who underwent pre-surgical MEG language mapping with the auditory word recognition task. To determine the language dominant hemisphere, late MEG responses from 200 to 2000 ms after stimulus onset were investigated by two methods; equivalent current dipole (ECD) modeling analysis and statistical analysis of event-related desynchronization/synchronization (ERD/ERS). In ECD analysis, the laterality index (LI) was calculated from the number of ECDs localized on the posterior language area in each hemisphere. LI values greater than 0.5 and less than -0.5 were considered to indicate left and right hemispheric dominance, respectively, and values between -0.5 and 0.5 to indicate bilateral activation. In ERD/ERS analysis, language dominance was determined based on statistically significant changes in ERD or ERS. The MEG findings were compared with functional magnetic resonance imaging (fMRI) findings during verb generation tasks.

Case	Age	Sex	Epilepsy Onset	Etiology	MEG ECD	MEG ERD/ERS	fMRI	ECS
1	67	M	12	HS	100.00%	HG ERS	Rt	-
2	17	M	16	HS	100.00%	HG ERS	Lt	-
3	15	F	1	HS	100.00%	Alpha ERD	Lt	-
4	26	M	22	Tumor	100.00%	Alpha ERD(Rt)	Lt	-
5	35	M	21	HS	94.30%	HG ERS	Lt	-
6	37	F	16	AVM	82.00%	Alpha ERD	-	-
7	19	M	17	HS	78.70%	HG ERD	Lt	-
8	24	M	4	HS	60.30%	LG ERD(Lt) / HG ERS(Rt)	Lt	-
9	44	M	25	HS	41.40%	Beta ERD	Lt	-
10	26	F	12	HS	39.50%	HG ERS	Lt	-
11	28	F	20	HS + Cystic lesion	37.50%	Beta ERS	Lt	Lt T
12	32	F	5	Ganglioglioma	26.50%	Beta ERD	NL	Lt T
13	21	M	10	HS	23.07%	Theta ERD	Lt	-
14	23	F	10	HS	-8.70%	HG ERS(Lt) / LG ERS(Rt)	Lt	-
15	21	M	13	Ganglioglioma	-74.40%	HG ERS(Lt&Rt)	Lt	Lt T
16	26	F	10	HS	-90.90%	Alpha-beta ERD	Rt	-
17	27	F	7	HS + traumatic lesion	-93.50%	LG ERD	Rt	No language, Lt T
18	24	F	15	HS	-100%	HG ERS	Lt	-

M: male; F: female; HS: hippocampal sclerosis; AVM: arteriovenous malformation; ERD: event-related desynchronization; ERS: event-related synchronization; HG: high gamma; LG: low gamma; Lt: left; Rt: right; NL: non-lateralization; T: temporal

Table1. The clinical findings of patients with Lt TLE

Case	Age	Sex	Epilepsy Onset	Etiology	MEG ECD	MEG ERD/ERS	fMRI	ECS
1	27	F	13	FCD)	100.00%	HG ERS	Lt	-
2	21	M	16	Tumor	79.40%	Beta ERD	Lt	-
3	34	F	21	Cystic lesion	53.50%	LG ERS	Lt	-
4	29	F	4	HS	33.90%	HG ERD(Lt) / Alpha(Rt)	Lt	-
5	36	M	28	Non-lesion	33.60%	HG ERS(Lt&Rt)	Lt	-
6	41	F	9	Non-lesion	23.50%	Beta ERD	Lt	-
7	40	M	18	HS	-13.04%	Beta ERD	Lt	-
8	22	F	6	Non-lesion	-16.52%	HG ERS(Lt&Rt)	Lt	-
9	53	F	7	HS	-32.10%	Alpha-beta ERD(Lt)	Lt	-
10	28	F	25	Non-lesion	-69.00%	HG ERD	Lt	-

FCD: focal cortical dysplasia

Table2. The clinical findings of patients with Rt TLE

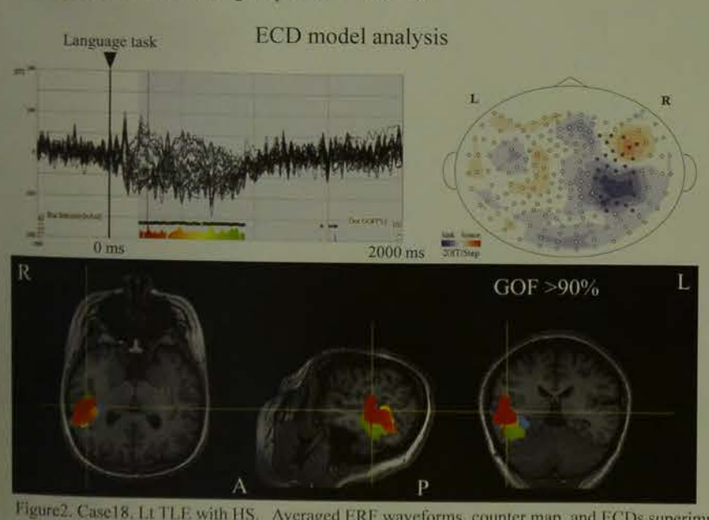

Figure2. Case18. Lt TLE with HS. Averaged ERF waveforms, counter map, and ECDs superimposed on the MRI for a auditory recognition memory task. Dipoles are localized on only the right hemisphere.

Modality	MEG		fMRI
Task	Recognition memory task		Verb generation task
Analysis	ECD model	ERD/ERS	BOLD change

Table 3. Difference of tasks and methods of analysis between modalities.

Laterality index (LI)

$$LI = \frac{(Lt - Rt)}{(Lt + Rt)} \times 100 \ (\%)$$

> 50% : Lt hemisphere dominant
-50% < and < 50% : Bilateral activation
< -50% : Rt hemisphere dominant

Fig1. laterality index (LI). LI was calculated from the number of ECDs localized on the posterior language area in each hemisphere. LI values greater than 50% and less than -50% were considered as indicative of left and right hemispheric dominance, respectively, and values between -50% and 50% were indicative of bilateral activation.

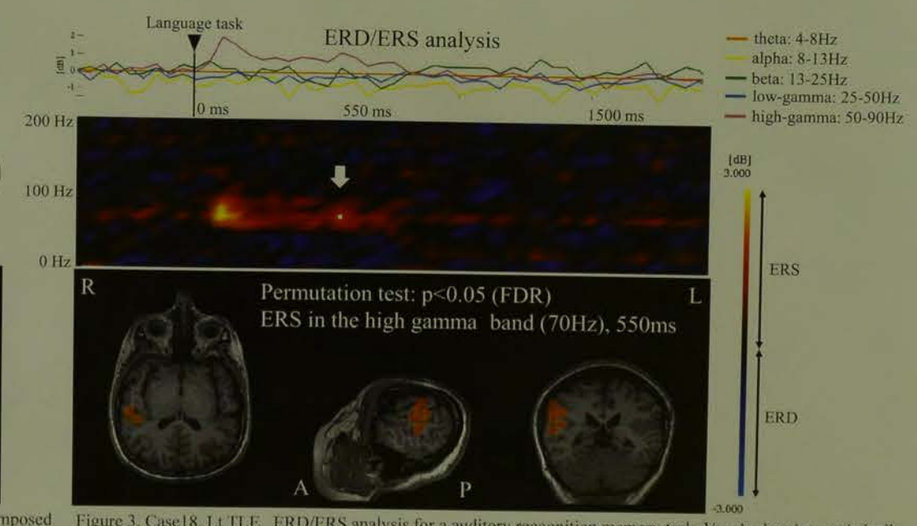

Figure 3. Case18. Lt TLE. ERD/ERS analysis for a auditory recognition memory task. Voxels showing statistically significant changes in high gamma synchronization are mapped onto the right temporal language area.

Results:

- The number of patients with bilateral activation judged by ECD analysis was larger than that judged by ERD/ERS analysis and fMRI (Table 4).
- In patients with left dominance, ECD analysis was highly concordant with ERD/ERS analysis and fMRI, while the concordance was lower in the other two groups (Table5).

	Lt TLE (n=18)			Rt TLE (n=10)		
	ECD	ERD/ERS	fMRI	ECD	ERD/ERS	fMRI
Lt hemisphere dominance	8	11	13	3	7	10
Bilateral activation	6	3	1	6	3	0
Rt hemisphere dominance	4	4	3	1	0	0

Table4. The results of language dominant hemisphere determined by ECD, ERD/ERS, and fMRI.

	Lt TLE (n=18)		Rt TLE (n=10)	
ECD	ERD/ERS	fMRI	ERD/ERS	fMRI
Lt hemisphere dominance	75.0 %	85.7 %	100.0 %	100.0 %
Bilateral activation	16.7 %	16.7 %	50.0 %	0.0 %
Rt hemisphere dominance	75.0 %	50.0 %	0.0 %	0.0 %

Table 5. The concordance between ECD model and ERS/ERD, fMRI.

Conclusion:

- The different MEG result between ECD modeling analysis and ERD/ERS
  - Averaged waveforms versus event-related changes in oscillations → Different sensitivity to language-related activity
- The different result between MEG and language fMRI
  - Different language tasks used
- Different analytical methods apparently indicate different language lateralization, so the specific functional aspects of language detected by MEG analysis must be considered for accurate determination of language dominance.

Reference:

1. Kamada K, Sawamura Y, Takeuchi F, et al. Expressive and receptive language areas determined by a non-invasive reliable method using functional magnetic resonance imaging and magnetoencephalography. Neurosurg 2007; 60: 296-306.
2. Papanicolaou AC, Simos PG, Castillo EM, et al. Magnetoencephalography: a noninvasive alternative to the WADA procedure. J Neurosurg 2004; 100: 867-876.
3. Hirata M, Goto T, Barnes G, et al. Language dominance and mapping based on neuromagnetic oscillatory changes: comparison with invasive procedures. J Neurosurg 2010; 112: 528-538.

Clinical Physiology

PG-03

PG-03

Effect of hypoxic training on renal function : a cross-over study in healthy subjects

Tsuneo Watanabe[1], Juri Nakayama[1], Hazuki Ohashi[1], Koichi Shinoda[1], Yuzuru Nohisa[1], Nobuyuki Furuta[1], Toshio Matsuoka[2], and Mitsuru Seishima[1]

[1]Division of Clinical Laboratory, Gifu University Hospital, Gifu, Japan; [2]Department of Sports Medicine and Sports Science, Gifu University Graduate School of Medicine, Gifu, Japan

INTRODUCTION

What is "hypoxic training"?

- First adopted by athletes in the late 1960s, the live-high train-high method of hypoxic training may increase performance in some.
- In a modern approach, live-high train-low altitude training was developed in the early 1990s in response to potential training limitations imposed on endurance athletes.

- Improvement of a cardiorespiratory function
- Fatigue recovery
- Weight control

The aim of this study was to investigate the influence of hypoxic physical exercise on renal function and to compare its effects on several parameters related to renal function to those of a control group who with training under normoxic conditions.

MATERIALS & METHODS

Subjects

Nine healthy men were examined (27.4±5.4 y).

Protocol

Hypoxia	Wash-out period	Normoxia
Normoxia	3 months	Hypoxia

Participants performed treadmill exercise under either normobaric hypoxic or normobaric normoxic conditions for 40 min. Exercise was performed at the target heart rate (HR), which was calculated as following formula: (220 – each individual's resting HR) × 0.7 + each individual's resting HR.

During the exercise session, HR was monitored not to exceed the target HR. Both blood and urine examinations related to renal function were determined before and after exercise.

Laboratory examinations

Blood test: blood urea nitrogen (BUN), creatinine (CRE), cystatin C (cysC), plasma osmolality (pOSM), sodium (Na), potassium (K), and chloride (Cl).

Urinary test: urea nitrogen (UN), CRE, Na, K, Cl, urine osmolality (uOSM), and urinary sediment.

RESULTS

Serum biochemical examinations

Parameters	Group	Training		Two-way ANOVA (F-value)		
		Before	After	Group	Training	Interaction
pOSM, mOsm/kg H_2O	Normo	290.2 ± 3.1	293.8 ± 2.9*	2.21	37.7 (P< 0.001)	2.00
	Hypo	292.3 ± 2.2	294.6 ± 1.6*			
BUN, mg/dL	Normo	12.8 ± 1.5	13.4 ± 1.5*	1.10	28.8 (P< 0.001)	0.9
	Hypo	13.8 ± 2.1	14.3 ± 2.1*			
CRE, mg/dL	Normo	0.83 ± 0.09	0.92 ± 0.11*	0.27	25.4 (P< 0.001)	0.03
	Hypo	0.81 ± 0.09	0.89 ± 0.11*			
Na, mEq/L	Normo	140.7 ± 1.2	141.9 ± 1.0*	0.23	42.9 (P< 0.001)	1.82
	Hypo	141.1 ± 1.4	141.9 ± 0.8*			
K , mEq/L	Normo	4.1 ± 0.1	4.4 ± 0.2*	4.45	44.3 (P< 0.001)	0.01
	Hypo	3.9 ± 0.2	4.2 ± 0.2*			
Cl, mEq/L	Normo	104.7 ± 1.2	105.3 ± 1.4*	0.16	5.6 (P= 0.031)	1.5
	Hypo	104.5 ± 2.3	104.7 ± 1.8			
CysC, mg/L	Normo	0.86 ± 0.07	0.92 ± 0.09*	0.41	7.6 (P= 0.014)	0.26
	Hypo	0.85 ± 0.09	0.88 ± 0.09*			

*P < 0.05 vs. before training

Urinary biochemical examinations

Figure 1. Changes in the urinary biochemical tests in the normoxic and hypoxic group.
A two-way ANOVA test was used to determine differences between several parameters. Tukey's HSD test was applied to assess differences among multiple comparisons when ANOVA indicated a significant difference for a particular factor. *P < 0.05 vs. before training

Urinary sediment examinations

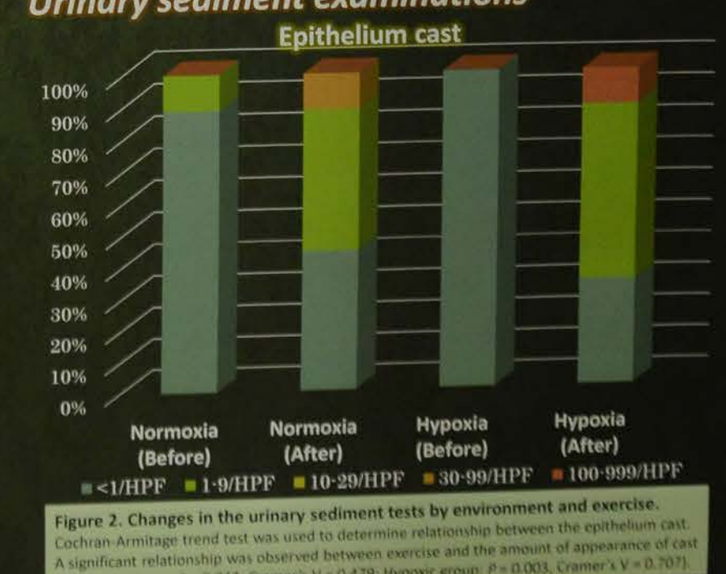

Figure 2. Changes in the urinary sediment tests by environment and exercise.
Cochran-Armitage trend test was used to determine relationship between the epithelium cast. A significant relationship was observed between exercise and the amount of appearance of cast (Normoxic group: P = 0.042, Cramer's V = 0.479; Hypoxic group: P = 0.003, Cramer's V = 0.707).

CONCLUSION

Our results suggest that hypoxic training may generate more load on the renal function than a similar exercise intensity under normoxic conditions.

GIFU UNIVERSITY

Clinical Physiology

PG-04

Vascular damage associated with CKD and laboratory medicine

Yusuke Nakade[1),3)], Tadashi Toyama[2)], Kengo Furuichi[2)], Yoshiyasu Miyajima[1),3)], Mihiro Fukamachi[1)], Hiroyasu Oe[1)], Mikio Nagahara[1)], Yoshio Sakai[1),3)], Takashi Wada[1),2),3)]

1) Clinical Laboratory, Kanazawa University Hospital, Kanazawa, Japan
2) Division of Nephrology, Kanazawa University Hospital, Kanazawa, Japan
3) Department of Laboratory Medicine, Faculty of Medicine, Institute of Medical, Pharmaceutical and Health Sciences, Kanazawa University, Kanazawa, Japan

【Background and Aim】

Carotid echo indexes [intima–media thick-ness (IMT)] are commonly used surrogate markers for cardiovascular disease.

Some studies reported the associations between decreased eGFR and increased IMT. Diabetes is also a well-known risk factor for increased IMT.

However, no previous longitudinal studies have assessed the associations between CKD and the severity of carotid atherosclerosis in patients with diabetes. Therefore, we conducted a prospective study to investigate the relationships between CKD and IMT in participants with and without type 2 diabetes.

Previous study

CKD → longitudinal studies → IMT
The Hisayama Study *Am J Kidney Dis* 2010

DM → longitudinal studies → IMT
Mitsuhashi N, *et al.* *Diabetes Care* 2002

This study

CKD + DM → longitudinal study → IMT

【Conclusion】

Low eGFR was associated with progression of carotid thickness independent of common cardiovascular risk factors in non-diabetic participants.

【 Inclusion and exclusion criteria 】

Carotid ultrasonography measured participants from 1 April 2005 to 30 June 2010 (n = 6,711)

→ Participants who had one time measurement excluded (n = 5,631)

Participants who had several times measurement included (n = 1,080)

→ Participants who did not have all baseline data excluded (n = 177)

424 participants included

【 Method】

Evaluated kidney and cardiovascular disease

・Kidney

$eGFR (ml/min/1.73 m^2) = 194 \times creatinine^{-1.094} \times age (year)^{-0.287}$ (multiplied by 0.739 for females)

Urinary protein (g/gCr) = spot urine protein–creatinine ratio

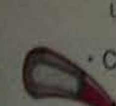

・Carotid

Mean carotid intima-media thickness (Mean IMT) (mm)

longitudinal study: Chang of Mean IMT (Mean IMT/year)

・Diabetes

Diabetes was defined as a clinical history of diabetes treatment or a glycated hemoglobin (HbA1c) ≧ 6.1 %
[National Glycohemoglobin Standardization Program (NGSP)]

Definition and Measurement of IMT

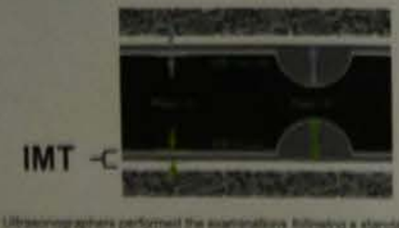

Ultrasonographers performed the examinations following a standard protocol. The common carotid arteries, bifurcation, and internal carotid arteries were measured in all participants. IMT from the right and left sides was measured from the far wall, the location of which was identified as the vertical distance from the leading edge of the first to the second echogenic line. Three IMT determinations were measured in the walls at the site of the greatest thickness of each common carotid artery, and these measurements of both arteries were averaged and expressed as the mean IMT.

Jpn J Med Ultrason. 2009 36 501–15

【Result】

Baseline data by yearly changes of IMT.

The study population was composed of 70.3 % male subjects. Participants with diabetes accounted for 64.4 % of the total population. The mean follow-up duration was 2.2 ± 1.5 years. Mean frequency of examination during the study period was 2.6 times. The majority (63.9 %) of participants were undergoing treatment with one or more antihypertensive drugs.

	All	Changes of IMT (mm/year)			p value
		≤−0.031	−0.030 to 0.017	≤0.018	
n	424	142	141	141	
Carotid factors					
IMT [mm/year (SD)]	0.00 (0.21)	−0.15 (0.21)	0.00 (0.01)	0.14 (0.21)	<0.01
IMT [mm, mean (SD)]	0.8 (0.2)	0.9 (0.2)	0.7 (0.2)	0.8 (0.2)	<0.01
Follow-up period [years, mean (SD)]	2.2 (1.5)	1.6 (1.2)	3.0 (1.5)	2.0 (1.4)	
Age [years, mean (SD)]	64.2 (12.6)	64.4 (11.7)	62.5 (12.6)	65.6 (13.4)	0.12
Sex [n (%) of males]	298 (70.3)	101 (71.1)	99 (70.2)	98 (69.5)	0.96
Kidney factors					
eGFR [mL/min/1.73 m2, mean (SD)]	69.1 (25.9)	66.5 (26.3)	72.3 (25.9)	68.5 (25.3)	0.16
Urinary protein					0.46
−/Trace [n (%)]	333 (78.5)	105 (73.9)	117 (83.0)	111 (78.7)	
1+ [n (%)]	38 (9.0)	16 (11.3)	9 (6.4)	13 (9.2)	
≥2+ [n (%)]	53 (12.5)	21 (14.8)	15 (10.6)	17 (12.1)	
Diabetes factors					
Diabetes [n (%)]	273 (64.4)	95 (66.9)	94 (66.7)	84 (59.6)	0.34
HbA1c [%, mean (SD)]	6.9 (1.9)	6.9 (1.9)	7.0 (1.8)	6.7 (2.0)	0.38
Duration of diabetes [years, mean (SD)]	13.6 (10.9)	9.2 (10.3)	8.0 (10.2)	8.3 (11.9)	0.63
Blood pressure (mmHg)					
Systolic blood pressure [mean (SD)]	129.3 (21.8)	131.2 (24.5)	129.1 (21.1)	127.5 (19.4)	0.36
Diastolic blood pressure [mean (SD)]	75 (14.0)	76.3 (15.5)	75.4 (12.4)	73.3 (13.7)	0.19
Pulse pressure [mean (SD)]	54.2 (18.1)	54.9 (21.1)	53.7 (16.9)	54.1 (16.1)	0.86
Smoking habit					0.45
Never smoker [n (%)]	187 (44.1)	61 (43.0)	67 (47.5)	59 (41.8)	
Ex-smoker [n (%)]	161 (38.0)	59 (41.6)	45 (32.0)	57 (40.4)	
Current smoker [n (%)]	76 (17.9)	22 (15.5)	29 (20.6)	25 (17.7)	
Smoking index [median (IQR)]	300 (0–900)	310 (0–1050)	100 (0–800)	300 (0–900)	0.25
Previous cardiovascular event [n (%)]	142 (33.5)	53 (37.3)	40 (28.4)	49 (34.8)	0.26
Other major risk factors					
Body mass index (kg/m^2) [mean (SD)]	31.2 (14.3)	24.2 (3.9)	24.3 (4.7)	24.2 (3.8)	0.98
Total cholesterol [mg/dL, mean (SD)]	185.6 (44.3)	190.3 (47.0)	181.8 (38.9)	184.6 (46.4)	0.26
Uric acid [mg/dL, mean (SD)]	6.9 (3.2)	7.1 (3.1)	6.8 (3.4)	6.6 (3.2)	0.46
Number of antihypertensive drugs					0.88
0 [n (%)]	153 (36.1)	48 (33.8)	53 (37.6)	52 (36.9)	
1 [n (%)]	83 (19.6)	27 (19.0)	30 (21.3)	26 (18.4)	
2 [n (%)]	65 (15.3)	22 (15.5)	21 (14.9)	22 (15.6)	
3 [n (%)]	77 (18.2)	25 (17.6)	22 (15.6)	30 (21.3)	
4 [n (%)]	32 (7.6)	13 (9.2)	10 (7.1)	9 (6.4)	
5 [n (%)]	13 (3.1)	6 (4.2)	5 (3.6)	2 (1.4)	
6 [n (%)]	1 (0.2)	1 (0.7)	0 (0.0)	0 (0.0)	
Use of statins [n (%)]	119 (28.1)	41 (28.9)	34 (24.1)	44 (31.2)	0.40

Percentages may not add to 100 % because of rounding.
SD standard deviation,
eGFR estimated glomerular filtration rate,
HbA1c glycated hemoglobin,
IQR interquartile range,
IMT intima–media thickness.

Cross-sectional study

The relationships between baseline IMT and potential risk factors.

Baseline systolic blood pressure was positively correlated between baseline IMT (a), and baseline eGFR was negatively correlated with baseline IMT (b). Both risk factors had relatively steeper correlations among participants without diabetes.

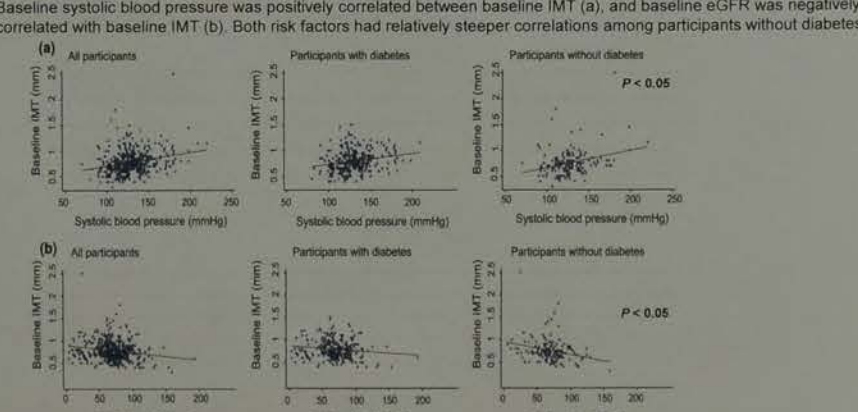

Systolic blood pressure was significantly associated with baseline IMT even after adjusting for confounding factors.

The magnitude of standard regression coefficient was higher in participants without diabetes than in those with diabetes. Baseline IMT was not significantly associated with eGFR.

	Unadjusted			Model 1			Model 2					
	All participants n = 424			All participants n = 418			Participants with diabetes n = 245			Participants without diabetes n = 150		
	β	SE	p	β	SE	p	β	SE	p	β	SE	p
Systolic blood pressure (+10 mmHg)	0.0265	0.0050	<0.01	0.0226	0.0049	<0.01	0.0159	0.0057	0.01	0.0312	0.0093	<0.01
eGFR (−10 mL/min/1.73 m^2)	0.0165	0.0042	<0.01	0.0040	0.0048	0.41	−0.0023	0.0056	0.69	0.0182	0.0103	0.08

Model 1: Regression analysis adjusted for age, sex, systolic pressure, total cholesterol, body mass index, eGFR, uric acid, smoking index, number of antihypertensive drugs, statin use, urinary protein levels, and past cardiovascular event
Model 2: Regression analysis adjusted for glycated hemoglobin and duration of diabetes added to Model 2 in participants with diabetes. The parameters were adjusted in the same manner as that as in Model 1 for participants without diabetes.

Longitudinal study

The relationships between annual changes in IMT and potential risk factors.

There was a negative correlation between eGFR and changes in IMT for participants without diabetes.

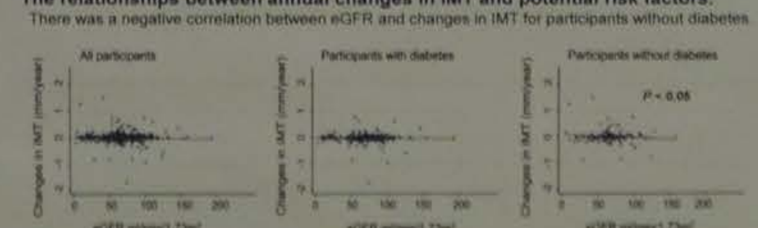

eGFR was significantly associated with increased IMT in participants without diabetes.

After adjusting for multiple risk factors, there was a tendency for increased IMT with lower eGFR in all participants. In participants without diabetes, eGFR was significantly associated with increased IMT even after adjusting for confounding factors. In contrast, no trend was observed in participants with diabetes.

	Unadjusted			Model 1			Model 2					
	All participants n = [illegible]			All participants n = 418			Participants with diabetes n = 245			Participants without diabetes n = 150		
	β	SE	p	β	SE	p	β	SE	p	β	SE	p
Systolic blood pressure (+10 mmHg)	[illegible]	[illegible]	[illegible]	[illegible]	[illegible]	[illegible]	[illegible]	[illegible]	[illegible]	[illegible]	[illegible]	[illegible]
eGFR (−10 mL/min/1.73 m^2)	[illegible]	[illegible]	[illegible]	[illegible]	[illegible]	[illegible]	[illegible]	[illegible]	[illegible]	[illegible]	[illegible]	[illegible]

An interaction term between eGFR and urinary protein in participants without diabetes was not significant (p = 0.792).

Clinical Physiology

PG-05

Usefulness of Virtual Touch Quantification for the Diagnosis of Pancreatic Solid Lesions

Yusuke Kudo[1,2], Mutsumi Nishida[1,2], Mamiko Inoue[1,2], Satomi Omotehara[1,2], Takahito Iwai[1,2], Rika Takasugi[1,2], Taisei Mikami[3] , Hitoshi Shibuya[1], Kaoru Kahata[1], Chikara Shimizu[1]

[1] Division of Laboratory and Transfusion Medicine, Hokkaido University Hospital
[2] Diagnostic Center for Sonography, Hokkaido University Hospital
[3] Faculty of Health Sciences, Hokkaido University

BACK GROUND

- Virtual Touch Quantification(VTQ) is a innovative ultrasound technique that evaluates tissue stiffness by Shear Wave Velocity(SWV) quantification.
- Clinical use of VTQ for the liver fibrosis has been established, however, few studies demonstrated its usefulness for the pancreatic solid lesions.

PURPOSE

To assesse the diagnostic usefulness of VTQ method in pancreatic solid lesions.

SUBJECTS and METHODS

- **Study design**
  Prospective study*
- **Research period**
  Between April 2014 and June 2016
- **Subjects**
  39 patients who had pancreatic solid lesion
- **Control group**
  30 healthy volunteers
- **Diagnostic equipment**
  SIEMENS ACUSON S2000, with the 4C1 convex probe
- **Sonographer**
  Y. K. and M. N. with 5 years experience of VTQ
- **SWV mesurement**
  SWV were measured 10 times in each of lesions
  The Median values were used for analysis
- **Statistical analysis**
  One-way ANOVA, Pearson's correlation coefficient
  P-value <0.05 was used to indicate significance

* Certification number of IRB at Hokkaido University Hospital 013-0090

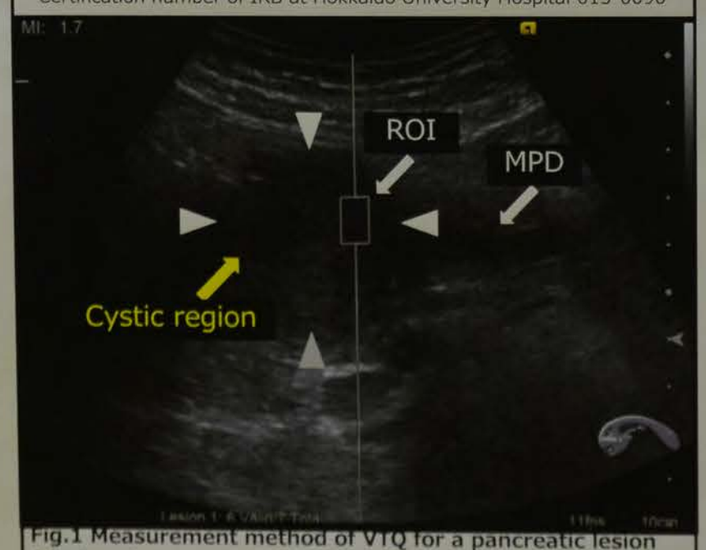

Fig.1 Measurement method of VTQ for a pancreatic lesion
A lesion of pancreatic adenocarcinoma in the pancreatic head is shown (arrow head). The ROI was located within the lesion, without including any cystic regions. ROI=region of interest, MPD=main pancreatic duct.

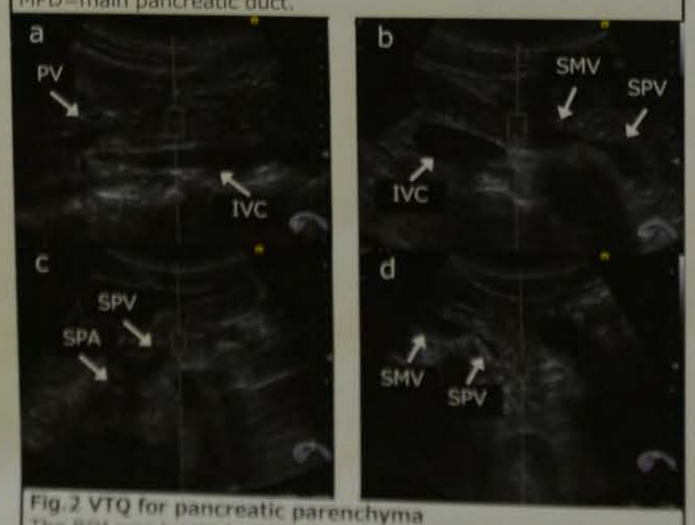

Fig.2 VTQ for pancreatic parenchyma
The ROI was located within the parenchyma, without including any vessels. **a.** Sagittal plane of the pancreatic head is shown. **b.** Axial plane of the pancreatic head. **c.** Sagittal plane of the pancreatic body. **d.** Axial plane of the pancreatic body. PV=portal vein, IVC=inferior vena cava, SMV=superior mesenteric vein, SPV=splenic vein, SPA=splenic artery.

RESULTS

Table.1 Baseline characteristics

Variable	Control n = 30	PC n = 21	NEN n = 14	META n = 4	P-value (ANOVA)
Age(years)	35.8±13.8	66.2±10.0**	56.9±17.0**	64.8±3.6**	<0.001
Male/Female	24/6	13/8	4/10*	3/1	0.009
BMI(kg/m^2)	21.6±2.4	21.0±3.0	21.8±3.4	24.5±4.1	0.194
Amylase(U/L)	71.9±19.4	126±124	91.7±66.7	129±84.3	0.173
HbA1c(%)	5.4±0.3	7.4±1.5*	5.9±1.0†	6.8±0.7	0.001
Depth of ROI(cm)	5.1±0.7	4.4±1.4	4.5±1.5	6.5±0.9†	0.021
Tumor size(cm)	-	3.4±1.3	2.3±2.0	3.3±0.6	0.156

Data are shown by mean±SD.
*P<0.01, **P<0.001 vs. control group; †P<0.05 vs. PC group
PC=pancreatic adenocarcinoma, NEN=neuroendocrine neoplasm, META=metastasis from renal cell carcinoma.

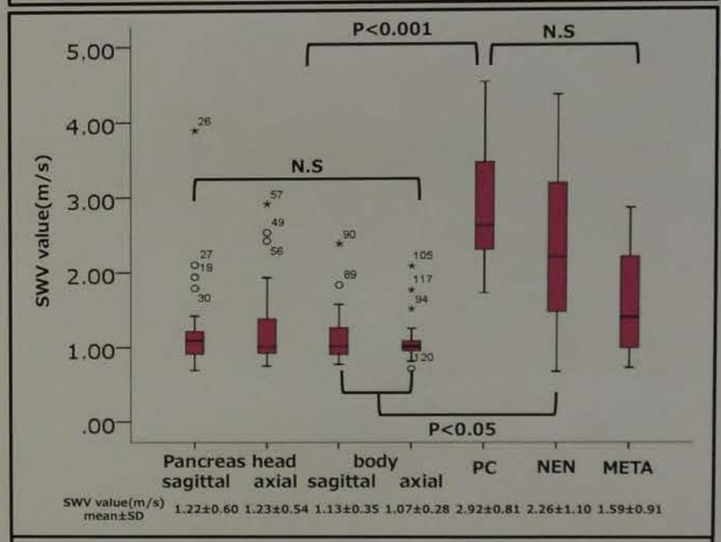

Fig.3 Comparison of SWV values

Table.2 Influence factors of SWV value

Variable	Control		PC		NEN	
	r	P-Value	r	P-Value	r	P-Value
Age(years)	-0.004	0.491	-0.179	0.247	0.414	0.117
Gender	0.476	0.004	0.224	0.194	-0.126	0.365
BMI(kg/m^2)	-0.109	0.284	-0.110	0.337	-0.294	0.205
Amylase(U/L)	0.041	0.414	-0.133	0.305	0.468	0.086
HbA1c(%)	0.170	0.185	-0.140	0.296	-0.088	0.404
Depth of ROI(cm)	0.018	0.462	-0.204	0.217	-0.578	0.040
Tumor size(cm)	-	-	0.216	0.203	0.110	0.381
Presence of cystic region	-	-	0.374	0.14	-0.533	0.056
cStage	-	-	-0.090	0.366	-	-
Grade	-	-	-	-	0.313	0.189

DISCUSSION

1. SWV values of PC were significantly higher than those of normal pancreatic parenchyma. This result was equivalent to D'Onofrio's report*. →SWV values are considered to reflect of fibrosis in tumor. VTQ method would be useful in the presence diagnosis of PC.

	Present study	D'Onofrio's
PC	2.62m/s	2.74m/s
Normal pancreatic parenchyma	1.01m/s	1.17m/s

1. In control, SWV values depended on gender. →In female pancreas is located shallower than male. Because of multiple reflection of abdominal wall would cause misdetection of SW, SWV might show higher value than as it really is.
2. In NEN, deeper ROI was associated with low SWV values. →The push pulse is attenuated before reaching ROI. The amplitude of SW might decrease, then SWV would show lower value than as it really is.

*D'Onofrio M, et al. Acoustic radiation force impulse with shear wave speed quantification of pancreatic masses: A prospective study. Pancreatology 2016.

CONCLUSION

VTQ method would be useful in the presence diagnosis of pancreatic adenocarcinoma provided that it takes gender and depth of ROI into consideration.

Clinical Physiology

PG-06

Controlled attenuation parameter for non-invasive assessment of hepatic steatosis in chronic hepatitis C

Naohiro Ichino[1], Keisuke Osakabe[1], Toru Nishikawa[2], Hiroko Sugiyama[2], Tadayoshi Hata[1], Naoto Kawabe[3], Senju Hashimoto[3], Kentaro Yoshioka[3]

[1]Faculty of Medical Technology, School of Health Sciences, Fujita Health University, Toyoake, Japan
[2]Center of Ultrasound Diagnosis, Fujita Health University Hospital, Toyoake, Japan
[3]Department of Liver, Biliary Tract and Pancreas Diseases, Fujita Health University, Toyoake, Japan

AIM

Hepatic steatosis can be a co-factor in many chronic liver diseases that can lead to liver fibrosis and cirrhosis. A novel non-invasive tool based on ultrasound attenuation, called controlled attenuation parameter (CAP), was attached with FibroScan502 for assessment of liver steatosis quantitatively. The aim of this study was to evaluate the performance of CAP for assessment of hepatic steatosis in chronic hepatitis C.

FibroScan502

SUBJECTS & METHODS

- In a total of 113 patients, 69 men and 44 women with chronic hepatitis C, CAP values were measured, and liver biopsies were performed.
- The measurement of CAP was done ten times on right lobe of the liver from the right intercostal space, and the median values were adopted for CAP values.
- The CAP values were compared with steatosis grade and also with the ratio of hepatic steatosis area that was calculated by digital image analysis liver specimen.

hepatic tissue area	hepatic steatosis area	ratio of hepatic steatosis area
2475795	488438	16.5 %

Fig.1 Digital image analysis liver specimen using Image-Pro Plus6.1J

RESULTS

Table.1 Hepatic steatosis grade of the subjects

Grade	Steatosis	n
Grade0	< 5%	53 (46.9%)
Grade1	5 - 33%	32 (28.3%)
Grade2	34 - 66%	18 (15.9%)
Grade3	> 67%	10 (8.8%)

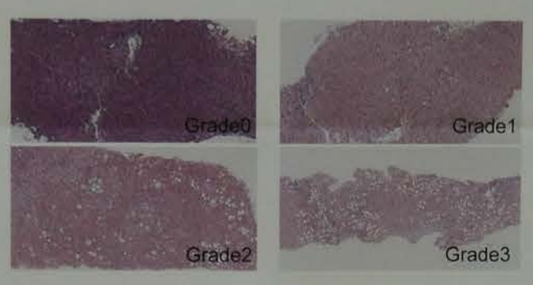

Fig.2 Hepatic steatosis grade

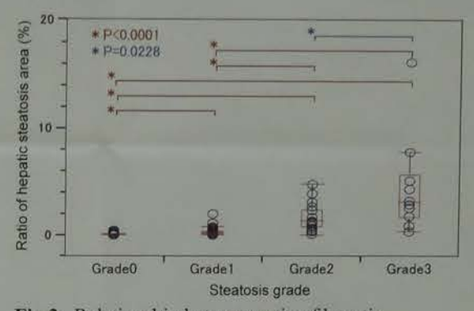

Fig.3 Relationship between ratio of hepatic steatosis area and steatosis grade

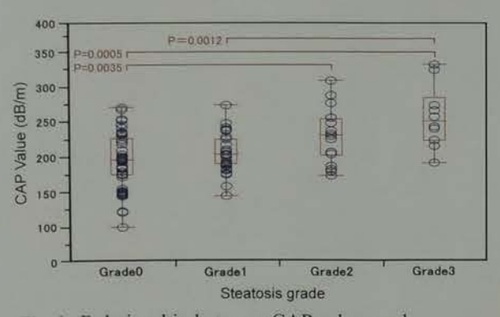

Fig.4 Relationship between CAP values and steatosis grade

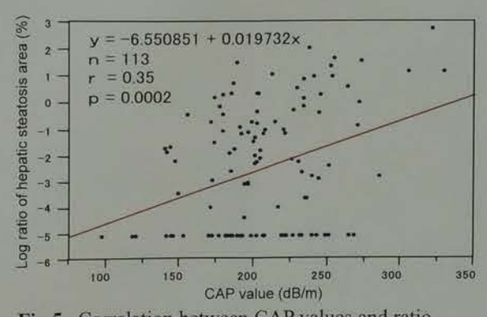

Fig.5 Correlation between CAP values and ratio of hepatic steatosis area

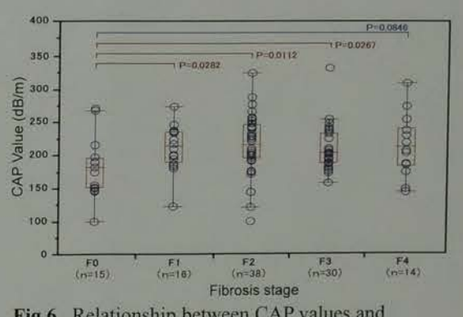

Fig.6 Relationship between CAP values and fibrosis stage

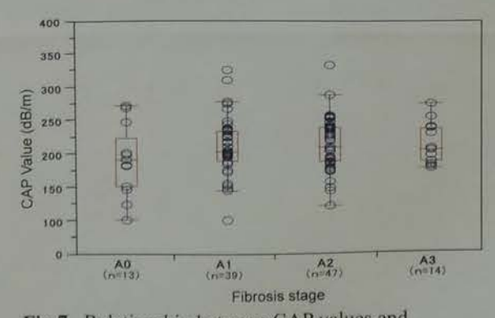

Fig.7 Relationship between CAP values and inflammatory grade

Table.2 Multiple regression predicting CAP value

	Estimated value	Standard error	P-value
Age	21.375904	83.12259	0.7977
Sex	-0.248454	0.34178	0.4694
BMI	4.751686	1.30597	0.0005
Ratio of hepatic steatosis area	6.568109	2.84319	0.0235
Fibrosis stage	30.312851	2.14000	0.0356
Inflammatory grade	3.494394	15.01754	0.8166
T-cho	0.196360	0.12864	0.1308
Hyaluronic acid	-0.005816	0.02435	0.8119
PT	0.150450	0.30669	0.6251
TP	-2.153036	7.52517	0.7755
AST	0.129683	0.08002	0.1090

BMI; Body mass index, T-cho; Total cholesterol, PT; Prothrombin time, TP; Total protein, AST; Aspartate aminotransferase

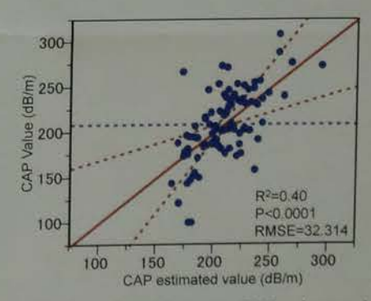

Fig.8 Correlation between CAP values and CAP estimated values

CONCLUSION

This study suggested that CAP is a promising tool for the non-invasive assessment and quantification of hepatic steatosis in chronic hepatitis C.

The authors have no conflict of interest related to the content of this poster.

FUJITA HEALTH UNIVERSITY

Clinical Physiology

PG-08

Evaluation of the Cross-Sectional Area by Ultrasound in Peripheral Neuropathy

Ako ITO*, Tsuneo WATANABE*, Megumi YAMADA**
Koichi SHINODA*, Yuzuru NOHISA*, Nobuyuki FURUTA*,
Hiroyasu ITO* and Mitsuru SEISHIMA*

Division of Clinical Laboratory, Gifu University Hospital*
Department of Neurology and Geriatrics, Gifu University Graduate School Medicine**

INTRODUCTION

- The diagnosis of peripheral neuropathy is based primarily on characteristic symptoms and is confirmed with a nerve conduction study (NCS).
- High-resolution sonography is a novel method that provides morphological information for peripheral nerves.
- **The purpose of this study was to evaluate the cross-sectional area (CSA) of the median nerve using ultrasonography (US).**

MATERIALS & METHODS

Subjects

We studied a total of 50 median nerves of 26 participants who underwent both NCS and US.

- **◆Carpal tunnel syndrome (CTS) group** (n = 12, mean age, 53.8±11.6 years)
- **◆Type 2 diabetes mellitus (DM) group** (n = 16, mean age, 61.1±6.1 years)
- **◆Other peripheral neuropathy(OPN) group** (n = 10, mean age, 59.3±20.0 years)
- **◆Healthy volunteers (controls) group** (n = 12, mean age, 53.3±5.3 years)

※OPN group is composed of following patients: 1 patient with CIDP, 1 patient with multifocal motor neuropathy, 2 patients with amyotrophic lateral sclerosis: 1 patient with hereditary motor sensory neuropathy and 1 patient with Guillain-Barre syndrome.

Methods

The CSA was measured by US at defined sites (CT, carpal tunnel inlet; FA, midpoint of the forearm; AM, midpoint of the arm), and one way analysis of variance (ANOVA) was carried out among the groups.

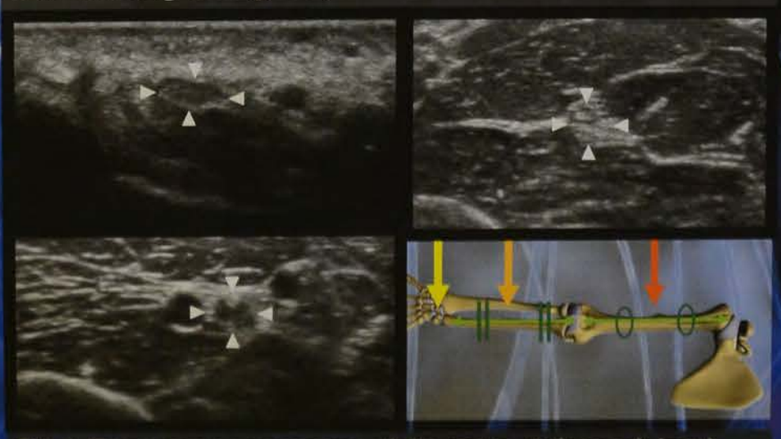

Fig 1. Transverse sonograms of the nerve at the each level. Arrow heads show the median nerve.

RESULTS

Significant differences were observed in CT [$F(3, 45) = 6.1$, $p = 0.002$] and AM [$F(3, 45) = 4.9$, $p = 0.005$] among four groups.

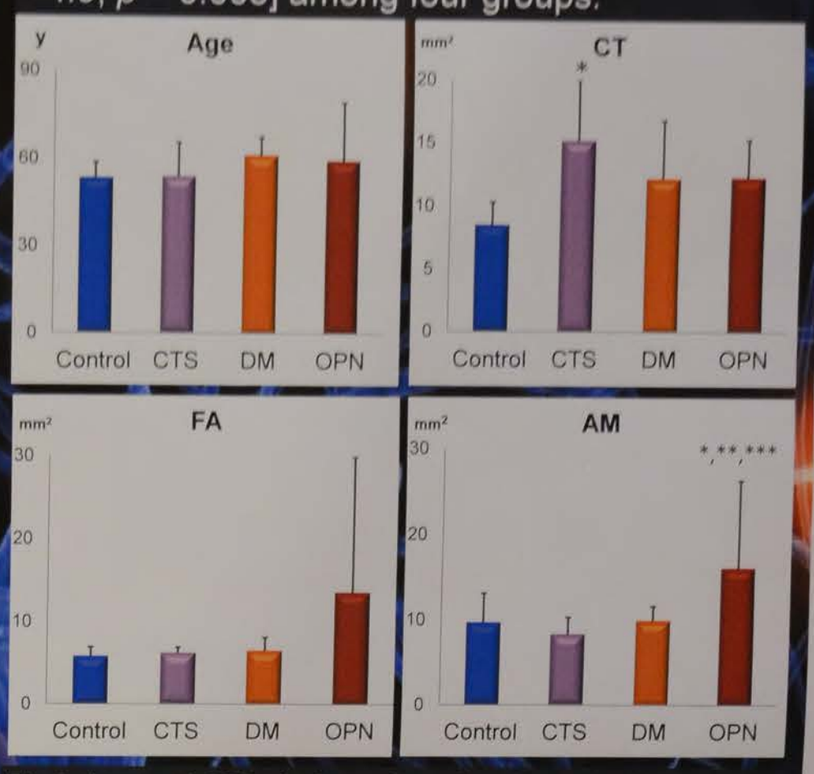

Fig 2. Ages and CSAs in three sites of median nerve in four groups.
The CSA in the CT was significantly higher in CTS group (15.2±4.8 mm²) than in controls 8.5±1.8 mm². The CSA in the AM was significantly higher in OPN group (16.1±10.2 mm²) than in other three groups. *$p < 0.05$ vs. Control, **$p < 0.05$ vs. CTS group, ***$p < 0.05$ vs. DM group.

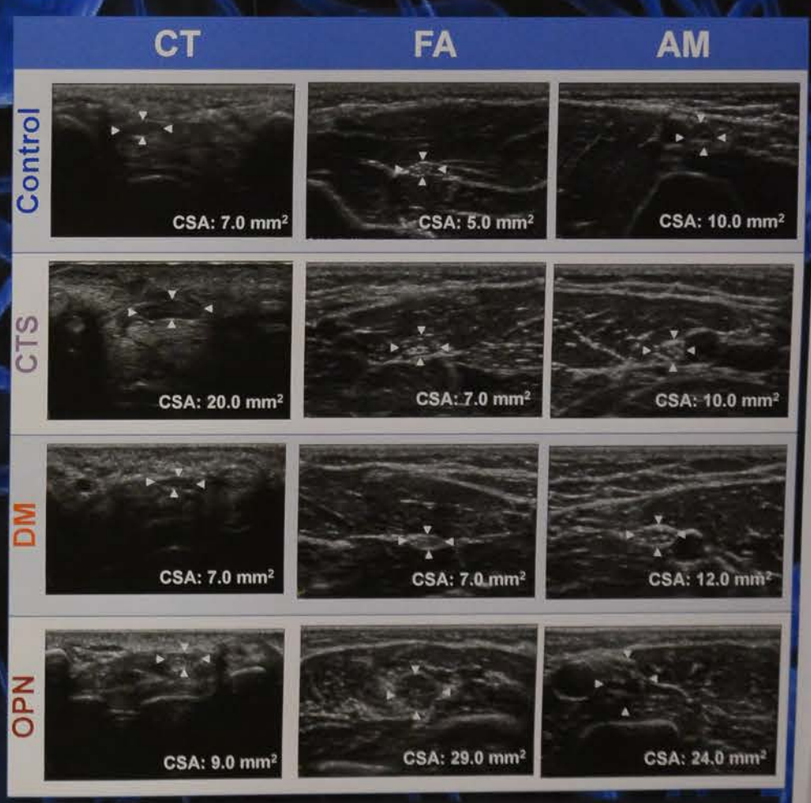

Fig 3. Determination of median nerve CSA in three sites by US.

CONCLUSION

Our study showed that nerve US is useful for diagnosis of peripheral neuropathy.

GIFU UNIVERSITY

C-3

Clinical Physiology

PG-09

Evaluation of peripheral neuropathy by sensory nerve action potentials comparison.

Msafumi Katayama, Yasuyuki Teramoto, Fumitomo Iwanaga, Kohei Nishimura, Takuya Matsunaga, Kaoru Matsunaga, Ryoji Nakanishi

International University of Health and Welfare
Neurophysiological laboratory Kumamoto Kinoh Hospital

Background

Sensory nerve action potential (SNAP) generally presents various changes due to the positional relation of electric stimulation and pickup electrode.

We investigated the SNAP recorded from different two positions and compared the data from normal subjects and patients with peripheral neuropathy.

Subjects and method

Twenty nine healthy volunteers, 18 cases of carpal tunnel syndrome (CTS) and 23 cases of diabetic peripheral neuropathy (DPN) participated in the present study.

SNAP were recorded after median nerve (MN) stimulation from the wrist, at proximal and distal position in the middle finger (fig.1).

We investigated SNAP recorded from proximal position (P-SNAP) and SNAP recorded from distal position (D-SNAP). The latency, amplitude and duration were measured at the two positions. Furthermore, The sensory nerve conduction velocity (SCV) in wrist-finger (W-F SCV) and finger-finger (F-F SCV) were calculated. The distance between the wrist and proximal recording electrode was 140mm. The two electrodes on the middle finger were set 25mm apart.

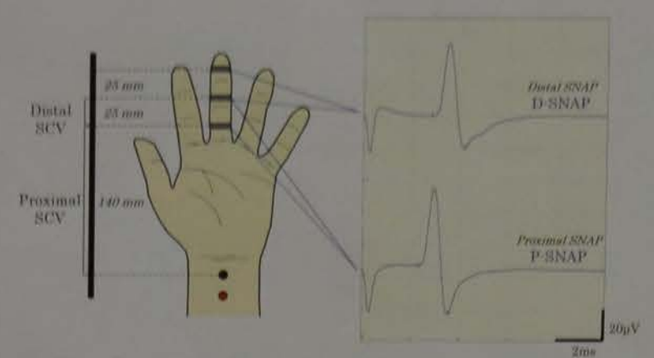

Fig.1 Design of experimental study

Results

In normal subjects and neuropathy cases, the latency delayed, the amplitude decreased, and the duration became wide in D-SNAP in comparison with P-SNAP (fig.2).

We compared the results in D-SNAP and P-SNAP and examined those relationships.

There was constant correlation between distal and proximal in all measurement items (fig.3-a,b,c). However different distribution of SCV was found in normal subjects , CTS and DPN cases (fig.3-a).

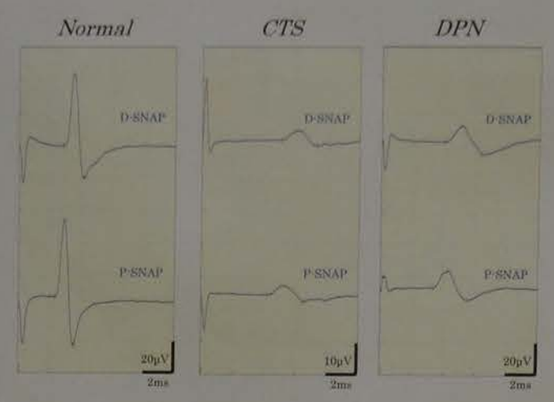

Fig.2 SNAP recorded from distal and proximal position.

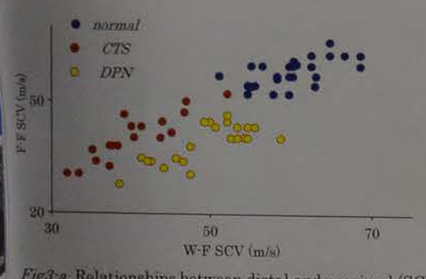

Fig3-a Relationships between distal and proximal (SCV)

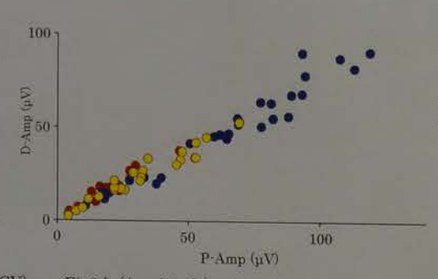

Fig3-b (Amplitude)

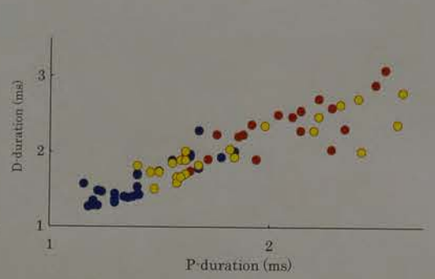

Fig3-c (Duration)

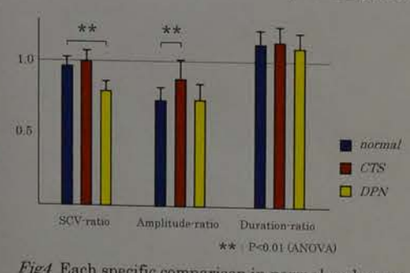

Fig4 Each specific comparison in normal and cases

We set rate of each measurement item of "SCV-ratio", "Amplitude-ratio" and "Duration-ratio" to clarify relation of distal and proximal and reviewed.
The Amplitude-ratio increase in CTS, and the SCV-ratio decrease in DPN cases in comparison with control.
(P<0.01) (fig. 4)

SCV-ratio: D-SCV / P-SCV
Amplitude-ratio: D-Amplitude / P-Amplitude
Duration-ratio: D-Duration / P-Duration

Case study

SNAP in cases of demyelinative and axonopathy type GBS and CIDP (fig. 5,6,7). SNAP in case of AIDP disappeared after IVIG (Intravenous immunoglobulin). However AMAN case showed normal with no changes by IVIG.

In CIDP case, slower SCV were shown both in distal and proximal segments. But SCV-ratio was within normal limits. On a distribution map of W-F and F-F SCV, CIDP positioned the same as severe CTS. AIDP case showed different results from other neuropathy, and presented severe neuropathy pattern (fig. 8).

Fig.5 25yo Male Rt

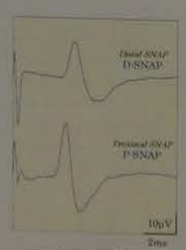

Fig.6 60yo Male Rt

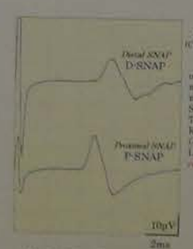

Fig.7 54yo Female Rt

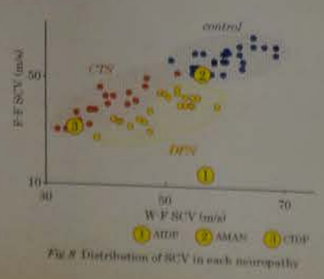

Fig.8 Distribution of SCV in each neuropathy

Conclusions

In case of CTS, conduction block may be occurred in faster fiber of conduction velocity by compression in carpal tunnel.
Therefore decreased SCV, slightly decreased amplitude in distal segment and normal SCV-ratio were presented.

DPN case showed the result that were typical distal dominant neuropathy. But Amplitude-ratio was within normal limit. It may be due to distribution of SCV and phase cancelation.

Demyelinative and axonopathy type GBS showed clearly difference in acute stage. Chronic course may have an influence on decreased SCV and normal SCV-ratio in CIDP case.

It seems that we were able to reflect peripheral dominance and diffusibility of neuropathy by this study.

Clinical Physiology

PG-10

Evaluation of Peripheral Sensory Perception Pre- and Post-Revascularization

Kaori Sugawara[1)] Mika Miki[1)] Takashi Miki[1)]
Daijiro Akamatsu[2)] Hitoshi Goto[2)]

1) Clinical Physiology Center, Tohoku University Hospital
2) Division of Advanced Surgical Science and Technology, Tohoku University Hospital, Sendai, Miyagi, Japan

Summary

We evaluate peripheral sensory perception at halluxes during pre- and post-revascularization.
We examined factors related to reduced functional sensory perception of the lower limbs after revascularization.
Some of the patients with ischemia might have the abnormal sense.
Some patients who were smokers and also aged might show a slight improvement in respect of a peripheral perception.
The PainVision™ system would be useful for the quantitative assessment of peripheral sensory perception in patients with ischemia who undergo revascularization.
Regarding total foot care, the assessment of the sensory function to recognize external stimulation leads to wound prevention, and finally amputation.

Evaluation of Peripheral Sensory

Evaluation of Peripheral Sensory is the ability to perceive perceiving external stimulation.
Minimum perceived current was defined as the minimum electrical stimulation sensed by the subject.
It is useful for patients who have a disease, such as peripheral neuropathy.

What is PainVision?

A new method for the quantitative measurement of sensory perception using a electrical stimulation system, PainVision® (NIPRO, Osaka, Japan) has been developed.
Assessment for the sensory perception in a quantitative manner
①put disposable electrode on the position you want
②turn on and strengthen gradually, measuring perception threshold
It takes about 10 min for examination
It costs 380 points (¥3,800) in Japan including diagnosis

Laghi et al reported that the somatic and autonomic nerve alteration may play a relevant role in the progression of the disease toward critical limb ischemia.(Peripheral neuropathy associated with ischemic vascular disease of the lower limbs, *Angiology* 1996 Jun; 47(6):569-77) Data regarding ischemia-related sensory perception of the fingertip is limited. We evaluate peripheral sensory perception at halluxes during pre- and post-revascularization. We examined factors related to reduced functional sensory perception of the lower limbs after revascularization.

Objectives & Subjects

The aim of this study was to determine the utility for evaluating how much patients can sense who need to undergo revascularization and to determine the factor why the progression of blood flow and sensory perception shows different tendencies.
16 patients enrolled(underwent revascularization and quantitative analysis of sensory perception from April 2015 to February 2016)
Retrospective review
19 limbs; mean age, 71.0 years; range, 47–82 years; 13 males [81.3%]

Methods

Before and after revascularization, sensory perception threshold was evaluated in the medial forearm and halluxes .
Indices compaired; sensory perception ratio between forearm and hallux improved or not, smoking, age, underlying disease, laboratory data
Use machinery

- Perception quantitative analysis PainVision®PS-2100 (NIPRO, Japan)
- Skin perfusion pressure analysis SensiLase®PAD4000 (KANEKA MEDICAL PRODUCTS, Japan)

Statistical analysis; Pearson's χ^2, decide $p<0.05$ as significantly

Definition of improvement of sensory perception

Normal range of peripheral sensory perception has not been established.
Based on our findings, a hallux–forearm ratio (HFR) of <1.99 was defined as normal sensory perception.
Cases in which HFR decreased after revascularization were considered to have improved sensory perception.

$$\text{Hallux-forearm ratio (HFR)} = \frac{\text{Sensory perception threshold of thumb}}{\text{Sensory perception threshold of forearm}}$$

Hallux-forearm ratio: abnormal sensory perception as high score

Results

All patients were not examined by electroneurographic evaluation of motor and sensory nerve conduction.
Our results showed that sensory perception threshold ration were raised in halluxes-forearm 47.4% of the patients at preoperative exam.

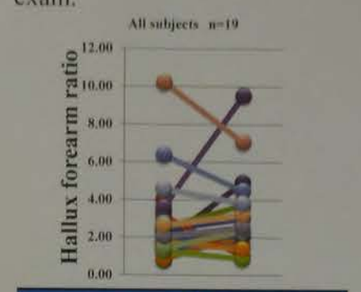

	Pre	Post
HFR mean±standard deviation	3.07±2.76	2.97±2.17

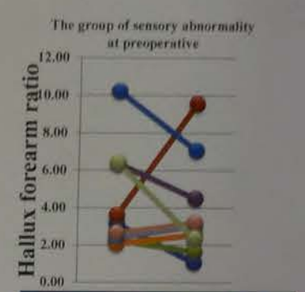

	Pre	Post
HFR	5.66±3.15	3.31±2.46

The value of HFR of all of the patients underwent revascularization was 3.07±2.76. Our study focuses on the abnormal sensory perception before operation. From here on we will discuss the results of patients who had sensory perception abnormality.

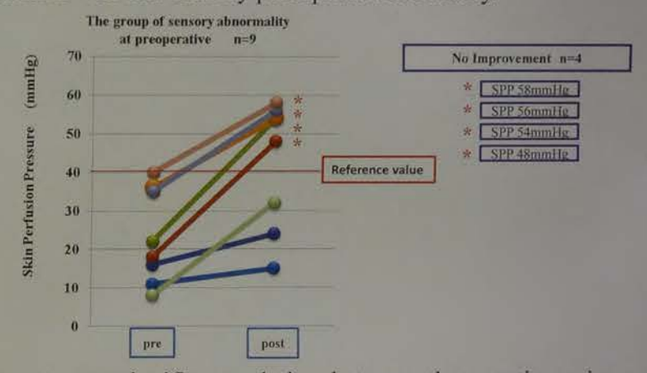

There was no significant relation between therapeutic region and improvement of sensory perception.

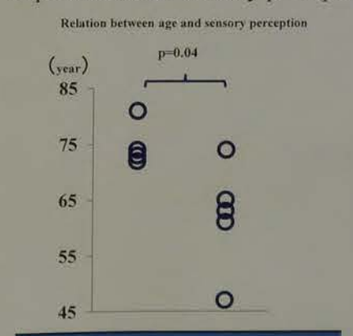

Sensory abnormality n=9	No improvement	Improvement
age±SD (y)	75.0±4.1	62±9.7

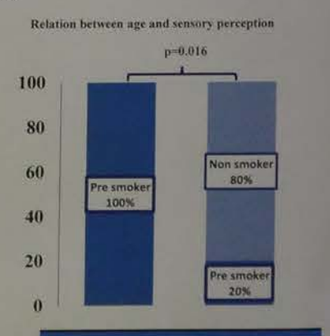

No improvement	Improvement
N=4	N=5

Those who were pre-smokers and aged tended to show a slight improvement in respect of a peripheral sensory perception.

Assessment

In micro circulation, endothelial cells transport oxygen. Because the function of endothelial cells doesn't work well in advanced atherosclerosis, the factor of atherosclerosis, including smoking and age might prevent the improvement of peripheral perception after revascularization.
Some of the patients with ischemia might have an abnormal sense perception. In that case, treatment might be delayed, patients would be had their legs amputated. Regarding total foot care, the assessment of the sensory function to recognize external stimulation leads to wounds.

Conclusion

We believe the PainVision™ system to be useful for the quantitative assessment of peripheral sensory perception in patients who undergo revascularization.

The author has no financial conflicts of interest to disclose concerning the presentation.

Clinical Physiology

PG-11

Novel Echocardiographic Method to Assess Left Ventricular Chamber Stiffness and End-Diastolic Pressure

Kazunori Okada[1], Rika Abiko[2], Sanae Kaga[1], Masahiro Nakabachi[3], Hisao Nishino[3], Shinobu Yokoyama[3], Mutsumi Nishida[3], Taisei Mikami[1]

[1]Faculty of Health Sciences, Hokkaido University, [2]Department of Health Sciences, School of Medicine, Hokkaido University, [3]Division of Laboratory and Transfusion Medicine, Hokkaido University Hospital

BACKGROUND

Difference between the atrial systolic pulmonary venous (PV) and transmitral flow durations have been reported to be useful to estimate the left ventricular (LV) end-diastolic pressure (LVEDP). We aimed to examine the usefulness of our novel parameters based on the time-velocity integral (TVI) measurements of the PV and transmitral flows during atrial contraction for assessing the LV chamber stiffness and LVEDP.

METHODS

Study Subjects

We retrospectively examined 50 consecutive patients who were admitted to Hokkaido University Hospital from January 2013 to December 2014 and underwent echocardiographic examination and left heart catheterization within 4 weeks under stable clinical condition.

Patients with atrial fibrillation, no spontaneous atrial contraction, frequent premature beats, complete atrio-ventricular block, congenital heart disease, mitral stenosis or severe mitral regurgitation were excluded.

Echocardiography

- Conventional parameters
- LV end-diastolic volume and pre-atrial systolic volume were measured by biplane disk-summation method, and LV volume change during atrial contraction was calculated and corrected for each patient's body surface area (ΔVa).

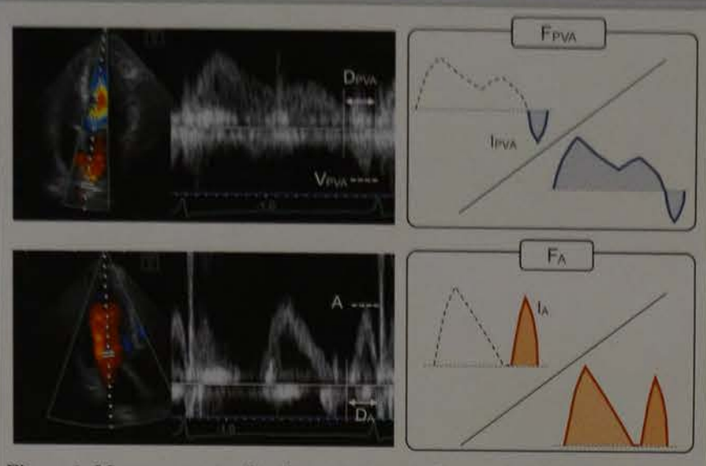

Figure 1 Measurements of pulmonary venous flow and transmitral flow parameters

From the pulmonary venous (PV) flow velocity record (upper panel), the peak velocity, duration and time-velocity integral of the backward flow during atrial contraction (V_{PVA}, D_{PVA} and I_{PVA}, respectively) were measured, and the ratio of I_{PVA} to the time-velocity integral of PV flow through a cardiac cycle (F_{PVA}) was calculated. From the transmitral flow velocity record (lower panel), the duration and time-velocity integral of the forward flow during atrial contraction (D_A and I_A, respectively), and the ratio of the I_A to the entire transmitral time-velocity integral during a cardiac cycle (F_A) were calculated. And then, $D_{PVA}-D_A$, I_{PVA}/I_A and F_{PVA}/F_A were calculated.

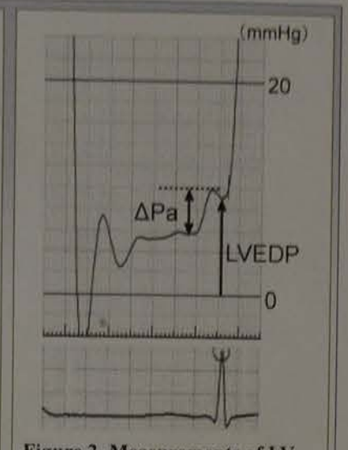

Figure 2 Measurements of LV pressure

The LV pressure increase during atrial contraction (ΔPa) and LVEDP were measured using a standard fluid-filled catheter, and their averaged values of 5 consecutive beats were calculated. The ratio of ΔPa to the echocardiographic ΔVa (ΔPa/ΔVa) was used as an index of LV chamber stiffness.

RESULTS

Table 1 Patient characteristics of the study population

Parameters	Mean ± SD	Range
Clinical characteristics		
Age (years)	65.5 ± 13.3	22–87
Male/female	28/22	
Body surface area (m^2)	1.64 ± 0.26	1.18–2.19
Systolic blood pressure (mmHg)	125 ± 22	72–190
Diastolic blood pressure (mmHg)	69 ± 16	33–106
Heart rate (bpm)	65.8 ± 11.6	42–100
Two-dimensional echocardiographic parameters		
LV end-diastolic dimension (mm)	51.3 ± 9.1	37–79
LV ejection fraction (%)	53.8 ± 14.3	22–82
LV mass index (g/m^2)	116 ± 34	45–216
Left atrial volume index (mL/m^2)	42.6 ± 15.3	19–76
Transmitral and pulmonary venous flow parameters		
E (cm/s)	66.6 ± 17.8	30.7–103.2
A (cm/s)	79.1 ± 20.0	18.5–116.0
E/A	0.92 ± 0.48	0.45–3.17
DT (ms)	249 ± 66	134–442
PVS (cm/s)	61.4 ± 16.8	24.7–98.3
PVD (cm/s)	47.7 ± 14.3	26.1–91.2
PVS/PVD	1.39 ± 0.52	0.27–2.78
V_{PVA} (cm/s)	35.0 ± 9.1	22.5–56.8
$D_{PVA}-D_A$ (ms)	0.3 ± 20.2	−50–66
I_{PVA}/I_A	0.49 ± 0.28	0.21–1.83
F_{PVA}/F_A	0.40 ± 0.24	0.10–1.24
Hemodynamic parameters		
LV pre-A pressure (mmHg)	9.1 ± 4.6	0.0–28.7
ΔPa (mmHg)	4.9 ± 2.8	0.7–13.5
ΔPa/ΔVa ($mmHg/mL/m^2$)	0.40 ± 0.37	0.03–1.80
LVEDP (mmHg)	13.8 ± 5.6	2.7–35.0

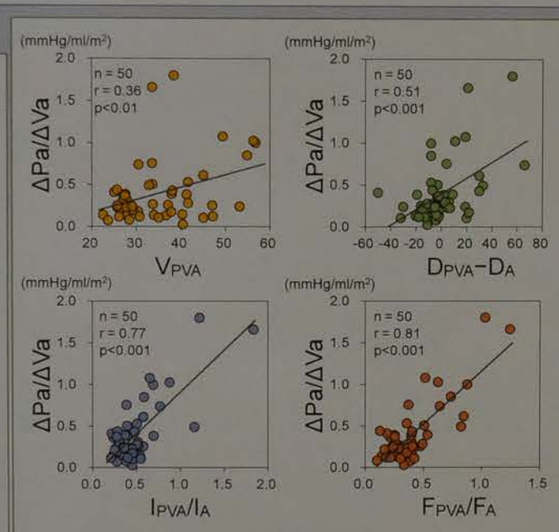

Figure 3 Correlation between the parameters derived from pulmonary venous and transmitral flows and the ΔPa/ΔVa

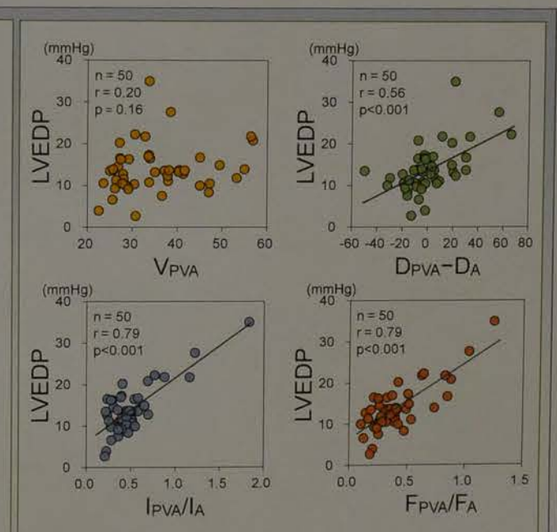

Figure 4 Correlation between the parameters derived from pulmonary venous and transmitral flows and the LVEDP

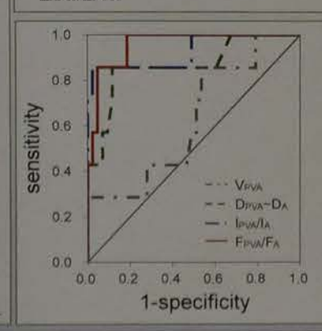

Figure 5 Receiver operating characteristic (ROC) curve of the pulmonary venous and transmitral flow parameters for differentiating patients with LVEDP >18 mmHg from those without.

Table 2 The results of the ROC analysis for estimating elevated LVEDP (>18 mmHg) by the pulmonary venous and transmitral flow Doppler parameters

	AUC	P value	Cut off value	Sensitivity	Specificity	Accuracy
V_{PVA} (cm/s)	0.63	0.28				
$D_{PVA}-D_A$ (ms)	0.87	0.002	10 ms	86%	88%	88%
I_{PVA}/I_A	0.93	<0.001	0.67	86%	98%	96%
F_{PVA}/F_A	0.96	<0.001	0.58	86%	95%	94%

CONCLUSION

Our novel parameters based on the time-velocity integral measurements of the backward PV and forward transmitral flows during atrial contraction are useful for the noninvasive assessment of LV chamber stiffness and LVEDP.

Clinical Physiology

PG-12

Changes in gender preference of female patients for repeated transthoracic echocardiography

Kenya Okada, Koji Kurosawa, Takao Kimura, Kanako Niwa, Takahiro Ikoma, Keiko Morita, Tetsuo Machida, Masami Murakami

Department of Clinical Laboratory Center, Gunma University Hospital

Backgrounds

It is reasonable to presume that some female patients, especially young ones, would prefer female sonographers for transthoracic echocardiography (TTE) because of the need to expose the chest.
This would interfere the logistics of echo labs. Because not all of the patients are familiar with what will happen during TTE exam, little is known about how they really feel about it and especially if they change their mind for the second time.

Purpose

We examined whether their preference for the gender of sonographers would change.

Methods

Since October 2013, female patients referred to TTE underwent the following questionnaire before the examination.

Dear female patients who undergo Electrocardiography or Echocardiography,
検査技師による心電図・心臓超音波検査を受けられる女性の患者様へ

Please check one of the followings
どちらかにチェックをお願いします

☐ I preferred a female examiner.
女性検査技師希望

☐ I do not care the sex of the examiner.
女性検査技師・男性検査技師どちらでも可

If you prefer a female examiner, your waiting time can be longer.
Thank you for your understanding and patients.
女性検査技師希望の場合、多少待ち時間が長くなることがございますが、ご了承下さい。

The TTE was performed according to their preference. Those who underwent TTE twice were included in this analysis.

Results

Duration: Oct 2013～Feb 2015
Number of subjects : 891
Age : 60 ± 16 y.o.

Fig.1 The preference of examiner's gender (n=891)

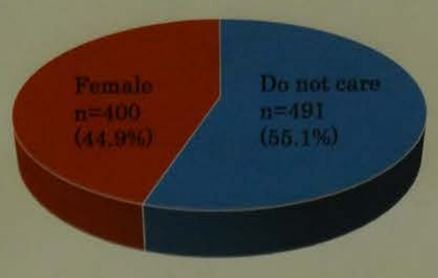

Table. The number of times of questionnaire

	1	2	3	4
Number of patients	725	68	6	3

68 answered the questionnaire twice (Fig 2 and 3)

Fig.2 The preference of examiner's gender (n=68)

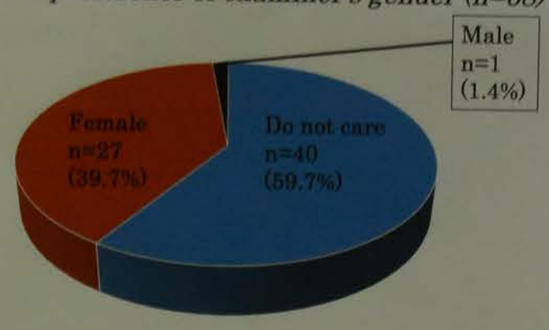

Fig.3-A The change of preference of examiner's gender (n=68)

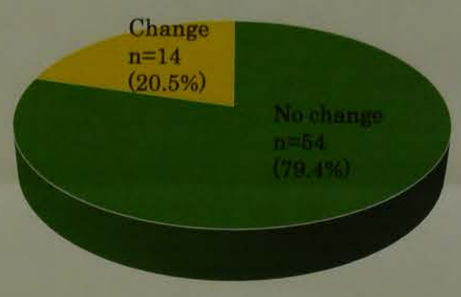

Fig.3-B The breakdown of the changes in preference of examiner's gender (n=68)

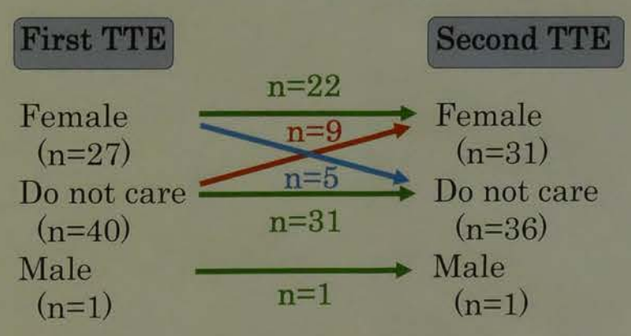

Do not care⇒Female (n=9)
(first examiner was male (n=3)
first examiner was female (n=6))

Summary

- ✔About half of the female patients preferred female sonographers.
- ✔Majority of them did not change their preference for the second time.
- ✔However, some changed their needs.

Conclusions

Repeated questionnaire would be one of the options for assessing patient preference.

Clinical Physiology

PG-13

Accuracy of the Estimation of Left Ventricular Relaxation and Filling Pressure: A Comparison of Single Doppler Parameters and Comprehensive Evaluation

Masahiro Nakabachi[1], Satoshi Yamada[2], Taichi Hayashi[2], Hiroyuki Iwano[2], Hitoshi Shibuya[1], Kaoru Kahata[1], Chikara Shimizu[1], Hiroyuki Tsutsui[2]

[1]Division of Laboratory and Transfusion Medicine, Hokkaido University Hospital
[2]Department of Cardiovascular Medicine, Hokkaido University Graduate School of Medicine, Sapporo, Japan

Background

- Many echocardiographic parameters are used in the estimation of left ventricular (LV) relaxation and filling pressure; however, we often have doubts about the accuracy of each quantitative parameter in clinical practice.
- An Algorithmic approach based on multiple parameters is widely used for the estimation of LV relaxation and filling pressure.
- In clinical practice, we comprehensively assessed LV relaxation and filling pressure using too many parameters for algorithm to be possible.

Objective

To compare accuracy in estimating LV relaxation and filling pressure among the following three methods: 1) single quantitative Doppler parameters, 2) simple algorithmic approach, and 3) Comprehensive evaluation based on multiple parameters.

Methods

- Institutions : Hokkaido University, Nagoya City University, Mie University, University of Tsukuba, Tokushima University
- Equipment: Artida, Aplio XG (Toshiba)
- Subjects: 77 patients (mean age 59±14, men 58) suspected of clinical heart failure who underwent cardiac catheterization
- Exclusion criteria: Non-sinus rhythm, frequent premature beats, moderate to severe aortic/ mitral stenosis/ regurgitation, post aortic/ mitral valve repair/ replacement, maintenance hemodialysis
- LV pressure measurements: Micromanometer-tipped catheter
  - Time constant of LV pressure decay (τ)
  - LV mean diastolic pressure (LVMDP)
  - Impaired LV relaxation: τ> 48ms, elevated filling pressure: LVMDP>15mmHg
- Echocardiographic parameters:
  - Early-diastolic mitral annular velocity (e') as a parameter of LV relaxation
  - The ratio of early-diastolic LV inflow velocity (E) to e' (E/e') as a parameter of LV filing pressure

Single quantitative Doppler parameters

Cutoff values were determined by method of relative cumulative frequency distribution.

- Impaired LV relaxation: e'<7.4 cm/s
- Elevated LV filling pressure: E/e'>11.0

Simple algorithmic approach

Normal : 0.75≤E/A<1.5 and E/e'<10
Abnormal relaxation : E/A<0.75
Pseudonormal: 0.75≤E/A<1.5 and E/e'≥10
Restrictive : E/A≥1.5

- Abnormal relaxation, pseudonormal, restrictive →Impaired LV relaxation
- Pseudonormal, restrictive→Elevated filling pressure

Comprehensive evaluation

Expert cardiologist in echocardiography evaluated LV relaxation and filling pressure based on clinical information, twenty-five echocardiographic parameters, and information about regional wall motion (table at right).

No.	
Age	
Gender (m/f)	
Height (cm)	
Weight (kg)	
Systolic blood pressure (mmHg)	
Diastolic blood pressure (mmHg)	
HR (bpm)	
QRS width (ms)	
Bundle branch block	
Hypertension	
Diabetes mellitus	
Dyslipidemia	
LVDd (mm)	
LVDs (mm)	
LVEF (%)	
IVS (mm)	
LVPWT (mm)	
LV mass index(g/m²)	
LA diameter (mm)	
E (cm/s)	
A (cm/s)	
E/A	
DT (ms)	
IRT (ms)	
e' sep (cm/s)	
e' lat (cm/s)	
E/e'avg	
Vp (Hokudai)(cm/s)	
E/Vp (H)	
Vp (Cleveland)(cm/s)	
E/Vp (C)	
PV S (cm/s)	
PV D (cm/s)	
S/D	
PVD-DT (ms)	
PV A (cm/s)	
ARd-Ad (ms)	
Wall motion score	
basal anterior	
basal anteroseptum	
basal inferoseptum	
basal inferior	
basal inferolateral	
basal anterolateral	
mid anterior	
mid anteroseptum	
mid inferoseptum	
mid inferior	
mid inferolateral	
mid anterolateral	
apical anterior	
apical septum	
apical inferior	
apical lateral	
apex	
Estimation of LV relaxation	N・A
Estimation of LV filling pressure	N・A

N, normal; A, abnormal

Results

Patient characteristics

Normal	14 (18%)
Angina pectoris	20 (26%)
Prior myocardial infarction	15 (19%)
Dilated cardiomyopathy	12 (16%)
Hypertrophic cardiomyopathy	8 (10%)
Hypertensive heart disease	8 (10%)

Hemodynamic and echocardiographic parameters

τ (ms)	49±13
τ>48 ms	37 (48%)
LVMDP (mmHg)	8.3±6.1
LVMDP>15 mmHg	11 (14%)
LVDd (mm)	51±8
LVEF (%)	58±17
LVEF<50%	29 (38%)
LV mass index (g/m²)	123±42
LV hypertrophy	41 (53%)

Correlations with τ

	r	p
E	0.25	<0.05
A	-0.26	<0.05
E/A	0.49	<0.001
DT	-0.14	0.23
IRT	-0.03	0.80
S/D	-0.24	<0.05
PVD-DT	0.20	0.14
PVA	-0.13	0.30
ARd-Ad	0.36	<0.01
e'	-0.32	<0.01
Vp	-0.22	0.08

Correlations with LVMDP

	r	p
E	0.47	<0.001
A	-0.24	<0.05
E/A	0.55	<0.001
DT	-0.12	0.31
IRT	-0.27	<0.05
S/D	-0.31	<0.01
PVD-DT	0.18	0.18
PVA	-0.06	0.61
ARd-Ad	0.35	<0.01
E/e'	0.50	<0.001
E/Vp	0.36	<0.01

e' vs τ, and E/e' vs LVMDP

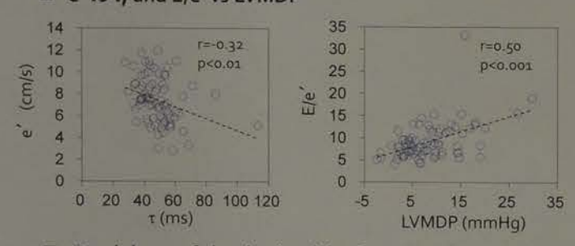

Breakdown of simple algorithmic approach

Normal	26 (34%)
Abnormal relaxation	34 (44%)
Pseudonormal	8 (10%)
Restrictive	9 (17%)

Comparison of accuracy

➢ Estimation of abnormal LV relaxation

	e'	Simple algorithm	Comprehensive evaluation
Sensitivity	32%	76%	81%
Specificity	30%	44%	68%
PPV	30%	57%	70%
NPV	32%	65%	79%
Accuracy	28%	60%	74%

PPV, positive predict value; NPV, negative predict value

➢ Estimation of elevated filling pressure

	E/e'	Simple algorithm	Comprehensive evaluation
Sensitivity	82%	64%	64%
Specificity	79%	85%	94%
PPV	39%	41%	64%
NPV	96%	93%	94%
Accuracy	76%	82%	90%

➢ Estimation of elevated filling pressure in patients with E/e'>11 n=22

	Simple algorithm	Comprehensive evaluation
Sensitivity	64%	64%
Specificity	85%	94%
PPV	41%	64%
NPV	93%	94%
Accuracy	82%	90%

Summary

- Regarding the estimation accuracy of LV relaxation, the simple algorithmic approach was superior to e', and comprehensive evaluation was further superior to the simple algorithmic approach.
- Regarding the estimation accuracy of LV filling pressure, E/e' had a high sensitivity, but a low positive predictive value; thus, the false positive rate was high. However, when E/e' is not high, we can consider LV filling pressure to be normal because of the high negative predictive value.
- In cases when E/e' is high, we can estimate the elevated LV filling pressure more accurately by using comprehensive evaluation.

Conclusion

Comprehensive evaluation of LV relaxation based on many conventional echocardiographic parameters was superior to both e' and the simple algorithmic approach in the estimation of impaired LV relaxation. Furthermore, LV filling pressure should be considered to be normal if E/e' is not high, and when E/e' is high, comprehensive evaluation based on multiple parameters is also indicated.

Clinical Physiology

PG-14

OKAYAMA UNIV. HOSPITAL

Factors Related to Residual Shunt After Transcatheter Closure of Atrial Septal Defect.

Madoka Ikeda, Hiroki Oe, Nobuhisa Watanabe, Yasufumi Kijima, Yoichi Takaya, Ken Okada, Hiroshi Ito

Okayama University Hospital

Case 1: Residual shunt from supero-anterior rim side.

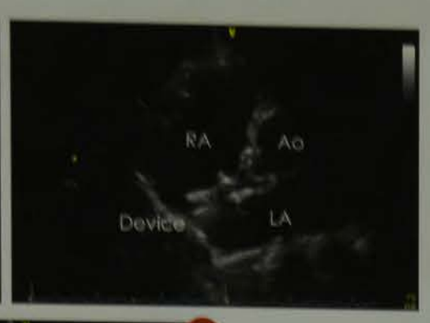

Case 2: Residual shunt from infero-posterior rim side.

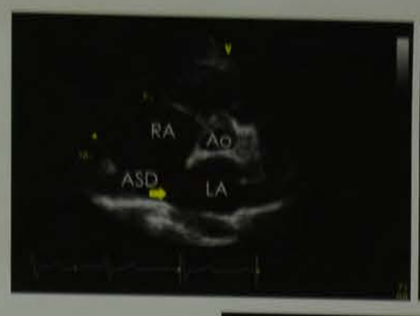

Backgrounds

- In recent years, transcatheter closure of atrial septal defect (ASD) with Amplatzer septal occluder has been established as a secure and effective treatment alternative to surgical repair for ASD.
  (J Am Coll Cardiol 2005;45:505-507.)
- Although, the incidence of residual shunt has reported very low with Amplatzer septal occluder (0-7.4%), the presence of a residual shunt is independently associated with an increased risk of recurrent ischemic events.
  (J Am Coll Cardiol 2002;39:1061–5)
  (Congenit Heart Dis. 2010;5:32–37)
  (J Interven Cardiol 2012;25:304–312)

Purpose

- Our purpose was to identify factors related to residual shunt after transcatheter closure of ASD with the Amplatzer septal occluder.

Methods

- Two hundred and fifty three patients who underwent transcatheter closure of ASD with Amplatzer septal occluder in our institution were included.
  Baseline characteristics are described in Table 1.
- The indication for ASD closure in all patients was a hemodynamically significant atrial shunt or the presence of right ventricular volume overload.
- Follow up transthoracic echocardiography was performed at 24 hours and 6 months after transcatheter closure of ASD.
- A residual shunt was considered to be present if color Doppler flow imaging showed a left-to-right shunt across the interatrial septum, and it was defined as shunt occurring from along the device rims. ***In color Doppler flow mapping, the velocity was set in the range of 50 cm/sec***. (Case 1,2)
- Deficient rim was determined as < 5mm measured by transesophageal echocardiography.
  Rim deficiency was defined as supero-anterior (SA), infero-anterior (IA), supero-posterior (SP) and infero-posterior (IP) rim deficiencies. (Table 2)

Table 1. Baseline characteristics.

	All patients (n=253)
Age (years)	46.6±20.9 (6-83)
Women	167 (66.0%)
Body Surface Area (m2)	1.54±0.22 (0.75-2.09)
Sufficient rim/Deficient rim	68/185 (26.9/73.1)
Single defect/Multiple defects	233/20 (92.1/7.9)
Qp/Qs	2.4±0.6 (1.2-4.1)
Defect size* (mm)	17.9±6.7 (2-40)
Device size (mm)	21.4±6.4 (7-38)

Data expressed as mean ± SD (range) or number of patients (percent).
* Measured using transesophageal echocardiography.

Table 2. Morphology of ASD in 253 consecutive patients

Morphology	Number of patients (%)
Sufficient rim	67 (26.9)
Deficient rim	185 (73.1)
SA rim deficiency	139 (54.9)
IP or IA rim deficiency	5 (2.0)
Multiple rim deficiencies	41 (16.2)

Multiple: more than a single rim deficiency.
Data expressed as number of patients (percent.

Results

- Precise echocardiographic examination at 24 hours and 6 months after the transcatheter closure of ASD showed residual shunts in 122 (48%) patients and 54 (21%) patients, respectively. (Figure 1)
- Patients with residual shunt had higher frequency of deficient rim than patients with complete closure both at 24 hours and 6 months examination (88% vs. 60%; p<0.01, 91% vs. 68%; p<0.01, respectively). (Figure 2)
- Defect size (20.5±7.4 vs. 17.4±6.5; p<0.01) and device size (24.1±6.4 vs. 20.6±6.3; p<0.01) in patients with residual shunt were significantly larger compared to patients with complete closure at 6 months follow up.

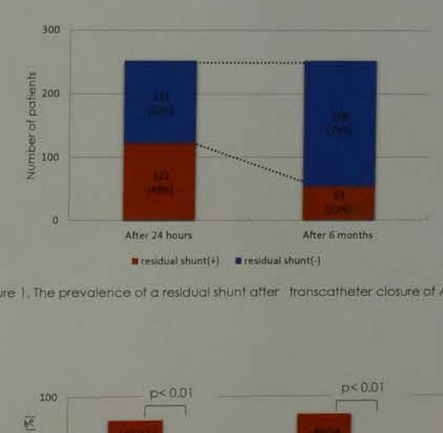

Figure 1. The prevalence of a residual shunt after transcatheter closure of ASD.

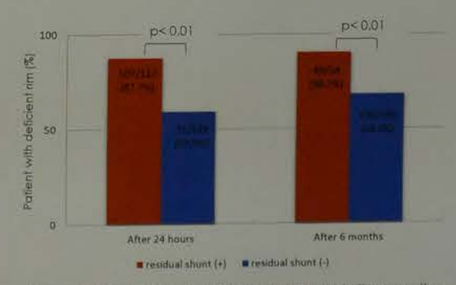

Figure 2. Comparison of a residual shunt after 24 hours and after 6 months.

- By multivariate analysis, age (p=0.0051) and deficient rim (p=0.0120) were independent predictors of a residual shunt after transcatheter closure of ASD at 6 months follow up.

Table 3. The independent features of residual shunt at 6 months follow up based on multivariate logistic regression analysis.

	Odds ratio	95% CI	p value
Age (years)	0.14	0.03 - 0.54	0.0051
Deficient rim	3.67	1.44 – 11.35	0.0120

CI, confidence interval

Conclusions

- Deficient rim, which is a morphological characteristic of ASD was an independent predictors of a residual shunt after transcatheter closure of ASD.

Disclosure
Teiji Akagi is a consultant of St. Jude Medical. There is no other potential conflicts of interest to report.

Clinical Physiology

PG-15

Electrocardiographic changes in patients with chronic obstructive pulmonary disease

Atsushi Ichikawa [1], Tetsuro Sugiura [1], Hiroshi Ohnishi [3], Hiromi Kataoka [4], Katsumi Ogura [2], Akihito Yokoyama [3], Yoshihisa Matsumura [1]

1. Department of Laboratory Medicine, Kochi Medical School, Kochi University
2. Clinical Laboratory, Kochi Medical School, Kochi University
3. Department of Hematology and Respiratory Medicine, Kochi Medical School, Kochi University
4. Kawasaki University of Medical Welfare

Background

Chronic obstructive pulmonary disease (COPD) is characterized by an airflow limitation that is not fully reversible. COPD is one of the leading causes of morbidity and mortality in both industrialized and developing countries because it significantly affects the lungs and the heart. Because COPD is related to the rate of cigarette smoking and length of history of smoking, symptoms of COPD usually manifest after the disease is in a progressive stage.

Statistical information of COPD deaths in Japan

Cause of death (2011) [1]

Rank	Men	Women
1	malignant neoplasms	malignant neoplasms
2	heart disease	heart disease
3	pneumonia	pneumonia
4	cerebrovascular disease	cerebrovascular disease
5	accidental death	accidental death
6	suicide	suicide
7	COPD	renal failure
8	renal failure	malignant neoplasm of liver
9	hepatic disease	hepatic disease
10	diabetes mellitus	diabetes mellitus
14	COPD	

Trends in the major disease-specific mortality [2]

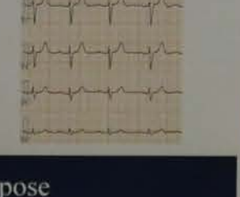

1) Ministry of Health, Labour and Welfare, Vital statistics 2011
2) Ministry of Health, Labour and Welfare, Vital statistics 2000, 2004, 2008,2011

Influence to the heart caused by COPD

Pulmonary hypertension

Burden on right side of the heart system aused by persistent pulmonary hypertension due to inflammation and hypoxemia of pulmonary blood vessels.

Pulmonary hyperinflation

Destruction of the alveoli, a decrease in lung elastic recoil, become a pulmonary hyperinflation by the gas exchange disorder, it is confirmed as a drop heart accompanied by a thoracic deformation and diaphragm flattening.

The electrocardiogram (ECG) in COPD

1. Frontal P axis more than 60°
   (Spodick DH. Circulation 1959;20(6):1067-72.)
2. Low voltage of QRS in lead I
   (Fowler NO. Am J Cardiol 1965;16(4):500-5.)
3. P wave greater in lead III than in lead I
   (Bajaj R. Int J Chron Obstruct Pulmon Dis 2013;8:41-4.)

A typical ECG in COPD

"lead I sign"
definition : less than 0.15mV

P axis; 90°, QRS amplitude in lead I; 0.07mV, FEV_1/FVC; 33%, Staging; GOLD III

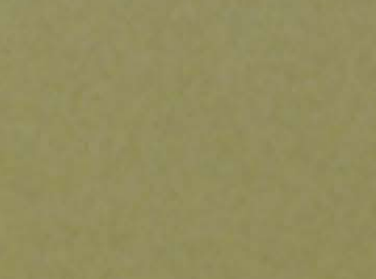

Purpose

The purpose of this study was to investigate the association between respiratory function and ECG characteristics in patients with COPD, and to identify the ECG results that indicate possible COPD.

Methods

Subjects

1. **Subject** : Patients consulted at the Kochi Medical School Hospital in Kochi
2. **Period** : October 2009 to March 2014
3. **Selection criteria** :
   All patients with COPD were in normal sinus rhythm and free of heart diseases and lungs diseases other than COPD. Patients in sinus rhythm and with normal respiratory function (vital capacity > 80%, FEV_1/FVC > 0.70) and neither heart nor lung diseases were selected as control subjects.
4. **Exclusion criteria** :
   Patients aged less than 45 years were excluded.
5. **Approval review** :
   Ethical Review Board of the Kochi Medical School

Used devices・Assessment indices

1. Used devices

① Electrocardiograph FCP-7541 (Fukuda Denshi Co., Ltd, Japan)
② Respiratory function test system C-8800 (CHEST M.I., Inc., Japan)

2. Assessment indices

① Standard 12-lead ECG indices
P axis, P interval, P amplitude,
QRS axis, QRS interval, QRS amplitude in V_1,
QRS amplitude in lead I, R amplitude in V_1,
R amplitude in V_5, QTc interval
② Respiratory function test measurements
FEV_1/FVC, Percent predicted value of FEV_1 (%FEV_1)

Statistics

1. Independence test (Chi-squared test)
2. Univariate analysis (Mann-Whitney U-test)
3. Multivariate analysis (Multiple logistic regression analysis)
4. One-way analysis of variance (Kruskal-Wallis test)
5. Correlation analysis (Pearson's correlation coefficient)
6. Receiver Operating Characteristic (ROC curve analysis)

Results

Clinical characteristics

Variables	COPD (n = 45)	Control (n = 100)	P value
Men, n (%)	41 (91)	93 (93)	0.953
Age (years)	74 ± 8	72 ± 7	0.226
Height (cm)	162.7 ± 7.8	162.4 ± 6.7	0.909
Body weight (kg)	58.4 ± 10.7	62.1 ± 9.5	0.042
Body mass index (kg/m^2)	22.0 ± 3.4	23.5 ± 3.1	0.014
FEV_1/FVC	0.52 ± 0.10	0.79 ± 0.04	< 0.001
%FEV_1 (%)	69 ± 21	101 ± 14	< 0.001

Date are represented as n (%) or mean ± standard deviation.

ECG indices

Variables	COPD (n = 45)	Control (n = 100)	P value
P axis (°)	64 ± 32	53 ± 24	< 0.001
P interval (sec)	115 ± 22	110 ± 16	0.019
P amplitude (mV)	0.11 ± 0.06	0.09 ± 0.04	0.027
QRS axis (°)	53 ± 33	45 ± 23	0.007
QRS interval (sec)	104 ± 18	99 ± 10	0.316
QRS amplitude in V_1 (mV)	1.01 ± 0.37	1.04 ± 0.36	0.554
QRS amplitude in lead I (mV)	0.50 ± 0.24	0.75 ± 0.26	< 0.001
R amplitude in V_1 (mV)	0.31 ± 0.33	0.22 ± 0.15	0.789
R amplitude in V_5 (mV)	1.44 ± 0.58	1.77 ± 0.49	< 0.001
QTc interval (sec)	0.43 ± 0.03	0.42 ± 0.02	0.089

Date are represented as mean ± standard deviation.

Predictive factors for COPD

Multiple logistic regression analysis

Coefficients	Partial regression coefficient	Std. Error	z value	P value
(Intercept)	-1.071	2.847	-0.377	0.706
Age	0.027	0.027	1.004	0.315
Body mass index	0.055	0.077	0.714	0.476
P axis	0.002	0.008	0.225	0.822
QRS amplitude in lead I	-4.208	1.351	-3.114	0.002
R amplitude in V_5	-0.287	0.476	-0.604	0.546

Correlation of FEV_1/FVC and QRS amplitude in lead I

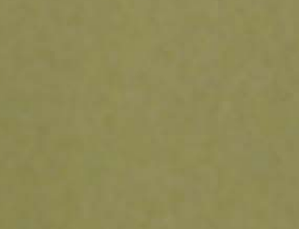

QRS amplitude in lead I in GOLD I, II, and III

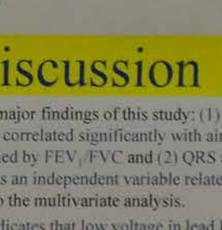

COPD group	GOLD I	GOLD II	GOLD III
(n = 45)	(n = 17)	(n = 17)	(n = 11)

Cut-off value of QRS amplitude in lead I in COPD diagnosis

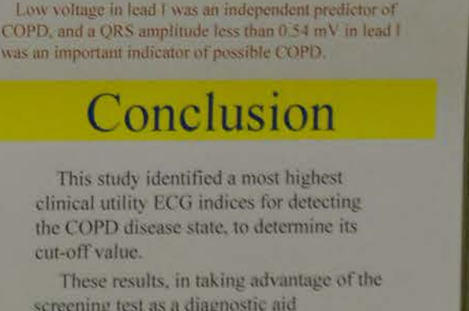

ROC curve analysis

Summary of Results

- There were significant differences between the groups for 6 (P axis, P interval, P amplitude, QRS axis, QRS amplitude in lead I and R amplitude in V_5) of the 10 ECG parameters.
- From the multiple logistic regression analysis, QRS amplitude in lead I emerged as a significant ECG parameter related to COPD.
- QRS amplitude in lead I correlated significantly with FEV_1/FVC.
- The ROC curve analysis showed that a QRS amplitude in lead I less than 0.54 mV indicated possible COPD (sensitivity: 71%, specificity: 76%).

Discussion

These were the major findings of this study: (1) QRS amplitude in lead I correlated significantly with airflow limitation determined by FEV_1/FVC and (2) QRS amplitude in lead I emerged as an independent variable related to COPD according to the multivariate analysis.

A finding that indicates that low voltage in lead I occurs during the early stage of COPD, because most of the patients with COPD (76%) in the present study had mild to moderate airflow limitation (GOLD stage I or II).

Low voltage in lead I was an independent predictor of COPD, and a QRS amplitude less than 0.54 mV in lead I was an important indicator of possible COPD.

Conclusion

This study identified a most highest clinical utility ECG indices for detecting the COPD disease state, to determine its cut-off value.

These results, in taking advantage of the screening test as a diagnostic aid examination of COPD, the efficiency of diagnosis can expect.

Clinical Physiology

PG-16

Value of Left Atrial Function in Patients with Aortic Stenosis: Assessment of Using Speckle-tracking Echocardiography

Kazuto Yamaguchi [1], Yoshitomi Hiroyuki, MD[1], Nitta Eri [1], Seiji Mishima[1]
Kazuaki Tanabe, MD[2], Atsushi Nagai, MD[1]

1. Shimane University Hospital, Laboratory Medicine
2. Shimane University Hospital, Department of Cardiology

Shimane University
Faculty of Medicine
Izumo, Japan

Background

- In aortic stenosis (AS), the chronically increased afterload is accompanied by several structural and functional changes as progressive left atrial (LA) enlargement and dysfunction.[1] In this situation, LA size may serve as a surrogate marker of chronic diastolic function and left ventricular (LV) filling pressure.[2] In severe AS, both LA dilatation and dysfunction have been shown to adversely affect the outcome. Assessing the relationship between LA size and function is thus of clinical importance.

- There is limited information regarding the role of LA function using the speckle tracking method in patients with aortic valve stenosis (AS).

Aim

The aim of the present evaluation was to assess the effect of AS progression on LA function, and relationship between LA function and symptoms.

Methods

- The study consisted of 25 consecutive patients (mean age 76±9 years) with moderate to severe AS.

- Patients were divided into 3 groups; moderate AS (aortic valve area 1.0~1.5 cm^2), severe AS (aortic valve area <1.0 cm^2) without symptoms, severe AS with symptoms and subsequent aortic valve replacement (AVR), and in 5 healthy control subjects. All patients underwent complete clinical assessment including comprehensive echocardiography and was included brain natriuretic peptide (BNP).

- Patients with atrial fibrillation (AF), prosthetic mitral valve, mitral valve stenosis, or pacemaker implantation were excluded from this study.

Figure 1. Atrial strain analysis from the apical 4-chamber view

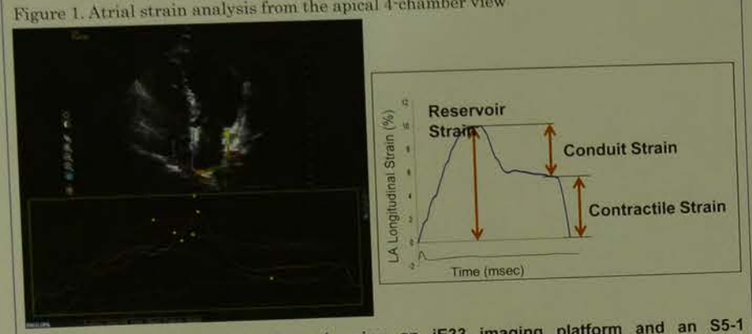

- Echocardiography was performed using an iE33 imaging platform and an S5-1 transducer (Philips, Andover, Massachusetts).

- The LA strain was obtained from apical 4-chamber view using semiautomated software (Cardiac Motion Quantification, Qlab version 8.0, Philips). The software produces a region of interest, and enable the strain curves. The strain curves were obtained from these strain profiles as averaged values of all regions of interest. 3 aspects of LA strain were recorded: contractile, describing deformation after the p-wave; conduit, describing passive atrial filling; and reservoir, representing the sum of these elements (Fig.1).

- Echocardiographic variables were performed by guidelines of the American society of Echocardiography , LAEF was derived: (LAVmax – LAVmin) / LAVmax x 100(%).

Results

Table 1. Echocardiographic characteristics

Variables	Moderate AS (n=9)	Severe AS without symptoms (n=9)	AVR with Symptoms (n=7)	ANOVA
Age (years)	74 ± 8	75 ± 9	80 ± 8	0.35
AVA (cm^2)	1.10 ±0.1	0.70 ± 0.18	0.47 ± 0.14 *	< 0.0001
PV (m/sec)	2.8 ± 0.6	5.0 ± 0.6	5.2 ± 0.4	< 0.0001
Mean PG (mmHg)	19 ± 7	63 ± 16	69 ± 10	< 0.0001
LVEDD (mm)	43 ± 6	47 ± 8	48 ± 7	0.26
LVESD (mm)	27 ± 5	28 ± 4	33 ± 8	0.11
LVEDV (mL)	67 ± 24	85 ± 25	99 ± 27	0.059
LVESV (mL)	24 ± 10	28 ± 10	44 ± 21	0.047
LVEF (%)	65 ± 6	69 ± 4	57 ± 10 *	0.033
LVGLS (%)	-13.9 ± 1.9	-12.6 ± 1.6	-10.2 ± 1.7 *	0.014
SV (mL)	72 ± 23	77 ± 13	55 ± 15 *	0.066
LAVI (mL/m^2)	40 ± 14	63 ± 19	68 ± 25	0.043
LAEF (%)	51 ± 6	41 ± 15	33 ± 9 *	0.031
Reservoir Strain (%)	13.8 ± 2.8	12.8 ± 3.3	8.8 ± 1.7 *	0.008
Conduit Strain (%)	5.6 ± 1.3	5.5 ± 2.2	3.8 ± 1.2	0.062
Contractile Strain (%)	8.2 ± 2.6	7.3 ± 2.3	4.9 ± 2.2	0.077
E wave	75 ± 36	65 ± 19	92 ± 51	0.94
A wave	101 ± 37	113 ± 23	116 ± 32	0.38
E/A ratio	0.8 ± 0.2	0.6 ± 0.1	0.8 ± 0.3	0.21
e'	5.1 ± 1.0	4.5 ± 1.4	4.0 ±1.5	0.19
E/e'	15.7 ± 6.4	16.4 ± 5.9	28.0 ± 15.9 *	0.08
RVP (mmHg)	37 ± 8	36 ± 4	43 ± 6	0.15
BNP (pg/dL)	74.3 ± 59.9	184.5 ± 132.5	459.0 ± 226.2 *	0.012

* vs Severe AS without symptoms $p < 0.05$

Results

- There were significant difference in severity of AS, LVESV, LV systolic function, LA volume, LA function parameters, E/e' and BNP among those three groups. Furthermore, symptoms and AVR group was significantly decreased AVA, LVEF, LVGLS, SV, LAEF and reservoir strain and had significantly increased values of E/e' and BNP compered to severe AS group without symptoms. Other LA strains (conduit and contractile strains) were slightly lower in AVR group with symptoms and (Table 1).

Figure 2. LA volume and LA function parameters

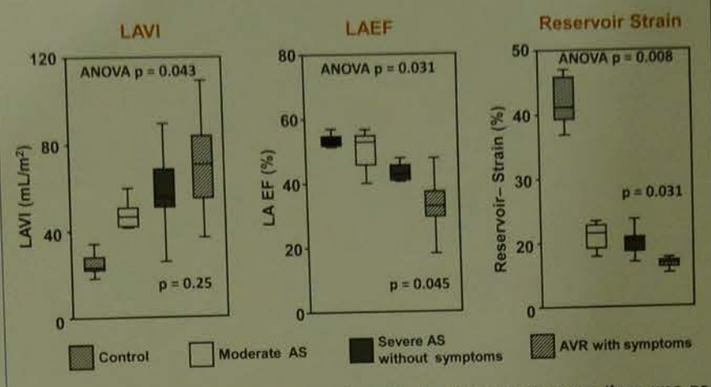

- In AS, LA size increased with progression of valve stenosis. However, there was no significant differences in LAVI between severe AS without symptoms and AVR with symptoms.

- LAEF decrease with progression of AS.

- LA reservoir strain significantly decreased with AS progression.

Discussion

- LA remodeling refers to complex pathophysiological changes in the LA in response to external stressors. LA dilatation, a hallmark of LA structural remodeling, is a result of pressure or volume overload . Increases in LA pressure help to maintain adequate filling of the LV under conditions of increased stiffness or decreased compliance of the LV .[3] The resultant increase in LA wall tension leads to its gradual dilatation, and the structural changes in the LA may reflect the chronicity of exposure to abnormal filling pressures. [4]

- In previous report, when cellular adaptation is exhausted, the increase in LV filling pressure may increase LA wall tension and myocyte stretch inducing myolysis, fibrosis and apoptosis.[1]

- LA reservoir function is determined by the longitudinal descent of the cardiac base and LA chamber stiffness.

- The quantitative assessment of LA function may be a useful additional tool in guiding clinicians in the optimal timing of surgery for AVR.

Conclusion

Impaired LA reservoir strain in patients with AS relates to AS progression, independently of the increase in LA volume. Increased LA stiffness may be associated with cardiac symptoms in patients.

References

1. Lancellotti P, Moonen M, Magne J, *et al*. Prognostic effect of long-axis left ventricular dysfunction and B-type natriuretic peptide levels in asymptomatic aortic stenosis. *Am J Cardiol* 2010;105:383–8.
2. Tsang TS, Barnes ME, Gersh BJ, *et al*. Left atrial volume as a morphophysiologic expression of left ventricular diastolic dysfunction and relation to cardiovascular risk burden. *Am J Cardiol* 2002;90:1284–9.
3. Abhayaratna WP, Seward JB, Appleton CP, *et al*. Left atrial size: physiologic determinants and clinical applications. *J Am Coll Cardiol* 2006;47:2357-63.
4. Simek CL, Feldman MD, Haber HL, *et al*. Relationship between left ventricular wall thickness and left atrial size: comparison with other measures of diastolic function. *J Am Soc Echocardiogr* 1995;8:37-47.
5. Mads Ersboll, Mads J.Anderson, Nana Valeur, *et al*. The Prognosis Value of Left Atrial Peak Reservoir Strain in Acute Myocardial Infarction Is Dependent of Left Ventricular Longitudinal Function and Left Atrial Size. *Circ Cardiovasc Imaging*. 2013;6:26-33.

The authors have no financial conflicts of interest to disclose concerning the presentation.

B-2

Clinical Physiology

PG-18

Effect of sleep stages on distribution of interictal fast ripples in intractable focal epilepsy

Rie Sakuraba[1)], Masaki Iwasaki[2)], Suguru Asagi[1)], Takashi Miki[1)], Nobukazu Nakasato[3)]

1) Clinical Physiology Center, Tohoku University Hospital
2) Department of Neurosurgery, Tohoku University Graduate School of Medicine
3) Department of Epileptology, Tohoku University Graduate School of Medicine

TOHOKU UNIVERSITY

Rationale:

High-frequency oscillations (HFOs) are EEG markers of epileptogenicity. Removal of the brain region hosting high-rate interictal HFOs is related to good seizure outcome after surgery. However, for the accurate diagnosis of epileptogenicity, pathological HFOs must be carefully distinguished from physiological HFOs. Occurrence of HFOs is strongly influenced by sleep stages. Recently, we reported that interictal ripples (80 – 200Hz) may provide a specific marker of epileptogenicity during REM sleep (Sakuraba et al., 2016). In this study, we investigated that effect of sleep stages on distribution of interictal fast ripples (200 – 500Hz, FRs) and correlation to epileptogenic area.

Methods:

The subjects comprised 12 patients (average age, 29.2 years; range, 14–58 years; 8 males) with drug-resistant epilepsy who underwent extraoperative intracranial EEG monitoring by a combination of depth (median, 8 contacts per patient; range, 0–20 contacts) and subdural electrodes (median, 45 contacts per patient; range, 24–52 contacts). All patients underwent surgical resection and ten achieved freedom from seizures postoperatively (Table 1). Intracranial EEG signals were sampled and recorded at 2000 Hz simultaneously with scalp EEG and electromyography for sleep staging. The recorded signals were filtered between 200 and 500 Hz, and interictal FRs were automatically detected on 5 min EEG samples derived from different sleep stages. FRs were defined by events above three times the standard deviation of baseline activities and containing at least four consecutive oscillations. The occurrence rate of FRs was compared between REM and NREM sleeps. High-rate FR electrode was defined as electrodes with the top 10% occurrence. The relationship of high-rate FR electrodes to the area of surgical resection was compared between REM and NREM sleeps in patients with postoperative seizure freedom (n = 10), with Fisher's exact test.

Results:

In total, 20,906 and 1,933 FRs were identified during NREM and REM sleeps, respectively, from 387 and 199 electrodes of a total of 568 intracranial electrodes across all patients. A total of 191 and 277 electrodes were located inside and outside the resection in patients with postoperative seizure freedom, respectively. The occurrence rate of FRs was significantly lower during REM sleep (mean, 0.7/min; range, 0.0–60.6/min) than during NREM sleep (mean, 7.3/min; range, 0.0–297.8/min) ($p < 0.0001$, Wilcoxon test).

In ten patients with postoperative seizure freedom, high-rate FR were identified in 25 (13.1%) and 4(1.4%) electrodes inside and outside the resection during NREM sleep, respectively, and in 33 (17.3%) and 12 (4.3%) electrodes inside and outside the resection during REM sleep, respectively. The relationship of the high-rate FR electrodes to the area of surgical resection was not different between NREM and REM sleeps ($p = 0.25$, Fisher's exact test, Figure 1,2).

Conclusions:

Sleep stages influence the occurrence of FRs. The occurrence rate of FRs was lower during REM sleep than during NREM sleep. REM sleep HFOs can serve as a specific marker of the epileptogenic zone (Supplementary Figure 1). However, influence of sleep stages may be lower on the FR than on ripples.

Patient	Gender /age	Epilepsy diagnosis	MRI	FDG-PET hypo-metabolism	Intracranial EEG seizure onset zone	Surgery	Pathology	Seizure outcome	Follow-up [M]
A	M/22	Lt OLE	Lt O CM	Lt O	Lt med O	Lt O lesionectomy	CH	F	28
B	M/36	Rt TLE	Normal	Rt a-med T	Rt lat T	Rt ATL	FCD type I	F	27
C	M/21	Lt TLE	Lt T CAPNON	Lt a-b-T	Lt b-T	Lt b-T lesionectomy	Ganglioglioma	F	26
D	F/28	Lt TLE	Lt HA, PHG cyst	Lt a-med T	Lt med, lat T	Lt ATL	HS, FCD type I	F	23
E	M/19	Rt FLE	Rt med F FCD	Rt med F, b-T	Rt med F	Rt med F cortex	FCD type II	F	22
F	M/36	Lt TLE	Lt HA	Lt a-med T	Lt med, lat T	Lt ATL	Gliosis	F	22
G	M/14	Lt FLE	Normal	Normal	Lt lat F	Lt F cortex	none	F	21
H	F/27	Rt TLE	Rt PHG lesion s/o	Normal	Rt med T	Rt ATL	Gliosis	F	16
I	F/28	Rt TLE	Bi lat HM s/o	Rt amy	Rt a-T	Rt ATL	Gliosis	F	15
J	M/22	Lt TLE	Normal	Lt a-med T	Lt med T	Lt ATL	none	F	14
K	M/58	Lt PLE	s/p removal Lt P lesion	Lt TPO	Lt TO	Lt TO cortex	Gliosis	R	23
L	F/39	Rt TOLE	Normal	Normal	Rt lat, b-O	Rt b-O cortex	FCD type I	R	17

Lt=left; Rt=right; OLE=occipital lobe epilepsy; TLE=temporal lobe epilepsy; FLE=frontal lobe epilepsy; PLE=parietal lobe epilepsy; TOLE=tempolo-occipital lobe epilepsy; CM=cavernous malformation; CAPNON=calcifying pseudoneoplasms of the neuroaxis; HA=hippocampal atrophy; PHG=parahippocampal gyrus; med=medial; lat=lateral; HM=hippocampal malrotation; a=antero; b=basal; amy=amygdala; FCD=focal cortical dysplasia; T=temporal; P=parietal; F=frontal; O=occipital; TPO=tempolo-parieto-occipital; TO=tempolo-occipital; ATL=anterior temporal lobectomy with amygdalohippocampectomy; CH=cavernous hemangioma; HS=hippocampal sclerosis

Table 1. Clinical characteristics of 12 patients

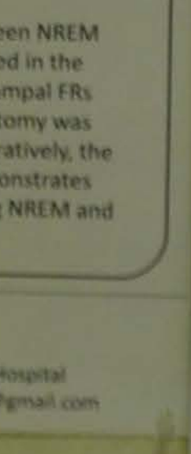

Figure 1. The relationship of the high-rate FR electrodes to the area of surgical resection was not different between NREM and REM sleeps in patients with postoperative seizure freedom ($p = 0.25$, Fisher's exact test).

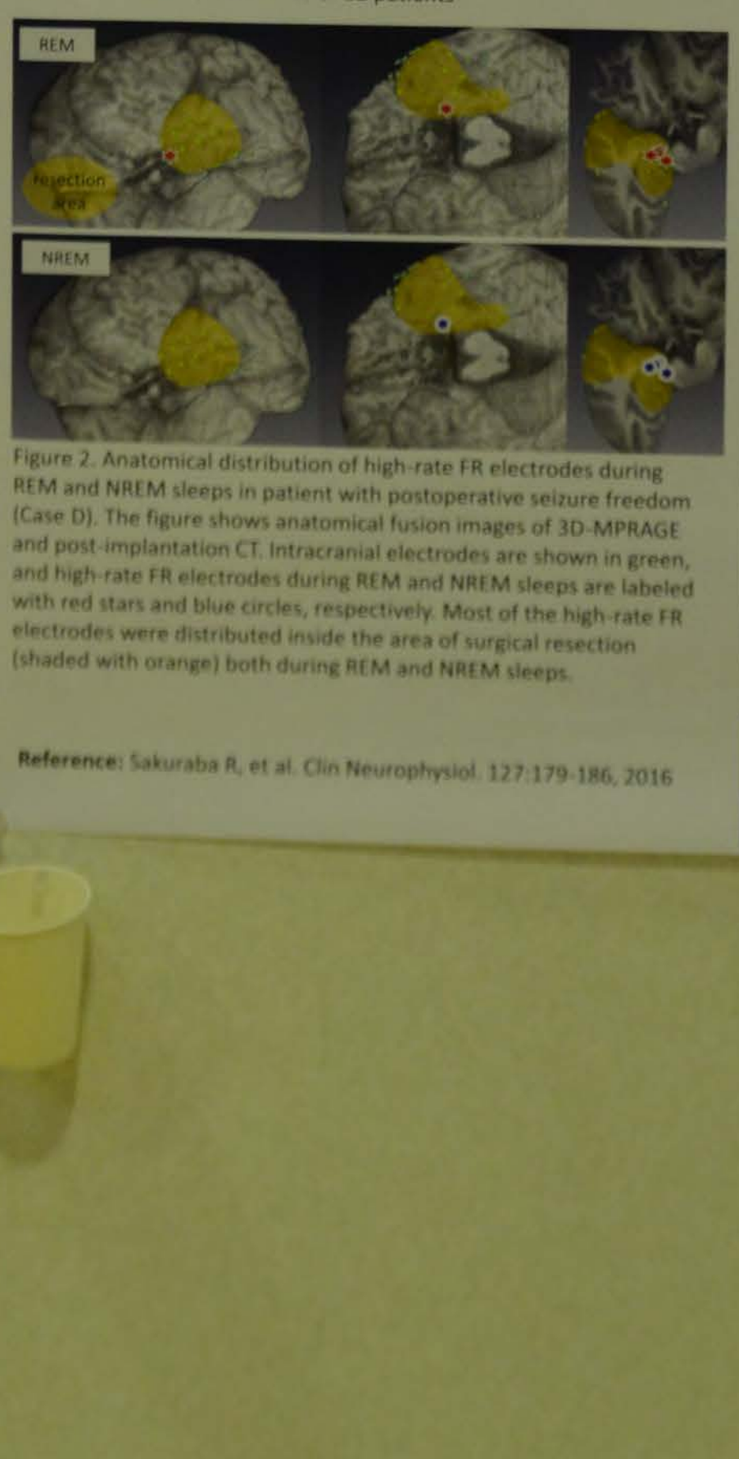

Figure 2. Anatomical distribution of high-rate FR electrodes during REM and NREM sleeps in patient with postoperative seizure freedom (Case D). The figure shows anatomical fusion images of 3D-MPRAGE and post-implantation CT. Intracranial electrodes are shown in green, and high-rate FR electrodes during REM and NREM sleeps are labeled with red stars and blue circles, respectively. Most of the high-rate FR electrodes were distributed inside the area of surgical resection (shaded with orange) both during REM and NREM sleeps.

Supplementary Figure 1. Different distribution of FR between NREM and REM sleeps in case C. Most frequent FRs were observed in the hippocampus during NREM sleep. However, these hippocampal FRs disappeared during REM sleep. Lt basal temporal lesionectomy was performed and the hippocampus was left intact. Post-operatively, the patient became seizure-free for 26 months. This case demonstrates that distribution of FR is critically different between during NREM and REM sleeps.

Reference: Sakuraba R, et al. Clin Neurophysiol. 127:179-186, 2016

CONTACT:
Rie Sakuraba, MHSc, Ph.D.
Clinical Physiology Center, Tohoku University Hospital
Tel: +81-22-717-7343 Email: r.sakuraba0817@gmail.com

Clinical Physiology

PG-19

KANAZAWA UNIVERSITY

Progression of Left Ventricular Diastolic Dysfunction in Patients with CKD

Yoshiyasu Miyajima[1)], Tadashi Toyama[2)], Hiroyasu Ohe[1)], Mikio Nagahara[1)], Kengo Furuichi[2)], Yoshio Sakai[1,3)], Takashi Wada[1,2,3)]

1) Department of Clinical Laboratory, Kanazawa University Hospital, Kanazawa, Japan
2) Division of Nephrology, Kanazawa University Hospital, Kanazawa, Japan
3) Department of Nephrology and Laboratory Medicine, Kanazawa University Hospital, Kanazawa, Japan

Background

・Left ventricular diastolic dysfunction is common among patients undergoing peritoneal dialysis.

Medicine Volume 94,Number 20,May 2015

Age,hypertension,obesity,and diabetes are established risk factors for the development of diastolic dysfunction

J Atheroscler Thromb,2015;22:1278-1286

Purpose

To investigate the relationships between CKD and progression of left ventricular diastolic dysfunction.

Methods

・Patients were examined their left ventricular peak velocity of blood flow across the mitral valve (E) and their diastolic peak velocities of mitral annulus (e').

・We calculated the ratio (E/e') as an index of left ventricular diastolic function.

・Low glomerular filtration rate (GFR) was defined as estimated GFR (eGFR) less than 60 ml/min/1.73 m^2.

・Relationship between changes of E/e' and status of CKD were examined using linear regression model.

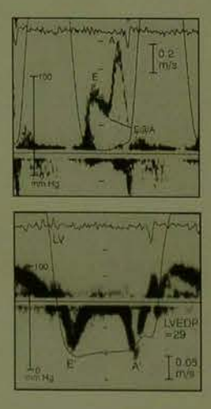

Inclusion Criteria

・Patients who were inpatient or outpatient of Kanazawa University Hospital.

・Patients who received echocardiography examination for more than once with intervals of more than one year.

Exclusion Criteria

・Congenital heart diseases
・Cardiomyopathy
・Valvular diseases
・Clinically diagnosed coronary artery disease.
・LV systolic dysfunction(EF≦55%)

Results

Flow diagram of participants inclusion

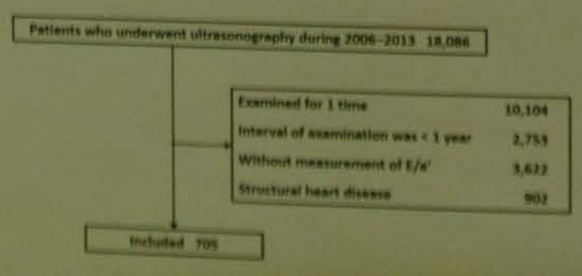

Baseline Characteristics (n=705)

Follow-up period (year)	3.3 ±1.4	LAD	37.2
Age (year)	61.7 ±13.5	IVSTd	9.3
Gender (male%)	46.8%	LVDd	46.6
BMI (kg/m²)	22.9 ±5.2	PWTd	9.3
eGFR (mL/min/1.73m²)	76.0 ±28.7	EF	68.7
BNP (pg/mL)	75.8 ±152.5	IVC	9.0
Tcho (mg/dL)	194.1 ±45.3	E/A	1.0
HDL−C (mg/dL)	53.7 ±16.5	E/e'	10.5
LDL−C (mg/dL)	108.7 ±43.5		
HbA1c (%) (NGSP)	6.1% ±1.1		
Diabetes(%)	12.7%		
Antihypertensive drugs (%)	45.3%		
Glucose lowering drugs (%)	17.1%		
Systolic blood pressure (mmHg)	125.7 ±20.2		
Diastolic blood pressure (mmHg)	74.6 ±12.4		
Urinary protein (g/g·Cr)	0.5 ±1.3	(n=421)	
Albuminuria (mg/g·Cr)	141.0 ±368.2	(n=313)	(mean±SD)

Relationships between changes in E/e' slope and risk factors.

Variables	Coefficient β(SE)	P
Age (+10year)	0.15 (0.01)	<0.01
Male (vs.Female)	-0.07 (0.11)	0.50
Low eGFR	0.31 (0.13)	<0.01
Antihypertensive drugs	0.05 (0.11)	0.70
Systolic BP (+10 mmHg)	0.01 (0.03)	0.70
BMI (+1kg/m²)	-0.01 (0.01)	0.36
Tcho (+10mg/dL)	-0.01 (0.01)	0.38
Diabetes	0.31 (0.12)	0.01

(n=705)

Low eGFR was related to rapid increase in E/e'

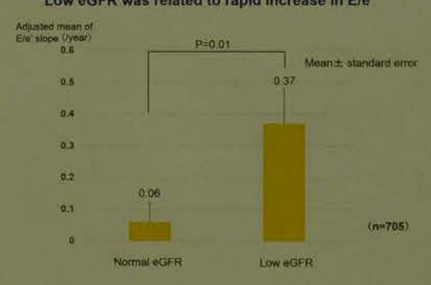

Low eGFR and proteinuria were related to rapid increases in E/e'

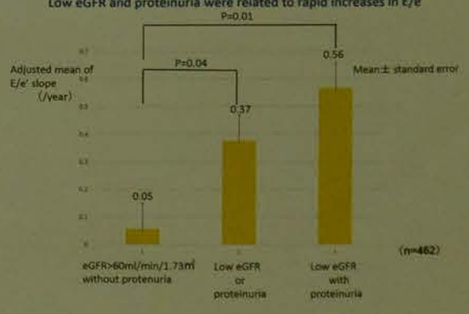

Severity of CKD was associated with progression of E/e'

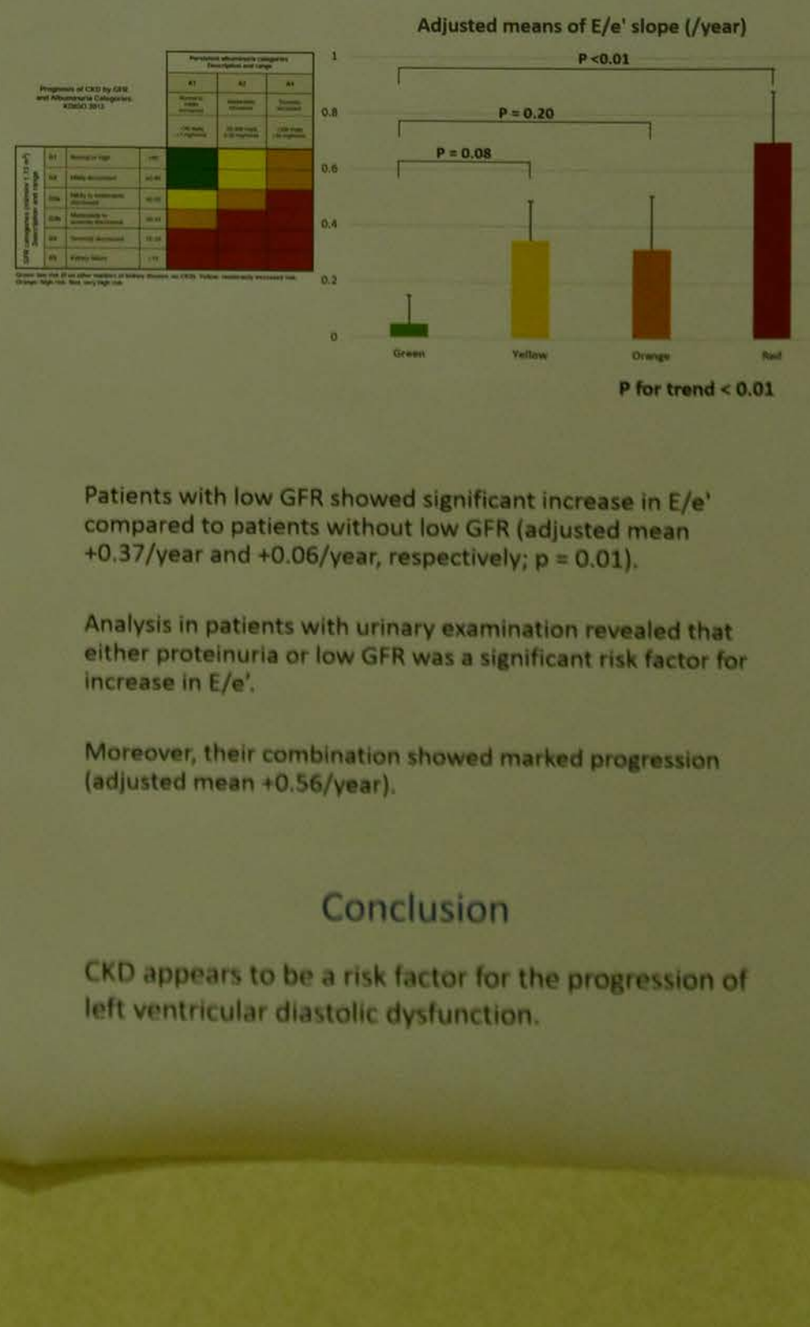

Patients with low GFR showed significant increase in E/e' compared to patients without low GFR (adjusted mean +0.37/year and +0.06/year, respectively; p = 0.01).

Analysis in patients with urinary examination revealed that either proteinuria or low GFR was a significant risk factor for increase in E/e'.

Moreover, their combination showed marked progression (adjusted mean +0.56/year).

Conclusion

CKD appears to be a risk factor for the progression of left ventricular diastolic dysfunction.

Clinical Physiology

PG-20

Experience of the first certification of ISO15189:2012 in physiological examination in Japan

Hidemasa Matsuo, Kanako Suzuki, Kuniko Iwata, Tomoya Yoneda, Yuko Nakayama, Takeshi Higuchi, Shuichi Shiga, Satoshi Ichiyama

Department of Clinical Laboratory, Kyoto University Hospital, Japan

Introduction

ISO 15189 is a well-known international standard for medical laboratories. More and more medical laboratories have been acquiring the certification in Japan. However, there had been no physiological laboratories certified by ISO15189, because the physiological examination is a unique task for medical technologists (MTs), and the accreditation system had not been established.

Here, we report the first case of acquiring ISO15189:2012 in physiological examination in Kyoto University Hospital.

Kyoto University Hospital
1,121 beds.
2,900 outpatients (average).
Approximately 3,000 staff.
The number of MTs is 82, including 22 MTs in the physiological examination room.

Acquisition of ISO15189:2012

Mar. 13, 2013 Kickoff meeting

Mar. 26, 2014 Acquisition of ISO:15189 except for physiological examination room

The accreditation system had not been established in JAB (Japan Accreditation Board)

Mid-Mar, 2015 Evaluation in physiological examination room by JAB

May. 27, 2015 Acquisition of ISO:15189 in physiological examination

Figure 1. Schedule of the ISO15189 certification.
There had been no physiological laboratories certified by ISO15189, because the physiological examination is a unique task for medical technologists, and the accreditation system had not been established.

A. Evaluation menu

- EKG, EEG, USG (Heart, Abdomen), and spirometry

B. Agenda

1st day	AM	1. Evaluation for documents
	PM	2. Tests for examination skill 3. Tests for knowledge
2nd day	All day	4. On-the-spot investigation

Figure 2. Evaluation menu and agenda for ISO15189.

Contact details:
Hidemasa Matsuo, MS, MLS(ASCP^{i})^{CM} E-mail: matsuo@kuhp.kyoto-u.ac.jp
Conflict-of interest disclosure:
Authors declare no competing financial interests.

A

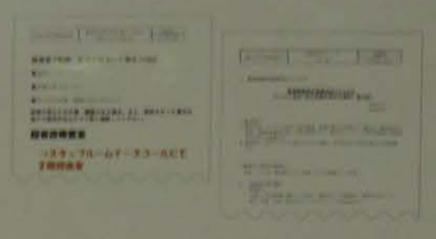

B

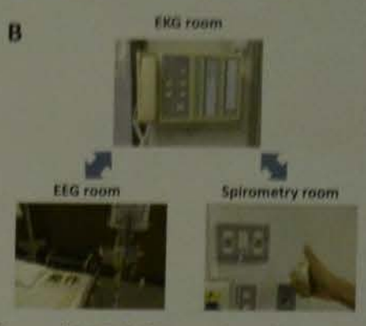

Figure 3. (A) Standard operating procedures (SOPs) for patients' falling and seizure in examination room. (B) Emergency call system between EKG, EEG, and spirometry room.

Problems	Solutions
There are no definitions of temperature and humidity suitable for physiological examination of patients.	We defined the acceptable temperature and humidity in physiological examination room and wrote them on SOP.
Procedure for when patient couldn't sleep during EEG with sleep activation is not defined.	We discussed with neurologist and defined as described below. 1. If we could observe stage-I sleep, we'll regard the examination as successful. 2. If we couldn't, we call the physician in charge, and discuss how we deal with it.
In spirometry, acceptable range in quality control (QC) is not defined.	We defined the acceptable range and we will continue to check the QC data using the range.

Figure 4. Major problems pointed out by JAB and the solutions.

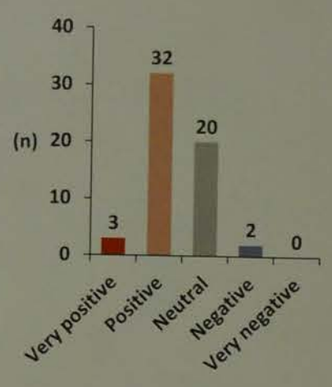

Positive comments

- SOPs are useful to teach new workers.
- We can ensure scheduled maintenance.
- The number of study meeting was increased.

Negative comments

- Making SOPs and checking the lists are time-consuming.

Figure 5.
Result of questionnaire survey for MTs on ISO15189 in Kyoto University hospital.

Conclusion

We have reported the experience of the certification of ISO15189 for physiological examination. At Kyoto University Hospital, multinational clinical trials including iPS cell research will be promoted as a medical institution with a physiological laboratory certified by ISO15189.

Acknowledgments

We thank all staff in physiological examination room:

Nakashima Y (MD), Hitomi T (MD), Kajita K, Fukuyama H, Murata M, Motoda H, Ishikawa Y, Kojima J, Narita Y, Yamashita M, Okamura Y, Sugimoto E, Wakita T, Ueda K, Ishii A, Masuda Y, Imai R, Yamamoto M, Ogawa M, Miyaura K, Isozumi M

Clinical Physiology

PG-21

Non-Invasive evaluation method of the liver fibrosis using ELF score and shear wave elastography

Koji yamamoto[1] Hiroko ushiba[1] Hiroshi nakano[1] Atsuya shimizu[2]

1) Department of Clinical Laboratory,Saiseikai Matsusaka General Hospital of Medicine 1-15-6 Asahimachi,Matsusaka,Mie 515-8557,Japan
2) Department of Internal Medicine,Saiseikai Matsusaka General Hospital of Medicine 1-15-6 Asahimachi,Matsusaka,Mie 515-8557,Japan

Diagnosis of chronic liver disease Background/Purpose

- Percutaneous liver biopsy is still now considered the gold standard as an indicator of liver fibrosis in chronic liver disease. However, it is difficult to keep the clinical observation over time because the liver biopsy is invasive with the risk of complications.
- Various non-invasive serological tests are used for measurement of liver fibrosis as the markers and the clinical usefulness has been reported . In this presentation, we set the reference value of ELF and examined the usefulness of liver fibrosis assessment in chronic liver disease. ELF Score® = 2.278 + 0.851 ln (C_{HA}) + 0.751 ln ($C_{P\,III\,NP}$) + 0.394 ln ($C_{TIMP\text{-}1}$)
- The other non-invasive measurements are ultrasonic tests such as Fibroscan, Real-time Tissue Elastography, Shear wave , and the usefulness of liver fibrosis assessment has been reported.
- We also examined the usefulness of liver fibrosis assessment in chronic disease with ELF and Shear Wave.

Subjects

The number of health subjects	700
Male (39.1±12.1)	154
Female (36.8±10.8)	546
Chronic hepatitis (8 cases of hepatitis B, 62 of C, 1 of NBNC)	71
Cirrhosis (3 cases of hepatitis B, 26 of C, 6 of NBNC, 8 of Alco)	45

Examination of ELF

Automatic chemiluminescence immunoassay system ADVIA Centaur XP

ELF Score® = 2.278 + 0.851 ln (C_{HA}) + 0.751 ln ($C_{P\,III\,NP}$) + 0.394 ln ($C_{TIMP\text{-}1}$)
Some data in European, but no report of the reference value in Japanese.

The normal liver was defined as healthy volunteers in cases of no abnormal liver function and negative hepatitis virus. For chronic hepatitis and cirrhosis, we used the cases of clinical diagnosis (including diagnostic imaging) and the cases of tissue diagnosis by liver biopsy (n = 33). Statistic software: Stat Flex Ver6

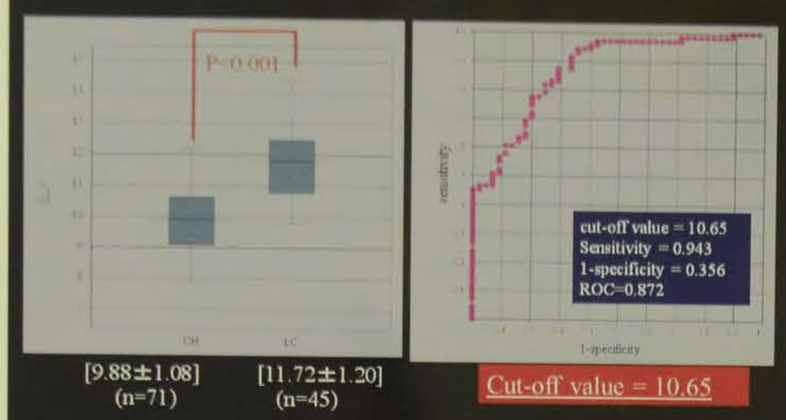

[9.88±1.08] (n=71) [11.72±1.20] (n=45) Cut-off value = 10.65

Cut-off value of cirrhosis diagnosis by ELF score

Summary ①

- **Setting of reference value of ELF score**

The reference value was 8.45±0.65 for the total, 8.65±0.66 for males and 8.39±0.63 for females. The reference values separated by age tend to differ significantly and we need to consider the age groups.

- **ELF score Evaluation for chronic liver diseases**

ELF scores were 9.88±1.08 for chronic hepatitis and 11.72±1.20 for cirrhosis, which showed a significant difference , considered to be useful for diagnosis. The cut-off value for cirrhosis was 10.65.

Chronic liver disease Ultrasonic diagnosis Examination of Shear Wave Elastography value

- Precutaneous liver biopsy is still now considered the gold standard as an indicator of liver fibrosis in chronic liver disease. However, it is difficult to keep observation over time because of the liver biopsy is invasive with the risk of complications.
- The other non-invasive methods are ultrasonic tests such as Fibroscan, Real-time Tissue Elastography, Shear wave , and the efficiency of evaluation for liver fibrosis has been reported.
- We examined the efficiency of evaluation for chronic liver diseases by using Shear wave in chronic disease at this time.

Subjects

Age	64.5±14.3
The number of subjects	97
Male	38
Female	59
Normal liver (healthy subjects)	20
Chronic hepatitis (5 cases of B, 26 of C, 3 of NBNC)	34
Cirrhosis (3 cases of B, 18 of C, 12 of NBNC)	33

Examination of Shear wave elastrography value

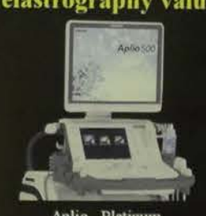

Aplio Platinum

The normal liver was defined as healthy volunteers in cases of no abnormal liver function. For chronic hepatitis and cirrhosis, we used the cases of clinical diagnosis (including diagnostic imaging) and the cases of tissue diagnosis by liver biopsy (n = 25).

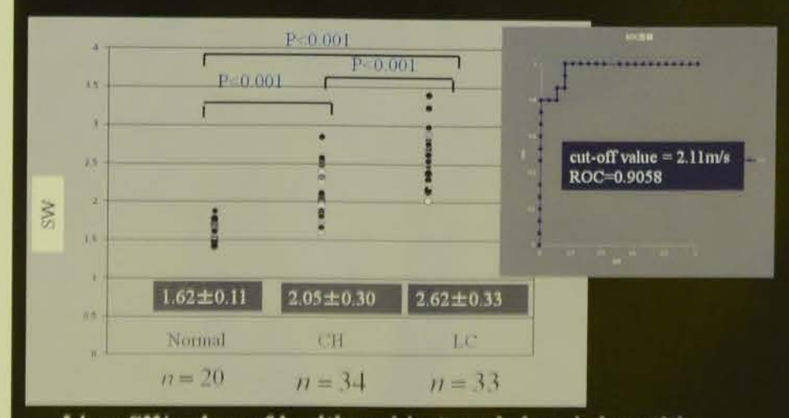

Liver SW values of healthy subjects and chronic hepatitis

Summary ②

- Shear Wave Elastography value

The values were 1.62 ± 0.11m/s for healthy subjects, 2.05 ± 0.30m/s for chronic hepatitis, and 2.62 ± 0.33m/s for cirrhosis, which showed a significant difference between each group, considered to be useful for diagnosis. The cut-off value for cirrhosis was 2.11 m/s.

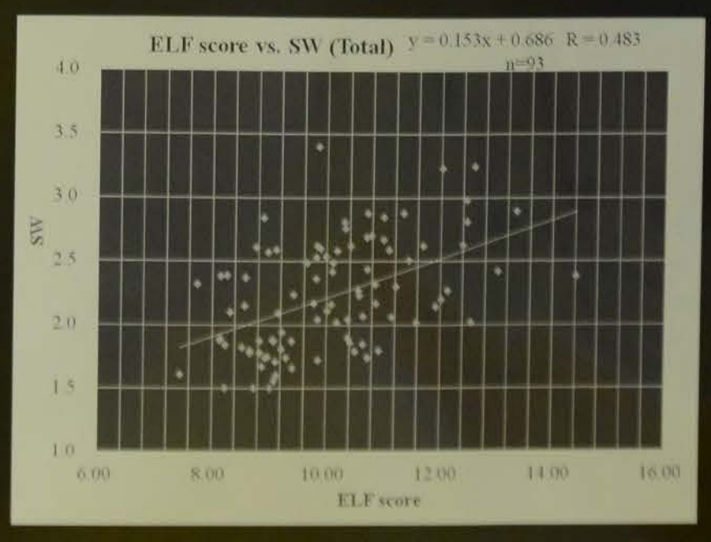

• Clinical application (liver) chronic liver disease

Cirrhosis patient (male, 70s) ; F4, A2 (cirrhosis)
SWE Velocity = 3.23 m/s ELF 13.87

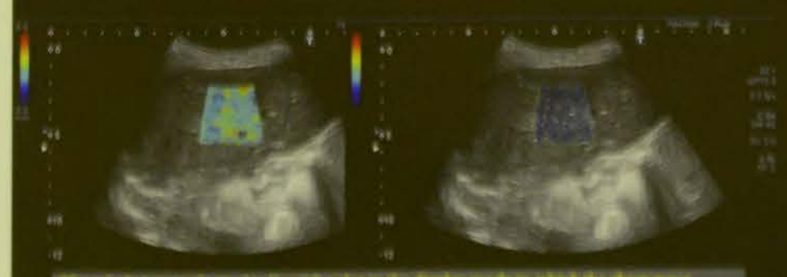

The whole image showed yellowish color in the display mode in which the shear wave propagation velocity can be measured, and it also showed some red area for easily assessing the tissue stiffness. In the contour display mode, we can observe it wider than healthy subjects and chronic hepatitis patients.
SWE value was 3.23m/s and ELF score was 13.87, and they were much higher than the reference values.

Conclusion

- ELF score and Shear Wave measurement are simple, non-invasive and useful as indicators of liver fibrosis in chronic liver disease.
- When the cut-off values of cirrhosis are set to 10.65 of ELF value and 2.11m/s of SWE value,

	sensitivity	specificity	Positive Predictive Value
ELF	80.0%	77.5%	69.2%
SWE	96.4%	62.2%	65.9%

- The histological examination (F category) is needed to be compared with them in the future.

Clinical Physiology

PG-22

Utility of monitoring spinal cord function during cervical cord surgery

Keita NISHIWAKI [1], Hiroka TAMURA[1], Natsumi AOKI[1]
Daichi KIYOHARA[1], Kazuya SAITO[1], Toshihisa FUNABASHI[1], Koichi SUGIURA[1]
1) Department of Physical Laboratory, Handa City Hospital

Spinal cord function monitoring is used to evaluate the neurological function of anesthetized patients during surgery, including detecting perioperative neuropathy and intervening to improve outcomes. In the patient study, the association between wave pattern changes and prognostic evaluation was monitored during cervical cord surgeries.

MATERIALS & METHODS

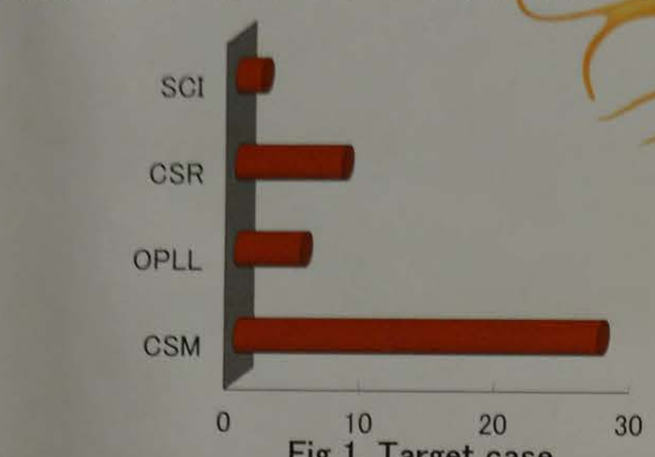

Fig 1. Target case

42 cervical vertebrae surgeries of the middle low rank (C5-7) domain ware performed, with monitoring. Participants were 30 men, and 12 women.

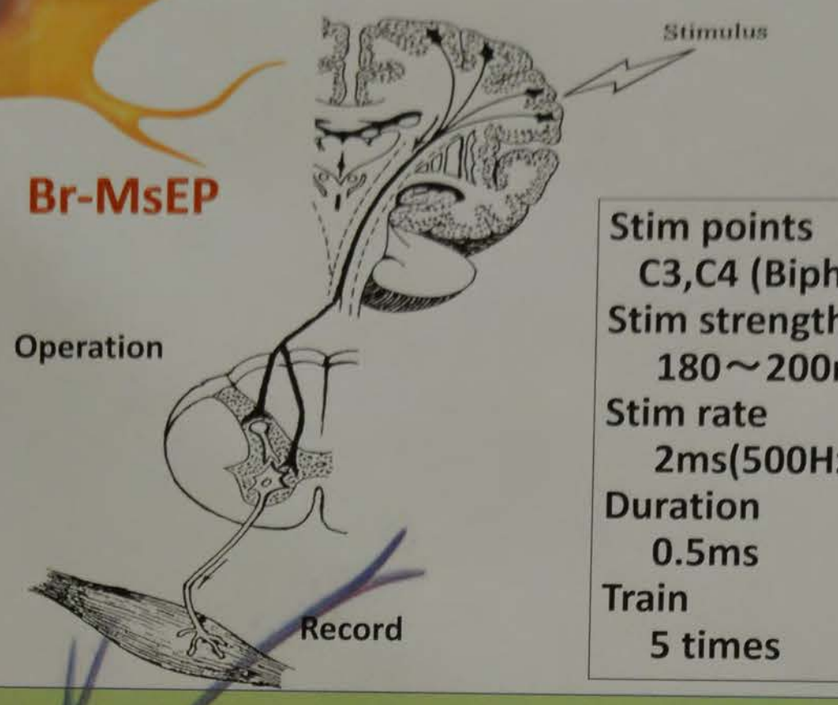

Stim points
C3,C4 (Biphasic)
Stim strength
180～200mA
Stim rate
2ms(500Hz)
Duration
0.5ms
Train
5 times

Anesthesia was achieved by complete vein anesthesia using propofol and remifentanil, with a muscle relaxant during intubation. Control waveforms were recorded after development after train of four was confirmed as >75%.

RESULTS & CONCLUSION

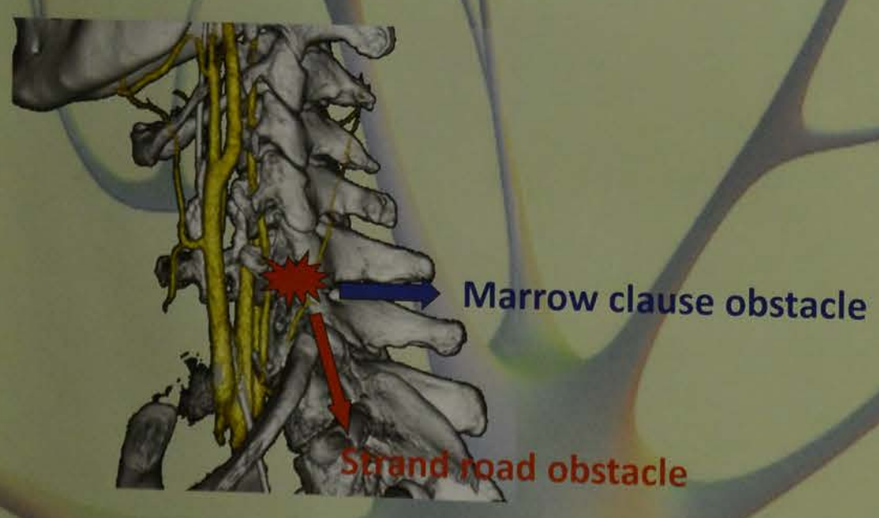

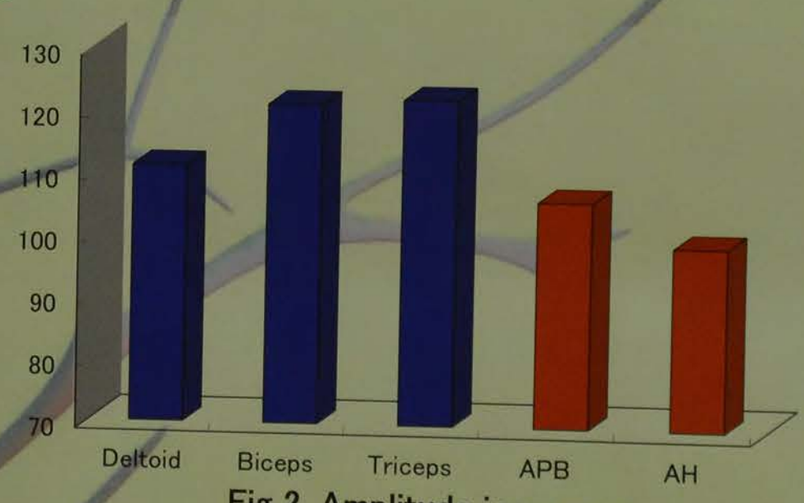

Fig 2. Amplitude increases

Increased amplitudes of evoked wave patterns reflected recovery of the marrow clause obstacle.

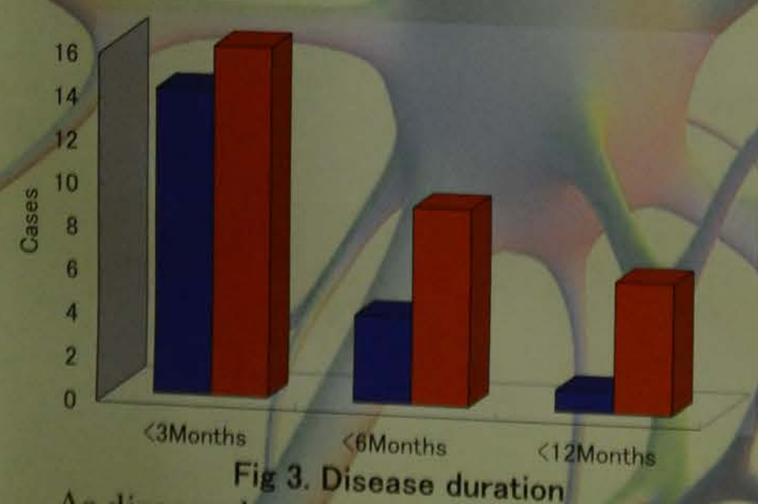

Fig 3. Disease duration

As disease duration is shorter cases, recovery of the waveform was remarkable.

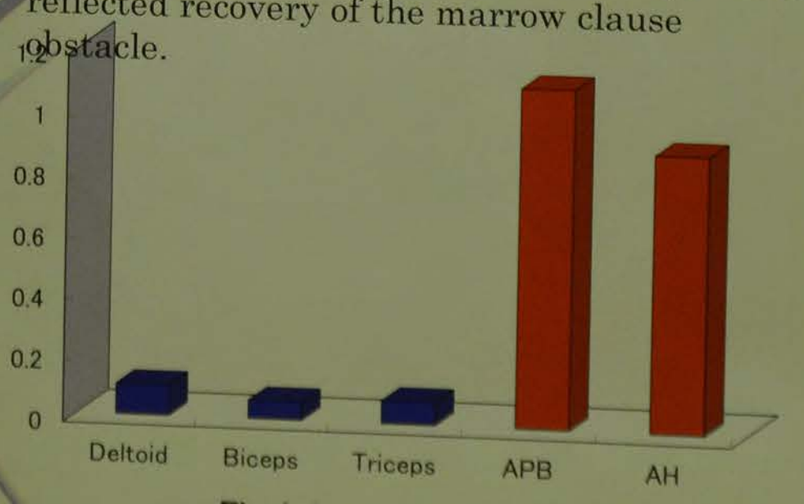

Fig 4. Latencies reduction

Latencies reduction suggests a recovery of the strand road obstacle.

Monitoring by sensing pressure on the nerve may not be required when spinal cord function is monitored during cervical spine surgery.

HANDA CITY HOSPITAL

Clinical Physiology

PG-23

Intraoperative motor evoked potential monitoring method utilizing cross-correlation coefficient

1) Hiroyasu OE, 2) Yusuke NAKADE, 3) Yuko NANBU, 4) Mikio NAGAHARA, 5) Mika MORI, 6) Kenshi HAYASHI, 7) Yoshio SAKAI, 8) Takashi WADA

1) ~8) Department of Clinical Laboratory, Kanazawa University Hospital
7), 8) Department of Nephrology and Laboratory Medicine, Graduate School of Medicine, Kanazawa University

Background

Measurements of motor-evoked potential (MEP) can be used to monitor nerve function during surgery. The induction of injury to the brain or spinal cord, or neuropathy in the perioperative period is judged by regular monitoring of nerve function in the operative field. MEP is measured by an electrophysiological technique to provide warnings of injury. However, the operative procedures frequently influence the operative environment such as temperature changes in the operative field, influenced by muscle relaxants, and electric noise. These factors affect the long-term recording of MEP, which makes their assessment difficult (Figure 1).

The present study aimed to determine the utility of a novel MEP monitoring method with the use of a cross-correlation coefficient (CR) to minimize the influence of environmental factors.

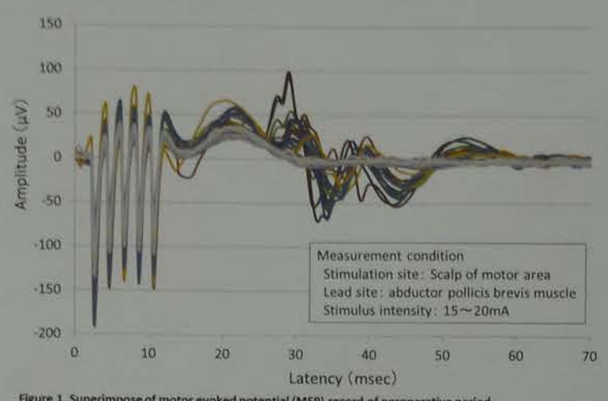

Figure 1. Superimpose of motor evoked potential (MEP) record of peroperative period.
All shapes of waves within the range of 0-25msec are artifacts that originate in stimulation. The muscular activity voltage caused by stimulation is admitted from 25-60msec. The artifact that originates in stimulation is larger than the evoked potential. In addition, the artifact is observed to influence the baseline. It causes it to measure the amplitude inaccurately.

Conclusion

The MEP-monitoring technique based on the CR has anti-noise characteristics, enabling the detection of slight changes in the evoked potential waveform. Therefore, this method could be useful as an intraoperative monitoring technique overcoming the issues associated with conventional methods.

Methods

MEP recording (Figure 2)

To record MEP, stimulation was achieved by puncturing the scalp with corkscrew electrodes at the area of the motor cortex (areas C3 and C4) and applying a voltage of 400–600 V and delivering a series of train stimulations (5; 500 Hz). Various muscles were used to measure MEP, including the abductor pollicis brevis (C6), quadriceps (L4), tibialis anterior (L4), gastrocnemius (S1), and inside plantar muscle (S1).

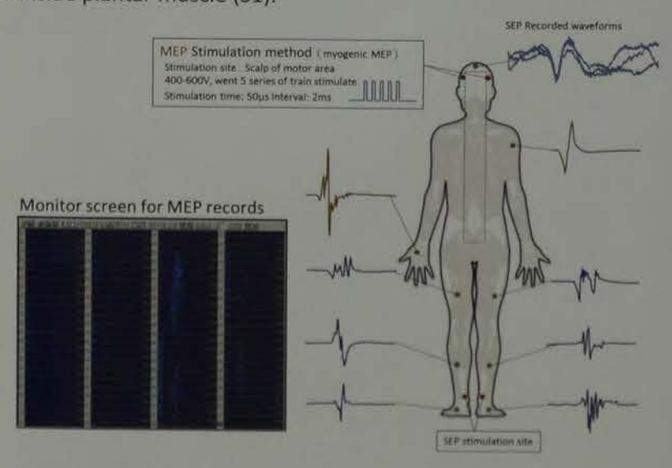

Figure 2. MEPs recordings.
The deriving site of MEP is properly selected according to the operative site. MEP is recorded with eight channels or less. MEP waveform is displaying that has been resampled. SEP is abbreviation of somatosensory evoked potentials. SEP records at the same time as MEP.

Calculation of the CR (Figure 3)

First, we re-sampled the recorded MEP waveform and excluded the background stimulation noise in it. Second, zero padding was performed for the reference MEP and object waveforms. Third, the crossing power spectrum was calculated from the reference and object waveforms processed by fast Fourier transform (FFT). Fourth, the cross-covariance function was obtained from the crossing power spectrum by reversely converting FFT. The cross-covariance function was normalized and the CR was calculated. The CR at cyclic time-zero point was τ0 CR and the maximum CR value was Max.CR.

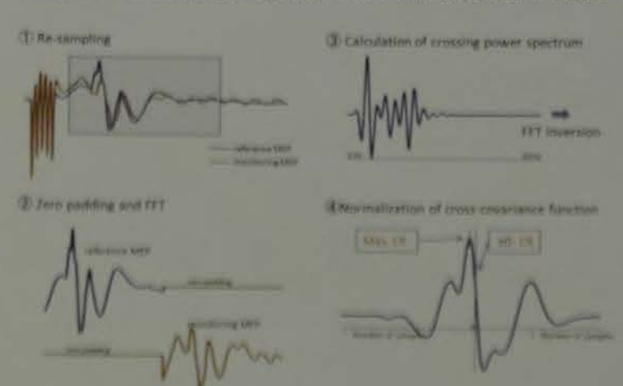

Figure 3. Calculation of cross correlation coefficient.
The part enclosed with the frame is a region where it is a resampling. FFT is abbreviation of fast Fourier transform. CR is abbreviation of the cross correlation function.

Results

Characteristics of the CR (Figure 4)

Scaling analysis was performed using a normal distribution model with a known probability distribution to clarify the character of the CR. The Max.CR did not decrease completely, however, τ0 CR displayed a tendency to decrease

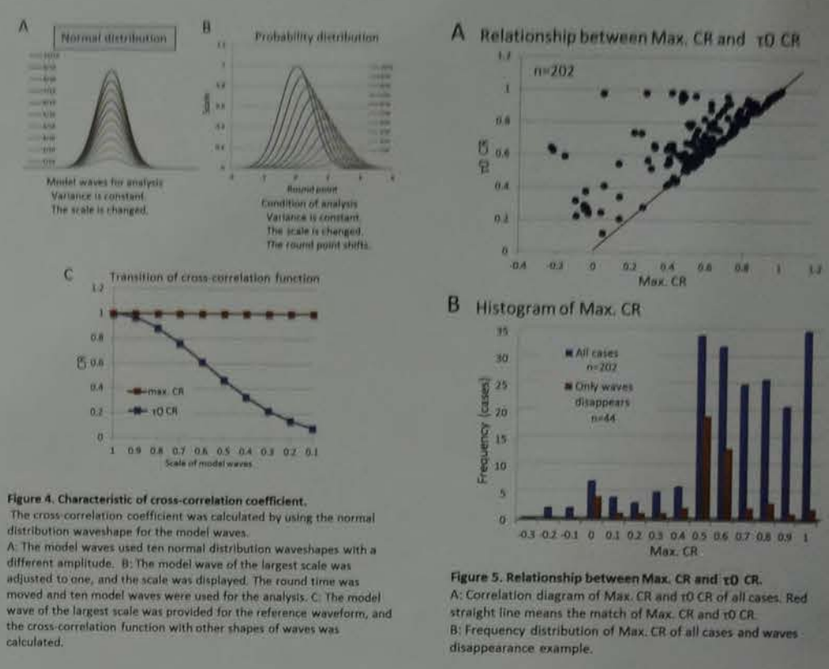

Figure 4. Characteristic of cross-correlation coefficient.
The cross-correlation coefficient was calculated by using the normal distribution waveshape for the model waves.
A: The model waves used ten normal distribution waveshapes with a different amplitude. B: The model wave of the largest scale was adjusted to one, and the scale was displayed. The round time was moved and ten model waves were used for the analysis. C: The model wave of the largest scale was provided for the reference waveform, and the cross-correlation function with other shapes of waves was calculated.

Figure 5. Relationship between Max. CR and τ0 CR.
A: Correlation diagram of Max. CR and τ0 CR of all cases. Red straight line means the match of Max. CR and τ0 CR.
B: Frequency distribution of Max. CR of all cases and waves disappearance example.

by the transition of the cross-correlation function along with a shift of the round point. The Max.CR detected a change in the attributes of the waveform rather than a change in its size.

Relationship between the amplitude of MEP, Max.CR and τ0 CR (Figure 5)

The relationship between the CR and the amplitude of MEP monitored by a conventional method showed no correlation. Identical and dissociated cases were observed between the Max.CR and τ0 CR. The cause of the dissociation was that the τ0 CR was lower than the Max.CR. A dissociation of Max.CR and τ0 CR was observed when there was a difference in the latency of MEP. A range of variation between -0.3 and 1 was observed in the MEP monitor, although, theoretically, it would have a variable range between -1 and 1 in the CR. Most CR values ranged between 0.5 and 1. In addition, the CR of the disappeared waveforms was not zero.

Case report

Case 1 (Figure 6). In accordance with the measurement parameters of the conventional method, only the appearance and disappearance of the waveform could be confirmed. On the other hand, a decreased tendency from 1.0 to 0.6 was gradually observed, and continuity was confirmed from the transition of the CR. However, even in a state of waveform disappearance, it was not zero. Thus, waveforms judged to have disappeared were not strictly of a zero potential.

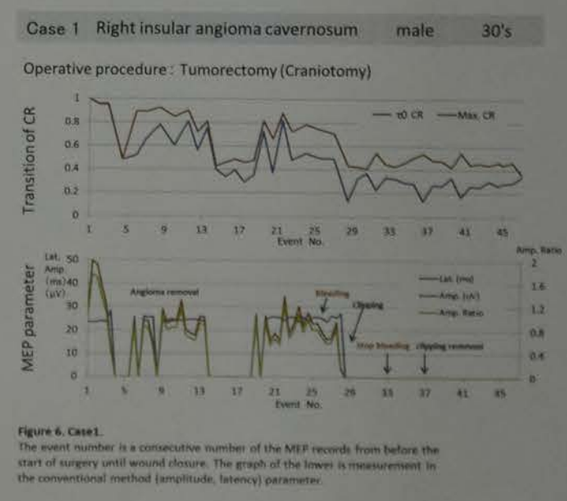

Figure 6. Case1.
The event number is a consecutive number of the MEP records from before the start of surgery until wound closure. The graph of the lower is measurement in the conventional method (amplitude, latency) parameter.

Case 2 (Figure 7). There was a remarkable dissociation of the CR in the waveform recovery period after tumor resection. In the first half of the progress, τ0 CR and Max.CR were almost in concordance, but a marked dissociation of Max. CR and τ0 CR was observed in the middle of recovery. The τ0 CR decreased because the recovery of the waveform had a short latency, which caused this dissociation.

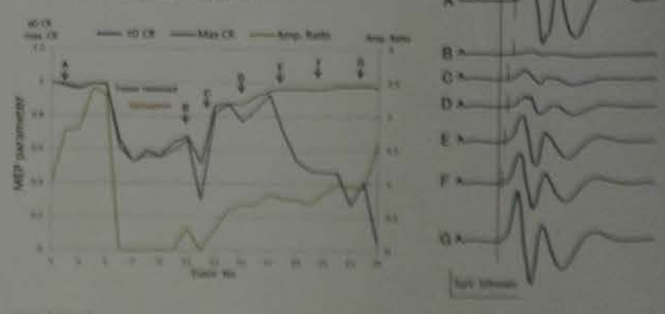

Figure 7. Case2.
The vertical letter alphabet in figure shows the CR and the actual waveform of each time point. A red straight line is indicating the latency time of the monitoring termination. A red, short line shows the latency of each waveform.

Discussion

- An MEP-monitoring technique based on the CR can capture a change in the entire waveform via the transition of continuous measurements. This method can observe partial changes in waveform that cannot be detected by methods with latency and amplitude measurements.
- Use of the CR is advantageous for recording measurements under loud environmental conditions because the CR removes random noise and only uses the periodic element of the waveform for calculations.
- Even when the waveform disappears, the CR is not zero, indicating that it may not explain all the variables.

Clinical Physiology

PG-24

Nocturnal sleep and respiration in pregnant women with and without obesity and non-pregnant women

Midori URA [1)2)], *Yuka Teramae* [3)], *Keisaku Fujimoto* [4)]

1) Department of Laboratory Medicine, Shinshu University Hospital
2) Graduate School of Medicine, Health Sciences, Shinshu University
3) Tokyo Metropolitan Ohtsuka Hospital
4) School of Health Sciences, Shinshu University

Introduction

Background

Obesity has become a major public health concern throughout the world. Serious global burden of overweight was reported the prevalence of obesity and overweight 2.1 billion worldwide in 2013[1)]. As a result, pregnant women with obesity have increased around the world. These women have a potential risk factor for the onset of complications associated with pregnancy; such as GDM[2)] and PIH[3)].

These complications may negatively correlate with maternal sleep and respiratory conditions. A number of previous study reported that pregnant women with or without obesity tend to suffer from sleep disorders, especially in the third trimester.

The cause of disordered sleep are thought to be movement of a fetus, difficulty in sleeping lying on the back, and frequent urinary urges due to oppression of the bladder by the fetus[4)]. In spite of these self-reported symptoms, little evidence is available regarding detailed nocturnal sleep and respiratory conditions in pregnant women.

GDM: gestational diabetes mellitus; PIH: pregnancy-induced hypertension

Purpose

We examined the nocturnal sleep and respiration of pregnant women with and without obesity and non-pregnant women in order to investigate the relationships between obesity and sleep disordered breathing in pregnant women.

Methods

Study subjects

- 10 pregnant women : at 37th week of pregnancy divided 2 groups based on BMI before pregnancy;
  - 5 pregnant women with obesity (BMI ≥30)
  - 5 pregnant without obesity (BMI <25)
  - 13 non-pregnant women (BMI <25)
- "BMI classification" of WHO[5)] were used.

Ethical issues

Informed consent was obtained from all the participants prior to study. This research protocol was approved by the Ethics Committee of School of Medicine, Shinshu University, Japan

Materials

- RDI (respiratory disturbance index): sensor sheet
- Oxygen saturation (SpO2): pulse oximeter
- Autonomic nerve activity : pulse wave sensor
- Quality of sleep : electroencephalogram (EEG)
- Self assessment on sleep : medical questionnaire

※photos were extracted from each HP of the device companies

Data collection & Statistical analysis

A number of participants increased after the abstract was accepted: Sample No. and results written here are different from the original abstract.

Subjects brought these 4 instruments home described above and put them on before going to bed to simultaneously record data during the night at least two nights to prevent from fault recordings. Ten of three pregnant women (with obesity) underwent recording in-hospital due to developing complications. Two women (with obesity) dropped out due to PIH at 37th and 34th weeks of pregnancy, respectively. Data for the same procedures were also collected from non-pregnant women for one night, as comparison controls. We analyzed these data including questionnaire (*P*SQI) and compare the pregnant women with obesity, non-obesity, and non-pregnant women. Data were expressed as mean ± standard deviation (SD). A Kruskal-Wallis *H* test was used for multiple data comparison, followed by post hoc analysis conducted with Mann-Whitney *U* test to compare between the two groups. *P* values under 0.05 were considered statistically significant. All data were analyzed using a software of StatFlex version 6 (Artech Co.,Ltd. Osaka, Japan).

Results

Table 1 Characteristics of study subjects (mean±SD)

	pregnant women BMI ≥30 (N=5)	pregnant women BMI <25 (N=5)	non-pregnancy BMI <25 (N=13)
Age (year)	32.0 ± 5.5 †	34.4 ± 4.7 †	22.5 ± 1.0
Height (cm)	158.2 ± 5.4	159.6 ± 3.6	160.7 ± 7.2
Weight (kg)	91.3 ± 12.3 *†	50.0 ± 4.1	52.2 ± 6.6
BMI	36.4 ± 3.3 *†	19.7 ± 1.4	20.2 ± 1.1
Gestational week	37th	37th	n/a

*p<0.05 vs. pregnant women BMI<25. †p<0.05 vs. non-pregnant women

Table 2 Comparison of sleep and respiratory conditions in 37th of gestational weeks of pregnant women with and without obesity and non-pregnant women

	pregnant women BMI ≥30 (N=5)	pregnant women BMI <25 (N=5)	non-pregnancy BMI <25 (N=13)
RDI	10.0 ± 2.6 *†	5.3 ± 2.3	3.6 ± 3.6
SpO2 (%)	94.4 ± 1.5 *†	96.6 ± 0.1	96.6 ± 0.5
Heart rate (bpm)	80.7 ± 12.2 †	70.5 ± 7.6 †	59.6 ± 5.8
EEG			
TIB (min)	396.4 ± 134.3	382.6 ± 59.8	377.7 ± 49.8
TST (min)	333.3 ± 119.9	301.9 ± 33.6	334.6 ± 55.8
Sleep latency (min)	32.2 ± 29.6	36.6 ± 19.4	22.8 ± 16.8
Arousal index	10.1 ± 6.7	11.7 ± 10.3	6.2 ± 4.1
REM sleep latency (min)	81.8 ± 33.4	67.7 ± 26.8	66.8 ± 24.8
Wake (%)	8.4 ± 5.6	9.8 ± 8.5	5.2 ± 3.4
N1 (min) (%)	39.1 ± 13.1 (12.3) †	24.9 ± 13.3 (7.6)	21.1 ± 5.7 (6.0)
N2 (min) (%)	213.4 ± 92.6 (57.5)	203.7 ± 21.8 (60.8) †	188.0 ± 37.6 (53.3)
N3 (min) (%)	2.0 ± 4.2 (0.4) †	0.4 ± 0.5 (0.1) †	29.8 ± 30.9 (8.0)
REM sleep (min) (%)	78.8 ± 31.3 (21.5) †	73.0 ± 14.7 (22.2)	95.7 ± 17.1 (27.5)
WASO (min)	27.9 ± 13.4	36.1 ± 35.1	18.2 ± 11.8
Sleep efficiency (%)	83.8 ± 9.5	79.7 ± 8.9 †	88.4 ± 5.8
Delta power	2439.2 ± 1168.3	3051.9 ± 1160.3	8848.7 ± 8549.8
*P*SQI score (1-21)	8.8 ± 3.7 *†	6.6 ± 1.9 †	3.9 ± 1.4
Complications	GDM: 4, PIH:3	none	n/a
Delivery: Vaginal / C/S	virginal:3, C/S:2	virginal:3, C/S:2	n/a
Infants	Healthy:5	Healthy: 4, FGR:1	n/a

BMI: body mass index; RDI: respiratory disturbance index; TIB: time in bed; TST: total sleep time; REM: rapid eye movement sleep; N1: non REM1; WASO: wake after sleep onset; PSQI: Pittsburgh Sleep Quality Index; C/S: Caesarean section; FGR: fetal growth restriction. PSQI score ≤ 5=no sleep disorder, 6-8=mild sleep disorder, ≥ 9=severe sleep disorder

Fig. Examples of visualized data

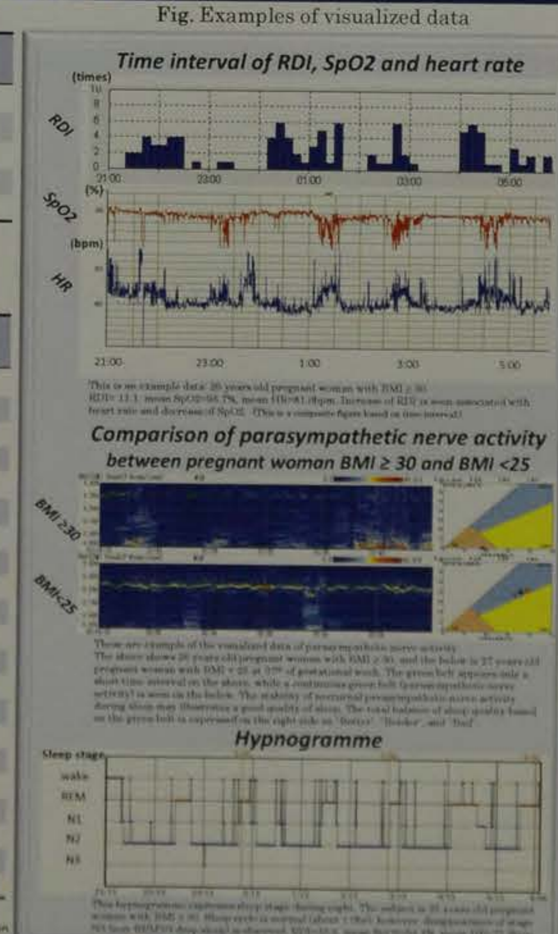

Fig. Comparison of indicators in 3 groups

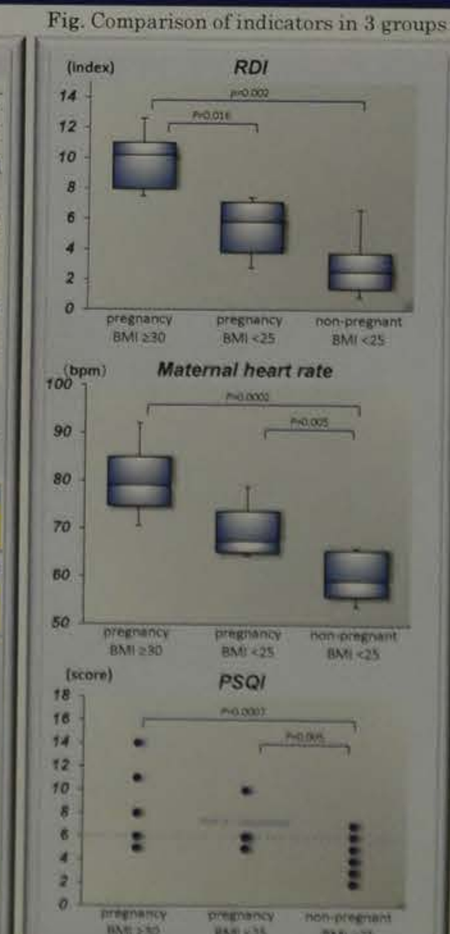

Discussions

*P*SQI(self-report questionnaire) indicates significantly increased sleep disorder in pregnant women regardless of BMI. In fact, sleep quality measured by the objective examinations deteriorated in pregnant women, particularly in those with obesity. Increased RDI with decreased SpO2, namely, sleep apnea syndrome was observed among pregnant women with obesity. These results may possibly be related to the onset of PIH because what the findings concurrently demonstrated is increases in heart rate, lack of deep sleep and unstable parasympathetic nerve activity. These indicators of sleep disordered breathing are reported to be a cause of hypertension in general population[6)]. Therefore, our findings may suggest a relationship between sleep disordered breathing and PIH in pregnancy. If the onset of sleep disordered breathing develop first followed by PIH, early diagnosis will be possible by measuring a quality of nocturnal sleep. As limitations, to deal with confounding factors and bigger sample size with longitudinal study are necessary to be addressed for further research.

Conclusion

The pregnant women with BMI≥30 experienced more serious sleep disordered breathing and complications during pregnancy. Deteriorated sleep quality may be related to the development of pregnancy-induced complications. Checking sleep quality in pregnant women with obesity might contribute to early diagnosis of pregnancy-induced hypertension.

References

1) [illegible] The Lancet [illegible]
2) [illegible] Diabetes Care [illegible]
3) [illegible]
4) [illegible] Sleep Medicine [illegible]
5) WHO. BMI classification. [illegible]
6) [illegible] New England Journal of Medicine [illegible]

Clinical Physiology

PG-25

Influence of changes of head position on balance assessed by the Gravicorder (Consideration of the output test and Frankfort horizontal plane)

Kinuyo Sasahara、Yukiko Toriumi、Yasuko Oda、Yuuko Tanaka

Kanagawa Dental University Yokohama Clinic Clinical Laboratory

Introduction

It has been reported that head position (submaxillary position) is important for balance.

We studied the relation between balance and head position, as well as the relations between balance and the output test or the Frankfort horizontal plane.

Subjects

The subjects were 49 persons (28 males and 21 females).

	Age	Height
Males	25.4±2.35	170.9±5.60cm
Females	25.1±3.00	159.7±5.87cm

Methods

They underwent assessment of balance by Gravicorder (Fig1)with head position changes. They also underwent the Mann test, one-leg test, blindfolded vertical writing test,(Fig2) stepping test(Fig3), hearing test, and assessment of the Frankfort horizontal plane.(Fig4)

Fig1

Body balance of Gravicorder

*Open and close eyes each one minute

*the 90 degrees head position
the 45 degrees head position

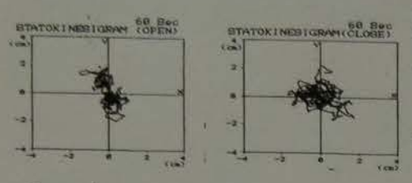

Check Item of Gravicorder

* Total Physical unrest trace Distance
* Envelope area

Fig2

blindfolded vertical writing test

*Black:open eyes
*Red:Close eyes

Angle with a red line and the black line
Less than normal level 10 degrees

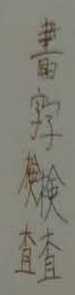

Fig3

Stepping test

*Close Eyes *Check Item
*100 Steps Shift distance
Shift angle

Fig4

The Frankfort horizontal plane.

Measurement angle

Root of nose and The pupil center — The porion and The orbitale

The front — The side

the Mann test: stand with other tiptoe to a heel, close eyes, 30 seconds
one-leg test : stand with one-leg ,close eyes , 30 seconds
hearing test :125Hz-8kHz pure tone ,hearing average dB(500Hz+1kHz+2kHz)/3

Results

1.Most of the subjects showed no problems in the hearing test, Mann test, one-leg test, and blindfolded vertical writing test.(table1.)

table1.

	mann test(%)	one-leg test(%)	writing test(%)	hearing test(Ave±SD)
Male	9.3	14.3	0.36	8.3±3.54dB
Female	0	9.5	14.3	7.7±2.50dB
	Ratio of the standard value outside(%)			

2.The Frankfort horizontal plane
It is a plane told to become approximately parallel to the verge surface of the earth where I stood straight. General average : 90degrees
I show the average of subjects in table 2.

The Frankfort horizontal plane(degrees of Angle).

Table2.

	The front(°)	The side(°)
Male	90.8±10.47	92.1±9.36
Female	84.5±19.95	89.3±6.50

3.When the influence of head position changes on balance was investigated, there was a significant difference of the deflection envelope area between the 90 degrees head position and the 45 degrees head position (t-test).(table3.)

Table3.

Head position 90 degree and 45 degree(Value of T-test) *P<0.05

	Distance (open-eyes)	Dostance(close-eyes	Envelope area(open-eyes	Envelope area(close-eyes)
Male	0.0735	0.2511	0.0965	0.2257
Female	0.4599	0.1443	0.4483	*0.0338

4.With regard to the Frankfort horizontal plane and the stepping test, a significant correlation between balance (deflection envelope area) and the Frankfort horizontal plane or stepping test was found (Pearson's test).(Fig5・Fig6)

Fig5

Frankfort horizontal plane and envelope area of 90degrees

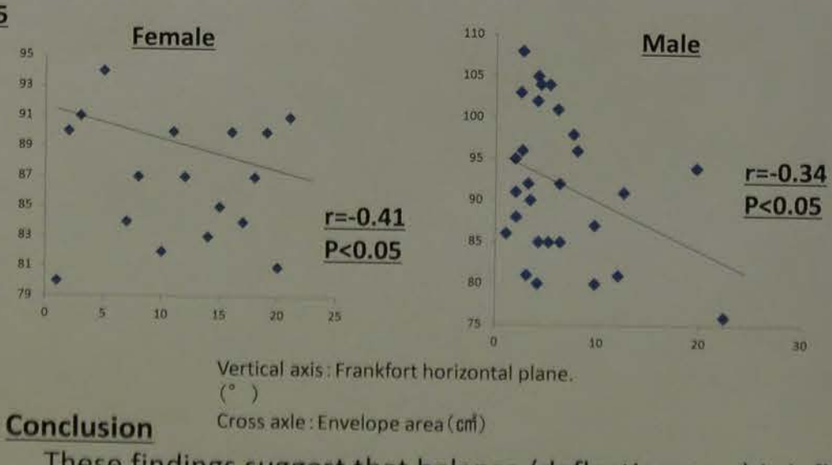

Vertical axis : Frankfort horizontal plane. (°)
Cross axle : Envelope area (㎠)

Fig6

Stepping test and envelope area of 90degrees

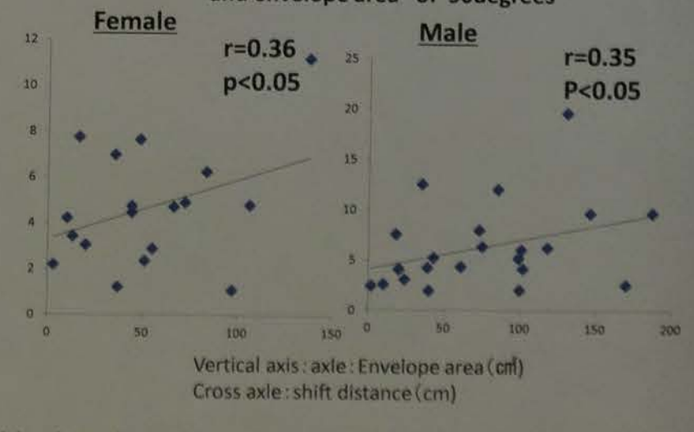

Vertical axis : axle : Envelope area (㎠)
Cross axle : shift distance (cm)

Conclusion

These findings suggest that balance (deflection area) is influenced by head position and the Frankfort horizontal plane in the stepping test.
At the position of the head, significant difference of 45 degrees and 90 degrees appeared to the woman who had low height, but it was thought that I was connected with a position and the height of the center of gravity.
However, in Frankfurt plane and stepping test, I was associated with an area of the unrest regardless of height.
It was guessed that the skewness of the face for the horizontal plane and the physical deviation were related to physical unrest.

Clinical Physiology

PG-26

The estimated pulmonary artery systolic pressure by echocardiography to grade the severity of heart failure

Shunsuke Suzuki[1)], Maki Naito[1)], Naoki Hiramatsu[1)], Akihiro Sonoda[1)], Hiroki Sakamoto[2)], Genichi Sakaguchi[3)], Toshio Shimada[1),4)]

1. Department of Clinical Laboratory Medicine, Shizuoka Prefectural Hospital Organization, Shizuoka General Hospital
2. Cardiovascular Medicine, Shizuoka Prefectural Hospital Organization, Shizuoka General Hospital
3. Cardiovascular Surgery, Shizuoka Prefectural Hospital Organization, Shizuoka General Hospital
4. Clinical Research Center, Shizuoka Prefectural Hospital Organization, Shizuoka General Hospital

Introduction

- Transthoracic echocardiography (TTE) method is one of the most reliable methods that can easily estimate pulmonary artery pressure. It is well known in clinical practice that the severity of heart failure sharply reflects the pulmonary artery pressure. A good positive correlation has been already reported between estimated pulmonary artery pressure (PASP, PADP) measured by TTE and pulmonary artery pressure (PASP, PAWP) by RHC.
- Natriuretic peptide family (NPF), such as BNP, NT-proBNP and ANP belonging to heart-derived sodium peptide family are already well known as plasma biomarkers that reflects sharply the severity of heart failure. In particular, BNP and NT-proBNP have been widely and clinically used, these biomarkers reflect on information on heart failure status involving both exercise closely related to everyday life and rest.

Object

We validate clinical usefulness of PADP and PASP through comparison between NPF and estimated PASP and PADP by TTE.

Materials and Methods

- This study subjects were 218 patients visiting our outpatient clinic from July, 2014 to January 2015 and in whom blood sampling was implemented at the same day.
- Tricuspid valve regurgitation pressure gradient (TRPG) were calculated from recorded tricuspid regurgitation velocity using continuous wave Doppler with the law of the Bernoulli's principle. Pulmonary atrial systolic pressure (PASP) (PASP=TRPG+RAP) was calculated by adding right atrial pressure (RAP), which was estimated from the inferior vena cava to TRPG.
- Statistical analysis was performed using logistic linear regression model which had a categorical dependent variable divided into two groups by the median of PASP and independent variables, including NPF and other variables.
- As a result, statistically extracted significant variables were compared among quartile groups by one way ANOVA and if necessary, followed by post-hoc test. A $p<0.05$ was considered statistically significant.
- Data with normal distribution were expressed with the average value (standard deviation), data without normal distribution were expressed with the median (range).

- Exclusion criteria :
  - ✓Heart failure of hyper-acute phase (1 to 3 postoperative day)
  - ✓Atrial fibrillation cases
  - ✓Renal dysfunction cases (cystatin C eGFR <30mg/l)
  - ✓Congenital heart disease (including post-operative).

218 patients undergoing blood sampling and PASP measurement at the same day.

↓

Multivariate logistic linear regression analysis.
Dependent variable :PASP category data. 1:PASP≥24mmHg(median), 2:PASP<24.2mmHg

←– (If NPF-significant variable)

One-way ANOVA → (if necessary) → Post-hoc test

Results

- The 218 patients consisted of 118 men (54.6%) and100 women (45.4%); mean age 71.1 years (11.4), 159 patients (73.6%)with CHF and 121 patients (56.0%)with HT.
- The average value of NPF was ANP: 32.8 pg / dl (5.3 ~ 339.6 pg / dl), BNP: 53.6 pg / dl (6.0 ~ 889.5pg / dl), NT-proBNP: 215.6pg / dl (18.6 ~ 4466.0pg / dl), respectively.
- The average value of EF was 60.1% (11.2%) and that of PASP was 25.5 mmHg (8.0mmHg).

Table Patient characteristic and echocardiographic measurements

age, year	71.1 (11.4)	LVDd, mm	48.3 (7.2)	AR, %	
sex, %	118 (54.6)	LVDs, mm	32.8 (8.0)	normal	87 (40.3)
	98 (45.4)	IVS, mm	8.8 (2.1)	trivial	67 (31.0)
height, cm	159.4 (9.2)	PWT, mm	8.8 (1.5)	mild	45 (20.8)
weigth, kg	56.5 (11.0)	LVMI, ml/m^2	95.1 (33.4)	moderate	17 (7.9)
BMI	22.1 (3.4)	EDV, ml	79.3 (38.4)	sevrer	0(0)
BMS	1.6 (0.2)	ESV, ml	34.9 (31.1)	AS, %	
sBP, mmHg	129.3 (20.8)	EF, %	60.1 (11.2)	normal	192 (90.1)
dBP, mmHg	72.1 (12.9)	LAVI, ml/m^2	39.7 (17.3)	mild	10 (4.7)
HR, bpm	72.0 (14.1)	E wave, cm/sec	62.3 (24.0)	moderate	6 (2.8)
NYHA (%)	131 (61.5)	A wave, cm/sec	75.7 (22.2)	severe	5 (2.3)
	51 (23.9)	E/A	0.9 (0.5)	MR, %	
	25 (11.7)	DecTime, sec	251.7 (196.6)	mormal	26 (12.0)
	6 (2.8)	E wave, cm/sec	5.5 (3.2)	trivial	102 (47.2)
		E/e	12.6 (6.0)	mild	68 (31.5)
Angina pectoris, %	45 (20.8)	TR peak vel, m/sec	2.3 (0.4)	moderate	15 (6.9)
Hypertension, %	121 (56.0)	TRPG, mmHg	22.0 (7.4)	severe	5 (2.3)
Hyperlipidemia, %	95 (44.0)	SPAP, mmHg	25.5 (8.0)	MS, %	
Chronic heart failure, %	159 (73.6)	PADP, mmHg	7.6 (4.7)	normal	213 (98.6)
Diabetes mellitus, %	53 (24.5)	PAEDP, mmHg	4.3 (3.8)	mild	2 (0.9)
Acute myocardial infarction,%	3 (1.4)	RAP, mmHg	3.0 [0, 15.0]	moderate	1 (0.5)
Dilated cardiomyopathy, %	7 (3.2)			severe	0(0)
Old myocardial infarction, %	10 (4.6)				
ANP, pg/dL	32.8 [5.3, 339.6]				
BNP, pg/dL	53.6 [6.0, 889.5]				
NT-proBNP, pg/dL	215.6 [18.6, 4466.0]				
Creatinine, mg/dL	0.8 [0.4, 2.0]				
Cystatin C, mg/L	1.0 [0.6, 2.0]				
cys.c EGFR	69.4 (22.1)				
eGFR.cre	67.3 (22.3)				

Table2 Multivariate logistic regression analysis

	Estimate	Odds ratio	95% CL	95% CL	p value
Intercept	6.12614		1.09624	11.52182	0.02070
age	-0.07244	0.00839	-0.11746	-0.03185	0.00090
BMS	2.00014	4.75714	-0.14256	4.23022	0.07200
LAVI	-0.02437	0.19062	0.05332	0.00329	0.08950
EA	-2.51601	0.00008	-3.94759	-1.23171	0.00030
Ee	0.01624	1.62593	0.07414	0.10891	0.72310
ANP	-0.02857	0.75147	-0.04597	-0.01246	0.00080

	Estimate	Odds ratio	95% CL	95% CL	p value
Intercept	7.51807		2.42072	13.02311	0.00530
age	-0.08967	0.00269	-0.13589	-0.04831	<.0001
BMS	1.63071	3.58649	-0.47593	3.81656	0.13430
LAVI	-0.02310	0.20784	0.05128	0.00380	0.09770
EA	-2.79381	0.00030	-4.24832	-1.50117	<.0001
Ee	0.02214	1.93993	-0.07035	0.11561	0.63820
NT_proBNP	-0.00146	0.98532	0.00255	-0.00051	0.00420

	Estimate	Odds ratio	95% CL	95% CL	p value
Intercept	8.27373				0.01810
age	-0.07841	0.00565	0.00030	0.08222	0.00030
BMS	1.82089	4.13661	0.79537	23.04140	0.09640
LAVI	-0.01941	0.26718	0.03858	1.73924	0.17100
EA	-2.51039	0.00069	0.00001	0.02945	0.00030
Ee'	0.01231	1.44540	0.09742	21.45169	0.78740
BNP	-0.00804	0.92279	0.00020	0.16579	0.00330

10 times odds for ANP, BNP or NT-proBNP were calculated and one unit odds for the other parameters were calculated.

Univariate logistic regression analysis was performed using 3 models that incorporate individually ANP, BNP or NT-proBNP as an independent variable. In each model, ANP,BNP or NT-proBNP was extracted as a significant independent variable, respectively.

Figure One-way ANOVA and post-hoc test

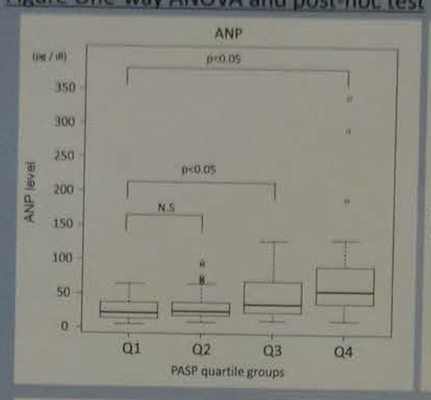

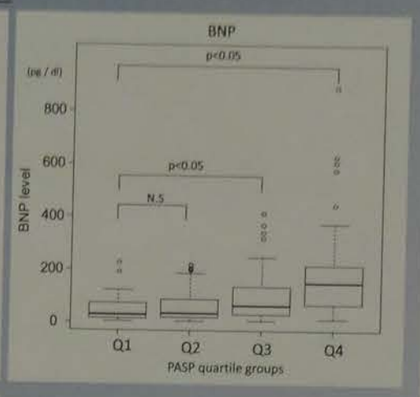

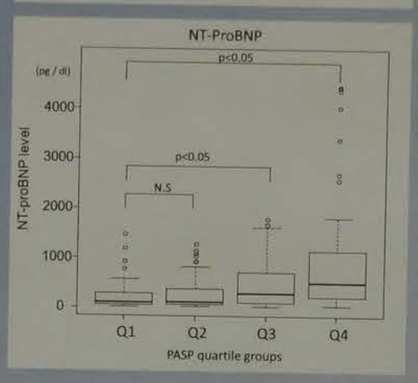

This graph showed the results of a post-hoc test. PASP has been divided into four groups of the quartiles.
Q1: 18.4mmHg (5.1-21.0mmHg),
Q2: 22.8mmHg (21.0-24.2mmHg),
Q3: 26.1mmHg (24.2-29.2mmHg),
Q4: 32.6mmHg (29.4-65.7mmHg).

NFP was analyzed by actual measurement values with no logarithmic transformation. The lowest quartile group of PASP was chosen as control group and as a result, each natriuretic peptide concentration was significantly higher in Q3 and Q4-group than in control group.

Discussion

- PASP increased proportionately with the increment of NPF and then, PASP may be able to assess the severity of heart failure correctly.
- In addition, in recent years, it has been reported that an increased PASP indicates a higher total mortality risk.
- In this study, irrelevant to age and cardiopulmonary diseases, a higher PASP indicated a higher mortality risk.
- Whenever PAWP is high, PASP is always high as we often experience in clinical practice.
- Therefore, this study was carried out to validate whether we were able to use PASP as an alternative pressure of PAWP or not.
- PASP rises up to a higher pressure when heart failure exacerbation usually increases peptides of NPF.
- As a result, PASP was a reliable parameter to evaluate the severity of heart failure.

Limitation

- PASP must be measured through TRPG. This study was planned only for cases to be able to visualize TR.
- However, in pathophysiological conditions (heart failure), it is convenient in clinical practice that pulmonary arterial pressure elevates to improve a detection rate of tricuspid regurgitation.

Conclusion

- PASP offers us an important information on overt heart failure.
- Judging from the fact that PASP is closely related to the NPF which reflect accurately the objective severity of heart failure, we conclude that PASP can be used as a potent biomarker for assessing the severity of heart failure, and monitoring therapeutic effect.

Clinical Physiology

PG-27

Novel Echocardiographic Method to Estimate Pulmonary Vascular Resistance Based on Measurements of Pulmonary Regurgitant velocities

Sanae Kaga [1], Kazunori Okada [1], Nobuo Masauzi [1], Masahiro Nakabachi [2], Hisao Nishino [2]
Shinobu Yokoyama [2], Mutsumi Nishida [2], Taisei Mikami [1]

[1] Faculty of Health Sciences, Hokkaido University, [2] Division of Laboratory and Transfusion Medicine, Hokkaido University Hospital.

Background

- Pulmonary vascular resistance (PVR) is an important hemodynamic parameter in patients with heart failure.
- Several echocardiographic methods to estimate PVR have been proposed, but their applications in patients with organic left-sided heart diseases have been limited.
- The early- and end-diastolic pulmonary arterial (PA) - right ventricular (RV) pressure gradients derived from pulmonary regurgitant (PR) velocities reflect the mean PA pressure and the PA wedge pressure, respectively, and may enable an accurate estimation of PVR.
- The aim of the present study was to examine the usefulness of our new method to estimate PVR (PVR_{PR}) based on the continuous-wave Doppler velocity measurements of PR in patients with left heart disease.

Methods

- **Subjects**
  - Study subjects were 43 patients who underwent right heart catheterization and echocardiography within one day.
  - 29 males and 14 females
  - 59±17 years (20 to 88 years)

  Exclusion criteria: patients with severe tricuspid regurgitation, non-sinus rhythm
- **Calculation of PVR from right heart catheterization parameters**
  - PVR_{CATH} = (mean PA pressure – PA wedge pressure)/cardiac output
- **Calculation of PVRs from echocardiographic parameters**
  - PVR-Scapellato
    $=-0.156+1.154\,[(ICT_{RV}/ACT_{RVOT})/TT_{RV}]$
  - PVR-Abbas-2003
    $=10\times TRV/TVI_{RVOT}+0.16$
  - PVR-Dahiya
    $=(TRPG+10-E/e')/TVI_{RVOT}$
  - PVR-Lindqvist
    $=0.95(2.44\times TRV^2-3)/CO_{LVOT}-0.29$
  - PVR-Abbas-2013
    $=5.19\times TRV^2/TVI_{RVOT}+0.4$
  - PVR-Kanda
    $=(TRPG-EDPG)/3CO_{LVOT}$
  - PVR_{PR}
    $=(RFPG-EDPG)/CO_{LVOT}$

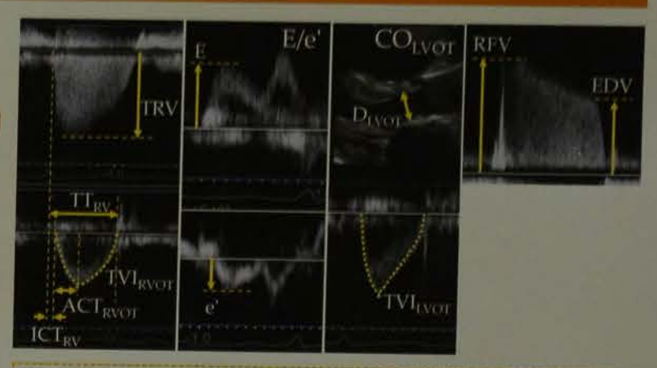

TRV: tricuspid regurgitant velocity, ICT_{RV}: RV isovolumic contraction time, ACT_{RVOT}: acceleration time of RV ejection flow, TT_{RV}: total RV systolic time, TVI_{RVOT}: time velocity integral of RV ejection flow, RFV: early diastolic PR velocity, EDPG: end diastolic PR velocity, E: early diastolic transmitral flow velocity, e': early diastolic mitral annular velocity, D_{LVOT}: diameter of the left ventricular outflow tract, TVI_{LVOT}: time velocity integral of left ventricular ejection flow, TRPG: systolic RV-right atrial pressure gradient, CO_{LVOT}: echocardiographic cardiac output, RFPG: early diastolic PA-RV pressure gradient, EDPG: end diastolic PA-RV pressure gradient

Results

- **Patient characteristics**

Age (yrs)	59 ± 17
Male/female	29/14
Heart rate (bpm)	71 ± 17
Body surface area (m^2)	1.69 ± 0.23
Systolic blood pressure (mmHg)	114 ± 26
Diagnosis	
Ischemic cardiac disease	20
Cardiomyopathy	11
Valvular heart disease	7
Others	5
Right heart catheterization	
Pulmonary artery systolic pressure (mmHg)	32 ± 14
Mean pulmonary artery pressure (mmHg)	21 ± 10
Pulmonary artery wedge pressure (mmHg)	14 ± 8
Cardiac output (l/min)	4.3 ± 1.1
Pulmonary vascular resistance (WU)	1.9 ± 1.1
Echocardiography	
Left ventricular end-diastolic dimension (mm)	60 ± 16
Left ventricular mass index (g/m^2)	137 ± 55
Left ventricular ejection fraction (%)	43 ± 19
Left atrial volume index (ml/m^2)	49 ± 25
Systolic RV-right atrium pressure gradient (mmHg)	29 ± 14
Early-diastolic PA-RV pressure gradient (mmHg)	16 ± 9
End-diastolic PA-RV pressure gradient (mmHg)	6 ± 5
Inferior vena cava dimension (mm)	15 ± 5
E (cm/sec)	82 ± 27
Septal e' (cm/sec)	6.2 ± 2.6
E/septal e'	14.5 ± 6.3

- **Correlation between PVR_{CATH} and the echocardiographic PVRs**
  - Our PVR_{PR} best correlated with PVR_{CATH} (r=0.81, p<0.001).

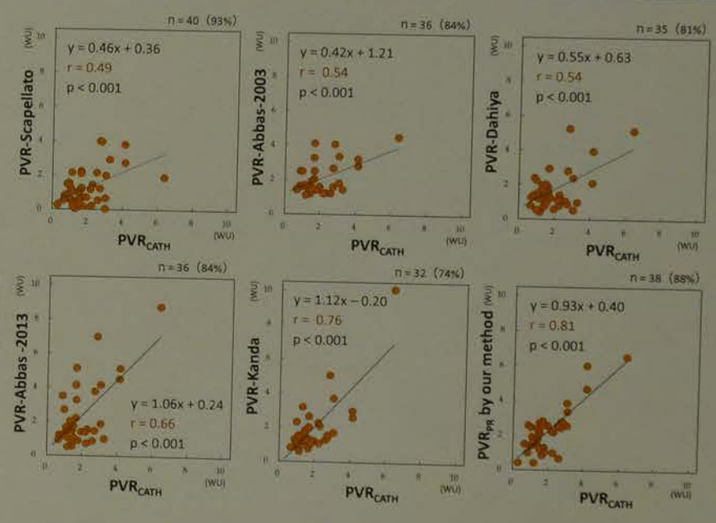

- **ROC curves to discriminate patients with PVR_{CATH} >3 WU by the echocardigraphic PVRs**
  - The AUC was the greatest for PVR_{PR} (0.964).

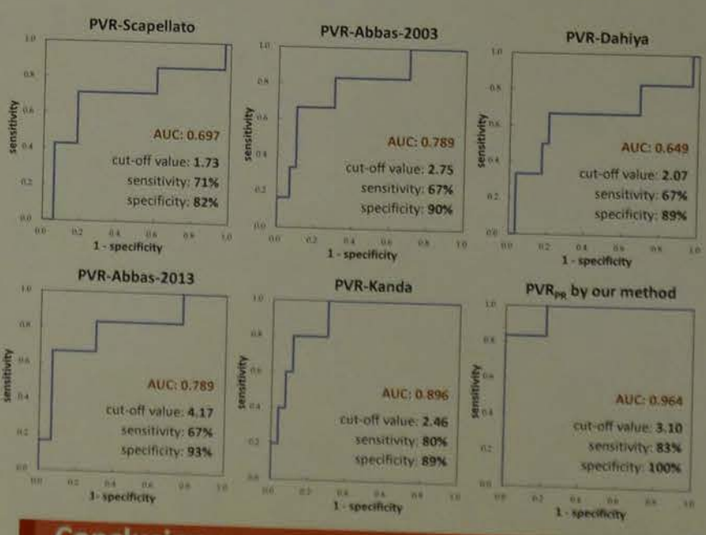

Summary of the results

- The PVR_{PR} better correlated with PVR_{CATH} (r=0.81, p<0.001) than any of the conventional echocardiographic PVRs.
- In the ROC analyses to determine the patients with abnormal elevation of PVR_{CATH} (>3 WU), the AUC was greater for PVR_{PR} (0.964) than the conventional PVRs (0.649-0.896).
- PVR_{PR} had 83% sensitivity and 100% specificity at the optimal cut-off value of 3.10 WU in identifying patients with PVR_{CATH} >3 WU.

Conclusion

- Our new method based on the continuous-wave Doppler measurements of early- and end-diastolic PA-RV pressure gradients is useful for the noninvasive estimation of PVR in patients with left-sided heart diseases.

Clinical Physiology

PG-28

Diagnosis of multiple atrial septal defects by transthoracic echocardiography

Nobuhisa Watanabe[1], Hiroki Oe[2], Teiji Akagi[3], Yoichi Takaya[3], Ken Okada[1], Hiroshi Ito[3]

1. Division of Medical Support, Okayama University Hospital, Okayama, Japan
2. Department of Cardiovascular medicine, Okayama University, Okayama, Japan
3. Division of Cardiac Care Unit, Okayama University Hospital, Okayama, Japan

BACKGROUNDS

- Atrial septal defect (ASD) has an variety of forms according to its anatomy and location. Centrally placed defects, defects with deficient rim, multiple defects, and perforated aneurysms of the interatrial septum are morphological variations of secundum type ASDs suitable for transcatheter closure using Amplatzer septal occluder (ASO) ®.

(Catheter Cardiovasc Interv 2001; 53: 386-391)

- The prevalence of multiple ASDs is approximately 8-10% of all ASDs and transcatheter closure of ASDs is currently a reliable alternative to surgery, even though challenging in patients with multiple ASDs.

(Clin. Cardiol. 2009; 32: 130–134)

- An accurate evaluation of the atrial septum is crucial to rule in or out the possibility of multiple defects. This has been done by careful interrogation of the atrial septum by color Doppler echocardiography, preferably by transesophageal echocardiography (TEE).

(Eur Heart J, 2000; 21: 941-947)

- This can be difficult to diagnose using transthoracic echocardiography (TTE) as abnormal color flow obscures the origins of the shunt, particularly if the second defect is situated inferiorly.

(Cardiovascular Ultrasound 2004;2:9)

- Transcatheter closure of multiple ASDs is safe and efficient. During the procedure, 2 occluders are necessary for the distance of 2 ASDs more than 7 mm, and a single occluder is sufficient for those 7 mm and less.

(Clin. Cardiol. 2009; 32: 130–134)

AIM

- In this study, we prospectively investigate the diagnostic ability of TTE for patients with multiple ASDs in our institution.
- Also, we investigate the morphological characteristics in patients with multiple ASDs diagnosable by TTE.

METHODS

- Between January 2006 and May 2012, we enrolled consecutive 420 patients with secundum ASD referred to our institute for transcatheter closure.
- All patients underwent TTE first and then TEE before the procedure.
- All TTEs were performed by well-trained sonographers.
  - ✓ We have defined considerable experiences for the well-trained sonographer. (more than 50 patients with ASDs / year)
- We have checked the timing when the accurate diagnosis was made.
  - ✓ First timing: preliminary diagnosed with multiple ASDs at the first visit.
  - ✓ Second timing: diagnosed by TTE
  - ✓ Third timing: diagnosed by TEE.
  - ✓ Final timing: diagnosed during the sizing balloon procedure.
- We have investigated the morphological characteristics in patients with diagnosable multiple ASDs by TTE.
  - ✓ Exact number of defects
  - ✓ Positional relationship of these defects to each other
  - ✓ Distance of these defects to each other
  - ✓ Diameter of minor defect

RESULTS

- Thirty-nine patients (9.3%) were diagnosed with multiple ASDs.
  - ✓ 30 females (76.9%)
  - ✓ Mean age: 42.0±23.0 years
- Thirty patients (76.9%) were diagnosed by TTE and 7 patients (17.9%) were diagnosed by subsequent TEE. Two patients (5.1%) were diagnosed during the sizing balloon procedure. (Figure 1)

Figure 1. Study flow-chart showing the diagnosis timing of 39 multiple ASDs.

Patients with multiple ASDs (n=39)
PRELIMINARY DIAGNOSED → 4 (10.3%)
DIAGNOSED BY TTE → 30 (76.9%)
↓ 9 patients
DIAGNOSED BY TEE → 7 (94.9%)
↓ 2 patients
DURING THE SIZING BALLOON PROCEDURE → 2 (100%)

- The diameter of the ASDs and the distance between the 2 ASDs of these patients are detailed in Table 1.

Table 1	Diagnosable (n=30)	non-diagnosable (n=7) *
Diameter of Major Defect	15.4±5.3 mm	20.9±9.2 mm
Diameter of Minor Defect	5.1±2.8 mm	4.1±1.6 mm
Distance between the defects	8.1±4.9 mm	4.1±1.6 mm

* Two patients diagnosed during the balloon sizing procedure were excluded.

- The morphological characteristics of patients diagnosable and non-diagnosable by TTE in table 2.

Table 2		diagnosable	non-diagnosable
Exact number of defects	2 defects	19	6
	>2 or fenestration	11	1
Positional relationship	Superior/inferior	13	5
	Anterior/posterior	10	2
	Diagonal	1	-
	Fenestration	6	-
Distance of defects	< 7mm	10	7
	≧7mm	20	0
Size of minor defect	≦5mm	19	5
	> 5mm	11	2
Number of deployment devices	Single device	12	6**
	Multiple devices	18	0

** One patient underwent surgical closure of defects.

SUMMARY

- Thirty patients (76.9%) were diagnosed with multiple ASDs by TTE and seven patients (17.9) were diagnosed by subsequent TEE. Two patients (5.1%) were identified multiple defects during the sizing balloon procedure.

- The morphological characteristics in patients with multiple ASDs diagnosable by TTE are ...
  - ✓ the distance of 2 ASDs more than 7mm. (Patient with multiple devices were deployed.)
  - ✓ minor defect of more than 5mm.
  - ✓ little association with positional relationship.

CONCLUSIONS

- Even in TTE evaluation, more than 70% of multiple ASDs can be diagnosed before the catheter intervention if it was performed by well-trained sonographer.

- Such pre-interventional information can be contributed to the valuable information for the establishment of therapeutic strategy.

Clinical Physiology

PG-29

Right ventricular FAC obtained in different echocardiographic views. Comparison with RVEF by cardiac-MRI

Rika Takemoto[1], Hiroki Oe[1], Nobuhisa Watanabe[1], Kazufumi Nakamura[2], Hiroshi Morita[2], Ken Okada[3], Fumio Ootsuka[1], Hiroshi Ito[2]

[1]Okayama University Hospital , Center of Ultrasonic Diagnostics,
[2]Okayama University , Cardiovascular Medicine,
[3]Okayama University Hospital , Division of Medical Support , Okayama JAPAN

Backgrounds

- Right ventricular (RV) function is a known predictor of outcome in a variety of cardiovascular diseases, including heart failure, pulmonary embolism, and myocardial infarction.
- Accurate imaging and assessment of right heart in a single 2-dimensional echocardiographic view is, however, difficult due to its unique structure.
- Echocardiographic measures of RV fractional area change (FAC) correlated well with RV ejection fraction (RVEF) by cardiac magnetic resonance (CMR).

Meyer P et al. Circulation 121 : 252-258, 2010
Ho S Y et al Heart 92 : i2-i13,2006
Anavekar N S et al Echocardiography 24 : 452-456,2007

- The ASE guideline recommends that multiple echocardiographic views should be obtained to evaluate RV function.

Rudski L G et al. J Am Soc Echocardiogr 23:685-713,2010

- However, there is no clear recommendation which echocardiographic view should be used to evaluate RV FAC.

Purpose

- We aimed to evaluate the usefulness of RV-FAC obtained in different echocardiographic views of right heart, and compared RV-FAC with RVEF measured by CMR.

Study Population

- The study population is consisted of 90 consecutive patients who underwent CMR and transthoracic echocardiography (TTE) for evaluation of RV.
- Exclusion criteria : Contraindication for CMR scanning
  - Implantable cardiac pacemaker,
  - Implanted surgical clips, wire sutures, screws
  - Implantable cardioverter defibrillator
  - Pregnancy

Methods : Cardiac MR analysis

- 1.5-T Philips Achieva magnetic resonance imaging system (Philips Medical Systems, Best, The Netherlands).
- RVEF measured by method of disc summation , using Extended MR Work Space (Philips Medical Systems).

Fig.1 RVEF measured by cardiac magnetic resonance

Methods : Echocardiographic analysis

- FAC provides an estimate of RV systolic function.
- FAC < 35% indicates RV systolic dysfunction.
- **RV-FAC (%) =(AreaED – AreaES) / AreaED**

Fig.2

RV focused A-4CV view (**F-FAC**) | Apical four-chamber view (**A-FAC**) | RV modified A-4CV view (**M-FAC**)

- Echocardiography was performed within 24 hours of the CMR examination.

Patients Characteristics

Age, year	53 ± 19
Sex (Male, %)	51 (57)
Dilated cardiomyopathy (%)	19 (21)
Hypertrophic cardiomyopathy (%)	17 (19)
Arrhythmia (%)	14 (16)
Cardiac sarcoidosis (included suspected case) (%)	8 (9)
Valvular heart disease (%)	5 (6)
Pulmonary hypertension (%)	4 (4)
Cardiac amyloidosis (included suspected case) (%)	3 (3)
Ischemic heart disease (%)	3 (3)
Other (%)	17 (19)

Echocardiographic Parameters

LV function	
LV end-diastolic volume (ml)	120 ± 65
LV end-systolic volume (ml)	66 ± 62
LV ejection fraction (%)	52 ± 18
LA volume index (mg/m²)	45 ± 18
E/e'	14.4 ± 8.7
Significant aortic regurgitation (%)	3 (3)
Significant mitral regurgitation (%)	20 (22)
RV function	
M-FAC (%)	40 ± 12
A-FAC (%)	44 ± 12
F-FAC (%)	45 ± 12
TAPSE (mm)	18.5 ± 5.9
s' (cm/s)	11.2 ± 3
Tricuspid regurgitation pressure gradient (TRPG)(mmHg)	26 ± 10
Significant tricuspid regurgitation (%)	5 (6)

Values are expressed either as mean±SD or numbers (%).

Results

Fig.3

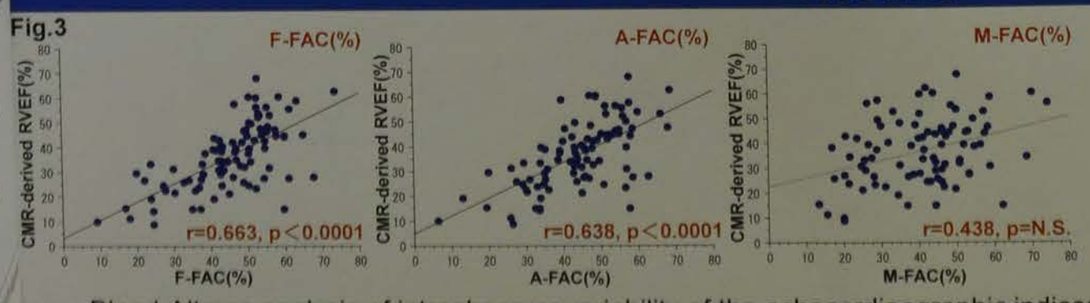

- Both A-FAC and F-FAC measurement were feasible in 90 patients (100%) and M-FAC measurement was feasible in 84 patients (93%).
- A-FAC and F-FAC were significantly correlated with CMR-derived RVEF.
- TAPSE and s' were significantly correlated with CMR-derived RVEF.
- Bland-Altman analysis of intraobserver variability of the echocardiaographic indices showed small mean differences and limits of agreements
  (A-FAC 6.82%, F-FAC 3.92%, M-FAC 8.5%).
- Regarding interobservre variability , Bland-Altman analysis showed similar small mean differences and limits of agreements
  (A-FAC 5.8%, F-FAC 9.8%, M-FAC 9.8%).

Discussion

- The ASE guideline recommends that A-4CV view should be used to measure RV FAC (not M-FAC.)
- RV modified A-4CV view should not be used quantitatively to assess RV due to its foreshortened and oblique image angle.

Fig.4

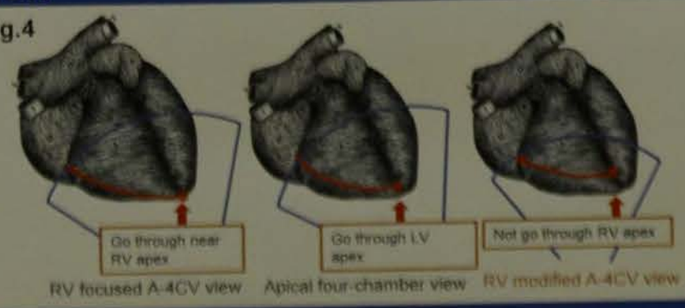

Summary

- Both A-FAC and F-FAC had good correlation with CMR-derived RVEF, and M-FAC didn't show correlation with CMR-derived RVEF.
- Bland-Altman analysis of intra- and inter-observer variability of FAC showed small mean differences and limits of agreements
- This study showed good correlation between TAPSE, s' and CMR-derived RVEF.

Conclusion

- RVFAC obtained in different echocardiographic views is feasible and useful.
- M-FAC may not be appropriate for measurement of RV-FAC.
- The standard A-FAC view is likely still to be informative.

The authors have no financial conflicts of interest to disclose concerning the presentation.

Clinical Physiology

PG-30

The dynamics of repolarization interval in children with ventricular septal defect

Yuri Mizutani[1], Yuka Takeuchi[2], Hirofumi Kusuki[3], Keiko Sugimoto[1], Keisuke Osakabe[1], Naohiro Ichino[1], Tadayoshi Hata[1],

[1] Graduate School of Health Sciences, Fujita Health University, Toyoake, Japan
[2] Division of Clinical Labortory, Ise Red Cross Hosepital, Ise, Japan
[3] Division of Clinical Laveratory, Chukyo Hospital, Japan Community Health care Organization, Nagoya, Japan

AIM

In patients with ventricular septal defect, left-to-right shunting increases left ventricular preload. This pathological change affects myocardial depolarization and repolarization and has the potential to evoke the arrhythmogenic substrate. We examined the effect of ventricular septal defect on myocardial repolarization using variability in the repolarization interval.

METHOD and SUBJECTS

- This was a retrospective study of 19 patients (mean age ± SD: 1.8 ± 2.1) who underwent surgical closure (mean ± SD left-to-right shunt ratio: 2.60 ± 0.55) and 26 age-matched healthy children as controls between 2008 and 2015.
- Two electrocardiogram measures were studied: heart rate corrected repolarization and variability of repolarization parameters.
- The repolarization parameters studied were QT, JT, J point to T peak (JTp), and T peak to T end (Tp-e) intervals, determined from preoperative electrocardiograms.
- The variability index (VI) was calculated from the logarithm of the repolarization parameter variance to heart rate variance ratio.

RESULTS

Demographic of ECG analysis

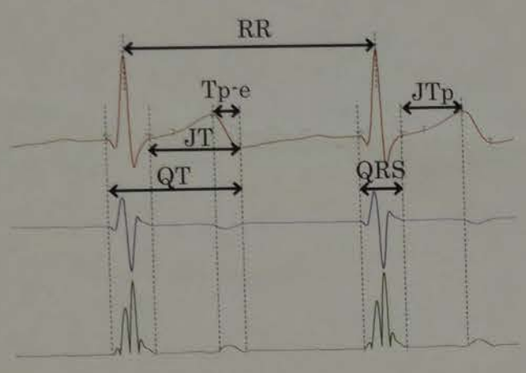

Comparison of electrocardiogram parameters and variability indices

	Control	VSD
RR	533.21±112.6	527.5±103.4
QRS	82.0±10.2	94.6±14.2†
QT	302.6±30.4	303.0±32.2
QTc (Bazett)	409.2±13.1	418.8±14.2*
QTc (Fridericia)	369.6±15.5	375.6±18.5
JT	220.1±23.5	208.4±22.7
JTc (Bazett)	297.7±12.4	288.1±12.9*
JTc (Fridericia)	268.9±13.6	258.4±14.6*
JTp	159.9±15.3	140.9±18.8†
JTpc (Bazett)	216.7±13.2	194.9±17.7†
JTpc (Fridericia)	195.6±11.0	174.8±16.7†
Tpe	60.2±10.6	67.4±10.4*
Tpec (Bazett)	81.0±8.2	93.2±11.0†
Tpec (Fridericia)	73.3±8.9†	83.6±10.4*

Comparison of repolarization variability indices

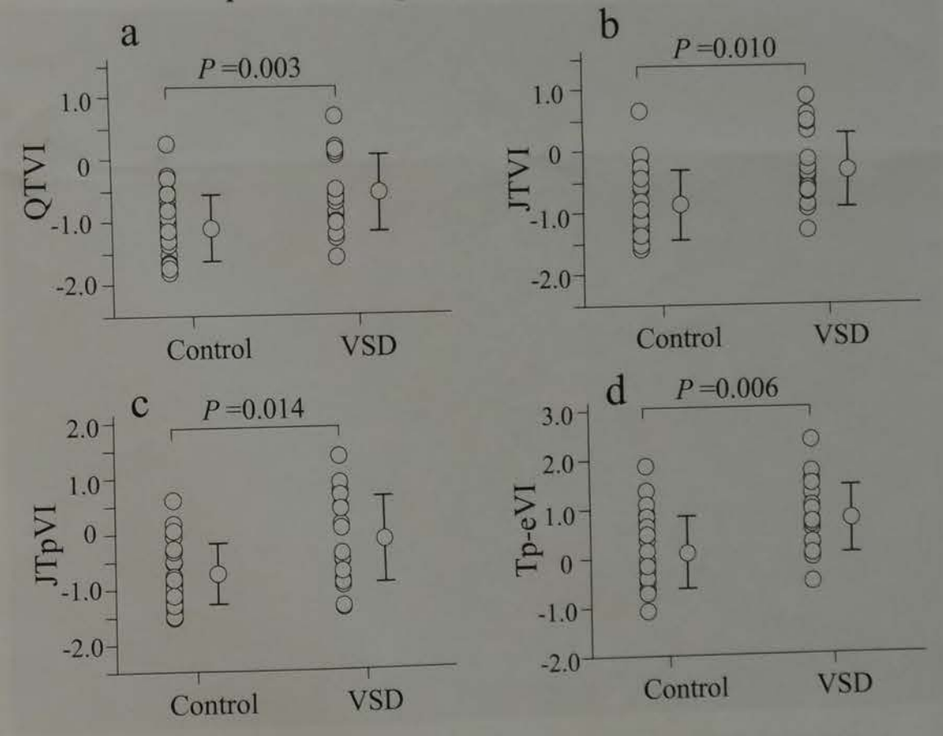

Relationship between the corrected QT interval and QTVI

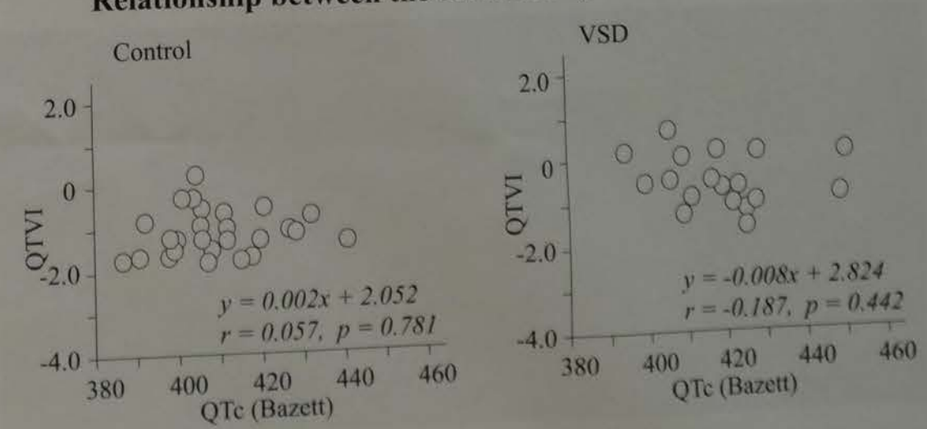

CONCLUSION

Variability of myocardial repolarizations in patients with VSD was evaluated and compared with a healthy control group. We found that early and late repolarization processes are influenced by left ventricular preload. It is suggested that these repolarization characteristics may serve as new indices to assess electrophysiology and pathophysiology of congenital heart disease in a non-invasive manner.

FUJITA HEALTH UNIVERSITY

The authors have no conflict of interest related to the content of this poster.

Clinical Physiology

PG-31

Diabetic patient with hypertensive response to light exercise is related to poor exercise tolerance

Motoki Otsuji , Ayaka Matsumoto , Katsunori Bettou

Ise Red Cross Hospital

Medical Technology Department Clinical Inspection Division

【Introduction】

Diabetic patients for education hospitalization in our hospital has implemented a treadmill stress test (TMT) for both detection of asymptomatic myocardial ischemia and evaluation of exercise tolerance. In TMT, hypertensive response to the short time of the load was often shown.

We evaluated whether hypertensive response to exercise (HRE) was related to exercise habits and exercise tolerance.

【Methods】

From September 2011 to September 2014, type 2 diabetic patients without myocardial ischemia were enrolled in our study.

One hundred sixty diabetic patients were divided into 3 groups, Control, HRE, and Hypertension (HTN).

The history of taking exercise habits, blood sampling, pulse wave velocity (PWV), and transthoracic echocardiography at rest were examined, and the association with blood pressure response to exercise was evaluated.

【 Definition 】

Systolic blood pressure at early exercise (e-SBP) was measured at 1.5METs at Bruce protocol.

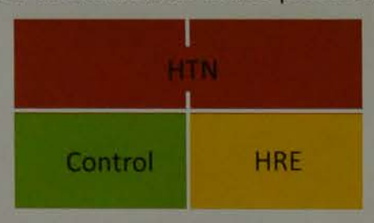

Control: resting systolic blood pressure (r-SBP) <130mmHg and e-SBP <160mmHg

HRE : r-SBP <130mmHg and e-SBP >160mmHg

HTN : r-SBP>130mmHg

【 measuring equipment 】

TMT; Nihon Kohden Q-Stress

PWV; OMRON-COLIN folm

Ultrasonic device ; PHILIPS IE-33

Blood sampling ; HITACHI 7350, LABOSPECT 008

HbA1c ; arkray HA-8181

【 Statistical processing 】

The level of significance, one-way analysis of variance and multiple comparison test It was a risk rate of less than 5% (Tukey).

【 Results 】

※P<0.05 ANOVA
※P<0.05 Tukey
(VS. Control)

	Control	HRE	HTN
number	78	26	56
Age	53±14	57±15	58±11
BMI (kg/m²)	24.8±5.1	27.3±5.7	26.5±5.1
Female ratio (%)	26	35	52※
Disease duration (month)	104	103	96
HbA1c (%)	10.9±2.4	10.3±2.7	9.9±2.7
Max IMT (mm)	1.4±0.7	1.6±0.9	1.4±0.6
LV wall thickness (mm)	9±1	9±1	9±1
LV End-diastolic diameter (mm)	47±3	46±4	48±5
LV End-systolic dimension (mm)	28±3	28±3	30±6

【 Exercise Habits 】

P<0.05 ANOVA
※P<0.05 Tukey
(VS. Control)

Control	HRE	HTN
44%	33%	21%※

「 exercise habits 」
; exercise satisfying all of the following conditions
①30 minutes or more at a time
②two or more times a week
③continued for more than a year
(Japan National Health and Nutrition Examination Survey compliance)

【E/e'】

P<0.05 ANOVA
※P<0.05 Tukey

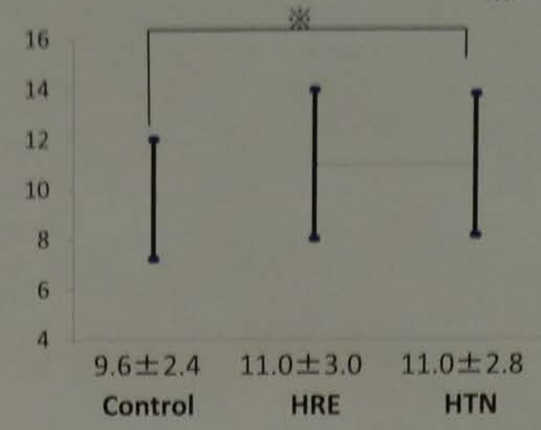

【PWV】

P<0.05 ANOVA
※P<0.05 Tukey

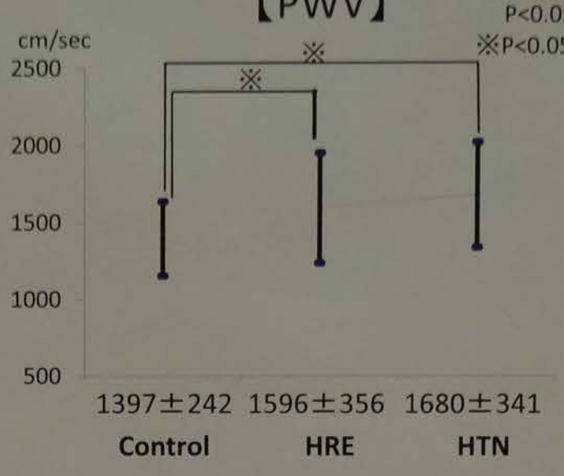

【 Exercise duration 】

P<0.05 ANOVA
※P<0.05 Tukey

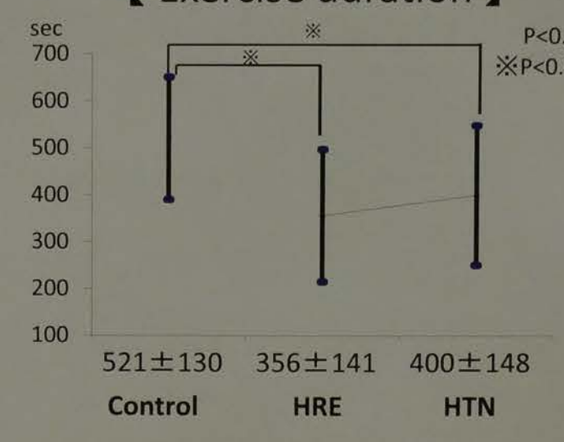

【 Multivariable regression analysis 】

Objective variable ; Exercise duration

Explanatory variable	standardized coefficient (β)	p
age	−0.159	0.0934
sex	0.1063	0.2123
BMI	−0.1318	0.1827
r-SBP	−0.0625	0.4861
e-SBP	−0.4538	<0.0001
HbA1c	0.0224	0.7907

【 Discussion 】

In diabetic patients, e-SBP rise due to the TMT submaxial load show a negative correlation with exercise duration despite resting blood pressure is controlled.

From this result, we suppose that rise of end-diastolic pressure accompanied by decline of left ventricular diastolic function and increase of cardiac afterload caused by decline of vascular elasticity is associated with the rise of e-SBP, and beside reduction of exercise duration.

【 Conclusion 】

Diabetic patients with hypertensive response to light exercise had poor exercise tolerance, regardless of resting systolic blood pressure.

Clinical Physiology

PG-32

Usefulness of the facial nerve motor evoked potentials in skull base surgery.

Subtitle : Development of transcranial facial motor evoked potentials using supra threshold level stimulation method.

Tsunenori Takatani[1)], Sayomi Yamamoto[1)], Hideko Yoshida[1)], Yayoi Umeki[1)]
Division of Central Clinical Laboratory[1)] Nara medical university hospital, Japan

【 Background 】

- The preservation of facial nerve function is one of the primary objectives in skull base surgery. Transcranial(Tc)-facial nerve motor evoked potential (FNMEP)s has been recognized as a good method for quantitative monitoring of facial nerve function in skull base surgery. Its function can be continuously monitored by obtaining compound muscle action potentials in facial nerve target muscles.
- In many papers authors use supra-maximum stimulation. However, there are some disadvantages in this method including high frequency of false negative findings and intraoperative movement.
  We develop a novel method of stimulation using supra-threshold stimulation and evaluate the validation and reliability of FNMEP by this method in comparison with the previous methods.

【 Methods 】

- 38 patients (56.4±13.7 years, 17 males and 21 females) undergoing elected skull base surgery using Tc-FNMEP monitoring were studied. General anesthesia was maintained by total intravenous anesthesia using propofol without neuromuscular blockade. Supra threshold level transcranial stimulation of Tc-FNMEP was established with minimum intensity to elicit the waveform from recording muscles plus 10%.
- A train of 4 pulses with 4inter-stimulation interval 1.5-1.7msec was delivered through corkscrew electrodes at C3/C4 (international 10/20 method). Subdermal needle electrodes were placed in the orbicularis oculi muscles at the lateral angle of the bilateral eyes and in the orbicularis oris muscles at the bilateral angle of the mouth for recording Tc-FNMEP. MEE-1232 (Nihon Kohden, Tokyo, Japan) was used as an electrophysiological device.
- Significant change of amplitude was defined as more than 50% decrease compared with control amplitude. Facial nerve function was evaluated preoperatively and postoperatively using the House and Brackmann grading system .
  The reliability of intraoperative Tc-FNMEP was assessed by sensitivity and specificity to detect postoperative facial nerve dysfunction.

Tc-FNMEP of electrode position
Tc-FNMEP Setting of the waveform

- Supra threshold level transcranial stimulation of Tc-FNMEP was established with minimum intensity to elicit the waveform from recording muscles **plus 10%.**

1) Suppression of stimulus intensity.

2) Measuring the threshold.

3) Setting the intensity to obtain a stable monitor waveform.

4) Supra threshold level + 10% above the minimum stimulation to elicit at least 20μV.

5) Deriving the only muscle groups of interest.

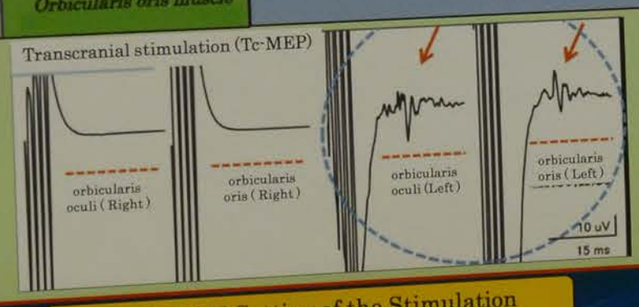

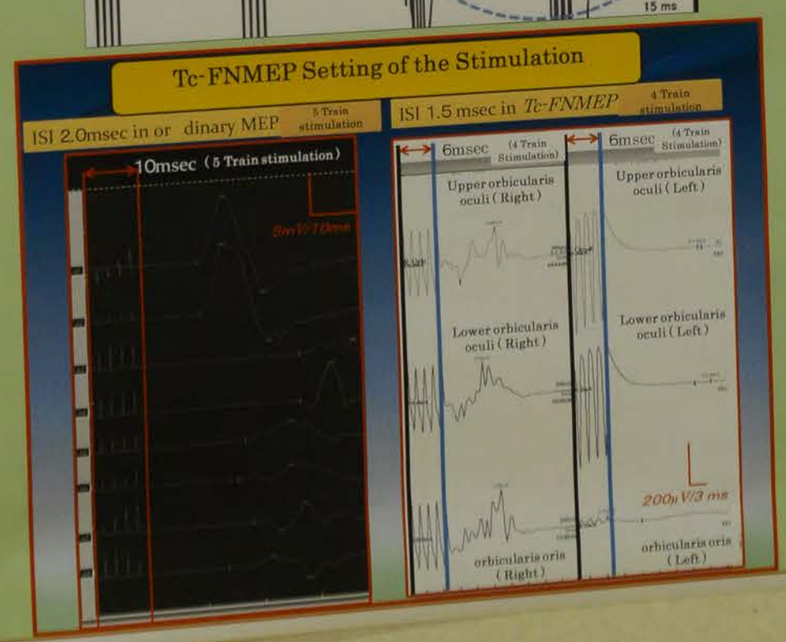

【 Case report of waveform disappearance 】

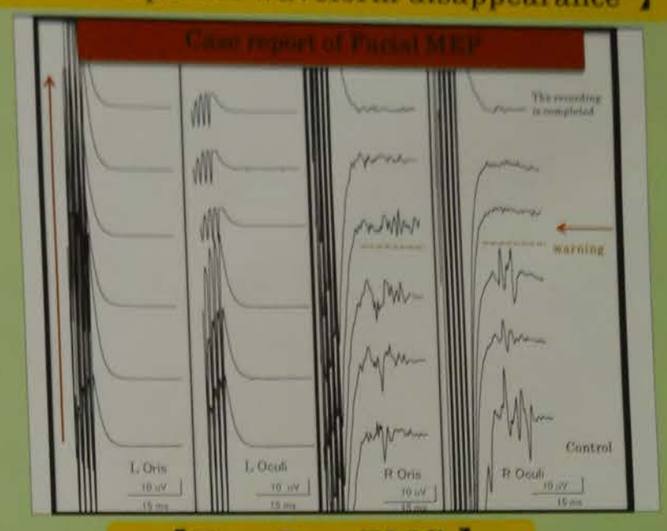

【Free Run EMG 】

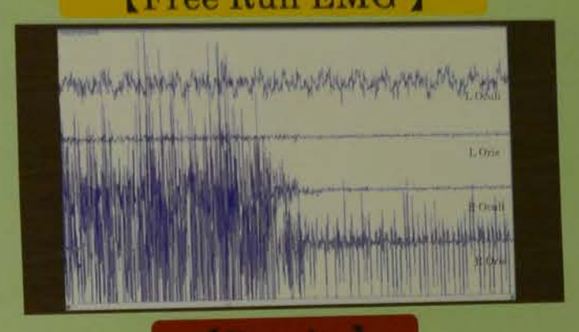

【Results】

- Control Tc-FNMEP waveforms were successfully recorded in all patients. Of 28 patients, significant sustained decreases of Tc-FNMEP until the end of surgery were observed in 10 patients.
- Postoperative new facial nerve dysfunction or worsen facial nerve function were observe in 6 patients. Of the 6 patients with postoperative deterioration of facial nerve function, 3 patients had intraoperative significant decline of Tc-FNMEP.
- The sensitivity and specificity of intraoperative Tc-FNMEP to detect postoperative facial nerve dysfunction were 82.4% and 100%, respectively.

Case report	Before surgery	After surgery	At discharge	more than 50% decrease	Free Run EMG reaction
1	normal	H-B Ⅱ	normal	○	–
2	normal	normal	normal	○	–
3	H-B Ⅱ	H-B Ⅱ	H-B Ⅱ	○	–
4	H-B Ⅱ	H-B Ⅲ	H-B Ⅱ	○	○
5	normal	H-B Ⅲ	normal	○	○
6	normal	H-B Ⅱ	H-B Ⅱ	○	○
7	H-B Ⅱ	H-B Ⅱ	H-B Ⅲ	○	○
8	normal	H-B Ⅱ	H-B Ⅱ	○	○
9	normal	H-B Ⅳ	H-B Ⅳ	○	○

House-Brackmann method

Grade	Description	Characteristics
I	Normal	Normal facial function in all areas
II	Mild dysfunction	Slight weakness noticeable on close inspection; may have very slight synkinesis
III	Moderate dysfunction	Obvious, but not disfiguring, difference between 2 sides; noticeable, but not severe, synkinesis, contracture, or hemifacial spasm; complete eye closure with effort
IV	Moderately severe dysfunction	Obvious weakness or disfiguring asymmetry; normal symmetry and tone at rest; incomplete eye closure
V	Severe dysfunction	Only barely perceptible motion; asymmetry at rest
VI	Total paralysis	No movement

Conclusion

- In Tc-FNMEP supra threshold level stimulation method, shortening inter-stimulus interval (ISI: 2.0ms → 1.5ms) were amenable to obtain stable waveform. Modification of the decrease of time in train of the stimulation from 5 to 4 was also helpful to elicit clearer waveform.
- The results in this study indicated that Tc-FNMEP using supra threshold level transcranial stimulation during skull base surgery was feasible and reliable.

Related to the abstract presentation,There is no such as a company that is in the COI relationship should be disclosed.

Clinical Physiology

PG-33

Relationship between olfactory function and gustatory function and pathophysiology in Alzheimer's disease

○Minoru Kouzuki, Syouta Nakamura, Yuto Katsumata,
Yuki Fujihara, Ayumi Takamura, Katsuya Urakami

Department of Biological Regulation, School of Health Science, Faculty of Medicine, Tottori University

Background / Objectives

Patients with Alzheimer's disease (AD) are well known to develop olfactory dysfunction in the early stage by senile plaques (SP) and neurofibrillary tangles (NFT) in olfactory-related domain. In addition, patients with dementia cause taste disorder by cerebral degeneration. However, no study investigates both olfactory and gustatory functions in mild cognitive impairment (MCI) which is a pre-AD state, and it is not clear about relationship between pathology.

【 Relationship of olfactory sense and AD 】

- Deposition of amyloid β (The main component of SP) in the brain
  Neocortex → Hippocampus CA1, Entorhinal region → Subcortical regions → ・・・
- Deposition of phosphorylated tau (The main component of NFT) in the brain
  Transentorhinal and entorhinal region → Hippocampus → Temporal lobe → ・・・

(Reference : Thal DR, et al. Neurology 2002; 58: 1791-1800. Braak H, et al. Acta Neuropathol 2006; 112: 389-404.)

【 Relationship of gustatory sense and AD 】

Stimulation of taste transmit through limbic cortex (hippocampus, insular cortex, etc.). Thus, the taste function is thought to be affected by general cerebral changes in AD.

(Reference : Steinbach S, et al. J Neurol 2010; 257: 238-246.)

【 Objectives 】

The aim of this study is to investigate;

1. To compare with olfactory and gustatory functions between AD, MCI and normal elderly subjects
2. To analyze correlation with olfactory and gustatory functions and pathophysiology

Subjects / Methods

【 Subjects 】

	AD	MCI	Normal
Number (n)	40	20	21
Age (y)	79.5±9.5	80.5±5.2	74.7±7.1
Sex (M : F)	12:28	7:13	4:17

Age and sex were not significant among three groups.
Exclusion criteria : Patients who are diagnosed olfactory disturbance and/or taste disorder.

【 Methods 】

1. Olfactory test (Odor Stick Identification Test for Japanese ; OSIT-J)

Each odors were enclosed in microcapsules made of melamine resin. The experimenter applied the odorous semisolid cream from an odor stick to a 2cm circle on a thin paraffin paper, folded this paper in half, rubbed it to grind the microcapsules, and passed it to the patient. The patient then opened and sniffed the paper, and answered from six possible answers : four items plus "detectable but not recognized" and "no smell detected".

(Daiichi Yakuhin Sangyo Co., Ltd)

【 12 kinds of odor 】
perfume, Japanese orange, rose, condensed milk (Sweet odors)
Indian milk, wood, menthol, Japanese cypress (Plants odors)
curry, roasted garlic (Spice odors)
cooking gas, sweaty smelling cloths (Offensive odors)

It is 12 points when the patient answers all correctly, but it is 0 point when the patient's answers are all incorrect.
(Reference : Saito S, et al. Chem Senses 2006; 31: 379-391.)

2. Gustatory test (Intraoral dropping method using taste solutions)

The experimenter dropped a drop of solution into the oral cavity from the lowest concentration. The patient answered from six possible answers: sweet, salty, sour, bitter, unidentifiable taste and no taste. If the patient answered correctly, the concentration was taken as the recognition threshold. If the choice was incorrect, the concentration was increased at the next trial.

(Sanwa Kagakukenkyusho Co., Ltd)

【 4 kinds of taste solution 】
Sweet (0.3, 2.5, 10, 20, 80% sucrose)
Salty (0.3, 1.25, 5, 10, 20% sodium chloride)
Sour (0.02, 0.2, 2, 4, 8% citric acid)
Bitter (0.001, 0.02, 0.1, 0.5, 4% quinine hydrochloride)

If the patient recognizes the lowest concentration ; 1 point
If the patient recognizes the highest concentration ; 5 points
If the patient doesn't recognize the highest concentration ; 6 points.

3. Cerebrospinal fluid (CSF) tests (By sandwich ELISA)

- Amyloid β (Aβ) 42
  (IBL Co., Ltd. : Human Amyloid β (1-42) Assay kit)
- Phosphorylated tau (p-tau) 181
  (Innogenetics Co., Ltd. : Innotest Phospho-tau (181p))

4. Cognitive function test

- Touch Panel-type Dementia Assessment Scale (TDAS)

Nihon Koden Co., Ltd

【 Consist of 9 tasks 】

- Word-recognition
- Following command
- Visual-spatial perception
- Concept understanding
- Naming fingers
- Orientation
- Money calculation
- Object recognition
- Clock time recognition

It is 0 points when the patient answers all the question correctly, but it is 101 points when the patient's answers are all incorrect.
(Reference : Inoue M, Urakami K, et al. Psychogeriatrics 2011; 11: 28-33.)

Results

1. Results of olfactory test and gustatory test among three groups.

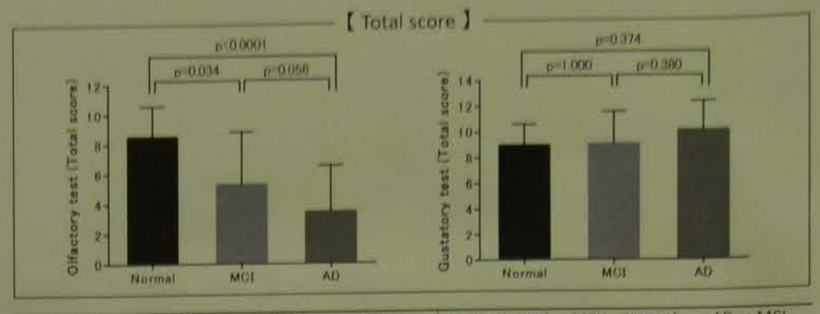

	AD	MCI	Normal	AD vs Normal p value (95% CI)	MCI vs Normal p value (95% CI)	AD vs MCI p value (95% CI)
Olfactory test score						
Sweet odors	1.2±1.3	1.6±1.2	2.3±1.0	0.057 (0.02 - 1.64)	0.501 (-0.42 - 1.54)	1.000 (-0.57 - 1.07)
Plants odors	1.0±1.2	1.7±1.4	3.0±1.0	< 0.0001 (0.85 - 2.45)	0.102 (-0.11 - 1.79)	0.042 (0.02 - 1.61)
Spice odors	0.6±0.8	0.9±0.8	1.8±0.4	< 0.0001 (0.61 - 1.62)	0.001 (0.30 - 1.49)	0.823 (-0.27 - 0.72)
Offensive odors	0.6±0.6	1.2±0.7	1.4±0.7	0.001 (0.26 - 1.27)	1.000 (-0.44 - 0.76)	0.012 (0.10 - 1.10)
Gustatory test score						
Sweet	2.2±0.8	2.0±0.5	2.2±0.5	1.000 (-0.47 - 0.53)	1.000 (-0.50 - 0.70)	1.000 (-0.57 - 0.43)
Salty	2.7±1.2	2.4±1.3	2.0±0.8	0.796 (-1.21 - 0.45)	1.000 (-1.06 - 0.91)	1.000 (-1.12 - 0.52)
Sour	3.0±1.2	2.5±0.9	2.7±0.6	0.838 (-1.08 - 0.42)	1.000 (-0.77 - 1.00)	0.429 (-1.19 - 0.29)
Bitter	2.3±1.0	2.2±1.0	2.0±0.7	0.815 (-1.03 - 0.39)	1.000 (-1.00 - 0.69)	1.000 (-0.87 - 0.54)

Data presented as mean ± standard deviation (SD).
(Analysis of covariance (ANCOVA), with age and sex as covariates.)

2. Receiver operating characteristic (ROC) analysis for olfactory test and gustatory test in patients with AD, MCI and Normal.

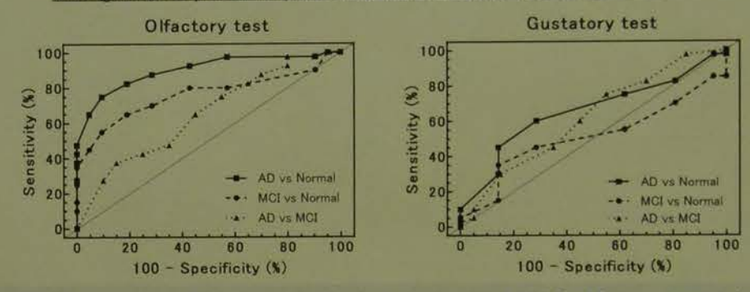

The area under the ROC curve of the olfactory test was 0.900 for AD versus normal group, 0.762 for MCI versus normal group, 0.649 for AD versus MCI group, whereas that for the gustatory test was 0.653, 0.508, and 0.618, respectively.

3. The correlation between olfactory test, gustatory test and CSF biomarkers, Cognitive function test.

	TDAS	p-tau181	Aβ42	p-tau181/Aβ42
	r	r	r	r
Olfactory test				
Sweet odors	-.350**	.002	.147	-.093
Plants odors	-.554**	-.054	.413**	-.285*
Spice odors	-.464**	-.067	.391**	-.308*
Offensive odors	-.440**	-.158	.108	-.223
Total score	-.555**	-.058	.320*	-.254
Gustatory test				
Sweet	.003	-.054	.154	-.104
Salty	.273*	.256	-.299*	.370**
Sour	.162	-.020	-.046	.020
Bitter	.298**	.033	-.153	.114
Total score	.368**	.061	-.197	.179

r ; correlation coefficients
p<0.05; ** p<0.01 (Spearman's rank correlation analysis)

Discussions / Conclusions

- Olfactory function was related to CSF biomarkers and cognitive disorders. Therefore, we confirmed that olfactory function likely to be impaired in the early stage of AD.
- However, it was not able to distinguish between AD and MCI. It is necessary to develop a more sensitive olfactory test.
- In gustatory function, there was specific correlation with TDAS scores. But, the total score of gustatory test, there was not associated with CSF biomarkers and no significant difference among three groups. Therefore, this study showed that gustatory function may not impaired in the early stage of disease.
- This study suggested that olfactory and taste functions deteriorate with AD pathology progress. But olfactory disturbance is probable earlier than gustatory disorder.

【 Ethical considerations and Conflict of Interest (COI) 】

- This study design was approved by the ethics committee of Tottori University.
- The presenter have no COI to disclose concerning the presentation.

Clinical Physiology

PG-34

Detection of left ventricular hypertrophy using electrocardiography in cases pre-identified by echocardiography

Maya Ishiguma, Toshiharu Umeki, Taemi Akiyoshi, Ichirou Tanabe
Takanori Higashitani and Eisaburo Sueoka

Department of Laboratory Medicine, Saga University Hospital

Ultrasound cardiography (UCG), is a reliable method to detect left ventricular hypertrophy (LVH). The 12-lead electrocardiogram (ECG) is often used for LVH screening as well. However, several different sets of criteria exist for diagnosing LVH by ECG, and their sensitivity and specificity differ by report depending on differences in race and body type. Therefore, we assessed the reliability of two sets of ECG criteria against that of UCG in the detection of LVH. Among 87 patients, 16 (18.2%) cases were incorrectly considered LVH-negative using S criteria, and 19 (21.6 %) cases tested negative using C criteria, respectively. The average UCG-measured wall thicknesses in cases that could not be detected by the combined ECG criteria were 13.5 ± 0.34mm (max 19mm) for ventricular septa and 12.4 ± 0.37mm (max 16mm) for posterior walls. Among 24 cases classified as LVH according to UCG, 12 were concentric remodeling, and 12 were concentric hypertrophy.

Objectives

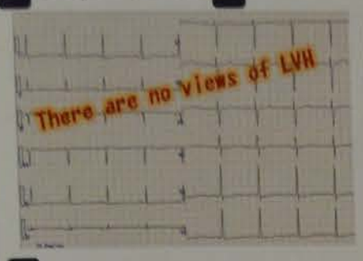

How many LVH patients are misdiagnosed by ECG examinations ?
Which factors have impact on the sensitivity of LVH detection with ECG ?

Materials & Methods

Eighty-seven patients who underwent UCG and were diagnosed with LVH at Saga University Hospital between January and December 2015 were included in our study. All subjects received ECGs; the percentage of correctly positive LVH diagnoses from ECGs was assessed using the UCG findings. Two sets of criteria for detecting LVH with ECGs were used: the Sokolow-Lyon criteria (S standard) and the Cornell voltage criteria (C standard). Statistical analyses were performed using t test of Welch.

Patient background

Item	Average
Age	68.4±1.2
Height(cm)	159.7±0.9
Weight(kg)	59.2±1.2
Body surface(m^2)	1.6±0.0

Main data elements

- Body Mass Index : BMI
- Interventricular septum thickness : IVST
- Posterior left ventricular wall thickness : PWT
- Left ventricular ejection fraction : EF (M. Simpson method)
- Left ventricular muscle mass : LVM (alea-length method)
- Left ventricular muscle mass index : LVMI
- Relative wall thickness : RWT
- Cardiac depth

Measurement of Cardiac depth

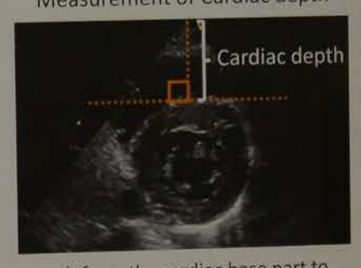

Length from the cardiac base part to ventricular septum was measured.

Results & Discussion

The group with negative for both S and C criteria for LVH with ECG

28% (n=87)

Comparison with positive group

Statistical analysis using *t* test

Item	P value
Body Mass Index : BMI	0.17
Interventricular septum thickness : IVST	0.17
Posterior left ventricular wall thickness : PWT	0.92
Left ventricular ejection fraction : EF (M. Simpson method)	0.13
Left ventricular muscle mass : LVM (area-length method)	<0.05
Left ventricular muscle mass index : LVMI	<0.05
Relative wall thickness : RWT	0.80
Cardiac depth	<0.05

- LVM, LVMI, and Cardiac depth showed statistically difference between the group with positive and negative for LVH criteria for LVH.
- LVM and LVMI in positive group were larger than those of negative group.
- Cardiac depth were longer in the group with negative compered with positive group.

Details of the results with three parameters showing statistically differences

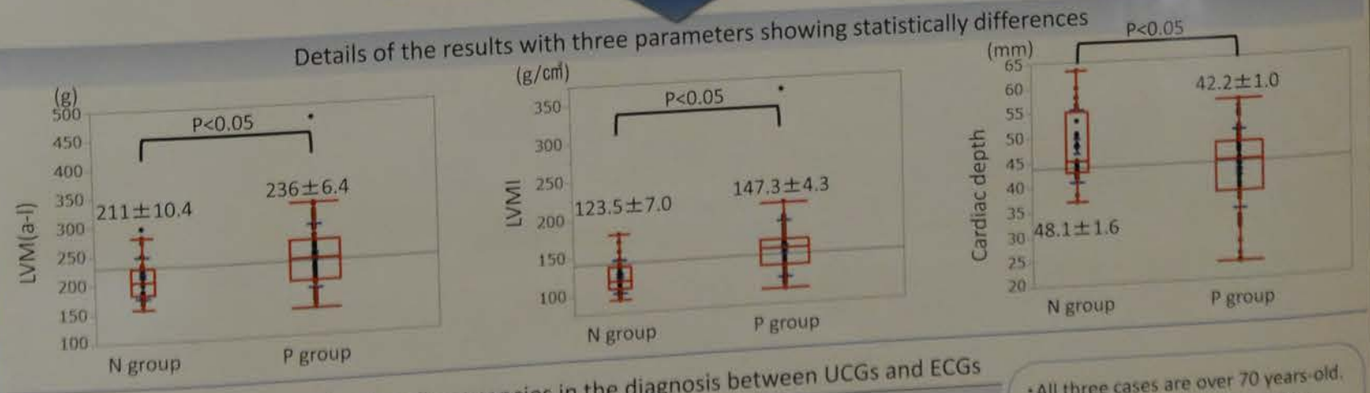

Clinical features of 3 cases showing discrepancies in the diagnosis between UCGs and ECGs

Case	1	2	3
Clinical diagnosis	・Hypertension ・Chronic kidney failure ・Hyperlipidemia	・Arteriosclerosis obliterans ・Hypertension ・Diabetes mellitus ・Hyperlipidemia	・Aortic stenosis ・Hypertension
Age	79	78	71
Sex	Male	Male	Female
BMI	23	25	17
IVST/PWT(mm)	12/11	19/11	12/13
LVMI	198	223	177
Cardiac depth	42.4	56	36.4
Others			Left pleural effusion(+)

- All three cases are over 70 years-old.
- Cardiac depth of case 2 was deep compared with the average of those of LVH negative group by ECG criteria.
- Case3 showed massive pleural effusion.

These results suggested that the distance from an electrode to heart and massive coelomic fluid may influence to the assessment of LVH.

Further investigation will be required.

Conclusion

We found about 28% LVH patients diagnosed by UCG were not detected by 2 ECG criteria for LVH. In our study, detection rate of LVH by ECG was not associated with each criteria for diagnosis of LVH. To improve the sensitivity for detection of LVH, assessment of physical condition and medical history of the patient are required in addition to ECG findings.

Clinical Physiology
PG-35

Evaluation of the effects of introducing exercise therapy in cardiac rehabilitation

Takeshi TERAJIMA
JA Niigata Koseiren Uonuma Hospital

Cardiac rehabilitation (CR)

CR is a comprehensive program focused on exercise therapy and includes lifestyle guidance, patient education, and counseling. Its goal is to improve motility, prevent disease relapse, and increase quality of life in patients with heart diseases such as myocardial infarction, angina pectoris, and heart failure, and in those with PAD after cardiovascular surgery, and with DM.

Target

52 subjects (32 men, 20 women)
mean age of 70.5±8.5 years.

Methods

CPX (peakVO2, AT, VE/VCO2), 6MWD,
UCG (EF, LVDd), CAVI, ABI, BNP, hs-TnT
The measurements were respectively performed before and after CR.

Results

Significant improvements were observed

Significant improvements weren' t observed

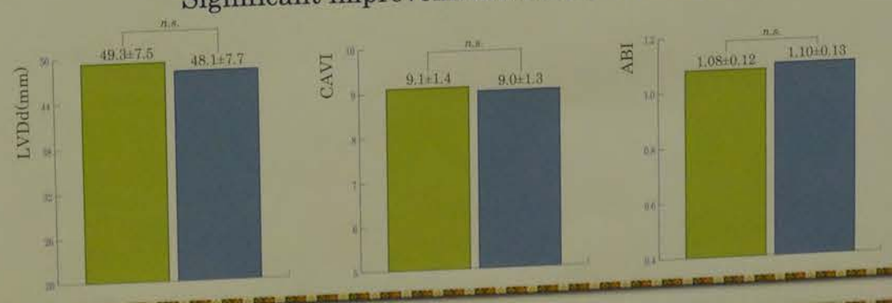

Discussion

The 150 days of CR caused skeletal and respiratory muscle to develop, vascular endothelial functions to recover, cardiac and peripheral circulating blood volume to increase, and exercise tolerance and motility to improve significantly. For cardiac functions, LV remodeling did not occur, and cardiac systolic and diastolic functions improved. Further, the hs-TNT results indicated exercise increased cardiac volume, attenuated sympathetic nerve activity, and suppressed myocardiopathy. Improvements were also seen in peripheral arterial hardness and blockage.

Conclusi

CR can improve exercise tolerance, which is
suppress diseases or prevent their recurren
activities;
of life.

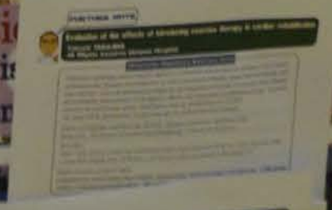

Feel free to take it.
Handout

Feel free to take it.
Further note

Clinical Physiology
PG-36

ASSESSMENT OF FEVER FOR INFECTION CONTROL USING THERMOGRA
—FACIAL THERMOGRAPHY IN PATIENTS WITH FEVER—

Osamu Horie[1], Hiromi Shibata[2], Gou Tsuji[2], Shunichi Kumagai[1], Masahiro Kodaira[1]

Introduction:

Methods:

Results:

Discussion:

Conflict-of-interest (COI)
We have no relevant relationships/interests to disclose.

Clinical Physiology

PG-36

ASSESSMENT OF FEVER FOR INFECTION CONTROL USING THERMOGRAPHY —FACIAL THERMOGRAPHY IN PATIENTS WITH FEVER—

Osamu Horie[1], Hiromi Shibata[2], Gou Tsuji[3], Shunichi Kumagai[3], Masahiro Koshiba[4]

[1]Tenri Health Care University, Department of Clinical Laboratory Science [2]Hyogo University of Health Sciences, School of Pharmacy
[3]Shinko Hospital, Department of Rheumatic Diseases [4]Hyogo College of Medicine, Division of Clinical Laboratory Medicine

Introduction:

To control infections such as Ebola haemorrhagic fever, thermography can be used to monitor patients with fever resulting from infection. However, evidence-based cut-off levels for the thermographic index to reasonably discriminate patients with fever from healthy individuals have yet to be established. We therefore compared facial temperatures between patients with fever and healthy volunteers, as measured using the diagnostic standards advocated by the Japanese Society of Thermology, and reconsidered assessment for infectious control using thermography.

Methods:

Subjects were acclimatized for 20 min in an environment with a room temperature of 25.0-26.0℃ and 40-50% humidity. Areas of the forehead, nose, right and left cheeks, and chin were measured by thermography, and mean temperature of these areas was regarded as the facial surface temperature(Fig.1). Axillary temperature was measured using a clinical thermometer. This study was performed with the approval of the Ethics Committee of Tenri Health Care University and Hyogo University of Health Sciences, and all human samples were collected after obtaining written informed consent. Thermographic examination was performed in 50 healthy volunteers (23 males, 27 females; mean age, 25 years), 48 patients (28 males, 20 females; mean age, 40 years) with influenza A, 13 patients (9 male, 4 female; mean age, 35 years) with influenza B and 65 patients (43 male, 22 female; mean age, 29 years) with the other pyrogenetic disease. We classified individuals with an axillary temperature over 37.5℃ as showing other pyrogenetic disease. Although all patients with influenza show positive results on antibody testing, they might not run a fever.

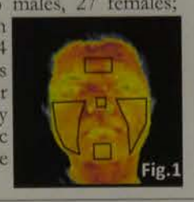
Fig.1

Results:

1. Facial temperatures were significantly higher for patients with fever than for healthy volunteers. It was statistically significant, otherwise standard deviation of the group of patients was larger than previously reported.

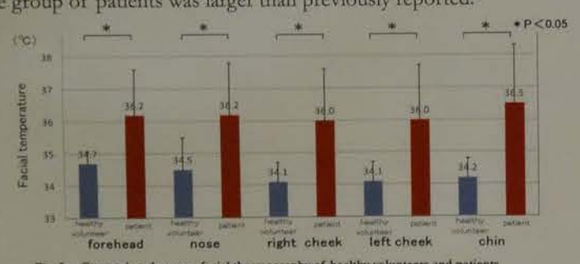

Fig. 2 Comparison between facial thermography of healthy volunteers and patients

2. The disease groups were compared after they were divided to three groups. The influenza A group showed a characteristic of higher facial surface temperature, and the other pyrogenetic disease group was characterized by a larger standard deviation than any other groups. As a result, each disease was considered to show specific characteristics in facial surface temperature.

Tab. 1 Comparison of facial and axillary temperature after divided to three disease groups (℃) (mean±S.D.)

	numbers	axillary temperature	forehead	right cheek	left cheek	nose	chin
influenza A	48	38.3±0.8	36.4±1.6	36.1±2.0	36.5±1.3	36.5±1.3	36.5±1.3
influenza B	13	38.2±0.8	36.7±1.2	35.6±2.1	35.8±1.2	35.8±1.2	35.8±1.6
other pyrogenetic disease	65	38.4±0.6	36.2±1.5	35.9±3.0	36.0±1.8	36.0±1.8	36.1±1.6
p-value (analysis of variance)			0.58	0.27	0.51	0.15	0.15	0.23

3. We compared facial surface temperature using thermography to axillary temperature in each age groups. Because significant correlations were not observed between the three age groups, degree of fever was not considered to show any difference. However, facial temperatures of the right and left cheek in the group 10 years old or less were significantly lower than in the others. Moreover, facial temperature of the forehead and nose were higher than those of the others, and that of chin was lower. For a temperature distribution pattern in the group 10 years old or less to be differentiated from other age groups, it is necessary to divide age groups for judgement of fever.

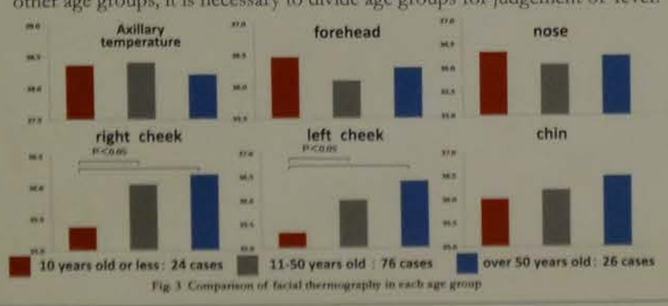

Fig. 3 Comparison of facial thermography in each age group

4. We compared facial thermography with axillary temperature as measured using a clinical thermometer in patients with fever. Significant correlations with axillary temperature were observed for all parts. Facial temperatures of patients with fever were higher than those of healthy volunteers. However, some patients showed lower temperatures than some healthy volunteers. Furthermore, the correlation coefficient was lower than previously report, and the reliability of the data was considered low. The correlations are not sufficiently strong to clearly detect patients with fever.

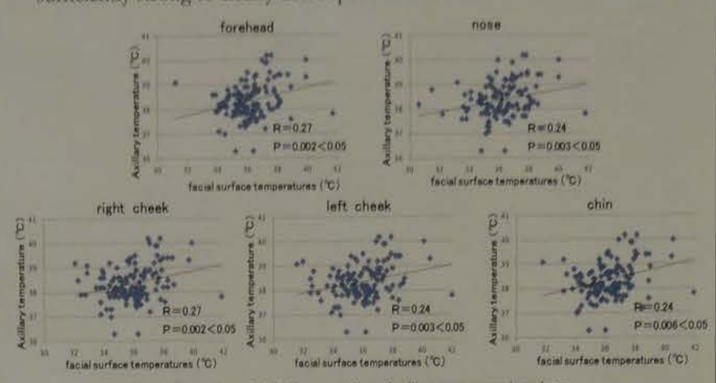

Fig. 4 Comparison of facial thermography and axillary temperature in patients

5. We therefore divided patients into three groups and compared correlation coefficients for facial surface temperature and axillary temperature. Correlations with forehead, both cheeks and chin were seen in influenza A group, and with forehead, nose and chin in other pyrogenetic disease group. Furthermore, the correlation coefficient was higher in influenza A group. No correlation was seen in influenza B. From these results, facial temperature was considered to differ from axillary temperature in some diseases.

Tab. 2 The comparison of correlation coefficient between facial surface and axillary temperature in three patients group

	numbers	forehead		right cheek		left cheek		nose		chin	
		c.c.	P	c.c.	P	c.c.	P	c.c.	P	c.c.	P
influenza A	48	0.44	0.002	0.43	0.002	0.44	0.002	0.27	0.07	0.47	0.001
influenza B	13	0.15	0.64	0.14	0.64	0.09	0.76	0.06	0.86	0.04	0.90
other pyrogenetic disease	65	0.26	0.04	0.19	0.13	0.18	0.15	0.30	0.02	0.26	0.04

(c.c. ; correlation coefficient P; p-value)

6. In patients with influenza, the effects on facial surface temperature with vaccine and medication were examined. No correlation in facial surface temperature was seen for all parts.

Tab. 3 The effects on facial surface temperature with vaccine and medication

vaccination	numbers	axillary temperature	forehead	right cheek	left cheek	nose	chin
with vaccination	28	38.3±0.7	36.2±1.3	36.1±1.6	36.1±1.6	36.4±1.4	36.5±0.3
without vaccination	16	38.3±1.1	36.1±1.5	36.0±1.3	36.0±1.5	36.1±1.4	36.1±0.4
p-value			0.91	0.75	0.87	0.81	0.56	0.43
medication	numbers	axillary temperature	forehead	right cheek	left cheek	nose	chin
with medication	24	38.3±0.8	36.2±1.4	36.1±1.2	36.0±1.5	36.5±1.2	36.4±1.3
without medication	31	38.3±0.8	36.1±1.3	35.9±1.6	36.0±1.6	36.1±1.4	36.1±1.5
p-value			0.96	0.82	0.62	1.00	0.30	0.44

7. The facial thermography patterns of 61 patients of influenza were abnormal in 29 patients, uncertain abnormal in 22 patients, normal in 6 patients, and impossible to judge in 4 patients.
8. The real purpose of assessment in infection control using thermography is not detection of fever, but of infection. Five patients who were positive for influenza antibody but showed an axillary temperature of 37.4 degrees or less were thus investigated. Vaccination was not effective for changing facial surface temperature, but medication did reduce this value. When the facial thermography of Case 3 with pneumonia was excluded, that of the other cases showed distinct differences from healthy individuals, even if the facial surface temperature was decreased. The diagnosis rate can thus be improved by adding the judgment of the facial thermography pattern to that of the cut-off value for facial surface temperature.

Tab. 4 Summary of five patients positive for influenza antibody but an axillary temperature 37.4 ℃ or less

case	age	sex	disease	axillary temperature	vaccination	medication	forehead	right cheek	left cheek	nose	chin	facial thermography pattern
1	27	F	influenza A	36.3	+	+	35.2	34.7	34.9	34.8	34.9	abnormal
2	48	F	influenza A	36.3	+	−	36.4	36.3	36.2	36.4	36.0	uncertain abnormal
3	86	F	influenza A pneumonia	37.0	obscure	+	34.5	34.5	34.5	35.1	34.1	normal
4	41	F	influenza A	37.1	−	+	34.1	33.8	33.9	35.3	34.2	abnormal
5	68	F	influenza A	37.2	−	−	37.2	37.1	37.0	38.8	38.5	uncertain abnormal

Discussion:

A thermography not only measure temperature, but also can provide the imaging. In our efforts to develop a universally accepted method for infection control, it would seem that thermography offers one of the more promising techniques. A new evidenced based standard of thermography for detection of patients with fever is necessary to avoid spreading pyrogenetic disease.

Acknowledgment: This work was supported by KAKENHI 15K15934 and 15K11492.

contact: horie@tenriyorozu-u.ac.jp

Conflict-of-interest (COI)

We have no relevant relationships/interests to disclose.

Clinical Physiology

PG-37

Potential use of measuring Controlled Attenuation Parameter (CAP) with the Fibroscan® during health checkups

ORie Mitsui,[1] Yosuke Sugioka, [1] Nobuki Fukuhara[1], Michitaka Kato,[3] Fumi Nihei,[2] Akira Kubo,[2,3,4] Yoshihiko Takeda[4]

1 Department of Clinical Laboratory, Ginza Hospital, Tokyo,
2 Anti-aging Center, Ginza Hospital, Tokyo,
3 Department of Shizuoka Physical Therapy, Faculty of Health Science, Tokoha University, Shizuoka,
4 Department of Internal Medicine, Ginza Hospital, Tokyo

Background:

Blood tests and ultrasound are common ways to assess liver function. Recently, the Controlled Attenuation Parameter (CAP), a new tool of quantifying the degree of hepatic steatosis using the FibroScan®, has been developed to allow simultaneous measurement of hepatic steatosis and liver stiffness. This study assessed the correlation between the degree of hepatic steatosis measured by the CAP and various test results to evaluate the usefulness of the CAP in assessing disease risks.

<How it works>

Transduser sends vibration waves to the liver.The speed is tracked and analyzed using ultrasound.

liver stiffness unit (Kpa)
C A P unit (dB/m)

How liver stiffness measurement works:
Propagation velocity of the shear wave emitted from the probe tip is analyzed with ultrasound to determine elasticity(kPa)

How CAP measurement works:
Ultrasound waves decrease in amplitude as they propagate through adipose tissues.
CAP uses this principle and estimates the amount of fat based on ultrasound attenuation.

Subject:

This study included patients who went through a medical checkup at Ginza Hospital between June 2014 and March 2016 and had their CAP and liver stiffness measured by the FibroScan®. Patients with known liver diseases, including those with positive HCV or HBV results, were excluded. A total of 293 patients (170 male and 123 female, mean age 51.8 years old) were included.

Methods:

We evaluated the association between the CAP and 227 measurements from the health checkup, including blood tests, physiological tests, radiological tests, and patient interviews.

Results:

The CAP showed significant correlations with 52 out of the 227 measurements, including total body fat (r=0.637 P<0.001), BMI (r=0.623 P<0.001), visceral fat (r=0.600 P<0.001), waist circumference (r=0.562 P<0.001), total-PAI-1 (r=0.490 P<0.001), cholinesterase (r=0.428 P<0.001), insulin (r=0.418 P<0.001), small-dense LDL (r=0.400 P<0.001), high-molecular weight adiponectin (r=−0.382 P=0.002),free testosterone (r=−0.380 P=0.042), ALT (r=0.374 P<0.001), triglycerides (r=0.351 P<0.001) and RLP-cholesterol (r=0.330 P =0.004).

measurements with the highest correlation coefficients

	Total fat mass	Abdominal fat mass	BMI	Visceral fat area	Total fat area	Waist circumference	Abdominal muscle mass
Correlation coefficient(r)	**0. 637**	0. 623	**0. 623**	**0. 6**	0. 597	**0. 562**	0. 552
p-value(p)	. 001	. 001	. 001	. 001	. 001	. 001	. 001

	Left arm fat mass	Right arm fat mass	Body weight	Total-PAI-1	Body fat percentage	Thigh circumference (left)	Subcutaneous fat area
(r)	0. 551	0. 547	0. 495	**0. 49**	0. 477	0. 476	0. 472
(P)	. 001	. 001	. 001	. 001	. 001	. 001	. 001

	Thigh circumference (right)	Buttocks fat mass	Leg fat mass(right)	ChE	Insulin	sdLDL	Leg fat mass(left)
(r)	0. 471	0. 463	0. 449	**0. 428**	**0. 418**	**0. 4**	0. 395
(P)	. 001	. 001	. 001	. 001	. 001	. 001	. 001

	Free testosterone	High molecular Adipon	Dihomo-γ-linolenic acid	Urinary creatinine	ALT	Total adiponectin	TG
(r)	**−0. 38**	**−0. 382**	0. 376	0. 375	**0. 374**	0. 361	**0. 351**
(P)	. 042	. 002	. 001	. 004	. 001	. 003	. 001

	RLP- cholesterol	Visceral fat area ratio	Uric acid	BAP	Albumin	HDL cholesterol	Reaction of L / H
(r)	**0. 33**	0. 322	0. 3	0. 299	0. 299	−0. 298	−0. 282
(P)	. 004	. 005	. 001	. 010	. 025	. 001	. 014

※ measurments that are associated with metabolic syndrome and have correlation coefficient above 0.3 are in red

Discussion:

The CAP correlated well with several diagnostic factors of metabolic syndrome, and unlike waist circumference, it could be useful in evaluating metabolic syndrome associated with visceral fat. The CAP could also be valuable in assessing the risks of thrombotic and arteriosclerotic diseases as it showed significant correlation with the total PAI-1 and other atherosclerotic markers.

Conclusion:

The CAP is a noninvasive measurement and may be useful in assessing and managing the risk of various diseases.

Clinical Physiology
PG-38

A Point-of-care Sural Nerve Conduction Device（DPNCheck™ ）for Identification of Diabetic Polyneuropathy

○Yuka Shibata[1], Taeko Kamiya[1], Ryuhei Kanda[1], Hiroya Tani[1], Takahiko Kishi[1], Minehiro Gotoh[1], Hideki Kamiya[2], Jiro Na[redacted]ra[2]

1.Department of Clinical Laboratory Aichi Medical University Hospital, Japan
2.Division of Diabetes, Department of Internal Medicine Aichi Medical University, Japan

Background

The diagnosis of diabetes polyneuropathy using objective electrophysiological tests (nerve conduction study: NCS) is golden standard method. But NCS examinations technique is limited access to the specialized laboratories and technicians.

Aims

This study is to evaluate that nerve conduction velocity and sensory nerve action potential amplitude were measured bilaterally with difference methods, that DPNCheck™ and electromyography standard method (Neuropack X1: NIHON KOHDEN CORORATION, Japan). And we did statistical analysis for evaluating interaction.

A Point-of-care Sural Nerve Conduction Device DPNCheck™

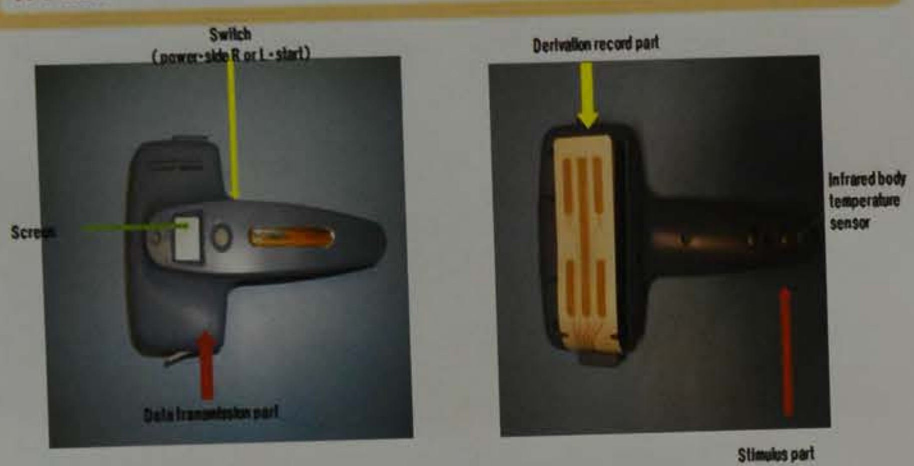

How to exam Sural nerve conduction study

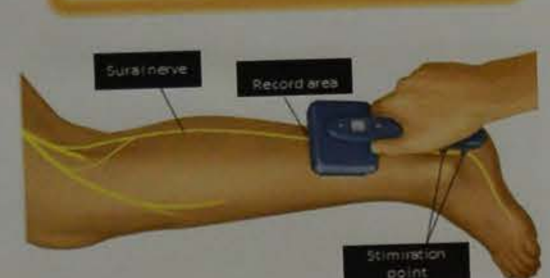

How to measure DPN Check™ wave

DPN Check™ nerve conduction waveform

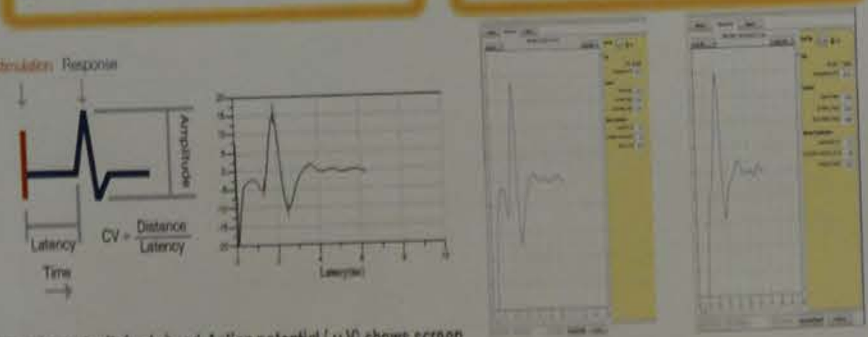

Conduction velocity(m/s) and Action potential (μV) shows screen

Difference points

	DPN Check™	electromyogram
Sampling frequency	10kHz	50kHz
Stimulus	orthodromic	antidromic
Stimulus derivation distance	92.2mm	140mm
Maximal stimulus	40～60mA	20mA

Methods

First we examined and measured both legs with electromyography standard method and after that measured with DPNCheck™.
To evaluate the reproducibility between two styles, one is same technicians twice examined DPNCheck™ and another is two technicians single examined DPNCheck™

Subjects

Diabetic in patients	57 persons
M:F	28:29
Mean Age	58.1 years old
Diabetes duration	8.9 years
HbA1c	9.55 %
BMI	26.6 kg/m²

Results

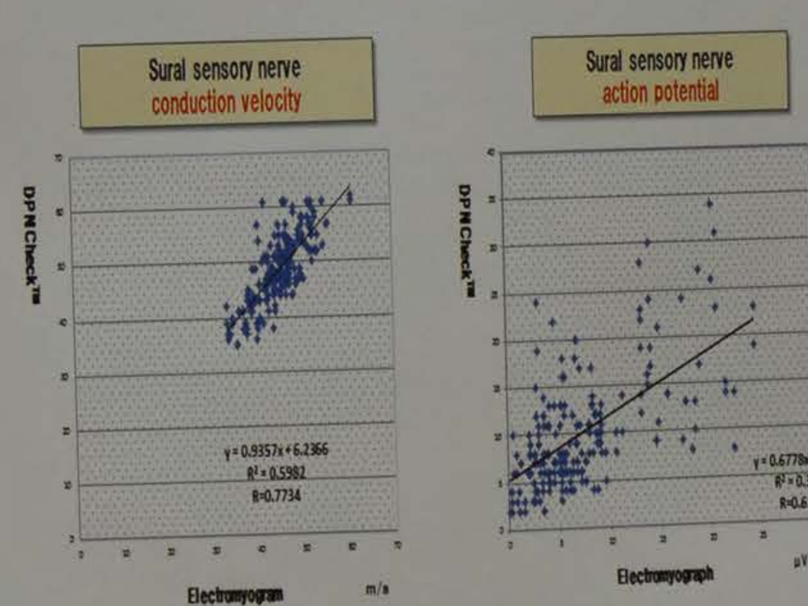

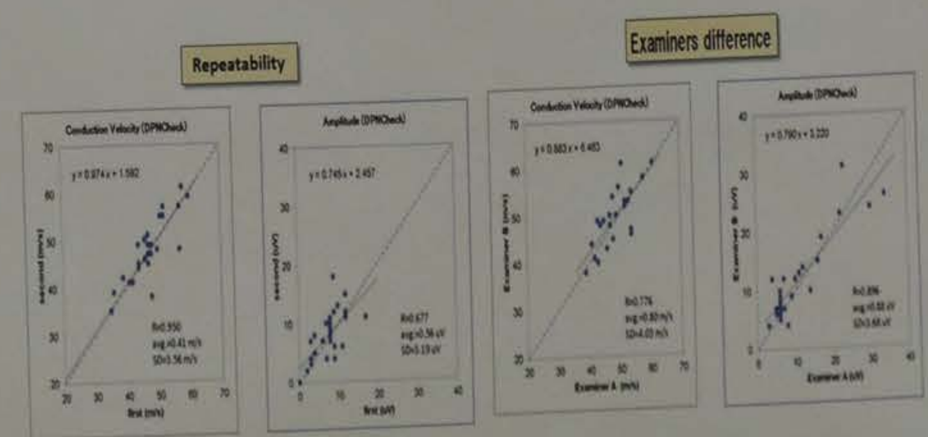

Pearson correlations were performed to determine the association between DPNCheck™ and electromyography standard method. The correlation coefficient (R) for velocity and amplitude were R=0.774 and 0.616 respectively. Comparison between of repeatability and the different examiner pattern showed admissible.

Conclusions

There is difference about stimulus principal' s method,. But however both examination results showed admissible statistical agreement correlation. DPNCheck™ is probably useful device for diagnosis of diabetes polyneuropathy.

AICHI MEDICAL UNIVERSITY HOSPITAL

E-mail address: yukau@aichi-med-u.ac.jp

禁　煙

Clinical Physiology

PG-39

About ABI value and pulse waveform numbers in ASO screening

Cases UT of blood pressure pulse waveform numerical value was useful

Michiko Enshu

Nara Prefecture General Medical Center

Introduction

Arteriosclerosis causes various vascular disorder. Nothing as for the arteriosclerosis obliterans (ASO) of those. The symptom of the ASO is pain, psychroesthesia, pain in rest, claudicatio intermittens. It is in one of a screening test of the ASO, and there are a crab, ABI measurement.

The examination for ABI (ankle-brachial index) measures an ankle and brachial blood pressure and calculates the ratio (ankle systolic blood pressure ÷ upper arm systolic blood pressure) Lower limbs blood pressure is usually higher than an upper arm. If there are a stenosis and obstruction, lower limbs blood pressure decreases.

Examination contents

If we have symptoms such as the intermittent claudication, pain, pain in rest, and ABI is low level, the likelihood that is ASO is very high.It is from around 70% of stenoses a blood vessel that we are reflected by an ABI level. Also, by the developments of the collateral pathway, we may not notice it with ASO. And we examined the complimentary number of obstruction, stenosis

Methods

We examine 47 people who underwent both blood pressure plethysmography and artery of lower extremity Eco - in 2014/1/1 - 2015/7/22 this hospital. We report 2 cases that suffered from the ASO that a symptom grieves at.

Use instrument : FUKUDA DENSHI CO.,LTD. (VaSera VS-1500A)

ASO screening reports in our hospital

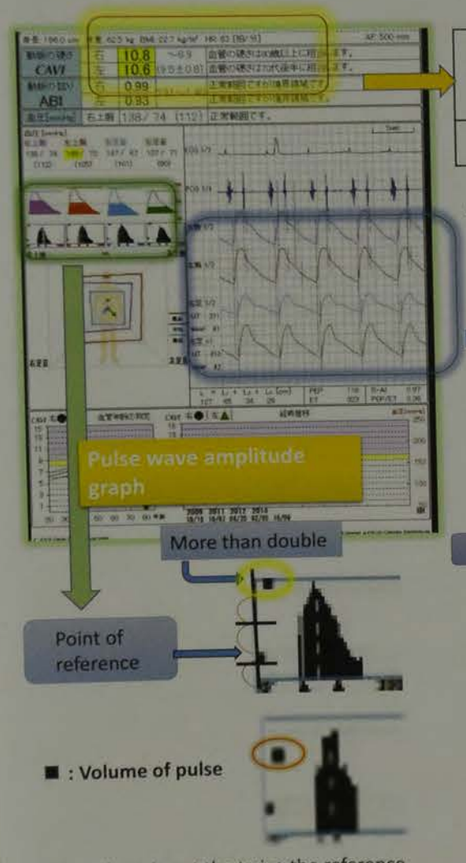

When there is not the twice the reference value, it is become constricted obstruction

Arterial hardness	The right	10.8	~8.9 (9.5±0.8)	The vascular hardness is considerable than 80 years old
	The left	10.6		The vascular hardness is considerable than 70 years old
ABI	The right	0.99	0.91~1.40	Is a normal range, but a boundary region
	The left	0.93		Is a normal range, but a boundary region

ABI reference values TASC Ⅱ (Japanese College of Angiology)

1.41: ABI ankle blood pressure higher 0.91: ABI ≤ 1.40 Normal range

0.00 ≤ ABI = 0.90 ASO doubt

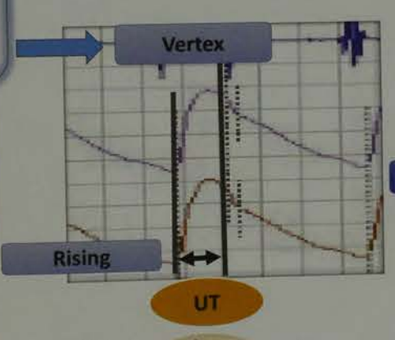

UT (Upstroke)

Rise time of the pulse wave

Normal value < 180 ms

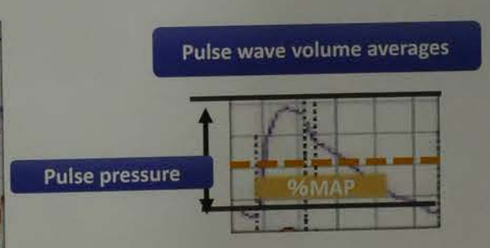

%MAP (Percent Mean Arterial Pressure)

Mean pulse pressure of the pulse wave /Pulse pressure × 100

Sharpness of the pulse wave

Normal value < 40

UT , %MAP flatten for a stenosis, obstruction

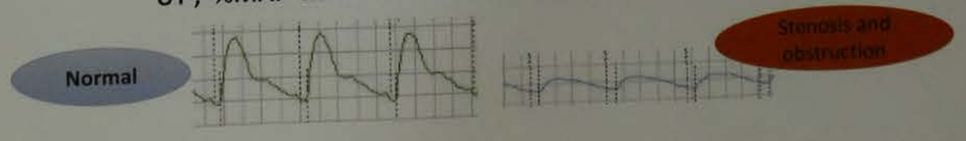

Case 1: 74 years old man

[chief complaint] It is a shoe sore in a left 5 digit
[clinical history] There is more tenderness for the left fifth finger than one month ago.
[medical history] Diabetes, angina

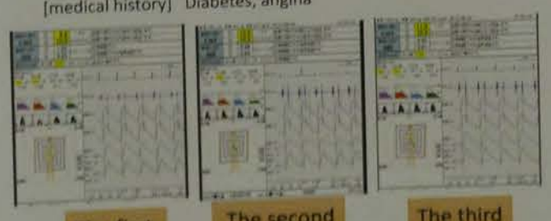

There is not a symptom, and, one and a half years later, the pain at walk develops.
50% of stenoses were detected in lower limbs Eco -.

	ABI		UT		%MAP	
	The right	The left	The right	The left	The right	The left
The first	1.03	0.93	199	219	37	37
The second	0.99	0.93	211	212	41	42
The third	0.95	0.91	214	215	40	41

Results

The ABI level is normal, but UT and % MAP exceed a reference value.

Case 2: 81 years old man

Results

UT ,% MAP is normal and the amplitude of the pulse wave amplitude graph is low.

Conclusion

There is not a symptom, and it cannot be said that ASO does not have it when an ABI level is normal. As for the ABI, it is more reliable ASO screening in what UT which is a complimentary measured value, % MAP, a pulse amplitude graph, the pulse wave form confirm without judging it only from the number of the blood pressure ratio.

FUJITA HEALTH UNIVERSITY

This work was supported by JSPS KAKENHI Grant Number 15K08656.

Clinical Physiology

PG-40

Comparison between FibroScan and virtual touch quantification for liver stiffness measurement in HCV patients

Keisuke Osakabe[1], Naohiro Ichino[1], Toru Nishikawa[2], Hiroko Sugiyama[2], Tadayoshi Hata[1], Naoto Kawabe[3], Senju Hashimoto[3] and Kentaro Yoshioka[3]

[1]Faculty of Medical Technology, School of Health Sciences, Fujita Health University
[2]Center of Ultrasound Diagnosis, Fujita Health University Hospital
[3]Department of Liver, Biliary Tract and Pancreas Diseases, School of Medicine, Fujita Health University

AIM

- ✓ Recently, various apparatuses for measurement of liver stiffness using the ultrasound have been developed.
- ✓ The liver stiffness values (LS) by FibroScan and the shear wave velocity (Vs) by virtual touch quantification (VTQ) was compared.

SUBJECTS

- ✓ LS and Vs were measured in 112(male; 68) patients with chronic hepatitis C virus infection who underwent liver biopsy consecutively in Fujita Health University Hospital from November 2010 to December 2014.
- ✓ LS and Vs were measured within a month of liver biopsy.
- ✓ Fibrosis stage by METAVIR score were, F0-1 in 26 patients, F2 in 25, F3 in 25 and F4 in 25.

EQUIPMENT'S & METHODS

- ✓ FibroScan 502 (EchoSens, Paris, France)
- ✓ ACUSON S2000 (Siemens , Japan Co., Ltd., Tokyo, Japan)
- ✓ LS values (kPa) and Vs values (m/sec) measured ten times
- ✓ at the right intercostal space, and the median value was adopted.

FibroScan 502 

ACUSON S2000 

METAVIR score

F0 : No fibrosis
F1 : Mild fibrosis – portal fibrosis without septa
F2 : Moderate fibrosis – portal fibrosis and few septa
F3 : Severe fibrosis – numerous septa without cirrhosis
F4 : Cirrhosis

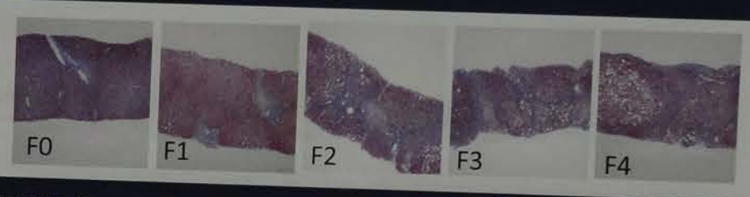

RESULTS

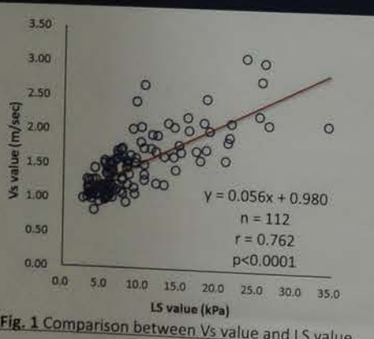

Fig. 1 Comparison between Vs value and LS value

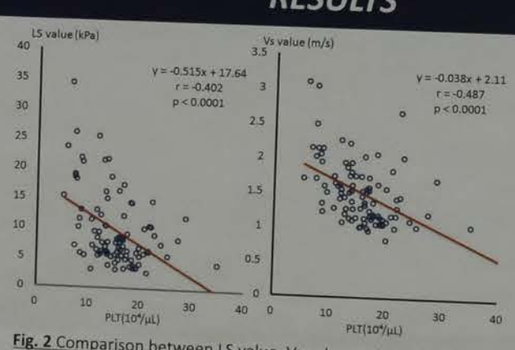

Fig. 2 Comparison between LS value, Vs value and platelet count

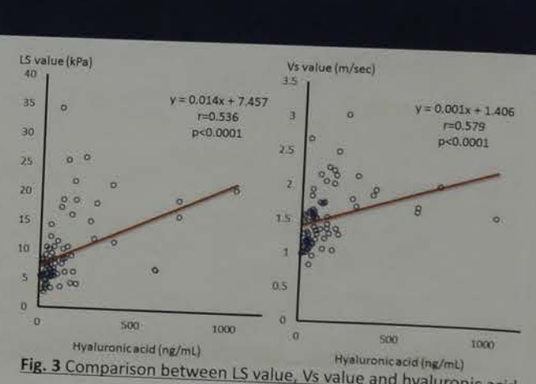

Fig. 3 Comparison between LS value, Vs value and hyaluronic acid

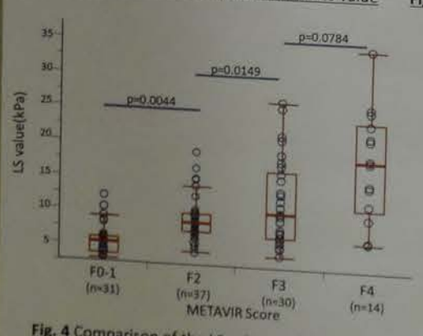

Fig. 4 Comparison of the LS value in METAVIR score

LS values were significantly correlated with fibrosis stage of the Metavir score ($r = 0.642$, $P < 0.0001$). LS values significantly differed between F0–1 and F2 ($P = 0.0044$); between F2 and F3 ($P = 0.0149$).

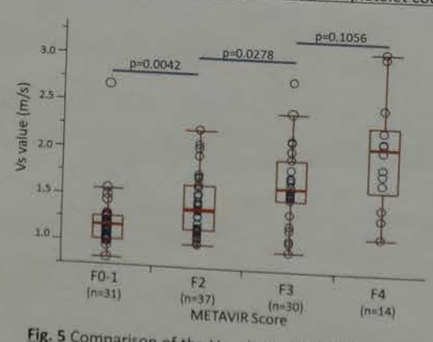

Fig. 5 Comparison of the Vs value in METAVIR score

Vs value were significantly correlated with fibrosis stage the Metavir score ($r = 0.600$, $P < 0.0001$). Vs values significantly differed between F0–1 and F2 ($P = 0.0042$); between F2 and F3 ($P = 0.0278$).

Table 1. Optimal cut-off value of LS and Vs for each fibrosis stage

F > or =2

	Cut off value	AUROC	Sensitivity(%)	Specificity(%)	Accuracy(%)	PPV(%)	NPV(%)
LS	6.0 (kPa)	0.826	82.7	97.4	72.3	89.3	37.8
VS	1.31(m/sec)	0.817	75.3	83.8	77.7	92.4	56.5

F > or =3

	Cut off value	AUROC	Sensitivity(%)	Specificity(%)	Accuracy(%)	PPV(%)	NPV(%)
LS	9.3 (kPa)	0.829	70.4	83.8	78.6	73.8	81.4
VS	1.51(m/sec)	0.805	79.6	75	76.8	67.3	85

F4

	Cut off value	AUROC	Sensitivity(%)	Specificity(%)	Accuracy(%)	PPV(%)	NPV(%)
LS	14.6 (kPa)	0.864	71.4	88.8	86.6	47.6	95.6
VS	1.81(m/sec)	0.824	71.4	85.7	83.9	41.7	95.5

AUROC : Area Under an Receiver Operatorating Characteristic
PPV : Positive Predictive Value, NPV : Negative Predictive Value

The optimal cut-off value of LS value was 6.0 kPa for F > or = 2, 9.3 kPa for F > or = 3 and 14.6 kPa for F4. The optimal cut-off value of Vs value was 1.31 m/sec for F > or = 2, 1.51 m/secfor F > or = 3 and 1.81 m/sec for F4. The optimal cut-off value of the LS had better on each stage than Vs.

CONCLUSION

- ✓ LS values and Vs values were confirmed to be correlated with each other and also with fibrosis stage of the METAVIR score.
- ✓ The ability to diagnose each fibrosis stage of FibroScan and VTQ is equivalent with each other.

Acknowledgements : This work was supported by JSPS KAKENHI Grant Number 15K08656.

The authors have no conflict of interest related to the content of this poster.

FUJITA HEALTH UNIVERSITY

禁 煙

alue and pulse waveform numbers in ASO screening

f blood pressure pulse waveform numerical value was useful

Michiko Enshu

a Prefecture General Medical Center

Introduction

disorder. Nothing as for the arteriosclerosis obliterans (ASO) of those. The esia, pain in rest, claudicatio intermittens. It is in one of a screening test of urement.

ndex) measures an ankle and brachial blood pressure and calculates the ratio rm systolic blood pressure) Lower limbs blood pressure is usually higher than obstruction, lower limbs blood pressure decreases.

tent claudication, likelihood that is stenoses a blood el. Also, by the we may not notice limentary number

Methods

We examine 47 people who underwent both blood pressure plethysmography and artery of lower extremity Eco - in 2014/1/1 - 2015/7/22 this hospital. We report 2 cases that suffered from the ASO that a symptom grieves at.

Use Instrument : FUKUDA DENSHI CO.,LTD. (VaSera VS-1500A)

creening reports in our hospital

terial dness	The right	10.8	~8.9 (9.5±0.8)	The vascular hardness is considerable than 80 years old
	The left	10.6		The vascular hardness is considerable than 70 years old
ABI	The right	0.99	0.91~1.40	Is a normal range, but a boundary region
	The left	0.93		Is a normal range, but a boundary region

reference values TASC Ⅱ (Japanese College of Angiology)
1: ABI ankle blood pressure higher 0.91: ABI ≤ 1.40 Normal range
00 ≤ ABI = 0.90 ASO doubt

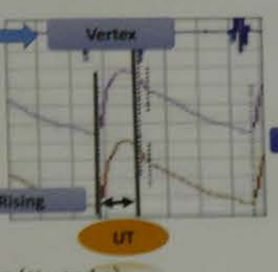

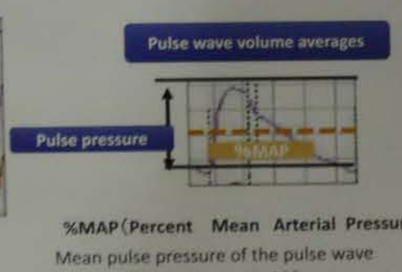

T (Upstroke)
tise time of the pulse wave
ormal value < 180 ms

%MAP (Percent Mean Arterial Pressure)
Mean pulse pressure of the pulse wave /Pulse pressure × 100
Sharpness of the pulse wave
Normal value < 40

UT , %MAP flatten for a stenosis, obstruction

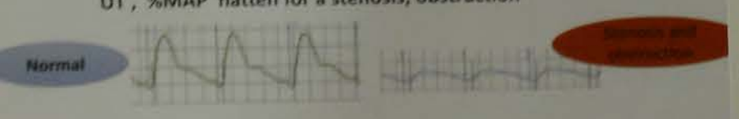

There is not a symptom, and, one and a half years later, the pain at walk develops.
50% of stenoses were detected in lower limbs Eco -.

	ABI		UT		%MAP	
	The right	The left	The right	The left	The right	The left
The first	1.03	0.93	199	219	37	37
The second	0.99	0.93	211	212	41	42
The third	0.95	0.91	214	215	40	41

normal, but UT and % MAP exceed a reference value.

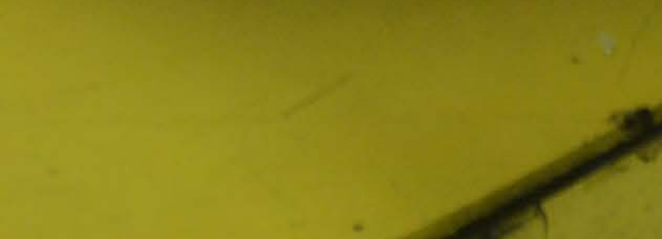

mal and the amplitude of the pulse wave amplitude graph is low.

d it cannot be said that ASO does not have it when an ABI level is normal.
sible ASO screening in what UT which is a complimentary measured value,
graph, the pulse wave form confirm without judging it only from the number

Clinical Physiology PG-41

A case of congenital biliary dilatation associated with gallbladder and common bile duct cancers

Rika Shimizu, Takako Oura, Harumi Fukuda, Yuko Sakurai, Makoto Morimoto, Kazushi Sugimoto, Kaname Nakatani

Department of Central Clinical Laboratory, Mie University Hospital, Mie, Japan

Case : 76-year-old female

Three years before, she underwent imaging studies for elevation of CA19-9 and was diagnosed as having adenomyomatosis and gallbladder polyp. Two years before, the follow-up studies showed the margin of gallbladder polyps becoming irregular and she was referred to our hospital.

Past medical history : tuberculosis, spinal canal stenosis, osteoporosis, dementia, hypertension, hyperlipidemia and glauzcoma
Social history : none Family history : none
Physical examination : no particular findings

A diagnosis of adenomyomatosis, gallbladder polyp and gallbladder stone were simultaneously made based on the findings of computed tomography (CT), endoscopic ultrasonography (EUS), and magnetic resonance imaging (MRI). Six months later, the follow-up CT showed gallbladder polyps became enlarged, raising the suspicion of malignancy. However, there was no remarkable change in the thickened gallbladder wall from body to fundus. One month later, abdominal ultrasonography (AUS) was performed and showed a cystic dilatation of the extrahepatic bile duct and a wide flat lesion on the wall of the dilated common bile duct. Then MRI and EUS were performed again. AUS and MRI revealed the dilated extrahepatic bile duct which had been taken as Gallbladder by CT findings .
By MRI findings, the patient was diagnosed as having Congenital biliary dilatation (Todani, Type Ia) associated with bile duct tumor and pancreaticobiliary maljunction. Surgical operation was performed.

Laboratory data

No abnormal values except for slight elevation of CA19-9 (79.5 U/ml).

Computed tomography -1st visit and 6months later-

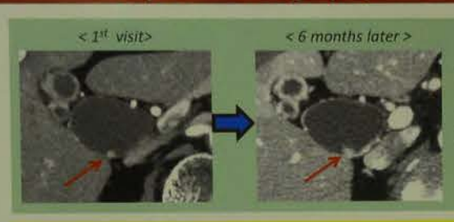

The elevated lesion suspected as gallbladder polyp became enlarged.

The thickened gallbladder wall from body to fundus showed enhancement in the vascular phase by contrast enhanced CT. High density area at the fundus was suspected as debris or stone.

6 months later, no remarkable change was seen on the thickened gallbladder wall and it was suspected as adenomyomatosis.

Magnetic resonance imaging -7 months later-

the tumor in the dilated common bile duct was revealed.

The elevated lesion on GB fundus had mild high intensity on T2WI and homogeneous high intensity on T1WI.

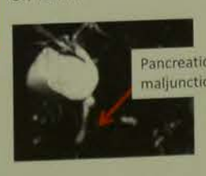

By MRI findings, the patient was diagnosed as having **Congenital Biliary Dilatation (Todani, Type Ia)** associated with bile duct tumor.

1st Endoscopic ultrasonography -1st visit-

Gallbladder wall was diffusely thickened. Hyperechoic lesion with acoustic shadow was observed at the fundus of gallbladder, suspected as gallbladder stone.

Abdominal ultrasonography -7 months later-

AUS showed a continuous cystic dilatation (ϕ38mm) from gallbladder and it was suspected as the dilated extrahepatic bile duct. In the dilated common bile duct, a wide flat lesion with a blood flow signal was also detected. The wall of gallbladder was diffusely thickened and hyper echoic lesion with acoustic shadow was seen in it, and gallbladder stones were suspected.

2nd Endoscopic ultrasonography -7 months later-

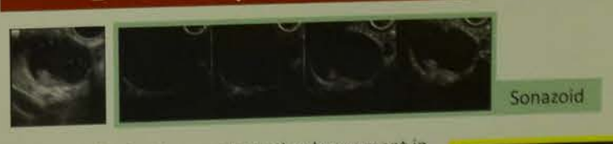

The bile duct tumor showed enhancement in the vascular phase by contrast-enhanced EUS with sonazoid .

Diffusely thickened wall and hyperechoic lesion with acoustic shadow at the fundus had no change. Irregularity of mucosa side was also detected.

Histological study

- The bile duct tumor was tubular adenocarcinoma, well differentiated and flat-infiltrating type, spreading to a lymph node.
- The lesion at the fundus of gallbladder was poorly differentiated adenocarcinoma, flat infiltrating type.

Congenital Biliary Dilatation (CBD)

CBD is a congenital malformation involving both local dilatation of the extrahepatic bile duct, including the common bile duct, and pancreaticobiliary maljunction. The prevalence is higher in Asia and occurred more frequently in women. The diagnosis of CBD is most often made during childhood. The surgical operation is required due to a high risk (2.5-26%) of cholangiocarcinoma. It is estimated that about 1% of CBD is associated with double cancers (GBCa+BDCa).

Discussion

- In this case, AUS was useful to detect cystic dilatation of extrahepatic bile duct.
- Detecting gallbladder cancer was difficult on AUS in this case. It was small and flat lesion hidden beneath stones.
- When the bile duct is dilated, we need to keep in mind the existence of CBD and check the tumor in the intra-,extra- bile duct and gallbladder carefully.

Conclusion

In this case, the patient was initially suspected as having gallbladder polyp which was later diagnosed as adenocarcinoma in CBD. AUS revealed the patient had CBD, which led to accurate diagnosis.

International Federation of Biomedical Laboratory Science
Disclosure of Conflict of Interest
Name of first author : Rika Shimizu

I have no COI with regard to our presentation.

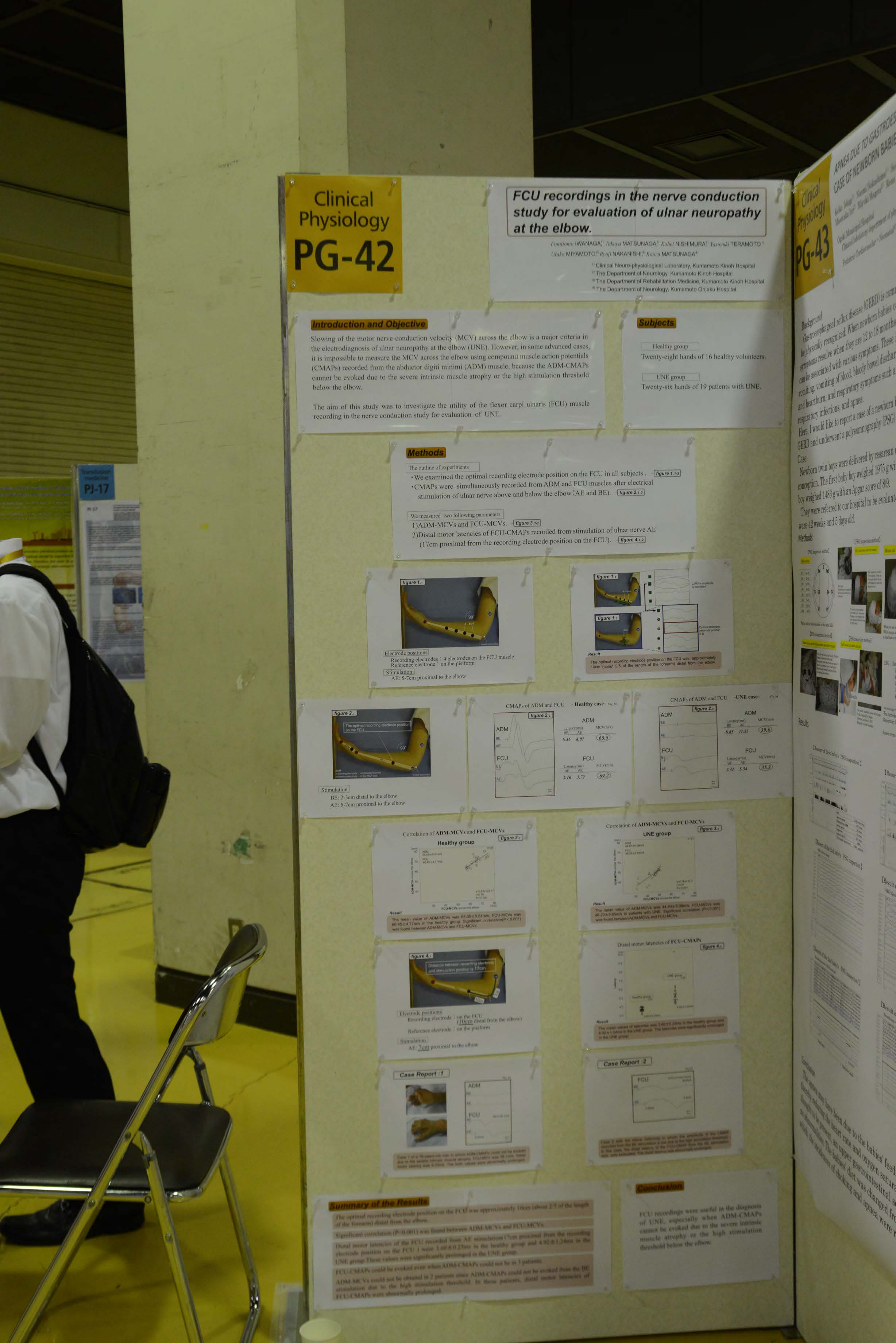

Clinical Physiology
PG-42
FCU recordings in the nerve conduction study for evaluation of ulnar neuropathy at the elbow.
Fumitomo IWANAGA[1] Takaya MATSUNAGA[1] Kohei NISHIMURA[1] Yasuyuki TERAMOTO[1]
Utako MIYAMOTO[2] Ryoji NAKANISHI[3] Kaoru MATSUNAGA[4]
[1] Clinical Neuro-physiological Laboratory, Kumamoto Kinoh Hospital
[2] The Department of Neurology, Kumamoto Kinoh Hospital
[3] The Department of Rehabilitation Medicine, Kumamoto Kinoh Hospital
[4] The Department of Neurology, Kumamoto Onjaku Hospital
Introduction and Objective
Slowing of the motor nerve conduction velocity (MCV) across the elbow is a major criteria in the electrodiagnosis of ulnar neuropathy at the elbow (UNE). However, in some advanced cases, it is impossible to measure the MCV across the elbow using compound muscle action potentials (CMAPs) recorded from the abductor digiti minimi (ADM) muscle, because the ADM-CMAPs cannot be evoked due to the severe intrinsic muscle atrophy or the high stimulation threshold below the elbow.
The aim of this study was to investigate the utility of the flexor carpi ulnaris (FCU) muscle recording in the nerve conduction study for evaluation of UNE.
Subjects
Healthy group
Twenty-eight hands of 16 healthy volunteers.
UNE group
Twenty-six hands of 19 patients with UNE.
Methods
The outline of experiments
・We examined the optimal recording electrode position on the FCU in all subjects. figure 1.1-3
・CMAPs were simultaneously recorded from ADM and FCU muscles after electrical stimulation of ulnar nerve above and below the elbow (AE and BE). figure 2.1-3
We measured two following parameters
1)ADM-MCVs and FCU-MCVs. figure 3.1-2
2)Distal motor latencies of FCU-CMAPs recorded from stimulation of ulnar nerve AE (17cm proximal from the recording electrode position on the FCU). figure 4.1-2
figure 1.1
Electrode positions
Recording electrodes : 4 electrodes on the FCU muscle
Reference electrode : on the pisiform
Stimulation
AE: 5-7cm proximal to the elbow
figure 1.2
figure 1.3
Result
The optimal recording electrode position on the FCU was approximately 10cm (about 2/5 of the length of the forearm) distal from the elbow.
figure 2.1
The optimal recording electrode position on the FCU
Stimulation
BE: 2-3cm distal to the elbow
AE: 5-7cm proximal to the elbow
CMAPs of ADM and FCU -Healthy case-
figure 2.2
ADM
Latency(ms) BE AE MCV(m/s)
6.36 8.01 65.5
FCU
Latency(ms) BE AE MCV(m/s)
2.16 3.72 69.2
CMAPs of ADM and FCU -UNE case-
figure 2.3
ADM
Latency(ms) BE AE MCV(m/s)
8.85 11.55 39.6
FCU
Latency(ms) BE AE MCV(m/s)
2.31 5.34 35.3
Correlation of ADM-MCVs and FCU-MCVs
Healthy group
figure 3.1
Result
The mean value of ADM-MCVs was 66.05±5.61m/s, FCU-MCVs was 66.45±4.77m/s in the healthy group. Significant correlation(P<0.001) was found between ADM-MCVs and FCU-MCVs.
Correlation of ADM-MCVs and FCU-MCVs
UNE group
figure 3.2
Result
The mean value of ADM-MCVs was 44.40±6.08m/s, FCU-MCVs was 46.29±5.65m/s in patients with UNE. Significant correlation (P<0.001) was found between ADM-MCVs and FCU-MCVs.
figure 4.1
Distance between recording electrode and stimulation position is 17cm
Electrode positions
Recording electrode : on the FCU (10cm distal from the elbow)
Reference electrode : on the pisiform
Stimulation
AE: 7cm proximal to the elbow
Distal motor latencies of FCU-CMAPs
figure 4.2
Result
Case Report :1
ADM
FCU
Case Report :2
FCU
Summary of the Results
The optimal recording electrode position on the FCU was approximately 10cm (about 2/5 of the length of the forearm) distal from the elbow.
Significant correlation (P<0.001) was found between ADM-MCVs and FCU-MCVs.
Distal motor latencies of the FCU recorded from AE stimulation(17cm proximal from the recording electrode position on the FCU) were 3.60±0.23ms in the healthy group and 4.92±1.24ms in the UNE group. These values were significantly prolonged in the UNE group.
FCU-CMAPs could be evoked even when ADM-CMAPs could not be in 3 patients.
ADM-MCVs could not be obtained in 2 patients since ADM-CMAPs could not be evoked from the BE stimulation due to the high stimulation threshold. In these patients, distal motor latencies of FCU-CMAPs were abnormally prolonged.
Conclusion
FCU recordings were useful in the diagnosis of UNE, especially when ADM-CMAPs cannot be evoked due to the severe intrinsic muscle atrophy or the high stimulation threshold below the elbow.
Clinical Physiology
PG-43
PJ-17

Clinical Physiology

PG-43

APNEA DUE TO GASTROESOPHAGEAL REFLUX DISEASE IN A CASE OF NEWBORN BABIES

Keiko Ishigo[1) Naomi Nakashima[1) Seiko Sawamura[1) Akari Tabata[1) Manayo Hattori[1)
Masataka Ito[2) Miyuki Magota[2) Rena Hyodo[2) Ryo Tanaka[2) Yoji Nomura[2)

Ogaki Municipal Hospital
Clinical labolatory department of physiology[1)
Pediatric Cordiovasalar・Neonatal[2)

Background

Gastroesophageal reflux disease (GERD) is common in newborn babies or infants and can be physically recognized. When newborn babies or infants have GERD, usually the symptoms resolve when they are 12 to 18 months old. However, severe cases of infant GERD can be associated with various symptoms. These include digestive symptoms such as vomiting, vomiting of blood, bloody bowel discharge, poor feeding or weight loss, rumination, and heartburn, and respiratory symptoms such as chronic coughing, wheezing, repeated respiratory infections, and apnea.

Here, I would like to report a case of a newborn baby who was not suspected of having GERD and underwent a polysomnography (PSG) check.

Case

Newborn twin boys were delivered by cesarean operation at 32 weeks and 5 days post-conception. The first baby boy weighed 1975 g with an Apgar score of 4/7. The second baby boy weighed 1483 g with an Apgar score of 8/9.

They were referred to our hospital to be evaluated for apnea and arrhythmia when they were 42 weeks and 5 days old.

Methods

【PSG inspection method】

EEG montage

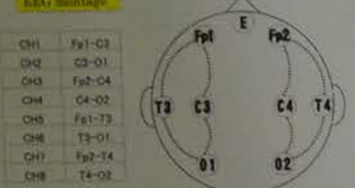

Bipolar and ear lobe recorded in the same side.

【PSG inspection method】

EEG electrodes attached example

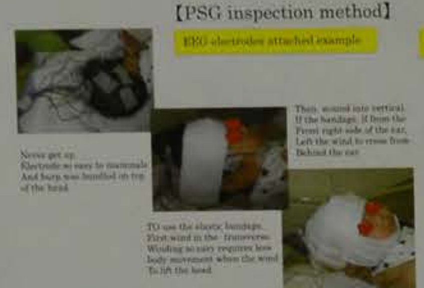

【PSG inspection method】

Mouse and nose breathing sensor

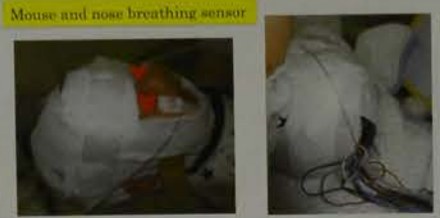

When you are with a lot of sensors even the small, You feel like crying. While using a sensor of the newborn, two mounting is unreasonable of a small hole in the nose thermistor sensor and pressure sensor.

【PSG inspection method】

Inductance method

In wound coil type sensor to belt a thin conductive wire to sign the form, Inductance changes when you change the spacing of the conductors by respiratory motion, the pulse of the period in accordance with the amount of change is oscillated.

【PSG inspection method】

Mouse and nose breathing sensor mounted example

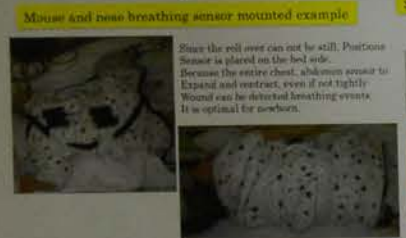

【PSG inspection method】

SpO2 sensor mounted example

Can not be installed sensor is too large. In the hands of the finger. Mounted as shown in FIG. Wrapped in elastic bandage.

【PSG analysis】

EEG : Determined by the sleep stage of newborn
keyboard 1: Active sleep
keyboard 2: Quiet sleep
keyboard 3: Indeterminate sleep
keyboard 4: Awake
keyboard 5: Indeterminable

Breathing events : Was carriedent in SUM analyzed using the Respiratory Inductance Plethymography(RIP)

Apnea event counts : 3 seconds

Results

【Resurt of first baby's PSG inspection 】

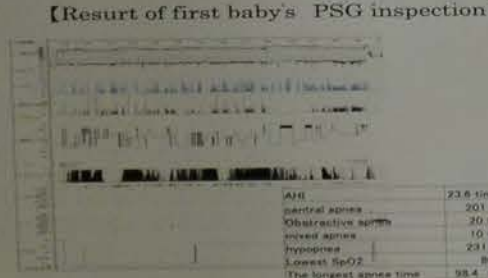

【Resurt of the 2nd baby's PSG inspection 】

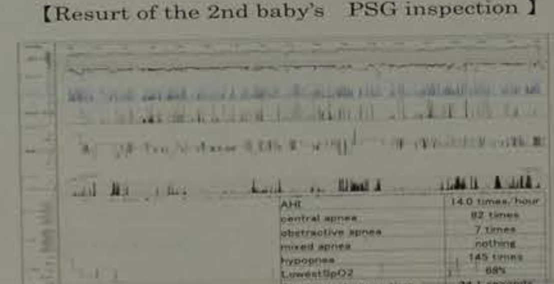

【Resurt of the 2nd baby's PSG inspection 】

EEG (Active sleep)

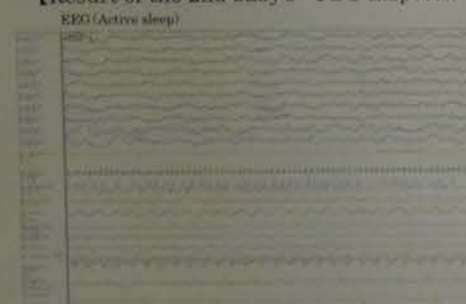

【Result of the 2nd baby's PSG inspection 】

EEG (Quiet sleep)

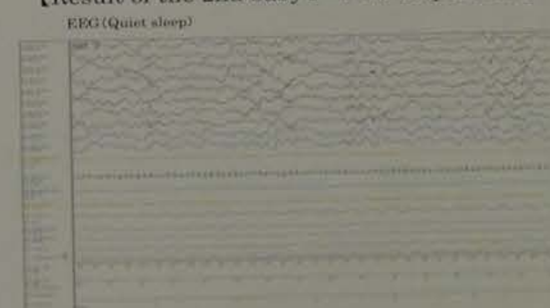

【Result of the 2nd baby's PSG inspection 】

Breathing events (SUM analysis)

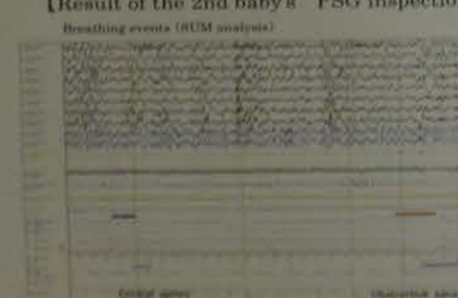

【Result of the 2nd baby's PSG inspection 】

Breathing events (SUM analysis)

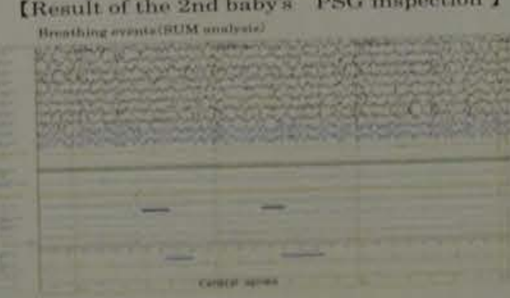

Conclusion

The apnea may have been due to the babies' feeding or sleeping, which caused choking, thereby reducing the heart rate and oxygen saturation. Although GERD was not thought to be present, an upper gastrointestinal series was performed, which revealed no abnormalities. The babies' diet was changed from breast-feeding to AR milk, after which, the incidences of choking and apnea were reduced.

Early detection of a latent cardiac dysfunction in Fabry disease by 2D speckle tracking

Toshihiko Hamada[1], Hiroyasu Uzui[2], Yuka Otake[1], Yumiko Tsuda[1], Norikazu Hashimoto[1], Kenichiro Arakawa[2], Yoshitomo Fukuoka[2], Masayuki Iwano[1], Hiroshi Tada[2], Hideki Kimura[1]
[1]Department of Clinical Laboratory Science, [2]Cardiovascular Medicine, University of Fukui, Japan

Clinical Physiology

PG-44

A Case of Intestinal Angina with Obstructive Hypertrophic Cardiomyopathy

Aya Ikeda, Takuto Hamaoka, Noriko Kawai, Wataru Omi, Yoshiteru Sekiguchi and Masako Kobayashi
Kanazawa Municipal Hospital

Background

Intestinal angina is characterized by recurrent postprandial abdominal pain and anorexia. Commonly, these symptoms are caused by severe stenosis of at least two vessels among celiac and mesenteric arteries, because of extensive collateral circulation. However, intestinal blood flows are dependent not only on individual vascular flows, but also on systemic supply. We experienced a unique case of intestinal angina with obstructive hypertrophic cardiomyopathy (HOCM) and relatively mild lesion of abdominal arteries.

Case presentation

An 86-year-old Japanese man was admitted with postprandial abdominal pain, anorexia and general malaise. He was previously diagnosed as HOCM with echocardiography, but had no medication because of no complaint about it. He had been suffering from repetitive and paroxysmal upper abdominal pain for one year. It occurred about 15 minutes after eating and usually disappeared within one hour, accompanied by watery diarrhea occasionally. He consulted to our department because the pain was suddenly getting worse and sustained longer a week ago. He was emaciated and exhausted with 7 kg loss of body weight for the last one year. Physical examination demonstrated low blood pressure (90/60 mmHg) and bradycardia (40 beats per minute).

The electrocardiogram revealed advanced AV block, left axis deviation and high R in V1 (Figure 1). Transthoracic echocardiography showed significant obstruction of left ventricular outflow tract (LVOT)(pressure gradient; 35 mmHg) and mitral regurgitation with systolic anterior motion (SAM) of anterior mitral leaflet (Figure 3A-C). The computed tomography (CT) with contrast enhancement demonstrated mild stenosis of the celiac artery and severe stenosis of the inferior mesenteric artery (Figure 2). Under the chronic low output condition with uncontrolled HOCM, exacerbating factors such as dehydration or bradycardia might have reduced systemic blood flow, especially intestinal perfusion.

We implanted a pacemaker with right ventricular apical pacing to improve hemodynamic condition, then his symptom was disappeared. After pacemaker implantation, LVOT obstruction and mitral regurgitation was reduced. AV delay was optimized to 100ms for minimum LVOT pressure gradient; 14.6mmHg(Figure 4A-C). The chest X-ray also showed reduction of intestinal dilatation (Figure 3D, 4D).

Electrocardiogram

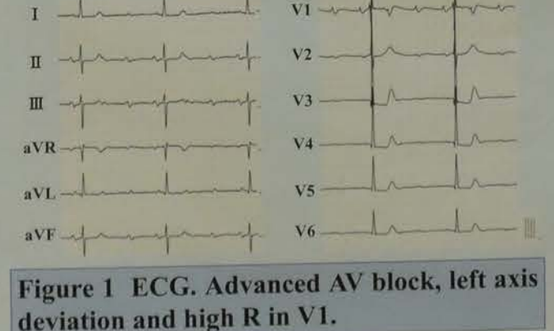

Figure 1 ECG. Advanced AV block, left axis deviation and high R in V1.

Computed tomography

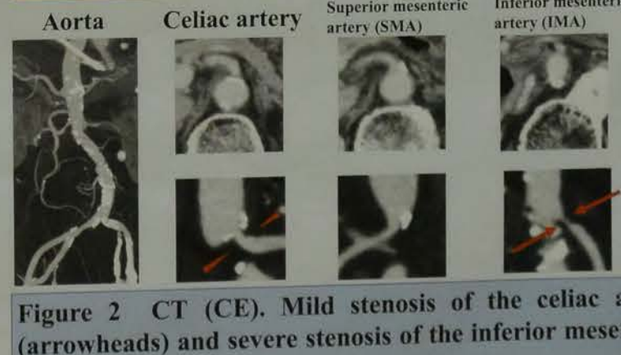

Figure 2 CT (CE). Mild stenosis of the celiac artery (arrowheads) and severe stenosis of the inferior mesenteric artery (arrows).

Images before pacemaker implantation

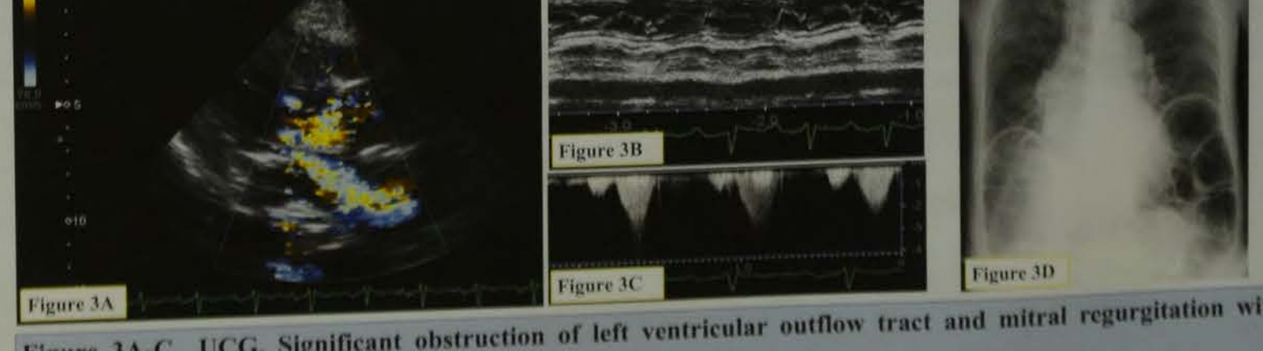

Figure 3A-C UCG. Significant obstruction of left ventricular outflow tract and mitral regurgitation with systolic anterior motion (SAM) of anterior mitral leaflet.
Figure 3D Chest X-ray. Mild cardiomegary and significant bowel dilatation.

Images after pacemaker implantation

Figure 4A-C UCG after pacemaker implantation. LVOT pressure gradient and mitral regurgitation are markedly reduced (AV delay 100ms for LVOT 14.6mmHg).
Figure 4D Chest X-ray showing significantly reduced of intestinal dilatation.

Conclusion

This case suggests that systemic hemodynamic change could contribute significantly to intestinal

Clinical Physiology

PG-45

Early detection of a latent cardiac dysfunction in Fabry disease by 2D speckle tracking

Toshihiko Hamada[1], Hiroyasu Uzui[2], Yuka Otake[1], Yumiko Tsuda[1], Norikazu Hashimoto[1], Kenichiro Arakawa[2], Yoshitomo Fukuoka[2], Masayuki Iwano[1], Hiroshi Tada[2], Hideki Kimura[1]

[1]Department of Clinical Laboratory Science, [2]Cardiovascular Medicine, University of Fukui, Japan

Background

- Fabry disease is induced by a mutation in the α-galactosidase A gene, causing a deficiency of the enzyme α-galactosidase A .
- The enzyme defect leads to progressive intracellular accumulation of globotriaosylceramide in lysosomes of various tissues and organs, including heart, kidney and nervous system.
- The pathology of cardiac Fabry disease primarily involves left ventricular hypertrophy, and reductions in cardiac function and progression of fibrosis are observed.
- Recently, same cases have been diagnosed before reductions in cardiac function based on clinical findings such as family history and measurement of α-galactosidase A activity.

We herein initiated a successive enzyme replacement therapy for two Fabry patients with normal cardiac function about 7 years ago, monitored the course of cardiac function over the time, and evaluated the usefulness of myocardial strain assessment by two dimensional (2D) speckle tracking echocardiography.

Case presentation

Family pedigree

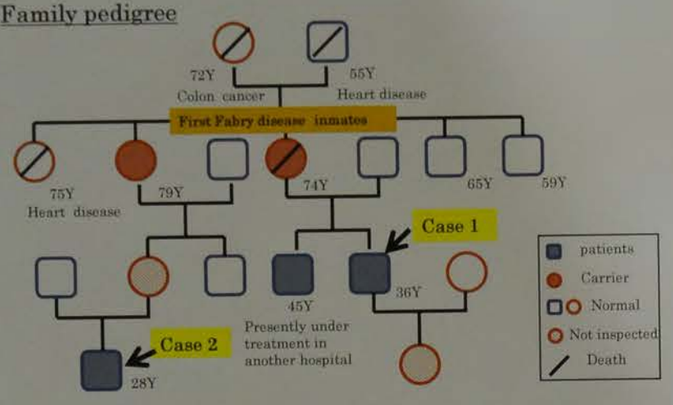

Case 1 36 y.o. Man

History of present illness

A 36-year-old man had noticed numbness in both arms and both legs after exercise as well as the symptom of not easily sweating in the summertime since his junior high school years.
When the patient was 29 years old, his mother was diagnosed with Fabry disease, and detailed examination was initiated.

Biomarker findings

BNP 12.1pg/ml , Plasma α-galactosidase A activity 0.2nmol/ml ,
Plasma Ceramide trihexoside (CTH) 7.6nmol/ml ,
Urinaly α-galactosidase A activity 11.2nmol/ml , Urinaly CTH 148nmol/ml

Changes in the echocardiography & MRI findings

* TTE

Dd/Ds/EF:
45mm/26mm/75%
Dd/Ds/EF:
44mm/29mm/64%

* MRI

(Neither demonstrated contrast delay)

* LV wall thickness & Mitral annular E' velocity

Date	Feb.27, 2013	Oct.16, 2013	Apr.9, 2014	Oct.22, 2014	Apr.9, 2015	Oct.8 2015	Apr.9, 2016
IVS (mm)	11.6	12.1	12.1	12.6	12.8	12.8	13
PW (mm)	11.3	11.6	12.1	12.3	12.1	12.8	12.5
E' (%)	7.1	7.4	6.8	8.1	8.1	7.3	6.4

* Longitudinal peak systolic strain of the LV

* Bull's – eye

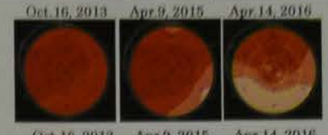

* Post systolic index

Case 2 28 y.o. Man

History of present illness

A 28-year-old man had noticed pain in the extremities and the symptom of hypohidrosis since around the age of 17 years. A relative of the patient was diagnosed with Fabry disease when the patient was 22 years old, and then the detailed examinations were initiated for the patient.

Biomarker findings

BNP 24.7pg/ml
Scrutiny at another hospital: Low plasma α-galactosidase A activity and increased levels of plasma CTH

Changes in the echocardiography & MRI findings

* TTE

Dd/Ds/EF:
44mm/29mm/62%
Dd/Ds/EF:
44mm/27mm/70%

* MRI

(Neither demonstrated contrast delay)

* LV wall thickness & Mitral annular E' velocity

Date	Apr.17, 2013	Oct.16, 2013	Apr.23, 2014	Oct.22, 2014	Apr.23, 2015	Oct.29 2015	May.12, 2016
IVS (mm)	9.7	9.5	9.1	9.1	9.5	9.6	9.5
PW (mm)	9.7	9.5	9.1	9.1	9.3	9.6	8.4
E' (%)	8.9	13.5	11.1	12.4	12.9	14.3	14

* Longitudinal peak systolic strain of the LV

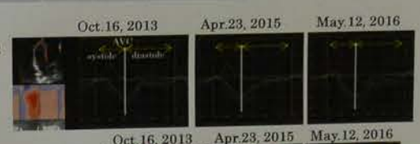

* Bull's – eye

* Post systolic index

Summary

In the seventh year, gadolinium-enhanced MRI showed no fibrosis, and conventional echocardiography showed no reduction in wall motion or left ventricular wall thickening. On the other hand, 2D myocardial strain assessment showed a reduction in the longitudinal strain of the lateral to posterior wall region.
In addition, a apparent reduction in the post-systolic strain in the lateral to posterior wall region was observed in both of two cases.

Conclusions

Measurement of the longitudinal strain using 2D speckle tracking enabled early detection of cardiac function abnormalities in two patients with Fabry disease who had not yet developed cardiac hypertrophy or fibrosis.
These findings suggest the more usefullness of 2D speckle tracking compared to conventional echocardiography in monitoring the time course of cardiac function status in patients with Fabry disease.

Clinical Physiology

PG-46

A case of the left atrium thrombus was difficult to visualize in transthoracic echocardiography

Yurina Kato[1], Akira Yabuki[1], Saori Abe[1]

[1] South Miyagi Medical Center

SMMC

【Introduction】
Transthoracic echocardiography(TTE) is the most popular test for the embolus source search today.
However we had a case of the left atrium thrombus was difficult to find in TTE.

【A case】
A man in his 60's

【Previous history】
Chronic atrial fibrillation, Chronic heart failure, Hypertension

【History of present illness】
He had had the numbness of the right hand since he woke up. He could walk but became able not to speak well.
He was admitted to our hospital owing to a diagnosis of cerebral infarction by brain MRI at another hospital. He received a diagnosis of cardioembolic ischemic stroke because of atrial fibrillation.

【TTE findings】
Transthoracic echocardiography (TTE) showed the left atrial dilatation and revealed that the inferior wall of the apex is moderate hypokinesis, but didn't show thrombus and any embolus source (fig.1, 2).

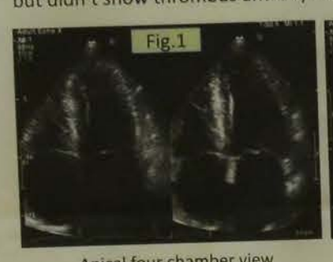

Apical four chamber view
→There were no thrombus

Apical three chamber view
→There were no thrombus

【TEE findings】
Transesophageal echocardiography (TEE) revealed a lesion like tumor (34.8 × 23.3mm) on esophagus side of the left atrium (fig.3) , but we couldn't diagnose it as myxoma or thrombus. It was thought an operation is necessary in either case.

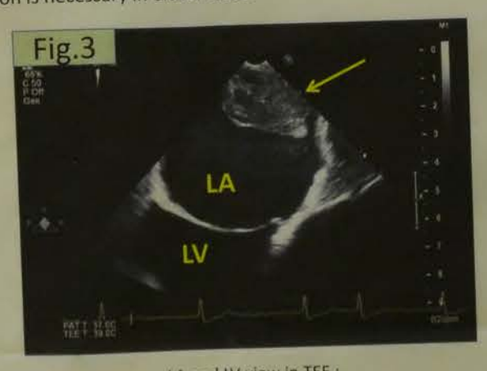

LA and LV view in TEE :
There was a 34.8 × 23.3mm size of thrombus in left atrium.

➡ He was operated at another hospital.

【TTE findings at another hospital (Before the operation)】

The medical technician in another hospital was able to view the lesion like tumor (fig.4) , because she knew there was something in his left atrium.

Apical four chamber view

【Operation findings】
There was a 4cm size of white thrombus on esophagus side of the left atrium (fig.5).
It was a thrombus in pathological findings too.

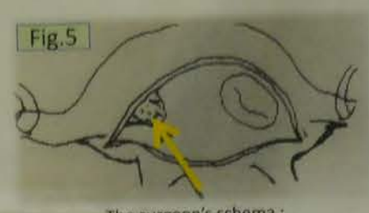

The surgeon's schema :
There was a 4cm size of thrombus in left atrium.

【Pathological findings】
The most parts of the thrombus are Fibrin, and we found few nucleated cells and few white blood cells . So, we diagnosed it as a white thrombus. (fig.6 - 10)

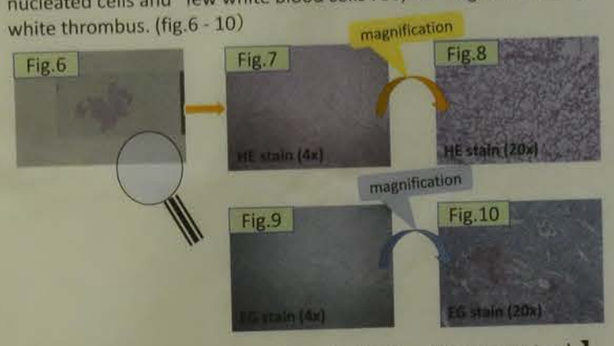

【TTE findings at another hospital (after the operation)】

There was nothing in the left atrium after the operation (fig.11).

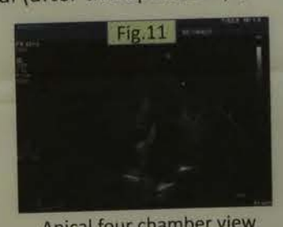

Apical four chamber view

【Comparison between Myxoma and Thrombus】
It's very important for a diagnosis to understand where tumor stick . Myxoma usually sticks to the interventricular septum, and thrombus usually sticks the posterior wall of left atrium or the lateral wall of left atrium . (Table 1)

	Myxoma	Thrombus
Character	· Form of strawberry jelly · Inside isn't uniform	· Fine, light, layered, and high brightness · Inside is uniform
Attachment site	· Nearby interventricular septum oval fossa	· Posterior wall of left atrium or lateral wall of left atrium
Basal disease	· Transmitral flow pattern like a MS	· MS,MR · Left atrial dilatation · Smoke like echo

Table.1

*Kawasumi S , Tsutsui H, Kuwana S, et al : Two cases of giant mass lesion in left atrium : Differential diagnosis of myxoma and ball thrombus. Shinzo 1995 ; 0586-4488(27)9 : 837-842

【Conclusion】
It was difficult to find the thrombus in TTE, because it is the farthest from chest wall. We became able to visualize this lesion, because we observed nearer to this lesion by using TEE. TTE has limitations, so we should carry out TEE. Therefore we can find an embolus source easily.

Clinical Physiology

PG-47

An 83-year-old asymptomatic female patient of Atrioventricular Septal Defect

Yuki Higuchi, Hiromi Umeda, Tamami Kudo, Kuninori Sugita, Takako Karube, Harushi Niu
Cardiovascular Medicine Akihiro Isotani

Kokura Memorial Hospital
Section of Medical Technologist, Department of Physiology

83 years old, Female

<Chief Complaint> Lower leg edema
<Past History> Uterine cancer
<Family History> No history

<Present Illness>
Asymptomatic atrial fibrillation and cardiomegaly was found in a primary care hospital in 2011. She was referred to our hospital for further workup.

<Physical Findings>
BP:133/45 mmHg, HR:70 bpm, irregular
SpO2:87% (room air), BT:37.8℃
Heart Sound:Pan-systolic murmur
Respiratory Sound:Normal

<Labo Data>
BNP 340.7pg/ml

<A Chest X-Ray Film>

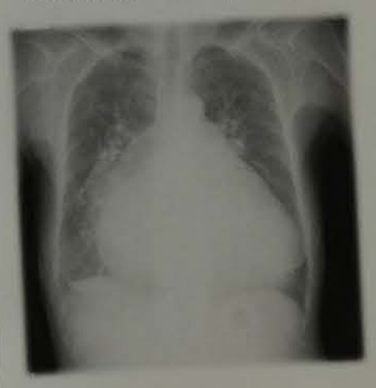

CTR 75%

<ECG>

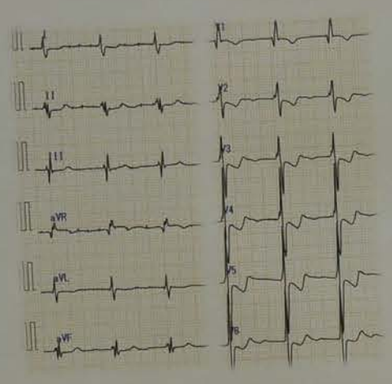

HR 61, af, abnormal ST-T, IRBBB (QRS 116 msec)

<TTE, TEE>
LVDd/LVDs 46.8/31.3mm, LVEF(Teicholz) 61.6%
Qp/Qs 3.64, TRPG 70.7mmHg

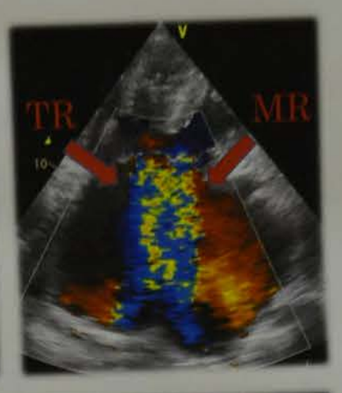

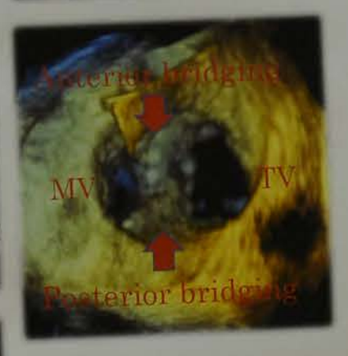

<Morphology>

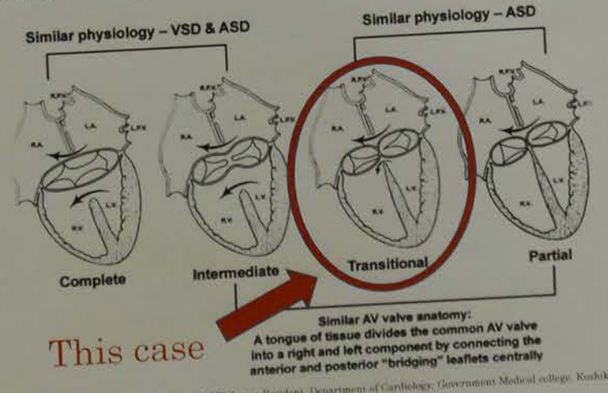

Atrioventricular Septal Defect, Dr Ramith MP,Senior Resident, Department of Cardiology, Government Medical college, Kozhikode

<Summary>
- AVSD (transitional type).
- Good LV function, reduced RV function with severe pulmonary hypertension.
- Very mild symptom despite desaturation due to right to left shunt from TR.

<Discussion>
- The discrepancy between significant heart abnormality and mild symptom can be explained by the small VSD. It might have lead to slow progression of PH.
- Desaturation might be influenced by direct TR jet into the LA.
- Quantitative estimation of valvular heart disease was difficult in this case, because of af, regurgitation in all valves in the heart.

<Conclusion>
TTE is effective for not only the diagnosis but also understanding of the hemodynamics of such a complex structural disease. TTE will be important even in the regular follow up of this complex congenital heart disease.

KOKURA MEMORIAL HOSPITAL

left atrium thrombus was difficult to visualize in echocardiography

[1], Akira Yabuki[1], Saori Abe[1]

Medical Center

SMMC

【Operation findings】

There was a 4cm size of white thrombus on esophagus side of the left atrium (fig.5).
It was a thrombus in pathological findings too.

Fig.5

The surgeon's schema :
There was a 4cm size of thrombus in left atrium.

【Pathological findings】

The most parts of the thrombus are Fibrin, and we found few nucleated cells and few white blood cells . So, we diagnosed it as a white thrombus. (fig.6 - 10)

Fig.6

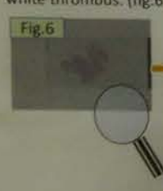

magnification

Fig.7

Fig.8

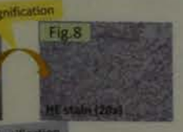

magnification

Fig.9

Fig.10

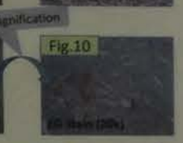

【TTE findings at another hospital (after the operation) 】

There was nothing in the left atrium after the operation (fig.11).

Fig.11

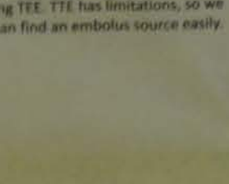

Apical four chamber view

【Comparison between Myxoma and Thrombus】

It's very important for a diagnosis to understand where tumor stick . Myxoma usually sticks to the interventricular septum, and thrombus usually sticks the posterior wall of left atrium or the lateral wall of left atrium . (Table 1)

	Myxoma	Thrombus
Character	· Form of strawberry jelly · Inside isn't uniform	· Fine, light, layered, and high brightness · Inside is uniform
Attachment site	· Nearby interventricular septum oval fosse	· Posterior wall of left atrium or lateral wall of left atrium
Basal disease	· Transmitral flow pattern like a MS	· MS,MR · Left atrial dilatation · Smoke like echo

Table.1

*Kawasumi S , Tsutsui H, Kuwana S, et al : Two cases of giant mass lesion in left atrium : Differential diagnosis of myxoma and ball thrombus. Shinzo 1995 ; 0586-4488(27)9 : 837-843

【Conclusion】

It was difficult to find the thrombus in TTE, because it is the farthest from chest wall. We became able to visualize this lesion, because we observed nearer to this lesion by using TEE. TTE has limitations, so we should carry out TEE. Therefore we can find an embolus source easily.

Clinical Physiology

PG-48

A case of shosin beriberi whose hemodynamics could be assessed serially by echocardiography

Natsuki Nakagawa[1], Ayano Hashizume[1], Ayaka Araki[1], Hiroomi Shimotsuka[1], Tsutomu Sakamoto[1], Hiroyuki Ihori[2], Tomoki Kameyama[2], Hiroshi Inoue[2]
[1]Dept of Clinical Laboratory and [2]Dept of Internal Medicine, Saiseikai Toyama Hospital, Toyama, Japan

Introduction

The Beriberi heart is a rare disease that is believed as high cardiac output heart failure due to vitamin B1 deficiency. Shoshin beriberi follows a fulminant course , resulting rapidly in hemodynamic collapse. Therefore, rapid diagnosis is mandatory. Herein, we report a rare case of shosin beriberi whose hemodynamics could be assessed serially by echocardiography.

Case

【Case】 Man, 65 years old
【Chief complaints】 Hypotension, Vomiting
【Present illness】 He was admitted to another hospital, because he fell down after drinking alcohol the previous day. In the next morning, he became collapsed (systolic BP 70 mmHg), and then was transferred to our hospital.
【History】 Alcoholic liver disease, Smoking(+), Drinking(+)
【Physical exam】 Height 165 cm, Weight 63.7 kg, HR 120 bpm, BP 70/44 mmHg, SpO_2 100 %(room air), Conjunctiva : jaundice(-), anemia(-), Abdominal : bowel(-), Jugular : vein distention(-), Breath sound : wheezes(-), Heart sound : Ⅲs(-), murmur(-), Consciousness(JCS I-1), Muscle weakness(-), Leg edema(+).

Clinical course after admission (Figure 3)

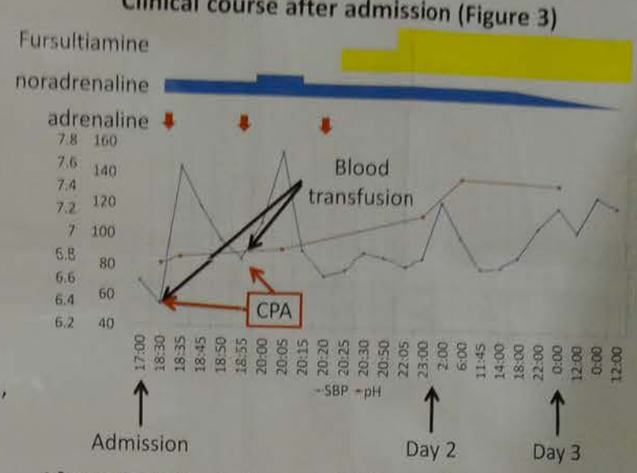

After admission to the ward, BP was decreased 50 mmHg, resulting in cardiopulmonary arrest(CPA). Cardiopulmonary resuscitation (CPR) with chest compression, intravenous adrenaline injection and blood transfusion were started. CPR was temporarily effective, but CPA recurred repeatedly. After reviewing his history of alcohol drinking, his shock was attributed to shoshin beriberi caused by vitamin B1 deficiency due to alcohol abuse. After a bolus intravenous injection of thiamine, his hemodynamics was improved immediately and dramatically.

Laboratory data on admission

AST 331 U/L	eGFR 16 ml/min/1.73m²	pH 6.762
ALT 112 U/L	NH3 577 μg/dl	pO2 110.9 mmHg
LDH 581 U/L	Troponin T (-)	pCO2 27.8 mmHg
γ-GTP 261 U/L	H-FABP (+)	HCO^{3-} 4 mmol/L
T-Bil 5.3 mg/dl	BNP 61.2 pg/mL	BE -28.3 mmol/L
TP 4.5 g/dl	HbA_1c 4.8 %	AG 28 mEq/L
ALB 2.2 g/dl		
UA 10.8 mg/dl	WBC 10.3×10^3 /μL	PT 22.1 L
UN 18.8 mg/dl	RBC 1.56×10^6 /μL	PT-INR 2.19
Cre 3.37 mg/dl	Hb 6.0 g/dl	APTT 68.2 sec
CK 602 U/L	Ht 19.1 %	D-dimer 36.6 μg/mL
CRP 0.2 mg/dl	MCV 122.4 fL	
Na 141.7 mEq/L	MCH 38.5 pg	
K 6.26 mEq/L	MCHC 31.4 %	
Cl 101.0 mEq/L	PLT 44×10^3 /μL	

Echocardiography after treatment (Figure 4)

EF 60.4 %

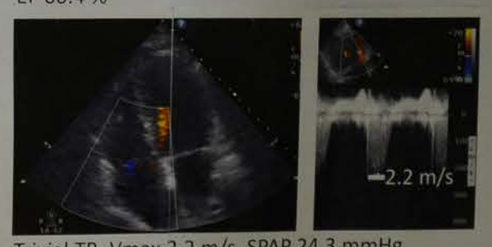

Trivial TR, Vmax 2.2 m/s, SPAP 24.3 mmHg

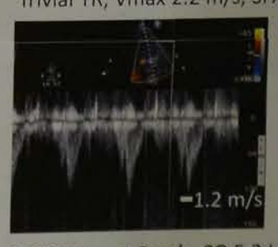

Abbreviations are as in Figure 2.

LVOT Vmax 1.2 m/s, CO 5.3 L/min, SVR 974.1 dyne·sec·cm^{-5}

ECG and XP on admission (Figure 1)

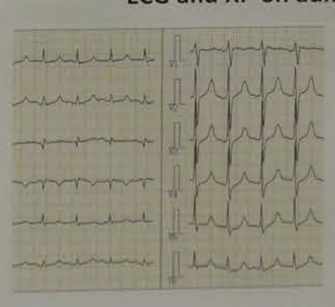

Echocardiography on admission (Figure 2)

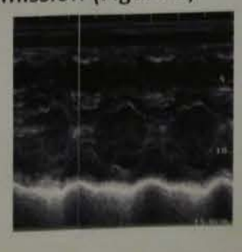

EF*1 83.8 %

Moderate TR*2, Vmax*3 3.6 m/s, SPAP*4 70 mmHg

LVOT*5 Vmax 2.8 m/s, CO*6 10.5 L/min, SVR*7 362.3 dyne·sec·cm^{-5}

*1 Ejection fraction
*2 Tricuspic regurgitation
*3 Maximum velocity
*4 Systolic pulmonary artery pressure
*5 Left ventricular outflow tract
*6 Cardiac output
*7 Systematic vascular resistance

Discussion

On admission, due to severe anemia and high cardiac output, we suspected he had hemorrhagic shock. He had severe metabolic acidosis and high cardiac output, and his hemodynamics did not improve after blood transfusion and catecholamine use. Therefore, we suspected he could have shosin beriberi. Indeed, after injection of vitamin B1, his hemodynamic state and echocardiographic findings improved dramatically.

Conclusion

We have reported a rare case of shosin beriberi whose hemodynamics could be assessed serially by echocardiography.
In patients with high cardiac output and anemia, beriberi heart should be considered as the underlying disease.

Clinical Physiology

PG-49

A pericarditis patient remission within

Abstract

We have recently encountered a patient with pericarditis who within one month. Here we show the clinical course of the pa

A pericardial hypertrophy and brightness, and respiratory fluctuations of ventricular inflow in the echocardiogram.

However, in this case the symptom was exacerbated and relie

In addition, the pericardium thickness was well correlated with

② Case Report

Case

A 62-year-old woman

Chief complaint: cough, chest pain

Medical history: cough variant asthma, hypercholesterolemia, fibromyalgia (suspected)

Family history: myocardial infarction (Mother)

Physical finding on admission

Laboratory findings on admission

clear

BH 160 cm weight 43.3 kg BMI 19.5

temperature 37.7 ℃ pulse 105 /min

blood pressure 80/68 mmHg

WBC 13.4 ×10³/μL

Fib ≥700 mg/dL

CRP 30.0 mg/dL

TP 6.1 g/dL

Alb 2.6 g/dL

BNP 232.7 pg/mL

wheeze (+) heart sound 3/3 (+)

jugular venous distention, Kussmaul's sign (+)

Imaging findings on admission

MRI, contrast-enhanced MRI

reinforced luminosity of the pericardium by contrast-enhanced MRI

③ Clinical Course

Changes in electrocardiogram

day 1 day 24

Symptom exacerbation

Changes of the p

On admission

The pericardial thickness w symptoms and the inflamma course.

④ Conclusion

It was concluded that the patient had been suffering from recurrent pe infection prevention. We learned from this case that there might be effective prevention who could be improved by proper treatm diagnosis by echocardiogram are clearly necessary in all the patients w vaccine prevention.

Clinical Physiology

PG-49

The 32nd World Congress of Biomedical Laboratory Science

A pericarditis patient who showed exacerbation and remission within a short period : a case report

Yoshinouchi T[1], Imamura K[1], Yasuda H[1], Nakanishi H[2], Ikeda K[1], Matsui H[1],
[1]Department of central clinical laboratory medicine, Kumamoto university hospital
[2]Department of cardiovascular medicine, Kumamoto university hospital

① Abstract

We have recently encountered a patient with pericarditis who showed repeated exacerbations and remissions within one month. Here we show the clinical course of the patient followed-up by the echocardiography.

A pericardial hypertrophy and brightness, and respiratory fluctuations of ventricular inflow in the echocardiogram. → Constrictive pericarditis was suspected at first.

However, in this case the symptom was exacerbated and relieved three times within one month.

In addition, the pericardium thickness was well correlated with inflammatory markers.

② Case Report

Case

- Patient: A 62-year-old woman
- Symptom: cough, chest pain
- Medical history: cough-variant asthma, hyperlipidemia, fibromyalgia (suspected)
- Family history: myocardial infarction (Mother)

Clinical history

- January, 20XX: Intermittent chest pain at inspiration occurred.
- September, 20XX: A chest pain at inspiration again, but there was no cardiac dilatation and pericardial effusion by X‐ray and CT examinations.
- November, 20XX+1: Cough and wheezing persisted. Thus a recurrence of the cough asthma was suspected and inhalational treatment was started.
- December, 20XX+1: The symptom did not change. Myocarditis and pericarditis were suspected by several examinations.

Physical finding on admission

- consciousness: clear
- height 149.0 cm weight 43.3 kg BMI 19.5
- body temperature 37.7 ℃ pulse 105 /min
- blood pressure 93 /68 mmHg
- respiratory sound: wheeze (+) heart sound: S3 (+)
- other: jugular venous distention, Kussmaul's sign (+)

Laboratory findings on admission

WBC	13.4 ×10³/μL
Fib	≧700 mg/dL
CRP	30.0 mg/dL
TP	6.1 g/dL
Alb	2.6 g/dL
BNP	232.7 pg/mL

ECG and Chest X-ray on admission

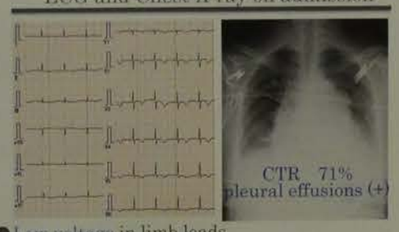

- Low voltage in limb leads
- Negative T waves in Ⅱ, Ⅲ, aVf and V1‐V6

Imaging findings on admission

- CT
- MRI, contrast-enhanced MRI

pericardial hypertrophy and effusion

reinforced luminosity of the pericardium by contrast-enhanced MRI

Echocardiogram on admission

- pericardial hypertrophy and brightness
- septal bounce
- adhesions of the pericardium

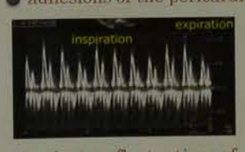

respiratory fluctuations of left ventricular inflow 30%

LVDd	37.3 mm
LVDs	27.4 mm
IVSTd	8.9 mm
PLVWd	8.7 mm
EF	67.3%(M.Simpson)
SV	35.4 mL
CO	3.8 L/min
E-wave DT	132.8 msec
e'	6.1 cm/sec
E/e'	14.8

③ Clinical Course

Changes in electrocardiogram

On admission — day 16 Symptom remission — day 24 Symptom exacerbation

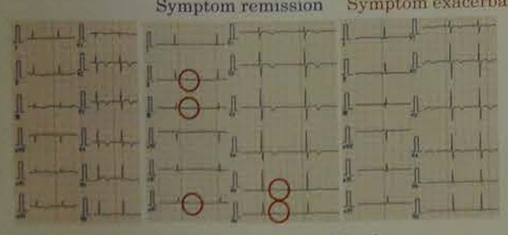

- Improvement of low voltage in limb leads
- Red circles: Flattened T-waves in Ⅱ, Ⅲ and aVF, Positive T-waves in V5 and V6

Progress of the disease and the treatment

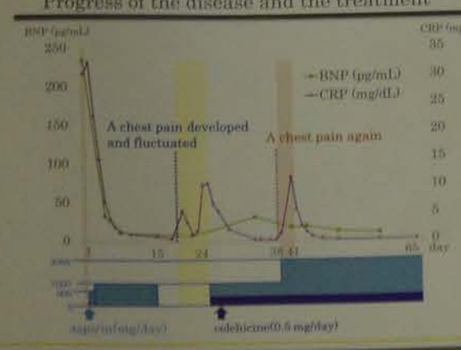

Changes of the pericardial thickness

On admission — day 16 — day 24

The pericardial thickness was well correlated with the clinical symptoms and the inflammatory markers during the clinical course.

④ Conclusion

It was finally concluded that the patient had been suffering from recurrent pericarditis accompanied by signs of constrictive pericarditis. We learned from this case that there might be pericarditis patients with the features of constrictive pericarditis who could be improved by proper treatments. Thus careful inspections and monitoring by echocardiogram are clearly necessary in all the patients who are initially diagnosed with constrictive pericarditis.

Clinical Physiology

PG-50

A case of Giant coronary artery aneurysms exceeding 5 cm in size

Chiho Ogawa[1] Hiroki Usuku[2] Hisayo Yasuda[1] Kanako Imamura[1]
Yuki Goto[1] Satoko Anai[1] Katsuyoshi Ikeda[1] Satoru Shinriki[1] Hirotaka Matsui[1]

[1] Department of Laboratory Medicine, Kumamoto University Hospital
[2] Department of Cardiovascular Medicine, Graduate School of Medical Sciences, Kumamoto University

Introduction

coronary artery aneurysms (CAAs)

- The coronary artery aneurysms with a diameter exceeding 20mm are usually referred to as "giant" coronary artery aneurysms (gCAAs).

Radiographics 2009; 29:1939–1954
J Cardiothorac Surg 2009; 4: 18

- gCAAs with a diameter exceeding 50mm are extremely rare and there had been few such reports.

J Jpn Coron Assoc 2013; 19: 30–35

We report an extremely rare case of gCAA with a diameter exceeding 50mm that was found by the echocardiogram.

Case Report

- Patient: a 74-year old man
- Chief complaint: chest pain
- Medical histories: hypertension, dyslipidemia
- Consciousness: clear
- Height 162 cm weight 47.7 kg BMI 18.2 kg/m^2
- Body temperature 37.5 ℃ Pulse 88/min
- Blood pressure 91 / 64 mmHg SpO_2 90% (O2 6L/min)

Present history

The patient has had a medical examination regularly in "A" hospital, because of hypertension and dyslipidemia.

In Year X, April	He became aware of a chest discomfort, but didn't go to a hospital because the symptom was within self-control range.
In Year X, October 16 am	He became aware of an intermittent epigastralgia.
In Year X, October 17	He was taken to the B Hospital by an ambulance because of the exacerbation of the symptom.

Blood test views (at the primary hospital)

WBC	14400	/μL	CPK	2180	U/L	Blood gas (O2 6 L/min)
Hb	12.3	g/dL	CK-MB	185	U/L	pH 7.522
PLT	3.71×10^5	/μL	TroponinI	65536	pg/mL	PaCO2 23.8 torr
CRP	4.85	mg/dL	BNP	941	pg/mL	PaO2 81.2 torr
T-Bil	0.9	mg/dL	TG	76	mg/dL	SaO2 97.1 %
AST	380	U/L	HDL-C	62	mg/dL	BE -3.3
ALT	71	U/L	LDL-C	90	mg/dL	HCO_3 19.7 mmol/L
LD	760	U/L	blood glucose	155	mg/dL	
γ-GT	167	U/L				
BUN	25.6	mg/dL				
Crea	1.6	mg/dL				
eGFR	33.7	mL/min				
Na	137	mmol/L	PT(INR)	1.02		
K	5.4	mmol/L	APTT	37.1	sec	
Cl	98	mmol/L	D-dimer	3.2	μg/mL	
Ca	8.8	mg/dL				

Electrocardiogram(at the primary hospital)

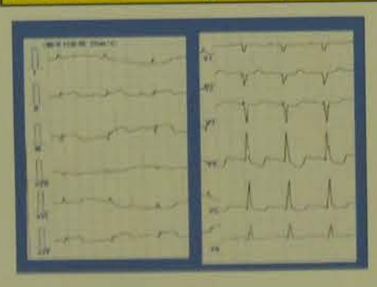

Rhythm: Sinus
Axis : normal
III,aVF : abnormal Q wave
V1-3 : QS pattern
II,III,aVF : ST-elevation
V3-5 : ST-depression

Chest X-ray examination (at the primary hospital)

Findings

- CTR 75%
- An enhanced pulmonary vascular shadow
- A decreased permeability of the right lung field

The summery of laboratory findings

blood examination
- The elevation of Troponin I, CK-MB

ECG
- II,III,aVF : ST-elevation
- V3-5 : ST-depression

The patient was diagnosed as myocardial infarction with ST elevation(STEMI) at the inferior wall.

His disease was suspected to be an acute coronary syndrome from lowered SpO2 and advanced cardiac dysfunction.

Coronary angiography was carried out under the insertion of the intra aortic balloon pump (IABP).

Echocardiography (at our hospital)

Arrows indicate a mass lesion (74x79mm) excluding right atrium, right ventricle, and the tricuspid valve.

〈epigastrium approach〉

Severe cardiac dysfunction
- LV Ejection Fraction (M. Simpson)=20.7%
- Severe tricuspid regurgitation
- Moderate mitral regurgitation

Contrast-enhanced CT examination (at our hospital)

The rupture of giant right coronary artery aneurysm

The perforation into the right atrium

Emergency surgery (at the division of cardiovascular surgery)

coronary artery aneurysms resection + coronary artery bypass + mitral valvuloplasty

- The gCAA, which was excised by the emergency surgery, was rich with organized thrombi.
- The pathological examination confirmed that the vascular wall had advanced arteriosclerosis lesions.

Discussion

〈The cause of CAAs〉

- Kawasaki disease (Most patients are Asians)
- Cardiac trauma
- Collagen diseases
- Coronary artery dissociation
- Coronary artery fistula
- Arteriosclerosis (the most common cause)

In this case

- No past history of cardiac trauma
- No Laboratory findings of collagen diseases
- No Coronary artery dissociation
- No Coronary artery fistula caused by CAAs

The blood vessels close to the gCAA in this patient was full of arteriosclerosis.

It has been reported that Kawasaki disease promotes arteriosclerosis.

It might be possible that the gCAA in this patient was caused by Kawasaki disease.

Conclusion

The echocardiography is highly useful for non-invasive morphological and functional evaluation, and enables us to make a proper decision for treatment strategy.

Clinical Physiology

PG-51

A case of AA amyloidosis with Castleman's disease that showed reversible ventricular hypertrophy

Kanako Imamura[1)] , Hisayo Yasuda[1)] , Sunao Kojima[2)] , Yuki Goto[1)] , Satoko Anai[1)] , Katsuyoshi Ikeda[1)] and Hirotaka Matsui[1)]

[1)] Department of Laboratory Medicine, Kumamoto University Hospital

[2)] Department of Cardiovascular Medicine, Graduate School of Medical Sciences, Kumamoto University

Introduction

Castleman's disease is known as not only one of the lymphoproliferative diseases characterized by hyperplasia of lymphoid follicles but also as an underlying disease of secondary AA amyloidosis.

Typical clinical symptoms

Chronic lymphadenopathy
Fever Anorexia Anemia

Aim

Here we report a report a case of Castleman's disease accompanied by AA amyloidosis who was followed-up for a long period with echocardiography.

Case

A 51-year-old man

- Major complaint : Dyspnea on exertion and attacks of unconsciousness
- Past medical history or family history : None
- Preference : Smoking of 12 cigarettes a day ×20 years
- Alcohol consumption : 2 glasses of distilled spirit per day

Clinical history

December / Year X	Palpitations after bathing and respiratory discomfort at walking on slopes
1 month later	After drinking alcohol, palpitation and unconsciousness lasting for about 10 sec. occurred. On the next day, palpitations and vomiting during asleep and unconsciousness for 10 sec. occurred again .
2 months later	Emergency hospitalization because of the attack of unconsciousness.

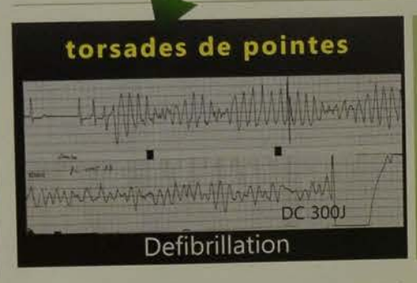

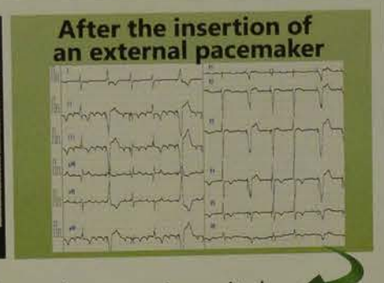

The patient was then referred to our hospital.

Physical findings on admission

- 170cm, 59 kg, 36.8℃
- Blood pressure : 98/62 mmHg
- Palpebral conjunctiva : Anemic
- Lymph node : Not palpable
- Heart sound : NP
- Abdomen : Palpating of liver in right hypochondrium (Two-finger breadths)
- Pulse : 72/min , irregular
- Bulbar conjunctiva : Yellowish
- Breath sound : NP
- Lower limb : No edema

Laboratory findings on admission

TP	6.7	g/dL	γ-GT	172	U/L	IgA	275	mg/dL
Alb	2.9	g/dL	UA	5.8	mg/dL	IgM	103	mg/dL
Na	138	mEq/L	Ch-E	69	U/L	P-Glu	114	mg/dL
K	5.3	mEq/L	CK	25	U/L			
Cl	103	mEq/L	Amy	69	U/L	WBC	5000	/μL
Ca	9.4	mg/dL	Fe	14	μg/L	Neut	73	%
BUN	28.3	mg/dL	UIBC	156	μg/dL	Lymp	22	%
Crea	1.77	mg/dL	T-Cho	145	mg/dL	Mono	3	%
T-Bil	0.6	mg/dL	TG	69	mg/dL	Eosin	2	%
AST	79	U/L	CRP	11.75	mg/dL	Baso	0	%
ALT	127	U/L	ESR	141/149	mm	RBC	311 × 10^4	/μL
LD	193	U/L	SAA	429	μg/mL	Hgb	7.4	g/dL
ALP	1923	U/L	IL-6	125	pg/mL	Hct	23.6	%
LAP	188	U/L	IgG	1640	mg/dL	PLT	36.2 × 10^4	/μL

- Serum immuno-electrophoresis : No polyclonal hyper-gammaglobulinaemia
- Urine immuno-electrophoresis and bone marrow biopsy : Negative for M-protein, plasma cells 1～3%

Duodenal biopsy

AA	(+)
TTR	(−)
AL κ chain	(−)
AL λ chain	(−)

Presence of the AA amyloid was confirmed

Abdominal US

6×4×4 cm solid mass

Abdominal CT

8cm Mesenteric tumor

Histopathological findings

Final diagnosis : Castleman's disease

Clinical course after the hospitalization

		2/15	3/18	3/28	5/1
AST	U/L	79		49	27
ALT	U/L	137	Mesenteric resection	42	26
TB	mg/dL	0.6		0.7	0.6
ALP	U/L	1923		791	263
LAP	U/L	188		132	73
γ-GTP	U/L	172		158	58
ChE	U/L	69		105	153
Cr	mg/dL	1.77		2.87	2.74
BUN	mg/dL	28.3		27.2	36.9
CRP	mg/dL	11.75		1.78	<0.05
IL-6	pg/mL	125		—	2.4
SAA	μg/mL	429		4.7	<2.5
WBC	/μL	5000		4600	3500
RBC	/μL	311 × 10^4		448 × 10^4	354 × 10^4
Hb	/dL	7.4		12.0	10.2
Ht	%	23.6		36.6	29.9
PLT	/μL	36.2 × 10^4		30.9 × 10^4	19.7 × 10^4

Changes of echocardiography findings

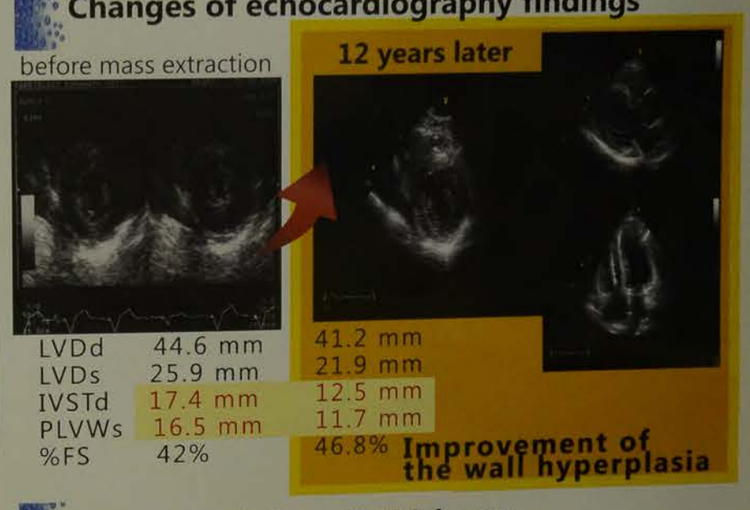

Changes of the wall thickness

The wall thickness was reduced to **12mm** in 8 years after the tumor resection.

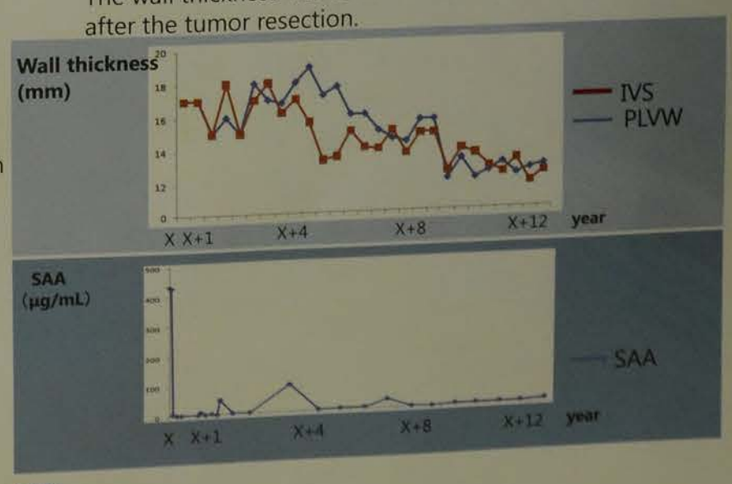

AA amyloidosis

- Most patients accompany renal failure, which is the main cause of death (40-60%).
- The amyloid deposition to heart is found in 5-10% of the patients, most of whom are accompanied with renal failure and high plasma SAA level.
- Better prognosis can be achieved when SAA level is maintained at **<10μg/mL by the treatment.**

Our cases of Castleman's disease who had been performed with echocardiography

			Left ventricular hypertrophy	SAA (μg/mL)	Renal failure	Organs with amyloid depositions (Biopsy point)	Sites of lymphadenopathy Type of the disease
Case 1 (This case)	51.M	+	17 mm	429	+	+ AA amyloid (Duodenum)	Mesenteric lymph node Plasma cell type
Case2	48. F	−	9 mm	1152	−	+ AA amyloid (Skin, duodenum,stomach,rectum)	From head to foot multiple lymphadenopathy
Case3	58. F	−	10 mm	51	+	+ AA amyloid (Duodenum)	Chest wall, axillary lymph node Plasma cell type
Case4	43.F	−	10 mm	Non measurement	−	−	Anterior mediastinum tumor Hyaline type
Case5	52. M	+	12 mm	263	+	(Duodenum, rectum)	Axillary lymph node Plasma cell type
Case6	48.M	−	10 mm	340	−		Cervical lymph node Plasma cell type
Case7	59. F	+	12 mm	Non measurement	−	−	Systemic lymphadenopathy Plasma cell type
Case8	46.M	−	10 mm	298	+	(Tumor mucosa cell)	Systemic lymphadenopathy Hyaline vascular type
Case9	15. F	−	7 mm	Non measurement	−	−	Retroperitoneal lymphoma Hyaline vascular type
Case10	79.M	−	10 mm	Non measurement	−		Unknown Plasma cell type
Case11	66. F	−	9 mm	Non measurement	−		Unknown Plasma cell type
Case12	66. M	−	9 mm	Non measurement	+		Cervical lymph node Hyaline vascular type mixt
Case13	55.M	−	8 mm	Non measurement	−		Clivus of lymph node Castleman node

We performed echocardiography in 13 patients among 33 cases of Castleman's disease diagnosed between April, 2004 to March,2014

Conclusions

Although this case is assumed to be very rare, it would be important not to overlook patients with Castleman's disease who present reversible ventricular hypertrophy.

Clinical Physiology

PG-52

Usefulness of Measuring Fractional Flow Reserve in Determining Renal Artery Stenosis due to Fibromuscular Dysplasia

Hiroki Kono[1], Naomi Bou[1], Naoki Kawabata[1], Kazuaki Shimizu[2], Kanichi Otowa[3], Kouichi Kifune[4]
([1]Municipal Tsuruga Hospital Medical Technology Department of Laboratory, [2]Department of Kidney Internal Medicine, [3]Department of Cardiology, [4]Department of Radiology)

Background -Fractional Flow Reserved : FFR-

Fractional flow reserved (FFR) determination is a technique used in coronary catheterization to measure pressure differences across a stenotic coronary artery, to determine the likelihood of the stenosis impeding Oxygen deliverry to the heart muscle.

(In the case of a cardiac catheter)

Coronary pressure(prox) Pd / Coronary pressure(distal) Pa = FFR

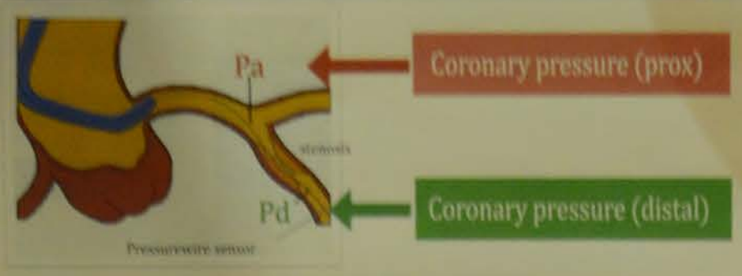

FFR Cutoff 0.80(0.75～0.80grayzone)

FFR is available for a diagnosis of renal artery stenosis

Background -Fibromuscular dysplasia : FMD-

Fibromuscular dysplasia (FMD) is a non-atherosclerotic, non-inflammatory disease of the blood vessels that causes abnormal growth within the walls of an artery. FMD is frequent in middle-aged women where it affects any arterial structure in the body.

FFR is the most effective for a diagnosis of FMD

Patient information

The patient was a 49-year-old woman with a history of hypertension. Sonography revealed a fast PSV in both renal arteries (PSV232cm/s,⊿PG22mmHg; left:⊿PSV171cm/s,⊿PG12mmHg). Contrast CT and angiography revealed a coffee bean-like appearance on both sides of the intermediate portion of the renal artery.

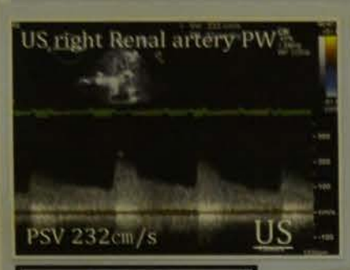

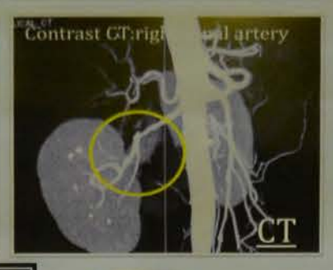

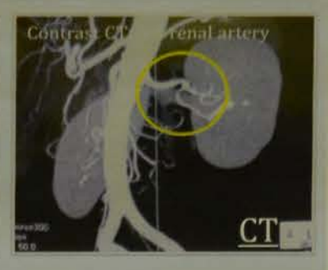

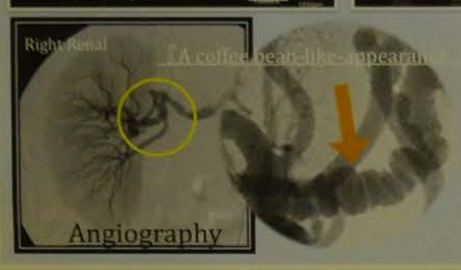

imaging study

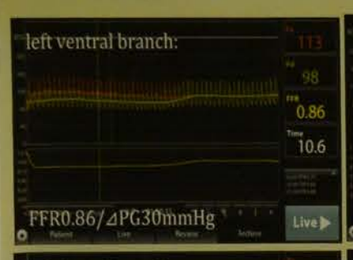

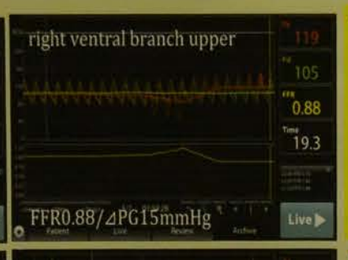

FFR

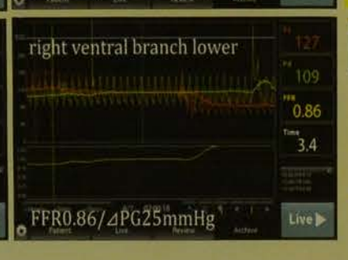

Case result

Pressures obtained were mostly in the upper limit, with the right dorsal branch having the highest measurement.

FFR is more execellent in a than diagnostic imaging study.

Conclusion

- FFR is available for renal artery
- FFR diagnoses a stenosis more exactry
- FFR is evaluable for a multiple lesion exactly

The disease severity of the stenosis disorder can be examined exactly by FFR.

Clinical Physiology

PG-53

Evoked potentials may predict of functional outcome in a case of acute necrotizing encephalopathy

Yuya Onozawa[1], Susumu Obata[1], Shinichi Munekata[1], Taira Toki[2], Yutaka Nonoda[2], Toshiyuki Iwasaki[2], Takahiro Iizuka[3], Yuhsaku Kanoh[4]
[1]Department of Clinical Laboratory, Kitasato University Hospital, [2]Department of Pediatrics, [3]Department of Neurology, [4]Department of Laboratory Medicine, Kitasato University School of Medicine

Objectives

- Acute necrotizing encephalopathy (ANE) is a severe form of acute encephalopathy characterized by bilateral thalamic lesions[1] and it mainly affects children in Asia and Western countries, with an estimated mortality rate of 30%.[2]
- To report a case of ANE, in which evoked potentials studies were useful in the prediction of functional outcome.

Methods

- A case report.

Results

- A 7-year-old boy was admitted to our hospital in Dec. 2013 with status epilepticus following influenza B infection.
- He was initially admitted to another hospital, and treated with IV peramivir hydrate. However, convulsive seizures developed in the next day, and he was transferred to our hospital.
- On arrival (day 1), he was in coma; the temperature was 40.6 ℃, BP 68/30 mmHg, PR 198 bpm, and SO2 70% (ambient air). Blood-test results showed metabolic acidosis, leukocytosis, DIC, increased CK, mild hypoglycemia, and renal dysfunction. CSF examination showed a few cells (WBC 7/μL) with protein level of 51 mg/dl, and normal glucose. Brain CT showed bilateral thalamic lesions.
- The patient was actively treated with therapeutic hypothermia (34 ℃, 48 hours), plasma exchanges (3 days), administering IV methylprednisolone (30 mg/kg/day, 3 days), and IVIg (1 g/kg/day, 1 day) under sedation with midazolam (0.2 mg/kg/hr, 6 days) and fentanyl (2μg/kg/hr, 6 days) from day 1. A brain MRI on day 4 showed symmetric thalamic DWI/T2 hyperintensities (Fig. 1). After the end of hypothermia he remained in coma for 26 days. EEG on day 8 showed burst-suppression pattern (Fig. 2A). However, evoked potential studies with ABR (day 8), Flash VEP (day 17), and SSEP (day 18) showed no abnormalities (Fig. 3). Following the treatment he gradually improved with resolution of thalamic lesions (Fig.1) and he was transferred to a rehabilitation hospital on day 48. He returned to school at 4 months after presentation. At the last follow-up (28 months after presentation), the pediatric cerebral performance category was scored 2 (Fig. 2B).

Conclusion

- Evoked potentials studies are useful in the prediction of functional outcome in ANE.

Fig. 1

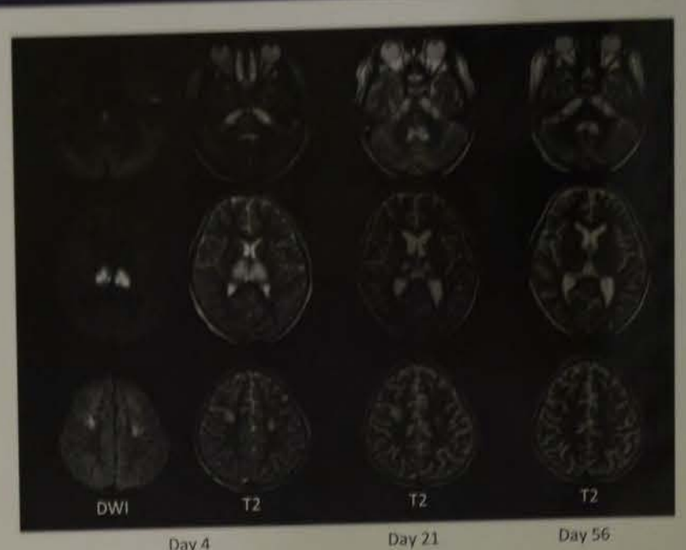

Serial brain MRIs showed resolution of initial increased signals in the thalamus, pons and frontal cortex. Note diffuse brain atrophy on Day 21 and 56.

Fig. 2

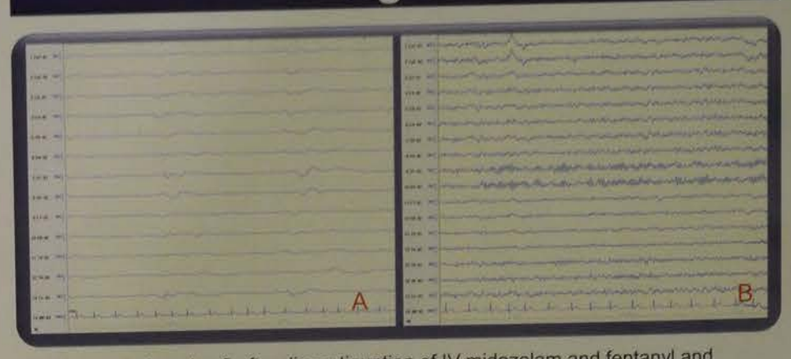

EEG recorded on day 8 after discontinuation of IV midazolam and fentanyl and recovery of therapeutic hypothermia showed burst-suppression pattern (A). The follow-up EEG showed recovery of background activities (B).

Fig. 3

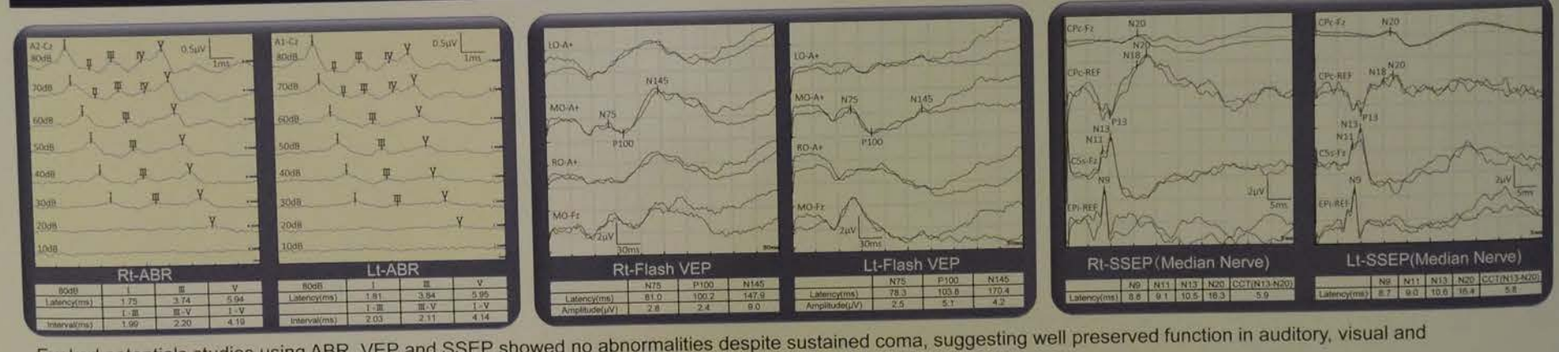

Evoked potentials studies using ABR, VEP and SSEP showed no abnormalities despite sustained coma, suggesting well preserved function in auditory, visual and somatosensory pathways.

Discussion

- This study demonstrated that burst-suppression pattern associated with bilateral thalamic lesions may not always suggest poor outcome in a case of ANE, particularly when each evoked potential is well-preserved on ABR, VEP and SSEP. It is suggested that evoked potential studies may be useful in the prediction of functional outcome. Similar association between evoked potentials and function outcome using somatosensory evoked magnetic field study has been reported in a case of ANE,[3] we also previously reported a similar experience in a adult case of anti-NMDA receptor encephalitis, in which despite prolonged decreased level of consciousness and diffuse delta EEG activity each SSEP was well preserved during the acute stage,[4] and the patient's long-term outcome was excellent 4-10 years after presentation.[5]
- In our case severe cytotoxic edema in the thalamus may result in coma, disrupting ascending reticular activating system and impairing cognition-related pathways. Such severe thalamic lesions is expected to cause irreversible severe deficits in adults; however, remarkable functional recovery may be due to compensatory mechanism associated with age at onset or early aggressive immunotherapy, which may have prevented further neuronal damage.

References

1. Mizuguchi M, et al., Acute necrotizing encephalopathy of childhood : a new syndrome presenting with multifocal, symmetric brain lesions. Journal of Neurol. Neurosurg. and Psychiatry 1995;58:555-561.
2. Mizuguchi M. Acute necrotizing encephalopathy of childhood : a novel form of acute encephalopathy prevalent in Japan and Taiwan. Brain & Dev. 1997;19:81-92.
3. Tran TD, et al. Varicella-associated acute necrotizing encephalopathy with a good prognosis. Brain Dev. 2001;23:54-7.
4. Iizuka T, et al. Anti-NMDA receptor encephalitis in Japan: long-term outcome without tumor removal. Neurology. 2008;70:504-11.
5. Iizuka T, et al. Association of progressive cerebellar atrophy with long-term outcome in patients with anti-n-methyl-d-aspartate receptor encephalitis. JAMA Neurol. 2016;73:706-13.

International Federation of Biomedical Laboratory Science
COI Disclosure

Name of Lead Presenter : Yuya Onozawa, Ph.D.
There are no companies, etc. in a relation of conflict of interest requiring disclosure in relation to the presentation.

[redacted] *Kitasato University Hospital* [redacted]

Clinical Physiology

PG-54

Evaluation of the validity of EEG toward the patients with possible dementia

Hiromi Minato[1], Saori Shibayama[1], Noriko Hatakeda[1], Ayumi Igaki[1], Yasunao Wada[1], Kouji Inuzumi[1], Masanaka Takeda[2], Masahiro Koshiba[2]

1, Hyogo College of Medicine Hospital, 2, Hyogo College of Medicine

Introduction

Electroencephalography (EEG) is an effective method for detecting diseases such as epilepsy and encephalitis. While, EEG is not routinely performed on the patients suspected to be dementia. Epilepsy patients might be misdiagnosed as dementia because these symptoms are similar to those of dementia, such as memory impairment or disorientation.

We examined EEG findings of patients with suspected dementia, and investigated how many cases except dementia were detected among them.

Table 1. Comparison of symptoms between adult onset epilepsy and dementia

Adult onset Epilepsy	Dementia
·memory loss	·memory impairment
·disorientation	·disorientation
· irritable	·violence, verbal abuse
·persistent disturbance of consciousness	·lack of understanding
·automatism	·hallucination

Materials and methods

Materials EEG findings of 70 patients with memory impairment or disorientation (29 males and 41 females, age 53-94)

Methods EEGs which were not found slow background activity and/or paroxysm activity were regarded as "Normal" for their age.
Digital EEG (Nihon Kohden, Tokyo, Japan), 10-20 system (with some exceptions)

Results

Abnormal findings were detected in 25 cases (36%).

Most of them were
- slow background activity
- θ and δ waves

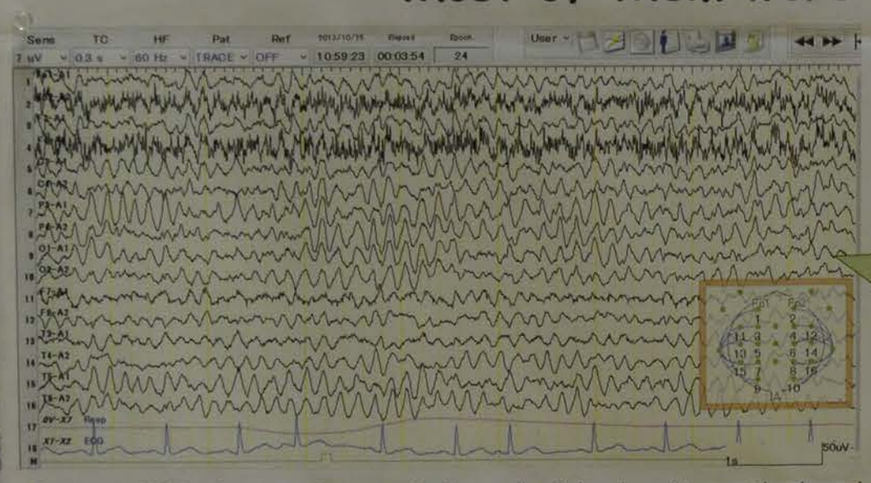

Figure 1. EEG showing θ wave during wakeful relaxation with closed eyes. (female, 89 years old). (Fp, front polar; F, frontal; C, central; P, parietal; T, temporal; O, occipital; even number, right; odd number, left).

These findings are indicated the brain disfunction, and this result is not consistent with dementia.

What is to be noted is

Spike and Periodic Synchronous Discharge (PSD)

localization-related epilepsy

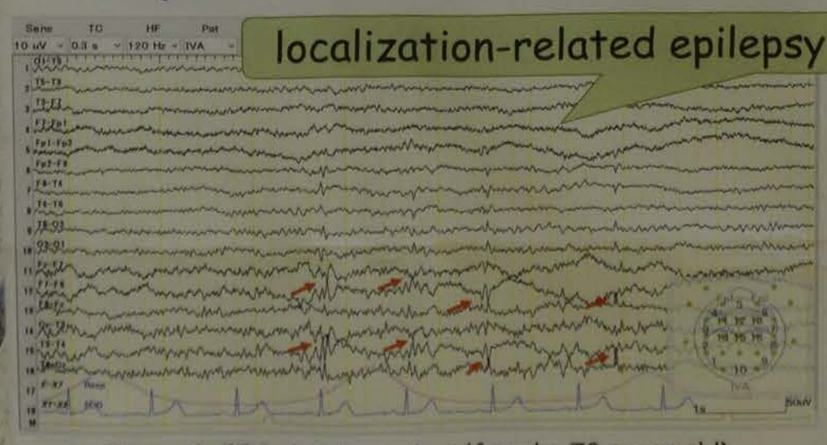

Figure 2. EEG showing spikes (female, 72 years old).

Creutzfeldt-Jakob disease (CJD)

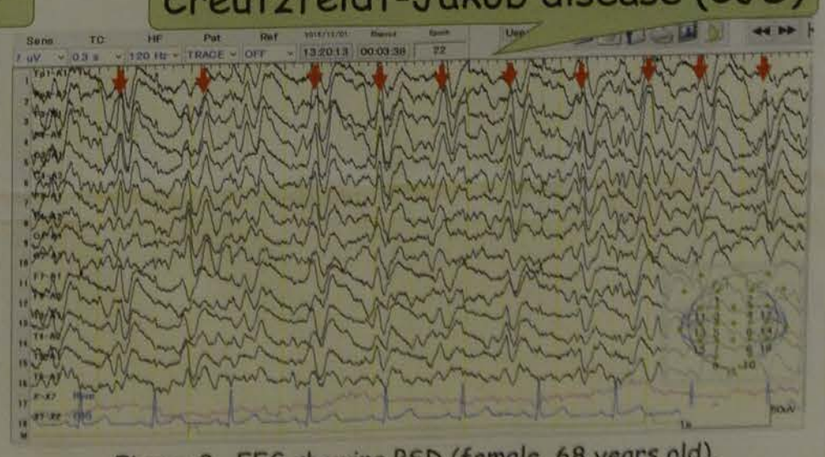

Figure 3. EEG showing PSD (female, 68 years old).

Conclusion

- Approximately 420 patients came to our Medical Centers for Dementia during study period. However, only 47 cases were performed EEG. This study suggested that patients with memory impairment or disorientation might be misdiagnosed as dementia.
- We concluded that to perform EEG for patients with suspected dementia will contribute to the detection and differential diagnosis of the diseases, and should be performed to them proactively.

Conflicts of interest: No potential conflicts of interest were disclosed.

Clinical Physiology

PG-55

Agreement rate of the sleep stage scoring in the PSG analysis

Sachiko Kurosaki , Yukio Yamadera , Ayumi Kikuchi , Chika Yasuda, Chiaki Suzuki , Naoko Sakurai , Kyouko Kaneta

Ohta General Hospital Foundation Ohta Nishinouchi Hospital, Japan

Introduction

The sleep stage scoring of PSG becomes an important indicator to use for diagnosing sleep disorders and judging the course of treatment. However, as scoring is performed visually, the inter-scorer difference may occur.

This time we will report on our investigation of the agreement rate and the factor that causes the inter-scorer difference by scoring the arousal and sleep staging on a same cases by multiple technologists.

Subject

Six Medical technologists (T－1～6) scored arousals and sleep stages on five PSG data (A～E) and made a comparative review of the following viewpoints with reference to the leading technologist's (T－1) results

Patient	age	sex	BMI	AHI	ArI
A	57	M	24.5	23.1	43.7
B	38	M	28.8	83.1	81.0
C	68	M	27.6	54.7	50.5
D	22	F	27.4	0.8	6.2
E	48	M	27.5	51.0	49.1
Mean	46.6		27.2	42.5	46.1

- The analysis performed according to "The AASM Manual for the Scoring of Sleep and Associated Events VERSION 2.1"

Methods: ① Agreement rate of the arousal scoring

- The decision if two events, Reference and Comparison, 'match' is taken by looking at the percentage of overlap. We used minimum overlap of 50% for our investigation.

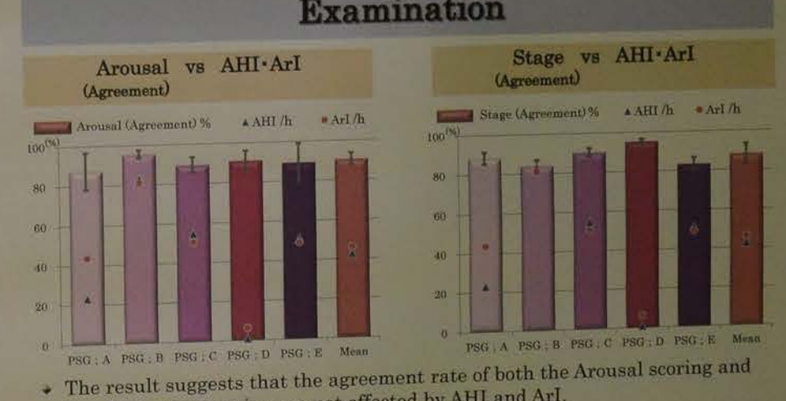

② Agreement rate of the sleep stage scoring
③ Agreement rate by each sleep stages

Results: ① Agreement rate of the arousal scoring

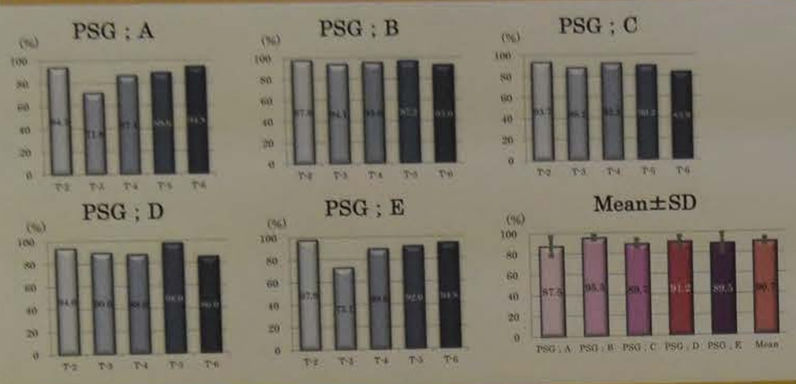

Results: ② Agreement rate of the sleep stage scoring

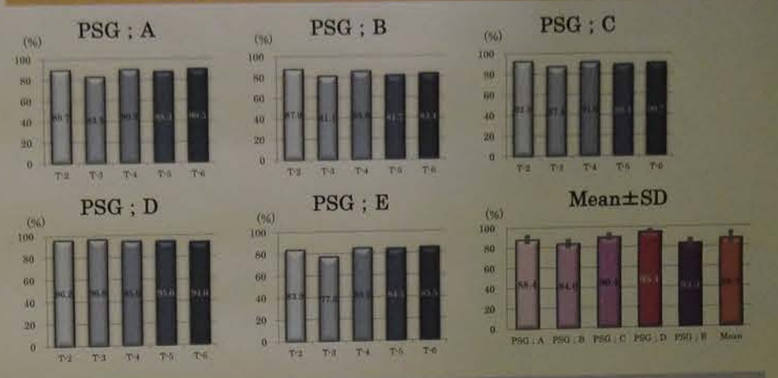

Results: ② Agreement rate of the sleep stage scoring

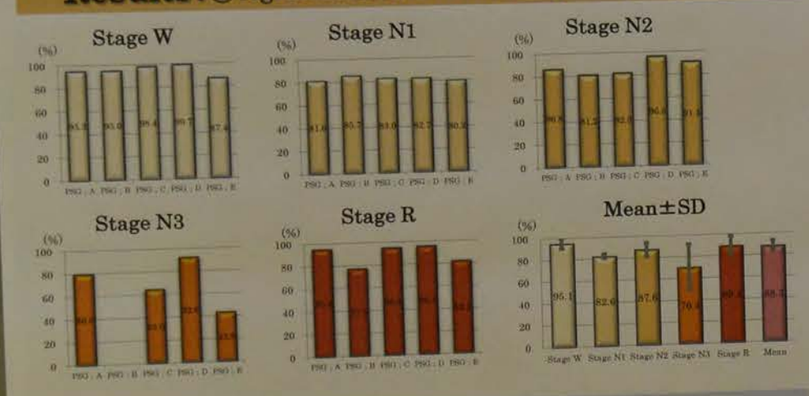

Examination

- The result suggests that the agreement rate of both the Arousal scoring and the sleep stage scoring are not effected by AHI and ArI.

Rate of disagreement epoch by sleep stage scoring

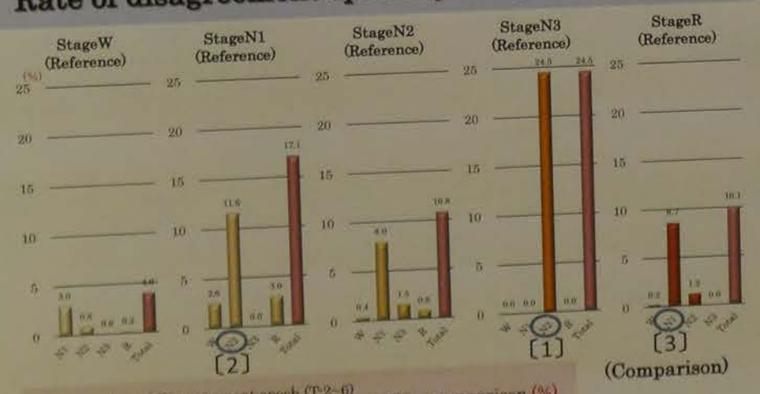

$$\frac{\text{Total number of Disagreement epoch (T-2~6)}}{\text{Total number of epochs of each stage} \times 5} \times 100 = \text{comparison (\%)}$$

[1] StageN3 ↔ StageN2

- F3-M2, C3-M2, O1-M2 ／ Filters: Hi pass : 0.3 Hz , Low Pass : 35 Hz
- F4-M1, C4-M1, O2-M1 ／ Filters: Hi pass : 0.5 Hz , Low Pass : 35 Hz

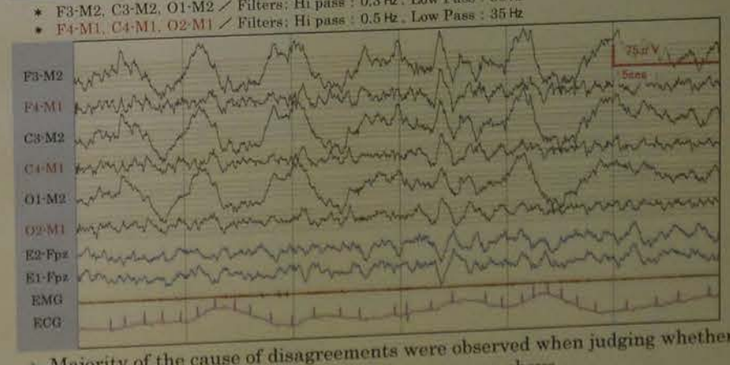

- Majority of the cause of disagreements were observed when judging whether it is an artifact due to sweating or a slow wave, as above.

[2] StageN1 ↔ StageN2

- Previous epoch : StageN1

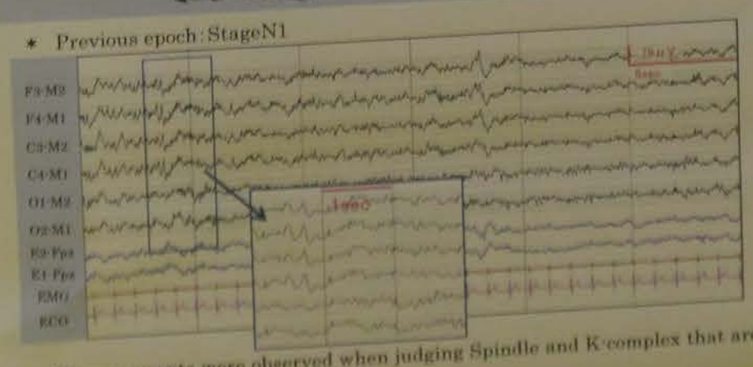

- Disagreements were observed when judging Spindle and K-complex that are used for staging N2, etc.

[3] StageR ↔ StageN1

- Previous epoch : StageR, Next epoch : StageR; Rapid eye movement (+)

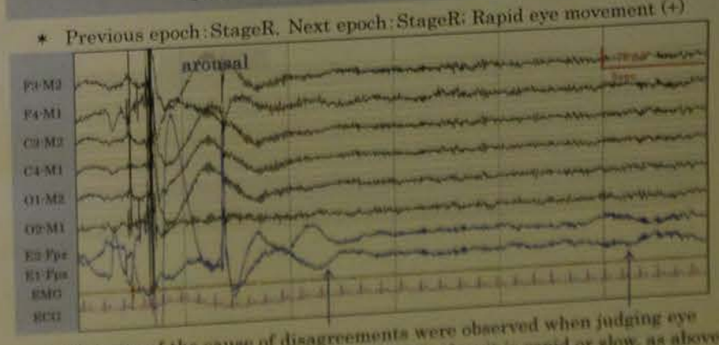

- Majority of the cause of disagreements were observed when judging eye movements that occurs after Arousals whether it is rapid or slow, as above.

Conclusion

Agreement rate were high in both arousal and sleep stage scorings. Regarding the agreement rate by each sleep stages, they were high in the order of Stage W > R > N2 > N1 > N3.Regarding StageN3 that was the lowest agreement rate, mix of artifact due to the sweating was particularly the factor that caused disagreement. We will push forward the approximation of the disagreement part within the scorers and, at the same time, we think it is important to set a rule for the bad quality signal recording cases.

Clinical Physiology

PG-56

Cancer associated thrombosis
The incidence of complication and positive rate

Harumi Ueda Chikako Ogino Satomi Isshiki Hidemi Yasugi
Masanori Nakamura Akiko Nonaka
Hyogo Cancer Center

Introduction

Deep vein thrombosis(DVT) has been found to be an important and critical complication of cancer patients.

However , there is scarce data on the incidence of DVT.

So we investigate the incidence of complication of DVT according to a type of cancer.

Methods

We investigated 423 patients who have a symptom likely to DVT, such as leg edema , and/or 1.0μg/ml D-dimer using by lower extremity ultrasound sonography among 3427 cancer patients who were consulted to our cancer from November 2014 to October 2015.

DVT separate

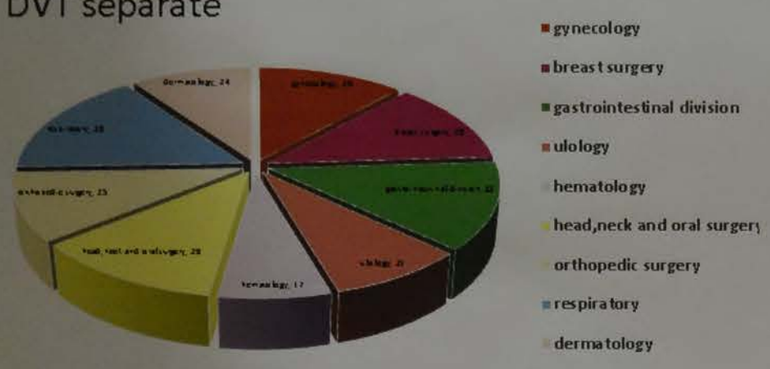

Results

Incidences of DVT complication according to cancer type were the peritoneal cancer (16.7%), soft tissue tumor (14.3%), ovarian cancer (11.8%), malignant melanoma (7.8%), multiple myeloma (7.1%), pancreatic cancer (6.1%), gastric cancer(5.6%), colon and small intestine cancer (5.1%), bladder cancer (3.5%), lung cancer (3%), prostate cancer (2.9%), endometrial cancer (2.4%), malignant lymphoma (1.7%), Paget's disease and Bowen's disease(1.5%), breast cancer (1.5%), kidney cancer (1.3%), esophageal cancer (0.6%) , pharynx cancer and larynx cancer (0.6%), cervical cancer (0.3%), liver cancer (0%), leukemia (0%), thyroid cancer (0%).

The positive rate of DVT according to cancer type were soft tissue tumors (50%),pancreatic cancer (42.9%), malignant melanoma (40%), ovarian cancer (34.4%),multiple myeloma (33.3%), lung cancer (33.3%), stomach cancer (31.7%), colon and small intestine cancer (27.9 %), kidney cancerthe frequency of the lower limbs DVT merger according to a malignant tumor disease (25%), breast cancer (23.5%), peritoneal cancer (20%), bladder cancer (18.2%), endometrial cancer (16.7%), malignant lymphoma (16.7%), pharynx cancer and larynx cancer (16.7%), prostate cancer (14.8%), Budget disease and Bowen's disease (12.5%), esophageal cancer (5.6%), cervical cancer (5%), liver cancer (0%), leukemia(0%), thyroid cancer (0%).

Incidences of DVT complication

Positive rate of DVT

Conclusion

①Peritoneal cancer, soft tissue tumors, ovarian cancer have higher incidence of DVT complication, respectively 16.7%,14.3%,11.8%.

②Soft tissue tumors, pancreatic cancer, malignant melanoma, ovarian cancer have higher positive rate of DVT, respectively 50%,42.9%,40%,34.4%.

Clinical Physiology

PG-57

Electrocardiography scoring is useful in predicting left ventricular wall motion abnormality after subarachnoid hemorrhage

Keiko Sugimoto[1], Akira Yamada[2], Risako Tanaka[3], Ayako Takahashi[3], Kazuhiro Nakamura[3], Kunihiko Sugimoto[3], Joji Inamasu[4], Tadayoshi Hata[1]

1. Fujita Health University School of Health Sciences Faculty of Medical Technology
2. Fujita Health University School of Medicine Department of Cardiology
3. Fujita Health University Hospital Clinical Laboratory
4. Fujita Health University School of Medicine Department of Neurosurgery

AIM

Patients with aneurysmal subarachnoid hemorrhage (SAH) frequently have cardiac such as arrhythmia, electrocardiographic change and cardiac wall motion abnormality (WMA). It is beneficial to detect WMA in the early stage of SAH, which contributes to more appropriate management of the patients. Electrocardiogram (ECG) is a routinely available diagnostic tool in many medical institutions.

The aim of this study was to examine whether ECG findings could predict WMA after SAH.

SUBJECTS & METHODS

- We studied 203 patients with SAH who were hospitalized in our institution between April 2007 and November 2010.
- A total of 161 patients with SAH (76%) were included in this retrospective study.
- Forty-two patients were excluded from analysis because either blood sample collection or Echocardiography and ECG had not been completed within 48 hours of SAH on-set.
- The exclusion criteria included an implanted pacemaker, a history of myocardial infarction , cardiomyopathy and significant valvular diseases .
- A 12-lead surface ECG was taken on the day of hospital admission at a paper speed of 25 mm/s (FX-8800 FUKUDA DENSHI Co).
- The ECG score was calculated by ECG findings (ST elevation, ST depression and T wave inversion) that were thought to be associated with WMA obtained from results of the univariate analysis.
- Each of following changes (ST elevation, ST depression and T wave inversion) was scored as 1 point. We defined the ECG score as the total points in every patient.

RESULTS

Patient Characteristics

	WMA(-) n=124	WMA(+) n=37	p-value
Age (years)	61.7±12.3	67.7±13.1	<0.05
Sex (female, %)	66.1	89.2	<0.01
Hypertension (%)	53.5	32.3	<0.05
Hypercholesterolemia (%)	11.4	9.4	NS
Diabetes (%)	8.0	3.3	NS
Aneurysm location (MCA / ACOM / ICPC%)	24.8/29.1/30.8	37.5/9.4/12.5	<0.01
SAH Grade (IV , V%)	35.0	83.8	<0.0001
Ejection fraction (%)	68.1±0.69	47.5±14.5	<0.0001
Troponin I (ng/ml)	0.15±0.38	1.65±3.17	<0.0001
Epinephrine (pg/ml)	197.3±1107.6	302±661.2	NS
Norepinephrine (pg/ml)	1077.1±3161.8	5036.4±2811.7	<0.01
Takotsubo cardiomyopathy (n)	—	14	—
Non-survivors	18 (16.8%)	19 (59.4%)	<0.0001

Univariate ECG Predictors of WMA

	p value	95% CI	OR
Sinus tachycardia	0.109	*0.21 – 1.20*	2.05
Sinus bradycardia	0.202	0.72 – 71.45	0.26
QT prolongation	0.089	0.21 – 1.09	2.02
PR shortening	0.243	0.16 – 1.72	2.00
PR prolongation	0.671	0.06 – 12.90	1.67
ST elevation	<0.0001	0.05 – 0.29	8.09
ST depression	<0.01	0.16 – 0.75	2.84
T wave inversion	<0.0001	0.04 – 0.23	9.85
U wave	0.360	0.53 – 13.51	0.49
Abnormal Q wave	0.198	0.11 – 1.72	2.38
PVC	0.582	0.30 – 35.16	0.55
PAC	0.671	0.06 – 12.90	1.69
LVH	0.317	0.60 – 8.57	0.52
CRBBB	0.720	0.15 – 5.29	1.36
Biphasic T wave	0.157	0.80 – 19.27	0.34

PVC: premature ventricular contraction, PAC: premature atrial contraction, LVH: left ventricular hypertrophy, CRBBB: complete right bundle branch block

Multivariate Predictors of WMA

	p value	95% CI	OR
QT prolongation	0.904	0.34 - 2.57	1.06
ST elevation	<0.001	0.06 - 0.45	5.97
ST depression	<0.05	0.11 - 0.75	3.44
T wave inversion	<0.0001	0.05 - 0.34	7.37

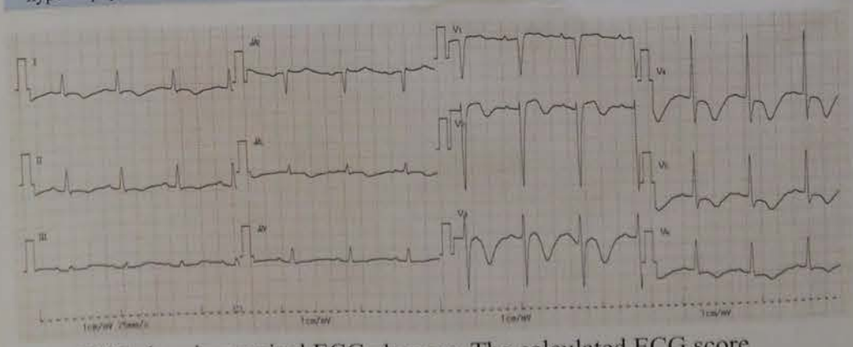

An ECG showing typical ECG changes. The calculated ECG score was 10points because of the T wave inversion in leads I, II, aV_L, aV_F, $V_{2\text{-}6}$ and positive T wave in lead aV_R.

The ROC curve for predicting WMA by ECG score

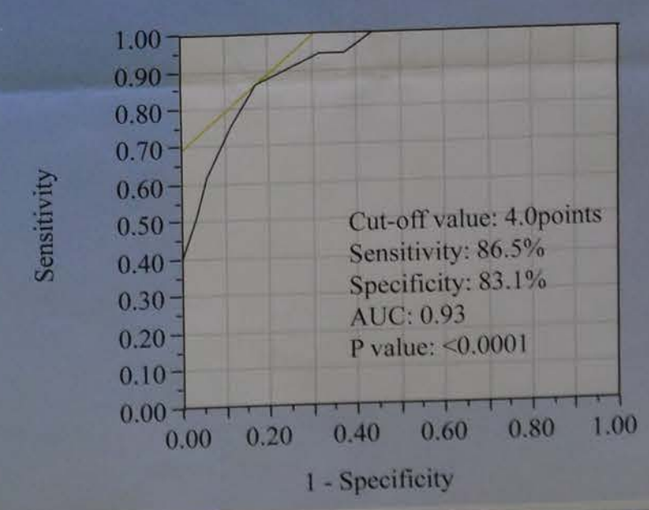

CONCLUSION

ECG scoring was very helpful in predicting WMA after SAH. ECG score over 4 could predict the occurrence of WMA.

The authors have no conflict of interest related to the content of this poster.

FUJITA HEALTH UNIVERSITY

Clinical Physiology

PG-58

Prognostic Significance of Right/Left Atrial Volume Ratio by Echocardiography in Interstitial Lung Disease Patients with Pulmonary Hypertension

Naka Saito[1], Shingo Kato[2], Ayumi Tanaka[1], Takako Ishikawa[1], Kozue Nakagomi[1], Noritaka Saito[1], Mamiko Nakamura[1], Kazuki Fukui[3]

1*Department of Clinical Laboratory, Kanagawa Cardiovascular and Respiratory Center, Japan
2*Department of Medical Science and Cardiorenal Medicine, Yokohama City University Hospital, Japan
3*Department of Cardiology, Kanagawa Cardiovascular and Respiratory Center, Japan

INTRODUCTION

Background

- Pulmonary hypertension (PH) is a well-known prognostic factor for interstitial lung disease (ILD) patients[1].
- In ILD patients, primary cause of PH is usually pre-capillary PH depending on pulmonary vascular resistance[2], resulting in increased right atrial (RA) dilatation[3,4].
- On the other hand, post-capillary PH is usually associated with left heart disease and accompanied with left atrial (LA) dilatation[2].
- We hypotheses that ILD patients accompanied with post-capillary PH have worse prognosis.
- Recently, we've shown that right/left atrial volume ratio (AVR) might be useful for the differentiation between pre- and post-capillary PH[5].

Purpose

- The aim of this study was to assess the prognostic value of echocardiography derived AVR in ILD patients with PH.

STUDY DESIGN

Study design

- Single center, retrospective observational cohort study

Population

- Inclusion criteria
  - ✓ ILD patients diagnosed by biopsy or chest computed tomography, who underwent echocardiography and right heart catheterization.
- Exclusion criteria
  - ✓ More than moderate aortic valve regurgitation (AR), and/or aortic valve stenosis (AS)
  - ✓ More than moderate mitral valve regurgitation (MR) and/or mitral valve stenosis (MS)
  - ✓ Chronic or paroxysmal atrial fibrillation (AF)
  - ✓ Congenital heart defect (CHD)
  - ✓ Lung cancer (LK)
  - ✓ History of myocardial infarction (MI)
  - ✓ Cardiomyopathy
  - ✓ Poor recording of UCG image

Figure 1. Flow chart of study enrollment

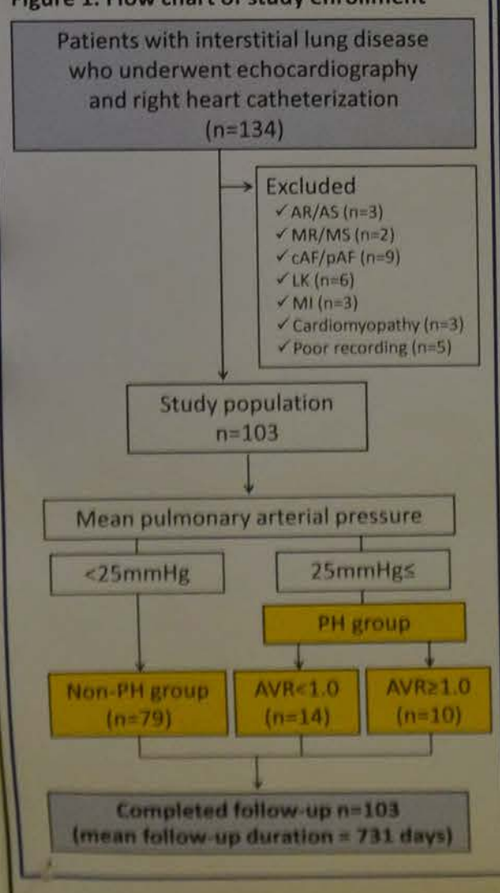

MATERIALS AND METHODS

Echocardiography

- Two dimensional gray-scale images were obtained using ultrasound system (iE33, Philips Medical System; Vivid E9, GE Healthcare)
- LA and RA measurement was performed using TomTec-Arena (Ver.1.0)

Echocardiographic measurement

✓ LA volume

Measured in both the LA focused apical 4- and 2-chamber views by area-length technique.

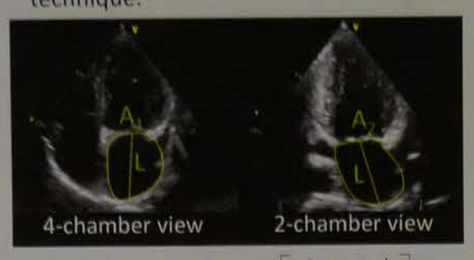

$$\text{LA volume (mL)} = \frac{8}{3\pi}\left[\frac{(A_1 \cdot A_2)}{L}\right]$$

※ A, area (cm²); L, length (mm)
※ L is defined as the shortest of the two long axes measured in the apical 2- and 4-chamber views.

✓ RA volume

Measured in RA-focused apical 4-chamber view by single plane area-length technique.

$$\text{RA volume (mL)} = \frac{8}{3\pi}\left[\frac{(A)^2}{L}\right]$$

※ A, area (cm²) ; L, length (mm)

- We defined atrial volume ratio (AVR) as following formula.

✓ $\text{AVR} = \frac{\text{RA volume}}{\text{LA volume}}$

RESULTS

Table 1. Patients characteristics

	non-PH (n=79)	AVR≥1 (n=14)	AVR<1 (n=10)
Demographics			
Age, year	71.3±7.2	62.1±10.6*	69.6±9.4
Male, n (%)	50 (63)	10 (71)	7 (70)
Height, cm	159.5±6.8	164.0±7.1	160.2±9.5
Weight, kg	57.2±10.0	62.8±12.4	60.1±12.9
BMI, kg/m²	22.4±3.3	23.3±3.9	22.6±3.6
BSA, m²	1.62±0.15	1.72±0.18	1.64±0.16
SBP, mmHg	134±18.8	125±10.9	140±24.5*
DBP, mmHg	74±9.8	76±9.3	82±11.2
HR, bpm	72±12.3	80±14.7	74±20.4
Right Heart Catheterization			
RAP, mmHg	2.1±3.0	3.8±3.7	6.1±6.5*
Mean PAP, mmHg	16.8±3.9	32.6±7.9*	33.2±10.4*
PCWP, mmHg	6.0±3.8	8.8±3.0*	13.0±5.7*,†
Echocardiography			
LVEF, %	65±5.9	64±7.2	64±6.9
LVDd, mm	42.7±5.1	41.5±3.1	44.4±3.7
LVDs, mm	27.2±3.6	26.7±4.2	29.4±3.9
IVSd, mm	9.3±1.8	9.7±3.0	10.2±2.2
LVPWd, mm	9.7±1.7	10.5±1.4	9.9±2.8
LV mass, g/m²	83.8±21.7	85.8±16.6	95.0±30.3
E/e'	11.1±3.4	10.0±3.1	11.0±6.6
LAD, mm	34.0±6.8	35.7±5.5	39.6±8.7*
LAVI, ml/m²	36.3±11.3	25.9±9.4*	38.9±12.2†
RAVI, ml/m²	41.5±16.3	65.4±25.5*	37.7±9.1†
RV FAC, %	39±9.7	33±10.9	35±9.2
TAPSE, mm	20.6±4.2	20.0±4.8	20.7±4.2
TV S', cm/s	13.4±3.4	12.8±2.5	13.9±4.3
RVSP, mmHg	40.1±12.1	60.9±18.0*	58.4±14.3*
Effusion, n (%)	1 (1)	2 (14)	3 (30)
Eccentricity index	1.05±0.13	1.30±0.44	1.21±0.31
AVR	0.76±0.3	1.40±0.3*	0.64±0.2*,†

*p<0.05, vs. non-PH; †p<0.05, vs. AVR≥1.0

RESULTS

Figure 2. All-cause mortality during follow-up

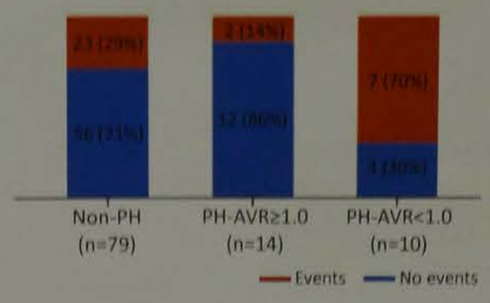

Figure 4. Kaplan-Meier Survival Curve

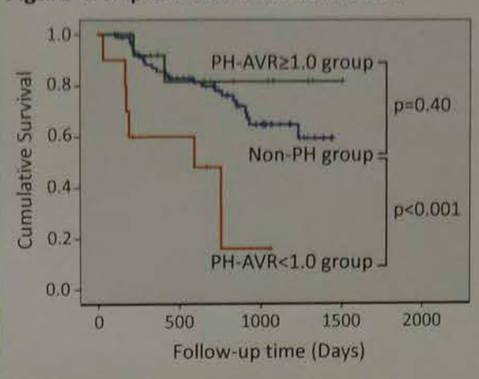

Figure 3. Comparison with atrial volume ratio between PH patients with death events and those without

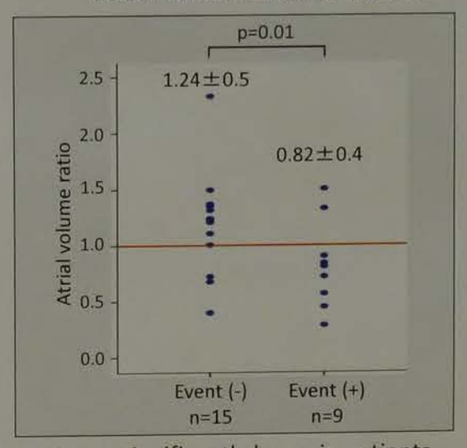

AVR was significantly lower in patients who died.

Table 2. Cox proportional hazard analysis in patients with PH

	Univariate analysis		
	HR	95% CI	p-value
LVEF	0.91	0.83-1.00	0.05
E/e'	0.95	0.81-1.12	0.58
Effusion	0.83	0.17-4.05	0.81
LAVI	1.02	0.98-1.07	0.35
RV FAC	0.93	0.87-1.01	0.08
TAPSE	0.93	0.79-1.09	0.38
RVSP	1.03	0.98-1.08	0.22
AVR	0.24	0.05-1.09	0.06
AVR <1.0	6.57	1.35-31.88	0.02

	Multivariate analysis		
	HR	95% CI	p-value
LV EF	0.94	0.82-1.06	0.30
RV FAC	0.93	0.84-1.03	0.17
AVR <1.0	11.1	1.90-65.26	<0.01

CONCLUSION

- In ILD patients with PH, lower AVR was associated with higher risk of death.
- AVR <1.0, might be useful as a simple and accurate parameter to detect the ILD patients with PH, at increased risk for death.
- The results indicated that assessment of AVR provides better risk stratification in ILD patients with PH.

Reference

1, Behr J et al. Eur J Respir. 2008; 31; 1357-1367.
2, Galie N et al. Eur Heart J. 2016; 37; 67-119.
3, Cioffi G et al. Eur J Echocardiogr. 2007; 8(5): 322-31.
4, Sato T et al. Int J Cardiol. 2013; 168; 420-426.
5, Saito N et al. AAE Scientific Session 2016

COI disclosure of first author

The authors have no financial conflicts of interest to disclose concerning the presentation.

Clinical Physiology

PG-59

Three dimensional left atrial speckle tracking may detect cardiac changes due to chemotherapy by trastuzumab.

Naoki Kimura, Yuji Masaki, Masashi Nagatomo, Minako Furukawa, Yasushi Kawabuchi, Katsuyuki Nagatoya

Osaka Rosai Hospital, Osaka, Japan

Background

Drug-induced cardiomyopathy often occurs in patients who undergo trastuzumab chemotherapy. Thus, it is important for these patients to undergo periodic echocardiography. In the early phase of drug-induced cardiomyopathy, a diastolic disorder appears first. By comparing two groups, with and without trastuzumab chemotherapy, we show that a three-dimensional left atrial speckle tracking echo may detect these changes.

Methods

This was a retrospective single-center observational study conducted from January 2014 to June 2015. We performed 140 three-dimensional echocardiographies and categorized them into two groups : a breast cancer postchemotherapy trastuzumab group (n=12) and a control group without heart disease (n=21). We analyzed three-dimensional left atrial speckle tracking using three indices: left atrial global longitudinal strain (LA GLS), left atrial global circumferential strain (LA GCS), and left atrial global radial strain (LA GRS). Using these three indices with diastolic index (E/A) and systolic index (LVEF), we were able to compare the differences between the two groups.

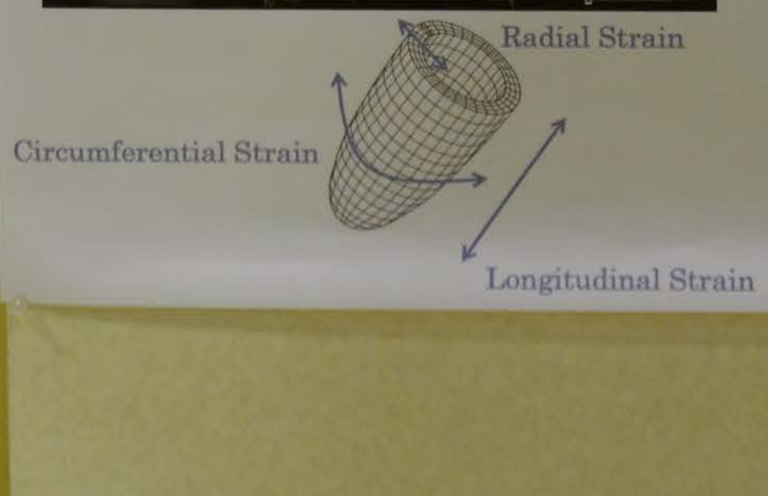

Results

No significant differences were observed for LVEF, but significant differences were observed for E/A. During the three-dimensional echo, only LA GLS yielded significant differences.

	chemotherapy group (n=12)	control group (n=21)	p value
age(years)	65±5.8	73±6.5	<0.05
gender male(number)	0	6	---
LA GLS(%)	21.8±6.1	16.8±4.7	<0.05
LA GCS(%)	27.3±21.6	17.9±10.9	0.08
LA GRS(%)	- 23.9±12.7	- 19.2±7.4	0.14
E/A	0.84±0.21	0.68±0.19	<0.05
LVEF (%)	70.1±3.2	69.1±5.5	0.26

mean±SD

Discussion

In the present study, we observed a difference in the two groups for E/A but not for LVEF. On the other hand, the three-dimensional echo revealed that only LA GLS yielded a difference, suggesting that LA GLS is a marker for E/A and could thus be used to detect early changes that result from trastuzumab chemotherapy.

Limitation

1. All the patients in the trastuzumab chemotherapy group had breast cancer. Thus, breast cancer could be a confounding factor. Similarly, the dose and/or duration of trastuzumab could also confound the results.

2. The cross-sectional nature of this study limits our ability to estimate the longitudinal effects as well as the causality of the interaction between trastuzumab chemotherapy and cardiomyopathy.

Conclusion

LA GLS can serve as a marker for E/A and can be useful to detect cardiac changes due to trastuzumab chemotherapy.